the LENSES project

LEarning and action alliances for NexuS EnvironmentS in an uncertain future

LENSES

WP7

D7.4 Flexible Approaches to Managing Competing Demands for Water

Mert Can Gunacti (EA-TEK), Cem Polat Cetinkaya (EA-TEK), Gulay Onusluel Gul (EA-TEK), Ali Gul (EA-TEK), Filiz Barbaros (EA-TEK), Sefa Nur Yesilyurt (EA-TEK), Mohamed NAJAR (Islamic University of Gaza), Claudia Panciera (Politecnico di Bari), Alessandro Pagano (IRSA), Ivan Portoghese (IRSA), Marwah Yaseen (Politecnico di Bari), Silvia Vanino (CREA), Estrella López (ECOADAPTA), Manuel Bea (ECOADAPTA), Vassilios Pisinaras (SWRI), Andreas Panagopoulos (SWRI), Anna Chatzi (SWRI), Dimitrios Malamataris (SWRI), Antonia Maragkaki (TUC), Maria Lillis (TUC), Nikolaos Nikolaidis (TUC), Luna Al-Hadidi (NARC), Nabeel Bani Hani (NARC), Zübeyde Albayram Doğan (UTAEM), Murat Çağatay Keçeci (UTAEM), Christina Papadaskalopoulou (DRAXIS), Marina Antoniadou (DRAXIS)

3/12/2023

Project coordinator

Project partners

Project Website

www.lenses-prima.eu

This project is part of the PRIMA programme supported by the European Union.
GA n° [2041] [LENSES] [Call 2020 Section 1 Nexus IA]

Project no. 2041

Project acronym: LENSES

Project title: Learning and action alliances for NEXUS environments in an uncertain future

Call: PRIMA call Section 1 – Nexus 2020, Topic 1.4.1-2020 (IA).

Start date of project: 01.05.2021

Duration: 36 months

Deliverable title: D7.4 Flexible Approaches to Managing Competing Demands for Water

Due date of deliverable: Nov 2023

Project Coordinator: Stefano Fabiani, Council for Agricultural Research and Economics (CREA)

Organisation name of lead contractor for this deliverable: EA-TEK (LEAD PARTNER)

Lead Authors Mert Can Gunacti (EA-TEK), Cem Polat Cetinkaya (EA-TEK), Gulay Onusluel Gul (EA-TEK), Ali Gul (EA-TEK), Filiz Barbaros (EA-TEK), Sefa Nur Yesilyurt (EA-TEK)

Email mert.gunacti@deu.edu.tr, cem.cetinkaya@deu.edu.tr

Contributions from

Internal Reviewer 1 **Vassilios Pisinaras**

Internal Reviewer 2

Dissemination level		
PU	**Public**	**PU**
CO	**Confidential, restricted under conditions set out in Model Grant Agreement**	
CI	**Classified, information as referred to in Commission Decision 2001/844/EC**	

History			
Version	**Date**	**Reason**	**Revised by**
01	04/12/2023	Internal review	Vassilios Pisinaras (SWRI)
02	04/12/2023	Revised version	Mert Can Gunacti (EA-TEK)

This project is part of the PRIMA programme supported by the European Union.
GA n° [2041] [LENSES] [Call 2020 Section 1 Nexus IA]

Executive summary

The document entitled "Flexible Approaches to Managing Competing Demands for Water" (Deliverable 7.4) endeavours to evaluate the functionality of our hydrological systems and their response to climate change. This initiative aligns with a Nexus perspective on integrated water resource management, encompassed in four steps: **(i)** Conducting water accounting at spatial and temporal resolutions acceptable for our Water-Ecosystem-Food (WEF) Nexus systems, as ecosystem boundaries encompass the examined irrigated farming systems. **(ii)** Assessing sectoral (irrigation, environmental, energy, urban) water demands for pilot areas with a focus on associated priorities, thereby linking to Work Packages 3 (WP3) and 6 (WP6) related to governance. **(iii)** Performing water balance simulations to scrutinize sectoral (irrigation, environmental, energy, urban) water allocation policies and practices, to evaluate current and future situation through the consideration of effect of climate change regarding Representative Concentration Pathways (RCP) 4.5 and RCP 8.5 scenarios to contribute to Work Package 4 (WP4). **(iv)** Planning water resources based on an adaptation framework, employing measurable Nexus indicators (NIs) to help a flexible and evidence-based allocation approach tailored to Nexus visions outlined in Work Package 2 (WP2) as ensuring all Nexus Domains does not compromise each other which also establishes a connection with Work Package 5 (WP5).

Methodological approaches were outlined to assess the water accounting of the project's pilot areas, namely Middle Jordan Valley – JO, Gediz Basin & Delta – TR, Guadalquivir Basin Donana National Park Area – ES, International Long Term Ecological Research Network Sites (Pinios and Koiliaris Basins – GR) and Tarquinia Plain – IT. Unfortunately, the examination of the Galilee and Hula Valley in Israel, as the other pilot case, could not be conducted due to unexpected circumstances. Given the distinct challenges in each pilot area, hotspots in their models were identified through active stakeholder involvement realized in other WPs of LENSES Project. Examples of such focal points include areas of national or international ecological significance, major water sources, and complexes of industrial sites. For each pilot area existing topological network consisting of supply, demand, diversion nodes and their connections identified, and their associated data requirements are investigated. Although data availability emerged as a constraining factor across all pilot areas, available utilized sources enabled a comprehensive analysis for each pilot. Moreover, models crafted for each pilot area underwent further validation through local experts and pilot leaders.

Furthermore, examinations of climate change scenarios have been undertaken based on the outcomes of the RCP 4.5 and RCP 8.5 scenarios, as provided by the DRAXIS Team. In addition to the findings derived from baseline and climate change scenarios, we computed water accounting indicators. These indicators are crafted to offer insights to the pilot areas regarding their current and future conditions within the context of climate change. Additionally, they function as inputs for other project tasks, specifically Task 4.2, which involves Participatory System Dynamics Modeling, and Task 5.4, focusing on Computational Advancements for Ecosystem Services Assessments.

This deliverable has been generated within the framework of Task 7.4, concentrating on "Water Accounting, Allocation, and Planning," as part of Work Package 7, titled "Nexus Operationalization for SDG Delivery" within the LENSES project.

Table of Contents

This project is part of the PRIMA programme supported by the European Union.
GA n° [2041] [LENSES] [Call 2020 Section 1 Nexus IA]

List of Figures

This project is part of the PRIMA programme supported by the European Union.
GA n° [2041] [LENSES] [Call 2020 Section 1 Nexus IA]

List of tables

List of main abbreviations

EMO-5	European Meteorological Observations
HEC-HMS	Hydrologic Engineering Centre-Hydrologic Modeling System
IWRM	Integrated Water Resources Management
SWAT	The Soil & Water Assessment Tool
USDA	United States Department of Agriculture
WEAP	Water Evaluation and Planning System

Report on Flexible approaches to managing competing demands for water

1. Background and key concepts

Water is an essential resource for life, supporting human activities from agriculture and industry to domestic use and ecosystem health. However, the world's water resources are facing increasing pressure from a variety of factors, including climate change, population growth, and economic development. As a result, effective water resources management has become increasingly crucial for ensuring sustainable water supplies and meeting the needs of various stakeholders. (Harmancioglu et. al.,2013)

Managing water resources is a complex task that requires an understanding of both the natural and socioeconomic systems that influence water availability and demand. Water resources are often shared across different sectors, such as agriculture, industry, and domestic use, leading to competing demands that must be balanced. Additionally, water resources are subject to various environmental pressures, such as climate change, pollution, and land use changes, which can further complicate management efforts.

To effectively manage water resources, it is essential to develop a comprehensive understanding of the systems involved. This involves gathering data on water availability, demand, and the various factors influencing these parameters. Once this data is collected, it can be used to develop models that simulate the behaviour of the system under different scenarios. These models can then be used to evaluate different management strategies and identify the most effective approaches for achieving desired outcomes (Cetinkaya & Gunacti, 2018).

Over the past 50 years, there has been significant progress in the development of water resources management models (Gleick, 1993; Waterbury, 2002; Meadows et al., 2004; Cetinkaya et. al, 2008; Gleick et al., 2013; WWAP, 2015). Early models focused primarily on the physical aspects of water systems, such as hydrology and hydraulics. However, as the complexity of water management challenges has increased, so has the sophistication of models to address these challenges.

In the last 10 years, there has been a growing emphasis on incorporating social aspects into water resources management models (Duncan and Cogan, 2022; Hoeffler and Crook, 2022; Tortajada and Lin, 2022). This is because social factors, such as stakeholder interests, economic considerations, and cultural norms, play a critical role in shaping water use patterns and management decisions. By incorporating social aspects, models can provide a more holistic understanding of water systems and help to identify more equitable and sustainable solutions (Harmancioglu et. al., 2020)

Several key concepts have emerged as central to effective water resources management. These concepts include:

- Integrated Water Resources Management (IWRM): IWRM is a holistic approach to water management that recognizes the interconnectedness of different water uses and the need to balance them in a sustainable way.
- Water Security: Water security refers to the availability of sufficient, reliable, and affordable water to meet the needs of individuals, communities, and ecosystems.

- Water Productivity: Water productivity is a measure of how efficiently water is used to produce goods and services. Improving water productivity is essential for conserving water resources.
- Water Governance: Water governance encompasses the rules, structures, and processes that determine how water resources are allocated, used, and managed. Effective water governance is essential for ensuring equitable and sustainable water use.

Effective water resources management is a critical challenge for the 21st century. To tackle this challenge effectively, it is crucial to develop a deep understanding of water systems, employ sophisticated modeling tools, and integrate social dimensions into management strategies. This holistic approach forms the foundation for progress towards a more sustainable future, characterized by the equitable sharing and efficient utilization of water resources to meet the diverse needs of all stakeholders.

2. Purpose of the deliverable

The objective of the report aims to summarize the modeling efforts undertaken in the 6 pilot areas of LENSES project. The report aims to present the results obtained through these initiatives, considering both baseline conditions and scenarios influenced by climate change. The process of constructing the water accounting models involves an initial phase based on the development of hydrologic models within the designated pilot areas. Hydrologic models, developed either collaboratively with pilot partners or exclusively by the EA-TEK team, have effectively depicted the present conditions of the pilot areas and assessed climate change projection estimates. In this scope, several one-on-one online meetings have been conducted with the pilot partners to conceptualize their pilot area's topology first, then collect the relevant data, and then validate the developed models. An offline topology guide has also been developed to help pilots further develop their pilot area topology (See Annex 1). After the water accounting models have been validated by the pilot partners, hydrological model results based on climate change scenarios generated according to the climate change parameters estimated according to RCP 4.5 and RCP 8.5 provided by DRAXIS were applied to the water accounting models.

The results of the baseline and the climate change scenarios were then utilized to calculate a series of water accounting indicators (sectoral water use, total amount of supply, total amount of demand, supply-demand ratio, unmet demand, reliability of source, coverage of demand, unmet instream/environmental flow requirements, average irrigation productivity, and crop unit gross revenue). The derived water accounting indicators summarize the baseline state of the pilot areas, offering a user-friendly platform for comparing various alternative states, including climate change impacts, demand management, and the implementation of Nature-Based Solutions (Figure 1).

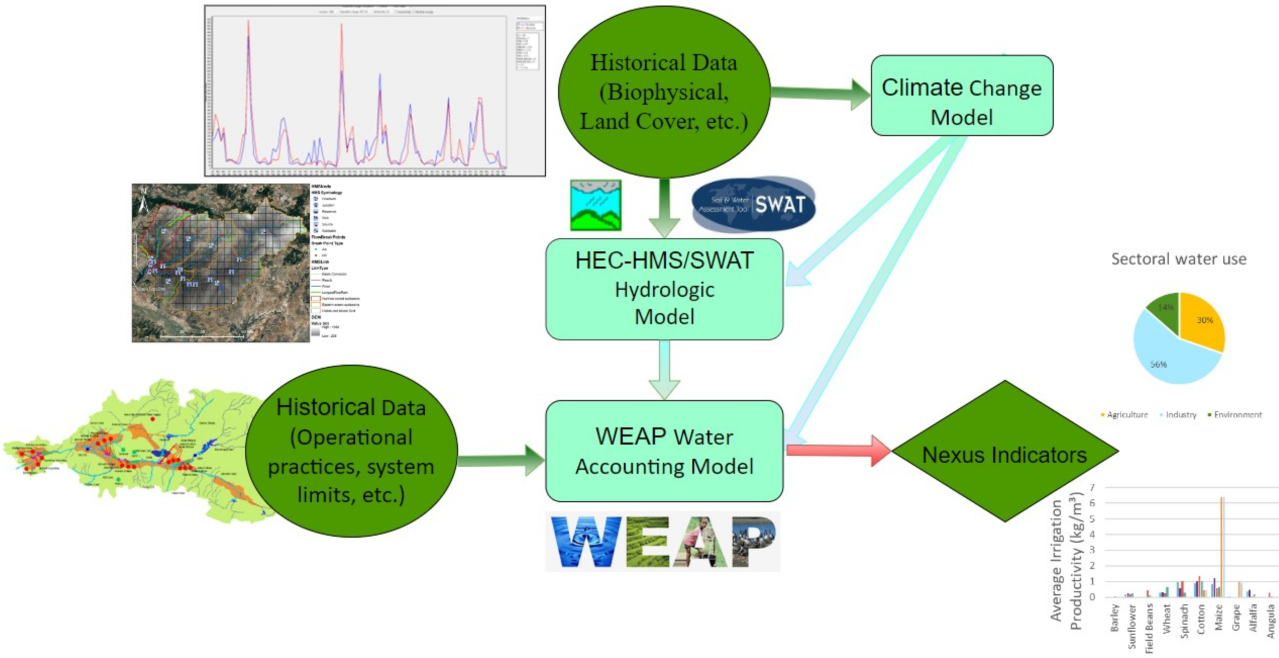

Figure 1 D7.4 Flowchart.

3. Models

3.1. Hydrological Models

Since hydrological processes have an overly complex structure, it is essential to accurately understand the modeling of hydrological system elements and their operational mechanisms. To achieve this understanding, the hydrological modeling of the pilot areas, as outlined in Task 7.4, utilized the Hydrologic Engineering Centre-Hydrologic Modeling System (HEC-HMS) and The Soil & Water Assessment Tool (SWAT), tailored to the study areas and the available data. These models allowed for the simulation of the hydrological behaviour of the basins, revealing the relationship between the model parameters and the characteristics of the river basin.

Climate change is having a profound impact on various environmental systems, including hydrology. One of the critical aspects of this impact is the alteration of streamflow. To understand and predict these changes, hydrologic modeling tools play a crucial role. In this task, we applied HEC-HMS and SWAT modeling tools in assessing climate change impacts on streamflow or other hydrologic budget constituents, depending on their significance for each pilot area.

3.1.1. Hydrologic Engineering Center- Hydrologic Modeling System (HEC-HMS)

The HEC-HMS is a software developed by the US Army Corps of Engineers. The model is capable of simulating rainfall-runoff events and directing hydrological processes. Integrated with HEC-Geo-HMS, it can seamlessly import spatial data for the study area, allowing the representation of key parameters such as infiltration, evaporation, and the overall hydrological dynamics of the river basin. HEC-HMS has a generalized modeling system that can represent a large number of different basins. The model comprises key components, including a catchment model, a meteorological model, control features, time series data, and grid data. It incorporates components for precipitation, potential evaporation, snowmelt, canopy, surface storage, infiltration, surface runoff, baseflow, channel routing, and channel losses. These components collectively enable simulation of land surface processes of the hydrological cycle. Users can tailor the model by selecting the most appropriate representation of catchment characteristics. Within the model, "Subbasin" is used to represent the physical basin, "Reach" to convey the flow, "Junction" to combine the flow from different upstream sources, "Source" to represent the water sources, "Diversion" to model the flow leaving the main channel and reservoir elements (HEC-USACE, 2008).

The modeling process begins with the input of meteorological data, such as rainfall and temperature, which can be obtained from weather stations or historical records. Users can also define the topography of the watershed, delineating the flow paths and drainage areas. Soil and land use information are crucial inputs, as they impact runoff and infiltration rates (Figure 2).

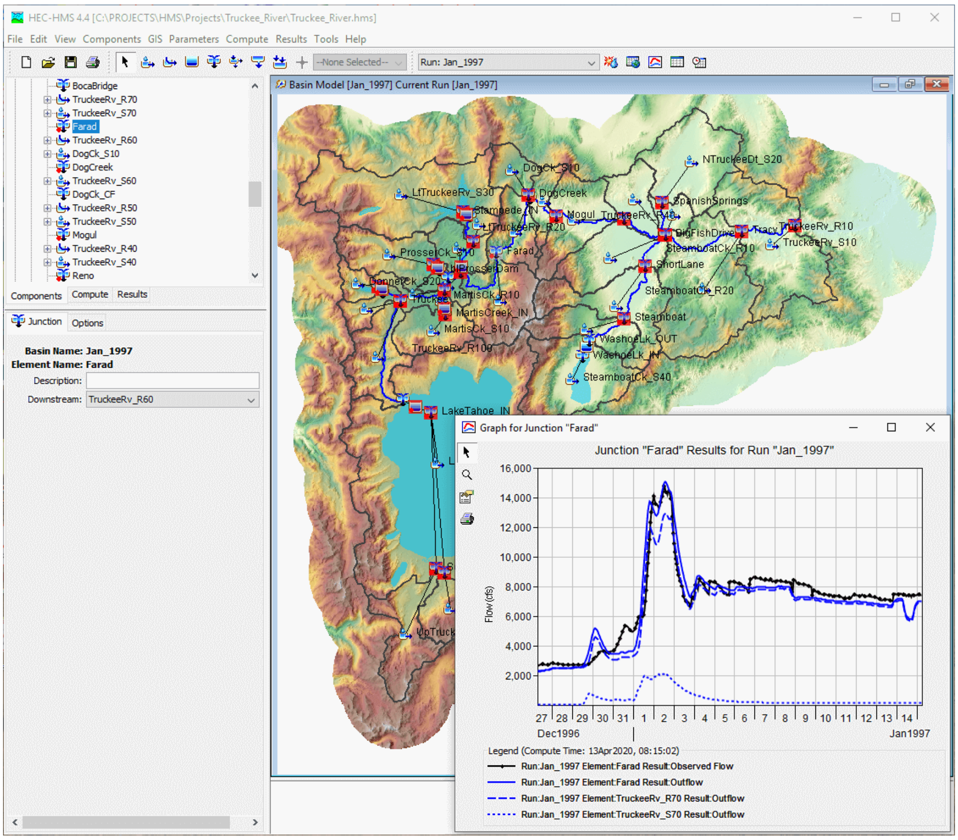

Figure 2 An example of HEC-HMS schematic and its hydrograph output (HEC-USAGE, 2008).

The selected methods based on the availability of the data, used in the hydrologic modeling phase of the project are given in Figure 3.

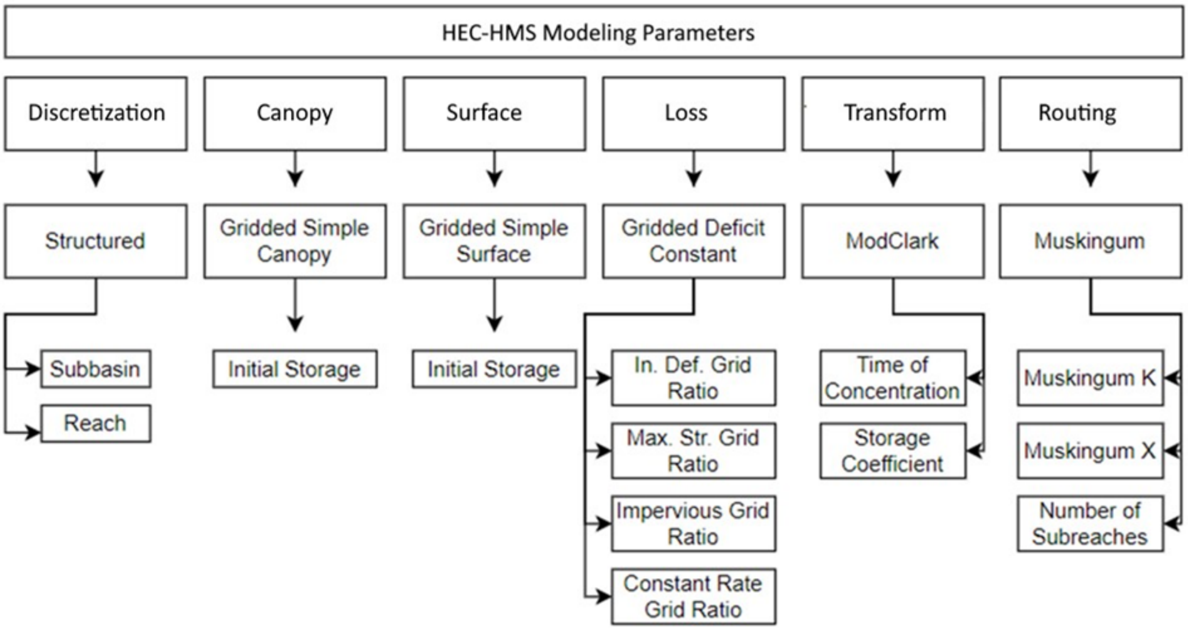

Figure 3 Selected methods and required parameters.

-The discretization defines how a subbasin is discretized. There are four types of Discretisation: Structured, Unstructured, File Specific, and None. In Task 7.4. the "Structured" method was used to create a Cartesian grid within the subbasin boundaries.

-The canopy is the component that can represent the presence of plants in the landscape. The choice of a canopy method is optional but should be used for continuous simulation applications. Users can choose between Dynamic Canopy, Gridded Simple Canopy or Simple Canopy to suit their model. For Task 7.4. the "Gridded Simple Canopy" method was used, which analyses each grid cell with separate parameter values and separate precipitation.

- The surface is one of the components that can be included in the sub-basin element. The surface is intended to represent the ground surface where water can accumulate in the depression tank. Users can choose either "Gridded Simple Surface" or "Simple Surface" method. In Task 7.4, the "Gridded Simple Surface" method, which uses the Simple Surface method on a grid cell basis, was selected.

- Loss represents the interaction of surface runoff and subsurface processes. A total of twelve different loss methods are provided. Some of the methods are primarily designed to simulate events. Others are designed for continuous simulation. All of the methods preserve mass. For Task 7.4. among the continuous simulation methods, "Gridded Deficit Constant", which analyses continuous events on a grid basis, was selected.

- Transformation calculations are performed with a transformation method that includes the sub-basin as opposed to infiltration. A total of nine different transformation methods are offered to users by the model. For Task 7.4, the ModClark method was used, representing the sub-basin as a collection of grid cells.

- The routing method represents the way the model realizes a section of a stream or river with a routing method within the reach. The model provides users with nine different methods. For Task 7.4. the

Muskingum method was chosen, which uses a simple conservation of mass approach to direct the flow along the river (Casuli, 2008; Minshall, 1960; Welle et al., 1980) (Figure 2.). Details of the methods and the required parameters are available on the software web page (HEC-USAGE, 2008).

One of the strengths of HEC-HMS is its ability to simulate various rainfall-runoff processes, from simple, lumped models to more complex, distributed models. This versatility makes it applicable to a wide range of hydrologic scenarios. The software also provides options for assessing flood risk, designing stormwater management systems, and evaluating the impacts of land use changes.

HEC-HMS is especially valuable when studying climate change impacts on streamflows. It allows users to incorporate future climate scenarios into their models, projecting how changes in temperature and precipitation will affect runoff and streamflow patterns. By comparing the results of different scenarios, hydrologists can gain insights into potential future challenges in water resource management.

In summary, HEC-HMS is a comprehensive tool for hydrologic modeling that is particularly useful in assessing climate change impacts on streamflow. Its versatility, user-friendly interface, and ability to simulate various hydrologic processes make it a valuable asset for researchers, water resource managers, and policymakers.

3.1.2. The Soil & Water Assessment Tool (SWAT)

The Soil & Water Assessment Tool (SWAT) is another influential modeling tool in the field of hydrology developed by the United States Department of Agriculture (USDA) (Arnold et al., 1998; Neitsch et al., 2011a). It is specifically designed for simulating hydrological processes at the watershed scale and has been widely used for assessing the impacts of climate variability, land use changes, and management practices on streamflow and water quality. SWAT's capabilities and flexibility make it well-suited for addressing the complex challenges posed by climate change. Successful applications of the SWAT model have been demonstrated across various disciplines in regions with diverse geographical conditions and different climate zones worldwide (Gassman et al., 2007; Onusluel Gül and Rosbjerg, 2010; Onusluel Gül et al., 2010) (Figure 4).

SWAT is particularly effective in capturing the interactions between land use, soil, and climate in a watershed. It integrates data on topography, land use, soil properties, weather, and management practices to simulate various hydrological processes, including evapotranspiration, runoff, infiltration, and groundwater flow. The model divides the watershed into sub-basins and uses a variety of algorithms to simulate the movement of water and sediments within the watershed.

Spatial and temporal datasets are the fundamental inputs for the SWAT model. Spatial datasets such as topography, land use, and soil maps are used to create the Hydrologic Response Unit (HRU), the smallest model component. The HRU is formed based on these spatial inputs, and it serves as the foundation for the model's water budget calculations. Additionally, the SWAT model requires climate time series data which includes precipitation, maximum/minimum temperature, relative humidity, solar radiation, and wind speed. These four essential data types (topography, land use, soil map, and climate) are mandatory for running the model. The physical processes considered in the SWAT model are illustrated in Figure 5.

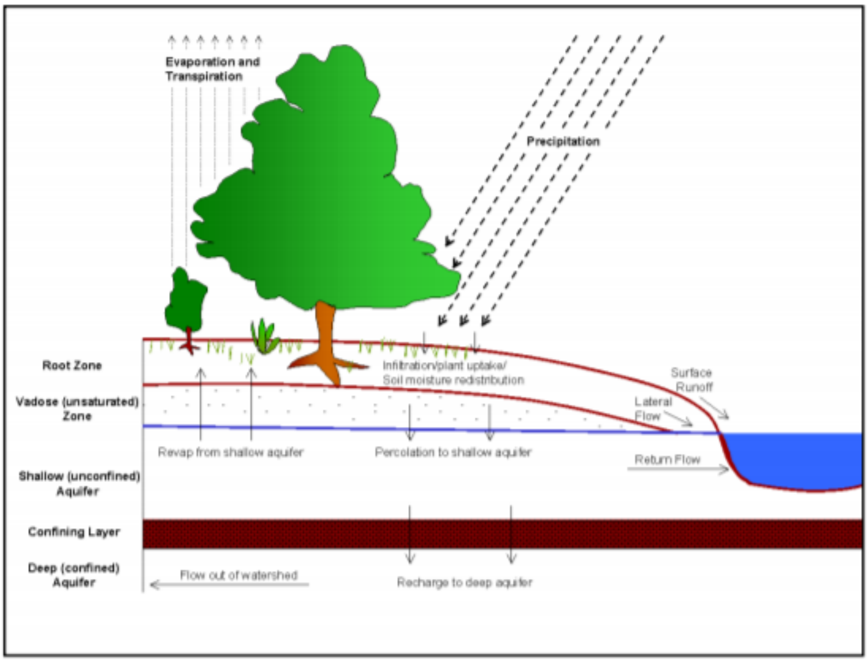

Figure 4 Physical processes considered in the SWAT model (Neitsch et al., 2011b).

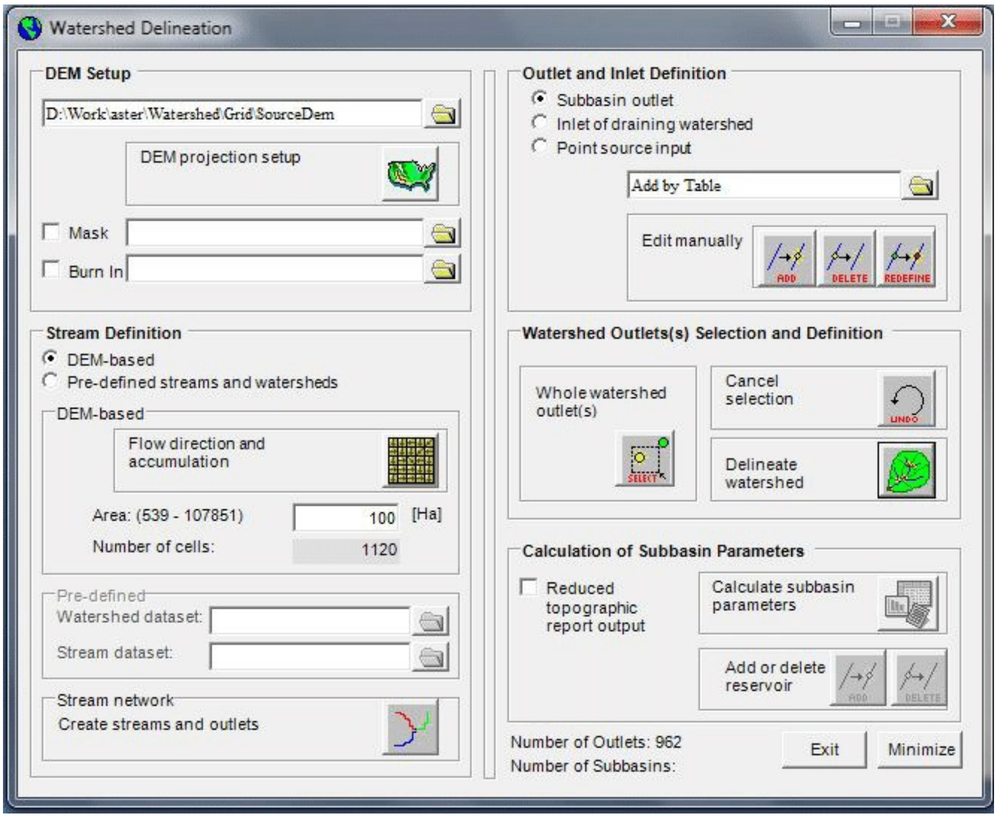

Figure 5 SWAT model (Merwade and Rajib, 2018).

The hydrological cycle in SWAT is based on the water balance given by Equation 1.

$$SW_t = SW_0 + \sum_{i=1}^{t}(R_{day} - Q_{surf} - E_a - w_{seep} - Q_{gw}) \quad (1)$$

Where SW_t is the final soil water content, SW_0 is the initial soil water content on day i (mm H_2O), t is the time in terms of days, R_{day} is the daily precipitation (mm), Q_{surf} is the amount of surface runoff on day i (mm H_2O), Ea is the amount of evapotranspiration on day i (mm H2O), w_{seep} is the amount of water entering the vadose zone from the soil profile on day i, and Q_{gw} is the amount of return flow on day i (mm H_2O). The subbasins allows the model to reflect differences in evapotranspiration for various crops and soils. The runoff is estimated individually for each HRU and is routed to obtain the total runoff for the basin, so it increases accuracy and gives a better physical definition of water balance.

One of the key strengths of SWAT is its ability to incorporate a wide range of data, allowing for a comprehensive representation of the hydrological system. Users can input historical climate data and, crucially, future climate scenarios to assess the potential impacts of climate change on streamflow. By running simulations under different climate scenarios, researchers can gain insights into how variations in temperature and precipitation patterns may influence streamflow dynamics.

3.2. Water Accounting Models - Water Evaluation and Planning System (WEAP)

Water allocation modeling component of the project is carried out by the WEAP software developed by the Stockholm Environment Institute (SEI). WEAP is a software tool that is commonly used in studies that are focused on integrated approaches to water resources planning problems. WEAP provides several built-in models for rainfall runoff and infiltration, evapotranspiration, crop requirements and yields, surface water/groundwater interaction and instream water quality on a monthly based time scale. It also serves to identify the variables and equations on relations between the elements of the basin or the processes involved. WEAP is linked to a GIS interface to build up the topology of the entire basin and the links between demand and supply nodes. The basin system is defined in terms of its supply sources (e.g., rivers, creeks, groundwater, reservoirs, and desalination plants); withdrawal, transmission, and wastewater treatment facilities; water demands; pollution generation; and ecosystem requirements (Figure 6). The modeling flowchart of a common WEAP Model is given in Figure 7.

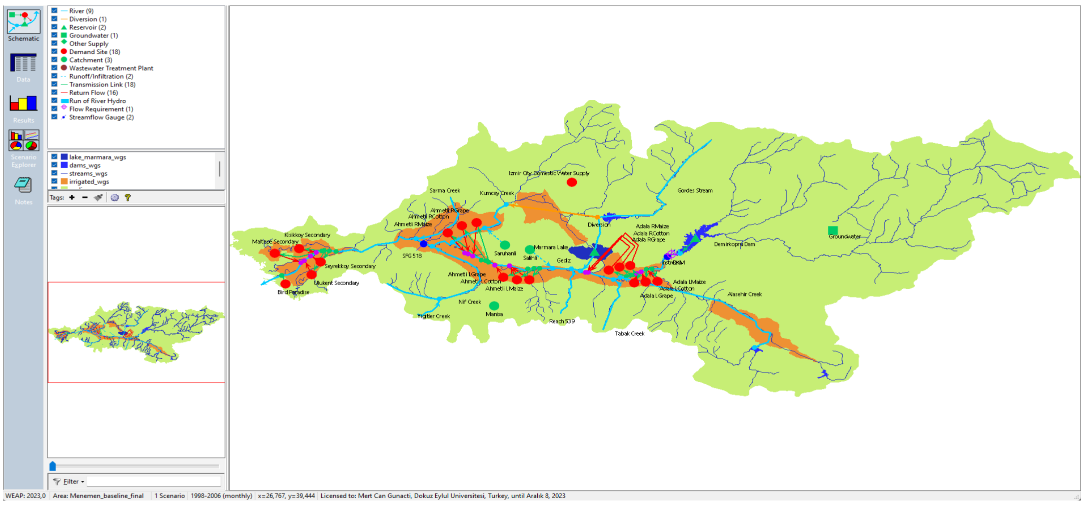

Figure 6 WEAP model.

This project is part of the PRIMA programme supported by the European Union.
GA n° [2041] [LENSES] [Call 2020 Section 1 Nexus IA]

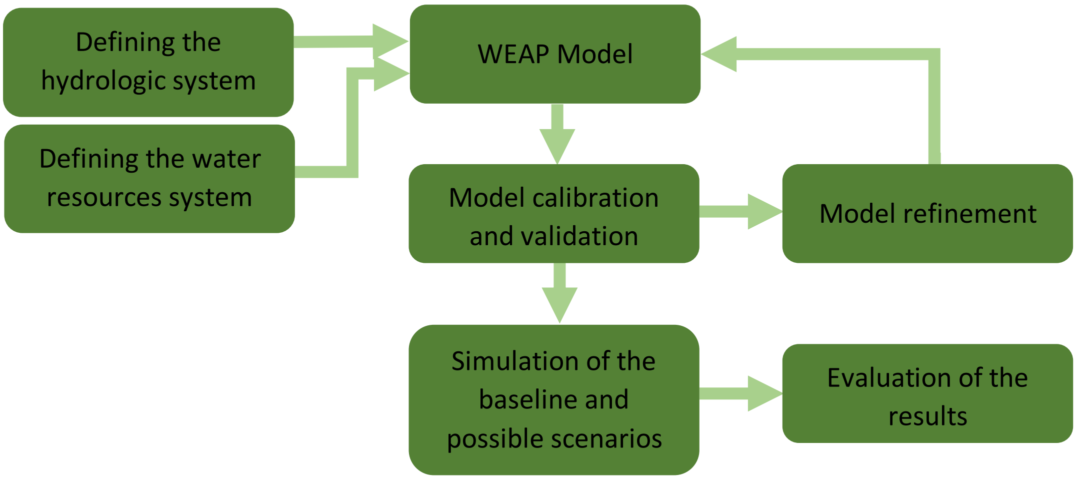

Figure 7 Modeling process of a common WEAP model.

Different allocation patterns lead to different responses by existing water demands. These patterns affect the whole system's Nexus indicators such as supply/demand ratios, reliability of the resource, socio-economic and environmental costs, and benefits. WEAP model relies on scenario analysis to evaluate the effects of policy changes. The scenarios generated in this project are based on climate change and implementation of Nature Based Solutions (NBS). Furthermore, some Nexus indicators are also calculated for each pilot area through the evaluation of WEAP model results obtained (Annex II). This deliverable will be covering results of the climate change scenarios specifically. Impacts of the NBS implementations will be examined on the Deliverable 5.4 "Guide for Ecosystem Services computational assessments."

3.3. Statistical Indicators

In hydrological modeling studies, statistical indicators are used to evaluate the model results. In D7.4., model outputs were analysed using R-Studio HYPERLINK "https://cran.r-project.org/web/packages/hydroGOF/index.html"package. The equations of the indicators are given in Table 1. For more information, please refer to the HydroGOF package. In these equations, S_i stands for simulation-model results, O_i for observation data, and N for the number of data. ME, MAE, MSE, D, MD, VE indicators take values in the range (0-1). These indicators achieve the best results at a value of 0. RMSE%, NRMSE%, indicators take values between (0-100). 0 value symbolizes the optimum result. The reference values of other indicators and their relationships with hydrological model performance are given in Table 2.2.

Table 1 Statistical Indicators for model performance.

Parameter	Description	Equation
ME	Mean Error	$ME = \frac{1}{N}\sum_{i=1}^{N}(S_i - O_i)$
MAE	Mean Absolute Error	$MAE = \frac{1}{N}\sum_{i=1}^{N}\lvert(S_i - O_i)\rvert$
MSE	Mean Squared Error	$ME = \frac{1}{N}\sum_{i=1}^{N}(S_i - O_i)^2$
RMSE	Root Mean Squared Error	$RMSE = \sqrt{\frac{1}{N}\sum_{i=1}^{N}(S_i - O_i)^2}$
NRMSE%	Normalized RMSE	$NRMSE\ \% = \frac{\sum_{i=1}^{N}(S_i - O_i)^2}{O_i^2}$
PBIAS%	Percent Bias	$PBIAS\ \% = \frac{\sum_{i=1}^{N}(S_i - O_i)^2}{\sum_{i=1}^{N} O_i}$
RSR	Ratio of Standard Deviations	(RSR) is calculated as the ratio of the RMSE and standard deviation of measured data.
Rsd	Relative Standard Deviation	RSD, used to determine if the standard deviation of a set of data is small or large when compared to the mean
NSE	Nash-Sutcliffe Efficiency	$NSE = \frac{\sum_{i=1}^{N}(S_i - O_i)^2}{\sum_{i=1}^{N}(O_i - \bar{O})^2}$
MNSE	Modified Nash-Sutcliffe Efficiency	$NSE = \frac{\sum_{i=1}^{N}\lvert(S_i - O_i)^2\rvert}{\sum_{i=1}^{N}\lvert(O_i - \bar{O})^2\rvert}$
D	Index of Agreement	$D = \frac{\sum_{i=1}^{N}(S_i - O_i)^2}{\sum_{i=1}^{N}(\lvert S_i - \bar{O}\rvert + \lvert O_i - \bar{O}\rvert)^2}$
MD	Modified Index of Agreement	$MD = 1 - \frac{\sum_{i=1}^{N}(S_i - O_i)^2}{\sum_{i=1}^{N}(\lvert S_i - \bar{O}\rvert + \lvert O_i - \bar{O}\rvert)}$
CP	Coefficient of Persistence	$CF = 1 - \frac{\sum_{i=2}^{N}(S_i - O_i)^2}{\sum_{i=1}^{N-1}(O_{i+1} - O_i)^2}$
R	Pearson Correlation Coefficient	$R = \frac{covariance\ (S,O)}{\sigma S * \sigma O}$
r^2	Coefficient of Determination	$R^2 = 1 - \frac{\sum_{i=2}^{N}(S_i - O_i)^2}{\sum_{i=1}^{N}(S_i - \bar{S})^2}$
Br^2	Modified Coefficient of Determination	br2=|b|R2,b<=1;br2= R^2/|b| ,b>1 (b=slope)
KGE	Kling-Gupta Efficiency	*KGE=1-ED* $ED = \sqrt{(s(1) * (r-1))^2 + (s(2) * (vr-1))^2 + (s(3) * (\beta - 1))^2}$ *r=Pearson product-moment correlation coefficient* *s=standardization factor* β *=inclination coefficient* *vr=variance*
VE	Volume Error	$VE = \frac{\sum_{i=1}^{N}\lvert(S_i - O_i)\rvert}{\sum_{i=1}^{N} O_i}$

Table 2 Relationship of indicators with hydrological model performance.

PBIAS%	NSE, MNSE, KGE	R2,BR2	Performance
0-10	0.75-1	0.85-1	Very Good
10-15	0.65-0.75	0.75-0.85	Good
15-25	0.5-0.65	0.65-0.75	Fair
25>	<0.5	<0.65	Poor

4. Data

Regarding meteorological data considered in hydrological modeling of the pilot area, it was considered to use observed values where meteorological observations are sufficient, and to apply the same meteorological database to ensure data consistency in areas where they are insufficient or missing. For this purpose, we used EMO-5 ("European Meteorological Observations", 5 km^2 spatial resolution), a European high-resolution, daily, multivariate meteorological dataset built on historical and real-time observations obtained by integrating data from 18 964 ground meteorological stations, four high-resolution regional observational grids (i.e. CombiPrecip, ZAMG - INCA, EURO4M-APGD and CarpatClim) and a global reanalysis (ERA-Interim/Land) (Figure 8) (Thiemig et al., 2022). EMO-5 provides daily resolution data including total precipitation, minimum and maximum temperatures, wind speed, solar radiation, and water vapor pressure.

This project is part of the PRIMA programme supported by the European Union.
GA n° [2041] [LENSES] [Call 2020 Section 1 Nexus IA]

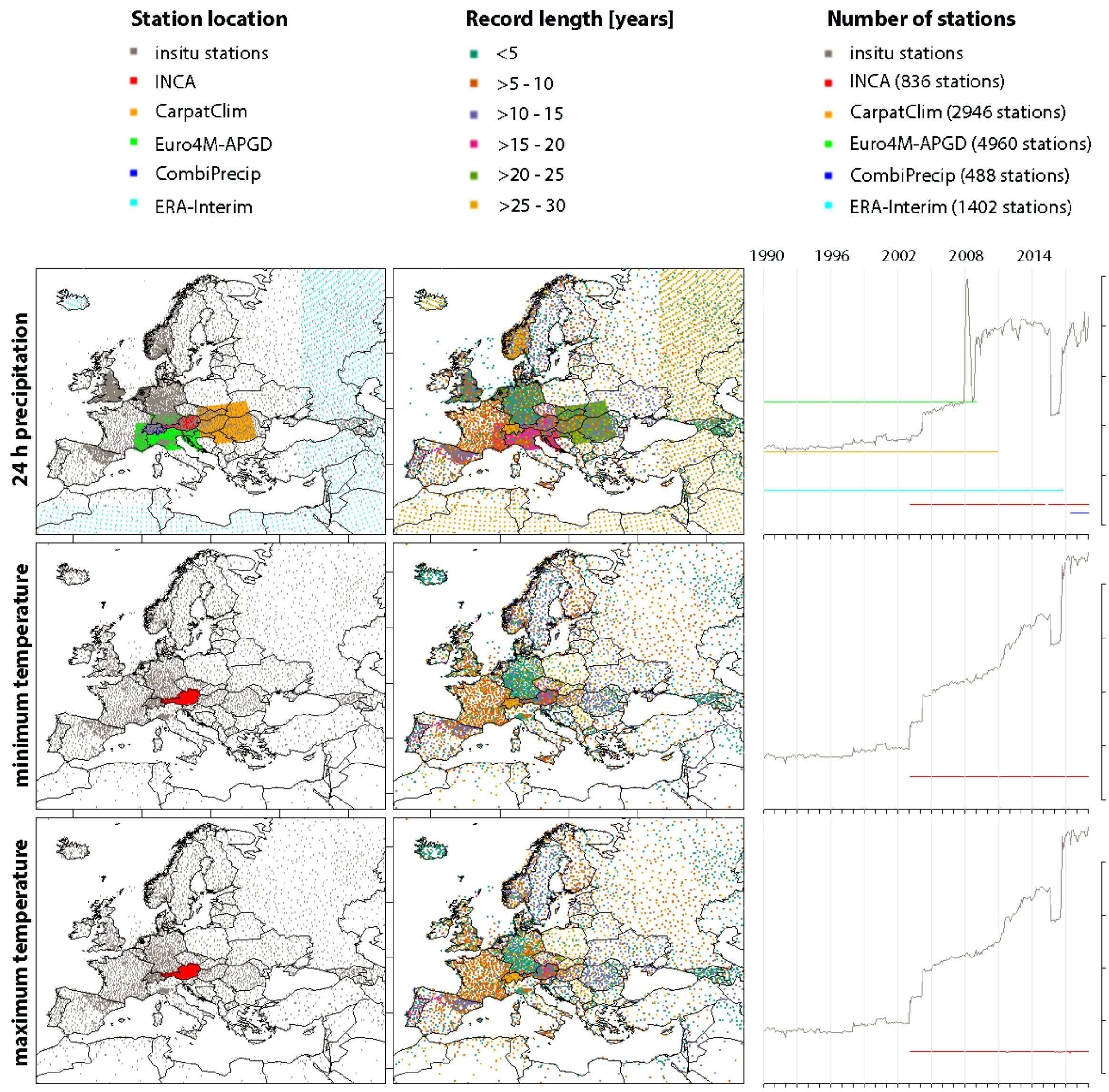

Figure 8 Data used for creation of daily EMO-5 precipitation and minimum and maximum temperature grids.

Climate change scenario data generated by DRAXIS under the Task 7.2 were used to monitor the impacts of climate change on streamflow in the pilot areas. These data cover 1971-2000 for the baseline period and 2011-2100 for the RCP 4.5 and RCP 8.5 scenarios.

5. LENSES Pilot Areas

5.1. Middle Jordan Valley (JO)

Jordan is located in the northwest of the Arabian Peninsula and covers an area of approximately 90,000 km^2 which are mostly semi-arid and arid regions. High population growth, socio-economic development and continuous deterioration of water quality cause water scarcity problems in the country. In Jordan, over 90%

of the territory experiences an annual rainfall of less than 200 mm. Water demand in the country is shared by irrigation (73%), municipalities (22 %) and industry (5 %). Notably, the overall water demand in the country nearly doubles the available water supply. (Al-Weshah, 2000; Al-Kharabsheh, 2000; Zagana et al., 2007; Dahamsheh and Aksoy, 2007).

Jordan is divided into four climatic zones: Ghor (Jordan Valley), the mountains (hilly region), the Badia region and the Gulf of Aqaba. Deir Alla, the area modelled under Task 7.4, is in the Ghor region. The area features a tropical climate characterized by scorching summers and mild winters, with an annual rainfall ranging from 150 to 250 mm. The altitude in this region varies between 200 and 416 m. The region spans 15 km in width to the north and 30 km in width to the south (Figure 9).

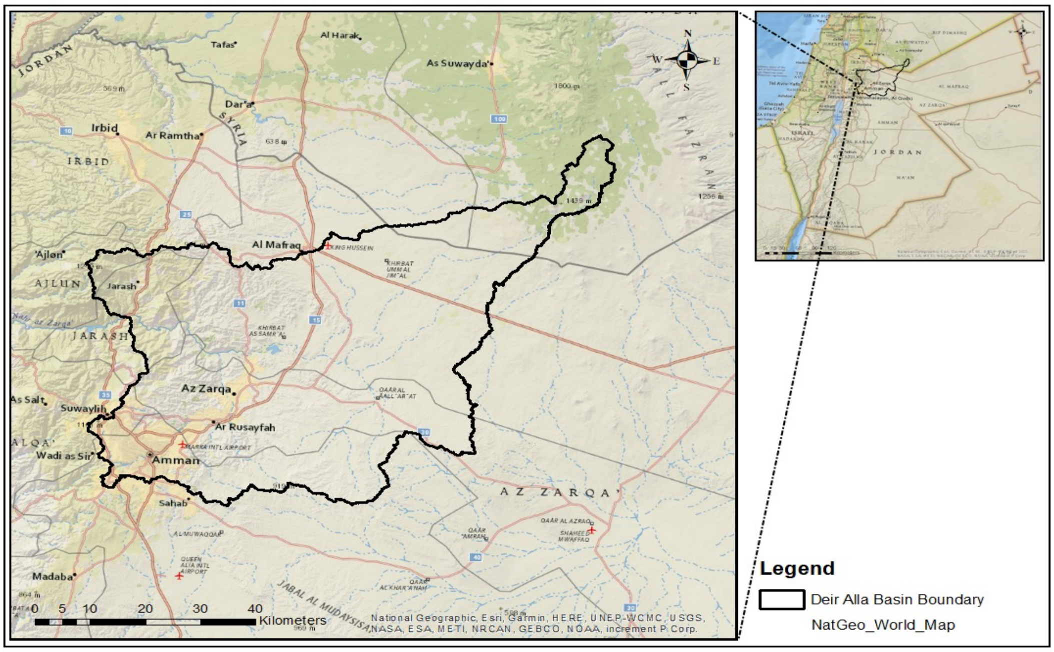

Figure 9 Jordan Case Study Area (Deir Alla).

Streamflow data input to the models employed has been acquired from the Deir Alla streamflow gauging station (SGS) which has daily flow observations between 1998 and 2017. EMO-5 dataset, provided in grid format at 5 km resolution, has been utilized for precipitation and temperature data input. Other parameters in the model were derived based on the HEC-HMS user manual and previous studies in the study area (HEC-USACE, 2008; Rawls et al., 1982). Local data concerning the water allocation such as cultivated crop types, total irrigated land area, other sectoral demand points and their water demand have been obtained from the Jordanian partner NARC in the development of the WEAP model.

5.2. Gediz Basin & Delta (TR)

Located in the western part of Turkey, the Gediz Basin is bounded by the Bakırcay Basin from the north and the Kucuk Menderes and Büyük Menderes Basins from the south. The region is located at the outlet of the Gediz River along the Aegean Sea coast and has a surface area of 149 km^2. The Gediz Delta is a Ramsar wetland of international importance. The part of the region between Emiralem Strait and the sea is called Menemen Plain, the pilot area in Türkiye (Figure 10). This plain, has a Mediterranean climate; summers are hot and dry, and winters are mild and rainy. The mean annual temperature is around 16-17°C, while the annual precipitation ranges from 600 to 610 mm. Beyond agriculture and farming, there is a well-established industrial sector in the region (Cetinkaya & Gunacti, 2018; Gül et al., 2018).

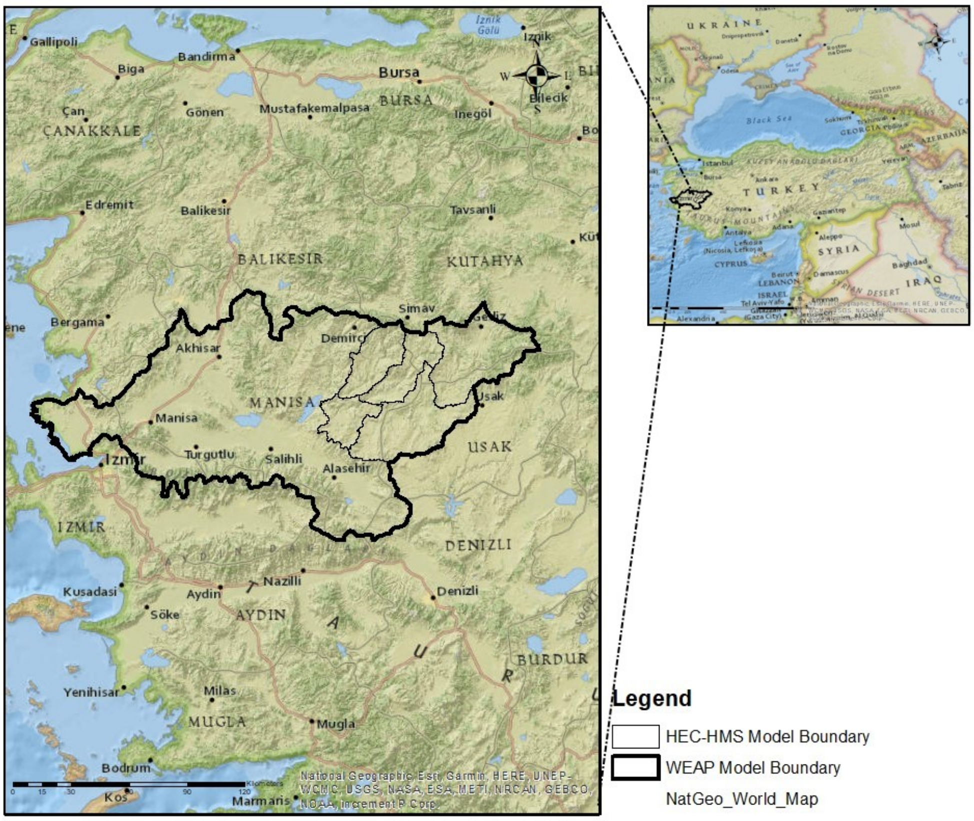

Figure 10 Gediz Case Study Area (Menderes).

The daily streamflow records used in hydrologic modeling were obtained from the General Directorate of State Hydraulic Works (DSI). Data from three distinct stations—Selendi Stream-Derekoy station no. 514, Deliinis Stream-Topuzdamları station no. 515, and Gediz River-Acısu station no. 523—within the study area were employed. Station-based precipitation and temperature data were obtained from Turkish State Meteorological Service.

Comprehensive data on sector-specific water demands, operational regulations, and constraints within the Gediz River Basin system were acquired from the Turkish pilot leader UTAEM, and previous studies that contributed to the development of the WEAP model.

5.3. Guadalquvir Basin, Doñana National Park Area (ES)

Doñana Ramsar site in Spain is fed by numerous river tributaries, with the Guadimar River being the largest among them. The total catchment area of Guadimar is 1879 km^2. Three SGSs were constructed to measure the flow values of the Guadimar tributary. Among these Gerena, Guijo and Aznalcazar stations, Gerena station, which has long-term complete data, was used in Task 7.4. Guijo station which is affected by the releases from Agrio Dam and Aznalcazar station which is affected by stagnant downstream water conditions has not been preferred in modeling studies (Gallart et al., 1999) (Figure 11).

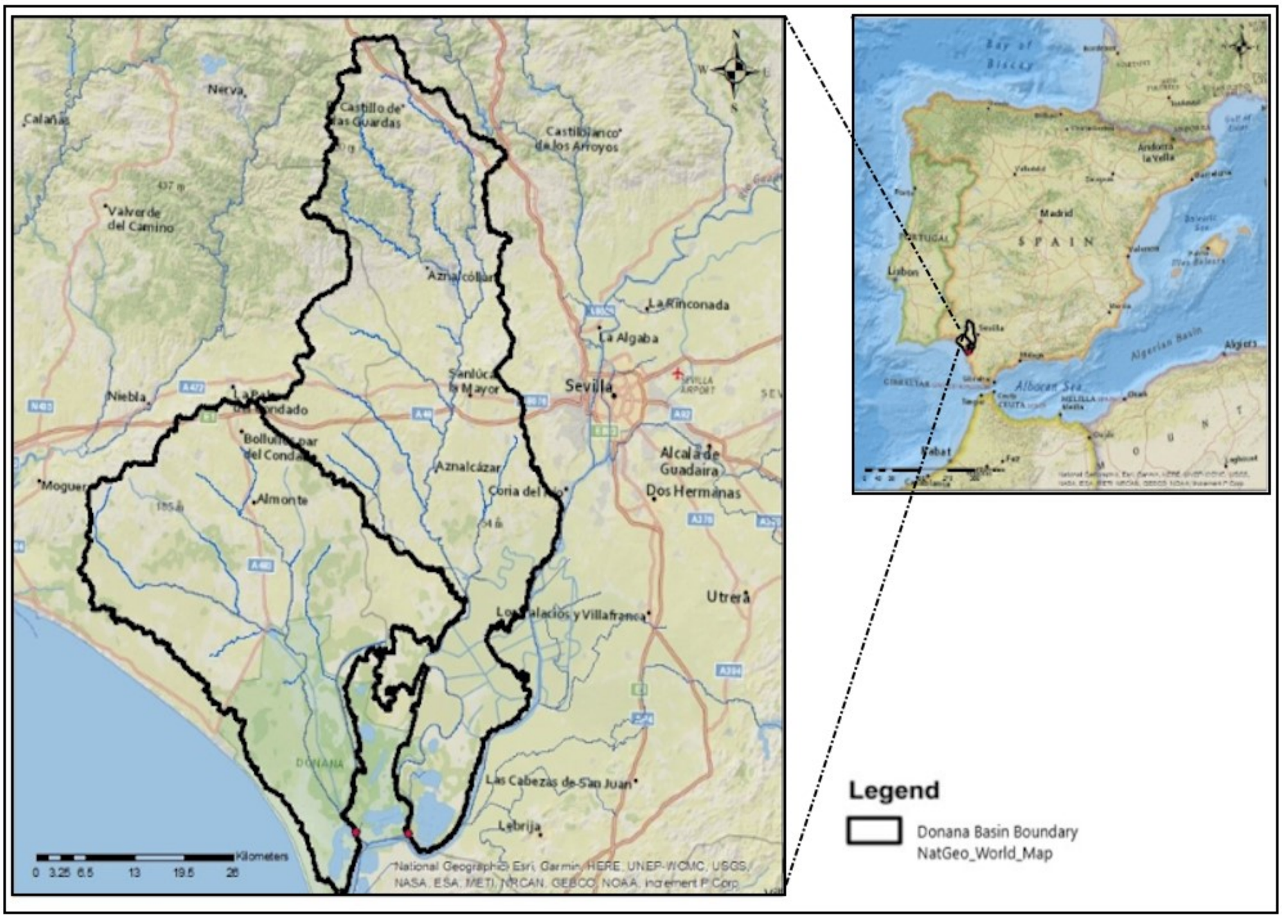

Figure 11 Doñana Case Study Area.

Another tributary in the region is the Guadalquivir River that spills to the Atlantic Ocean through the Gulf of Cadiz. On this tributary, El Partido, El Rocio and Partido Nuevo stations were used for Task 7.4. The basin is characterized by a Mediterranean climate, featuring an average annual precipitation of approximately 550-600 mm and has an average annual temperature range of 16-17 °C, as reported by Trick and Custodio in 2004. Streamflow data, integral to the study, has been procured from The Centre for Studies and Experimentation of Public Works OA and MP (CEDEX) database. Sectorial water demand data and the topological network system specific to the case study were acquired with the collaboration of the Spanish pilot leader ECOADAPTA during the developmental phase of the WEAP model.

5.4. International Long-Term Ecological Research Network Sites (Pinios - GR)

The Pinios River Basin is situated in central Greece, covering an area of approximately 11,000 km^2 and ranking as the second largest fully developed basin in Greece. The region experiences a combination of continental and Mediterranean climatic conditions, characterized by dry and hot summers and winter rainfall. The average annual rainfall in the basin is estimated to be 700 mm (Arampatzis et al., 2018). Renowned as one of Greece's most intensively cultivated and productive agricultural areas, agricultural activities encompass around 45% of the total basin area. A significant portion of the basin's water, nearly 94%, is allocated for irrigation purposes (Stephenson, 2003). However, since the 1980s, the escalating demand for water in irrigation, coupled with imprudent water management practices, has resulted in the over-exploitation of groundwater resources. Presently, over 65% of the total water consumption is sourced from groundwater, underscoring its pivotal role in ensuring the region's sustainability (Pisinaras et al., 2023). In the context of LENSES project, two sub-basins were considered, namely the Pinios River Deltaic plain and Agia sub-basins which are shown in Figure 12. Irrigation constitutes the major water consumer for both sub-basins. For the case of Pinios River deltaic plain, irrigation needs are satisfied by both groundwater and surface water, while for Agia irrigation needs are almost exclusively covered by groundwater.

Sectorial water demand data, topologic network system of the case study has been acquired from the Pinios pilot leader SWRI in the development of the WEAP model.

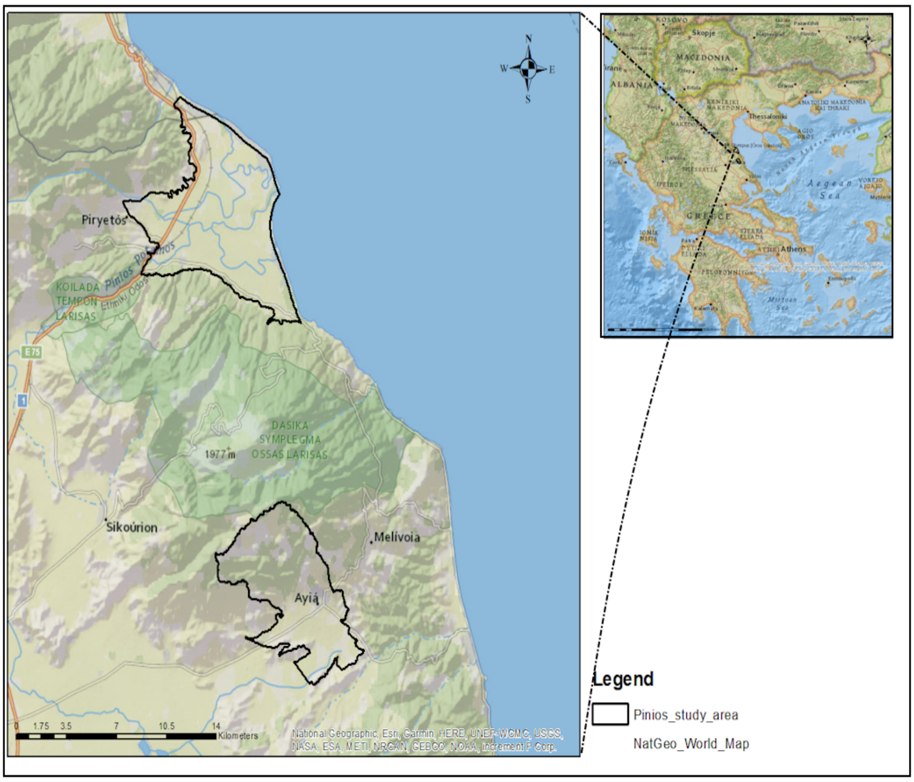

Figure 12 Pinios Case Study Areas.

5.5. International Long-Term Ecological Research Network Sites (Koiliaris and Keritis -GR)

The Koiliaris River Basin is located 15 km east of the city of Chania in Crete and the total watershed area is 130 km^2 and the main supply of water originates in the White Mountains. Over the past 15 years, up until today, the Koiliaris River watershed has undergone comprehensive investigation. The study area consists of karst systems that exhibit a unique characteristic: a spring can receive contributions from karst formations extending beyond the confines of the watershed to which the spring belongs. Alternatively, the spring can also be fed by karst systems stacked on top of each other, each with distinct hydraulic properties and transmissivities. This trait emphasizes the importance of identifying the extended karstic area that contributes to a spring's discharge. This identification is crucial for accurately assessing the hydrological and geochemical balances within the system. The karst system is characterized by rapid infiltration and direct connection to underlying conduits. Within this system, two primary groups of springs exist: the Stilos springs, located at an elevation of +17 meters above mean sea level (a.m.s.l.), and the intermittent spring known as Anavreti, situated at an elevation of +24 meters a.m.s.l. Both springs ultimately contribute to the flow of the Koiliaris River. The collective recharge area for these springs extends beyond the boundaries of the Koiliaris River Basin, stretching south-eastward from the watershed boundary. The geological composition of the region, combined with a significant fault running in a northeast–southwest direction, guides water movement towards the springs within the Koiliaris River Basin.

Geologically, the area features consist of 71.8% Plattenkalk which is comprised mainly by dolomites, marbles, limestone and re-crystallized limestone with cherts 9.5% calcaric marls in Neogene formations; 6.1% marls in Neogene formations 6.1% schists and 6.4% quaternary alluvial deposits. Land use includes cropland and pasture (35%), olive and orange groves (32.1%), shrub and brush (32.3%) and mixed forest (0.6%). The total length of the river is 36 km. Koiliaris is joined by four tributaries, two of which are temporary rivers (Keramianos and Anavreti), and two are permanent ones. The basin contains three telemetric hydrometric stations and three telemetric meteorological stations. Additionally, two hydrometric stations are situated outside the basin, one within the extended karstic area. Data at each station is recorded every 5 minutes.

The Keritis River Basin is one of the two main drainage basins in the Chania region. It is located in the north-central part of the Chania region, 12 kilometers west of the city. It is situated between the geographic coordinates of 35°15' - 35°32' north latitude and 23°45' - 23°55' east longitude. The hydrological basin covers an area of 210 km2, with an average elevation of 734 meters, and falls within the authority of the Platanias Municipality.

The hydrographic network begins in the southern and higher part of the basin (approximately 2000 meters), the White Mountains, and flows north of the village of Platanias. This basin is one of the most important hydrological basins in the region due to its abundant water resources. Numerous boreholes and wells serving the water supply and irrigation purposes of the wider area are in this drainage basin. The geological formations of the Keritis-Therisou basin exhibit different hydrogeological and hydraulic behaviours due to their lithological and tectonic characteristics, thereby determining the hydrological regime of the study area. The study area is characterized by the presence of two main deep hydrogeological systems and one secondary surface system. The deeper system is represented by permeable carbonate formations and is located in the southeastern part of the drainage basin. Underground springs mainly originate from the southwestern sector, where the carbonate formations of the White Mountains recharge primarily from the carbonates of the area. In the northern part, the carbonate rock formation is interrupted by a northeast-southwest fault, which leads to the formation of karst springs in the Agia region. The second major hydrogeological system is an impermeable system of marls and clay deposits, extending in the central part of the drainage basin. The rich hydrographic network in this area prevents rainfall from infiltrating the soil. This results in intense surface runoff and, consequently, the formation of numerous streams that feed the main flow of the Keritis River. The sources of Meskla are fed by carbonates and surface runoff from the marl of the Keritis, which is located southwest of the village of Meskla. The secondary hydrogeological system consists of quaternary deposits, extending north of the marls in the central part of the Keritis drainage basin. It is fed by surface runoff from the marls as well as by underground lateral flows to the east of the basin. The study area is shown in Figure 13.

Sectorial water demand data, topologic network system of the case study has been acquired from the Koiliaris pilot leader TUC in the development of the WEAP model.

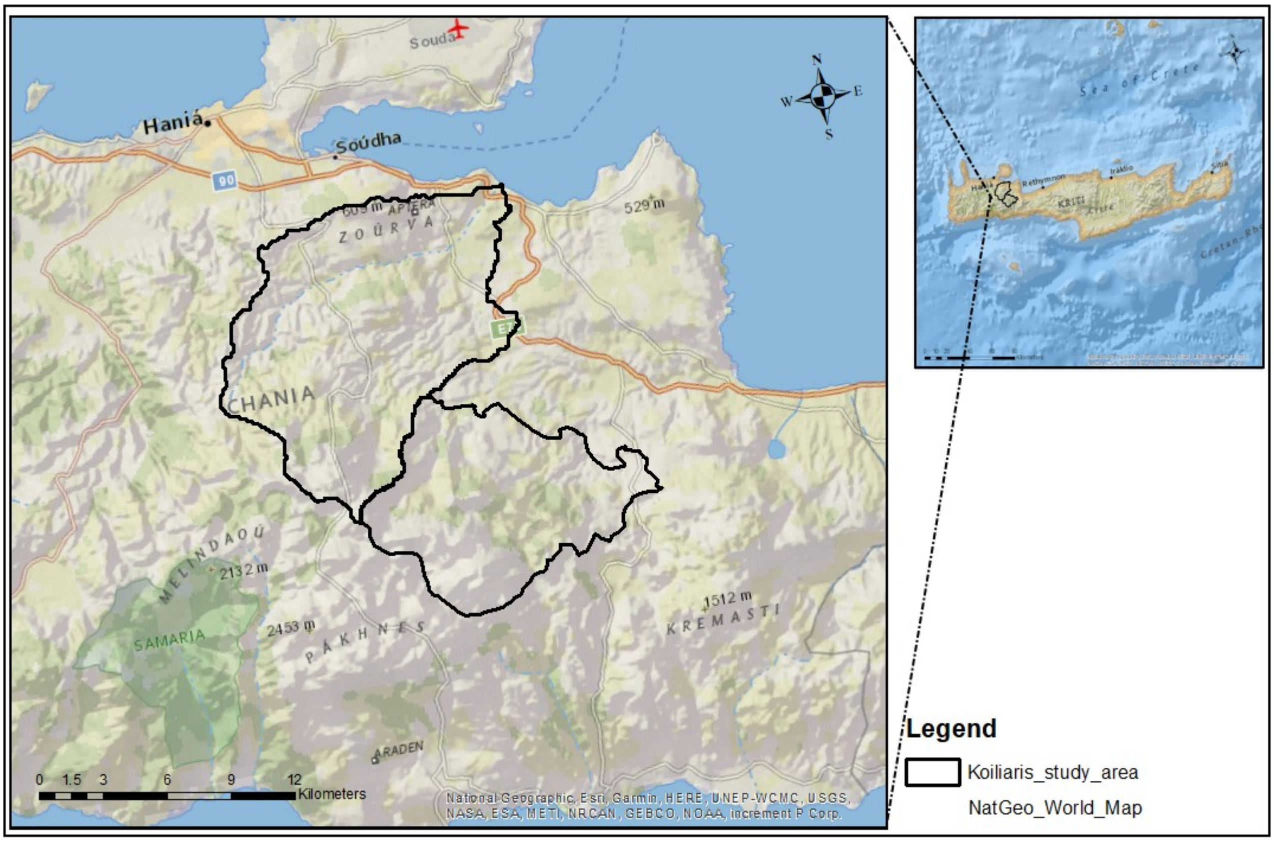

Figure 13 Koiliaris Case Study Area.

5.6. Tarquinia Plain (IT)

The Tarquinia plain spans an expansive 27,000 hectares in the region of Lazio, located approximately 90 km north of Rome in central Italy with the settlements including Lido di Tarquinia, Voltone, and Marina Velca. The predominant economic activities in Tarquinia and its surroundings revolve around tourism and agriculture, contributing to its designation as a UNESCO World Heritage site since 2004.

The area is characterized by a flat topography in a 1039.53 km^2 drainage area, making it an intensive agricultural zone, with 67% of the land dedicated to agricultural production. Notably, 85% of this pilot area has been identified as a nitrate-sensitive area. Around 45% of the agricultural land is subjected to irrigation, with 2,195 hectares of land actually irrigated in 2014. The spatial extent of the study area is depicted in Figure 14. Observed meteorological data were obtained from Tarquinian Hydrological Survey (ARSIAL), and discharge data were obtained from Regione Lazio - Agenzia Regionale Di Protezione Civile (Figure 14).

Sectorial water demand data, topologic network system of the case study has been acquired from the Italian pilot leader CREA in the development of the WEAP model.

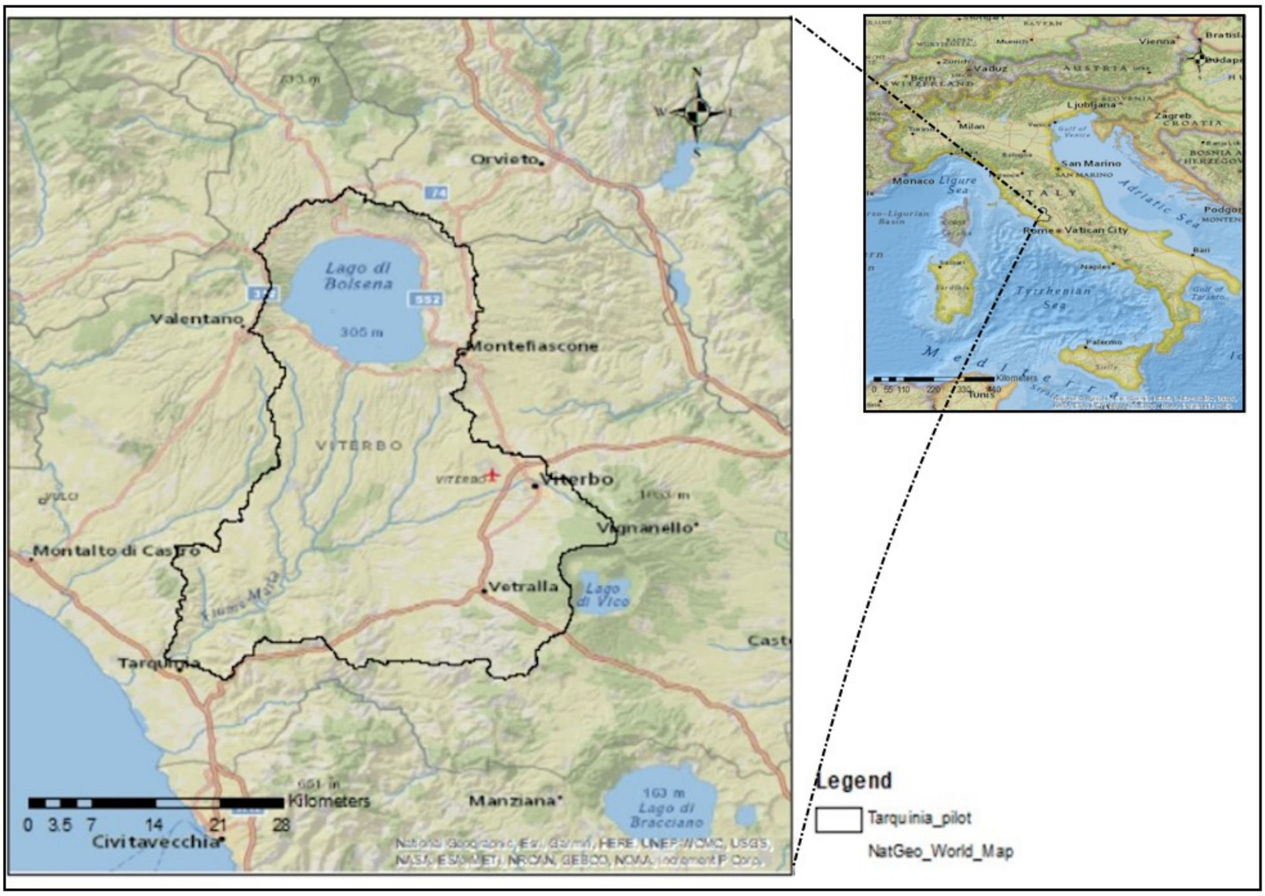

Figure 14 Tarquinia Case Study.

6. Results

6.1. Hydrological Modeling

6.1.1. Middle Jordan Valley (JO)

Within the scope of the study, the HEC-HMS model for the Deir Alla region was developed (Figure 15), and the periods of 1998-2007 and 2008-2017 periods are selected for calibration and validation respectively. For modeling purposes in the region, a sole streamflow station was employed. The parameters required for hydrological modeling have been fine-tuned to optimize their applicability to the region. The results of the monthly calibration and validation processes are given in Figure 16 and 17, respectively.

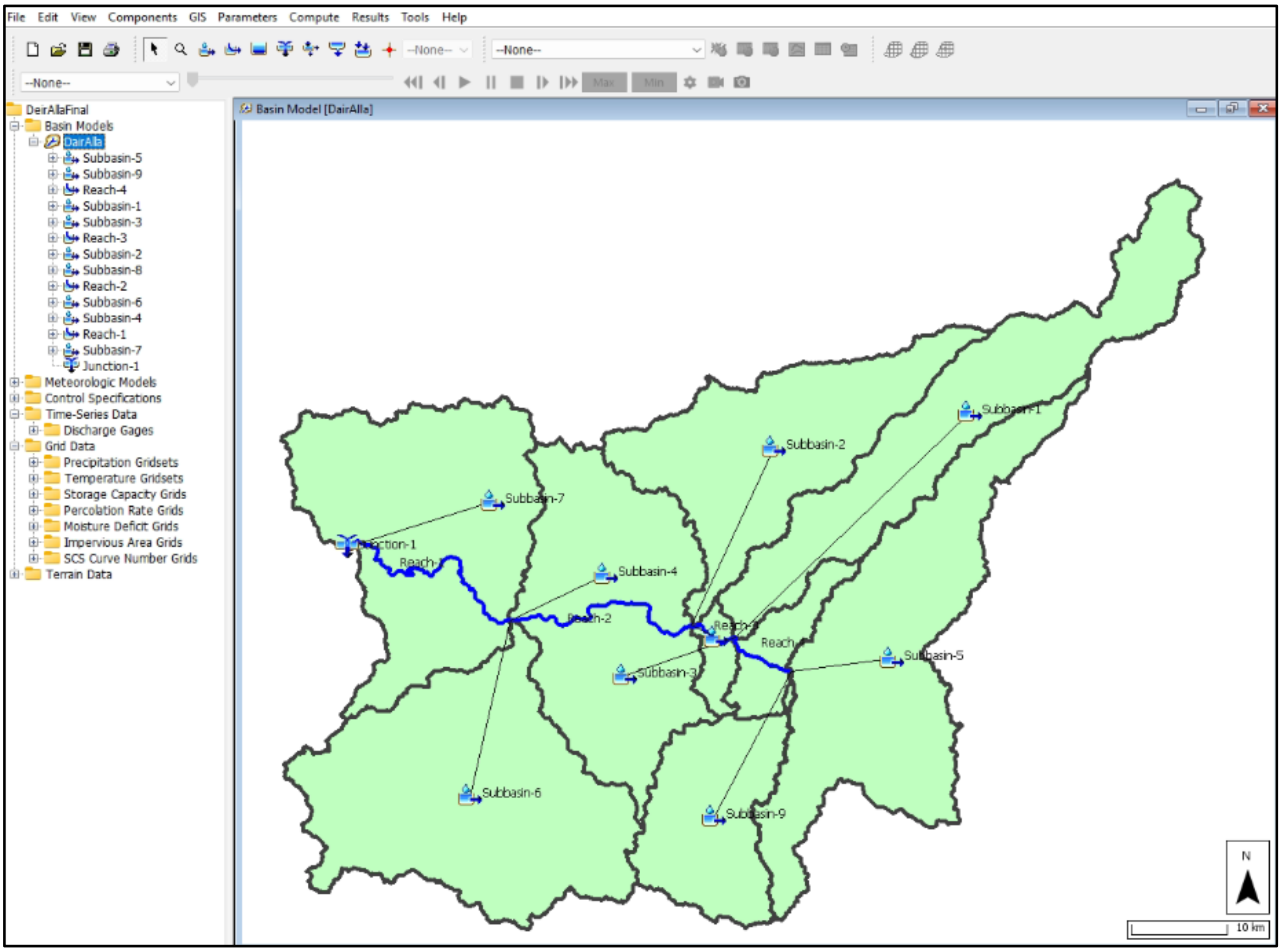

Figure 15 HEC-HMS schematic diagram for Jordan study area.

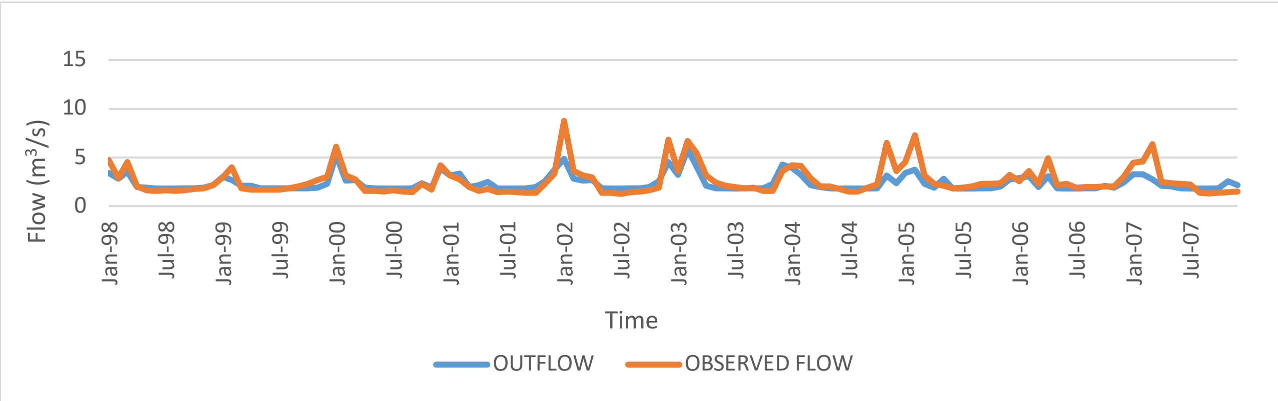

Figure 16 Deir Alla Calibration Period Result.

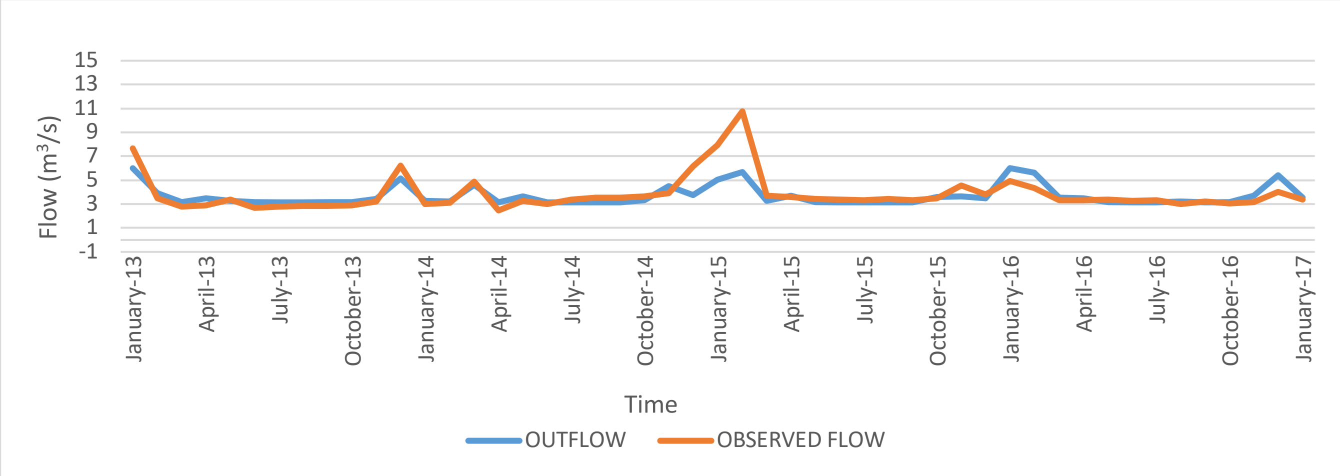

Figure 17 Deir Alla Validation Period Result.

The graphs derived from the model outputs demonstrate significant patterns. Following this, a thorough statistical analysis was conducted to delve into and interpret the obtained model results. This analytical process aimed to assess the reliability and robustness of the model outcomes, providing a comprehensive understanding of their significance and implications in the context of the study (Table 3).

Table 3 Statistical indicators for Deir Alla Hydrological Modeling Results.

Calibration				**Validation**			
ME	-0.24	MNSE	0.47	ME	-0.15	MNSE	0.38
MAE	0.55	D	0.84	MAE	0.59	D	0.78
MSE	0.77	MD	0.68	MSE	1.09	MD	0.64
RMSE	0.88	CP	0	RMSE	1.05	CP	0.58
NRMSE%	61.50	R	0.86	NRMSE%	68.80	R	0.75
PBIAS%	-9.20	r^2	0.73	PBIAS%	-4.00	r^2	0.57
RSR	0.61	Br^2	0.59	RSR	0.69	Br^2	0.50
Rsd	0.56	KGE	0.53	Rsd	0.56	KGE	0.49
NSE	0.62	VE	0.79	NSE	0.52	VE	0.85

This study conducts a comprehensive hydrological modeling analysis, assessing the overall effectiveness of the developed model in conjunction with findings from both calibration and validation phases (Table 3). The obtained values verifies that the model outputs adequately fit the observed hydrological data and the NSE and KGE values indicate that the model successfully captures the hydrological processes. The results obtained in the validation phase also emphasize the stable performance of the model. These results show that the model can be used as a reliable tool for predicting future hydrological events.

This project is part of the PRIMA programme supported by the European Union.
GA n° [2041] [LENSES] [Call 2020 Section 1 Nexus IA]

6.1.2. Gediz Basin & Delta (TR)

In Gediz pilot, the HEC-HMS modeling was performed in three subbasins (Figure 18) which are the main tributaries contributing to the inflows to Demirköprü Reservoir that is the main governing water resource for irrigation activities along the downstream basin. Table 4 summarizes the calibration and validation periods determined for each subbasin.

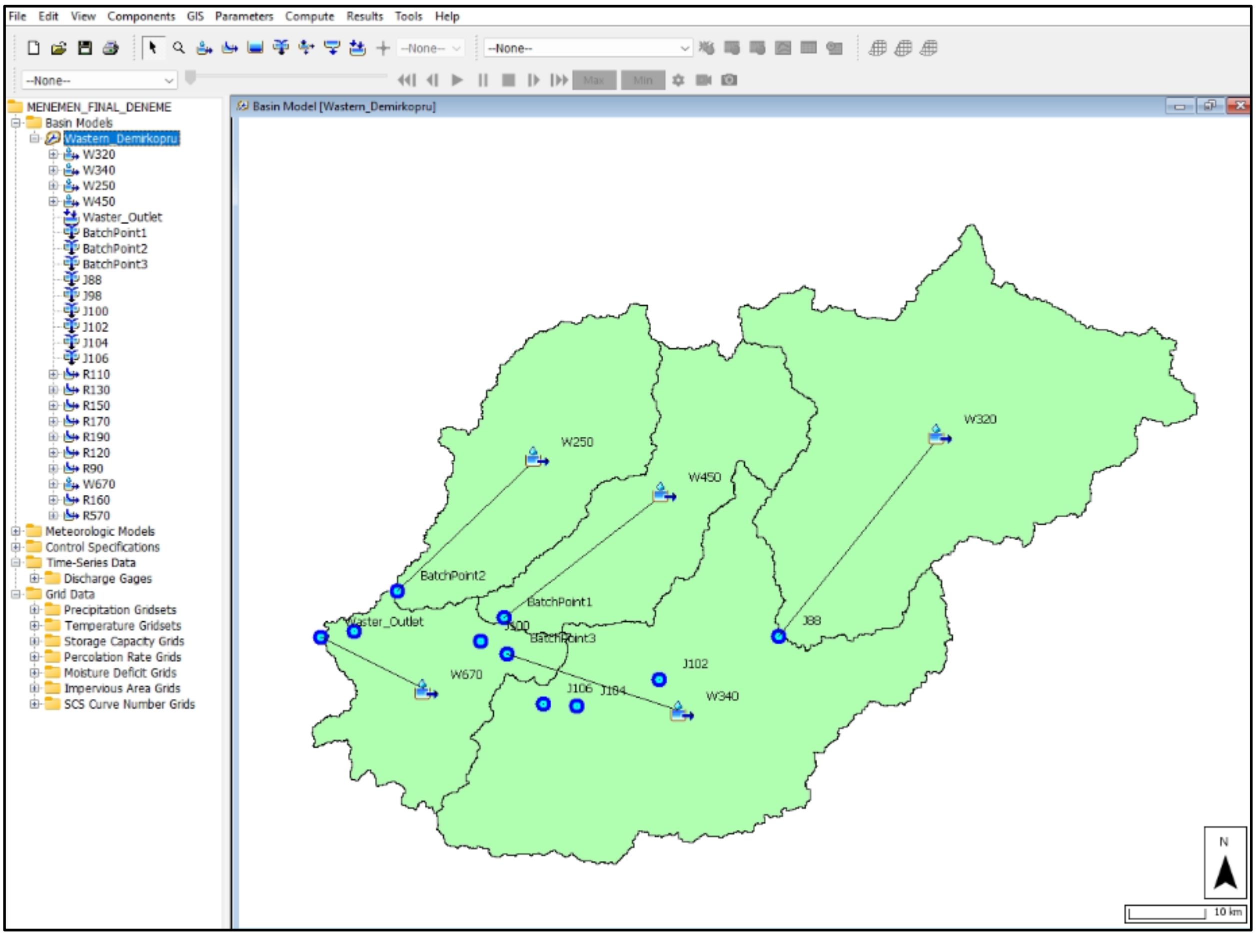

Figure 18 HEC-HMS schematic diagram for Gediz Case Study.

Table 4 Gediz Case Study Discharge Stations and their calibration and validation periods.

Discharge Gages	Meteorological Gages	Calibration Time	Validation Time
514	17748	01JAN1998-31DEC2006	01JAN2007-31SEP2015
515	17746	01JAN1998-31DEC2002	01JAN2003-31DEC2006
523	17750	01JAN1998-31DEC2005	01JAN2006-31SEP2012

This project is part of the PRIMA programme supported by the European Union.
GA n° [2041] [LENSES] [Call 2020 Section 1 Nexus IA]

Figure 19 and Figure 20 summarize the results for calibration and validation processes for station number 514, as in Table 5 the statistical indicators are given.

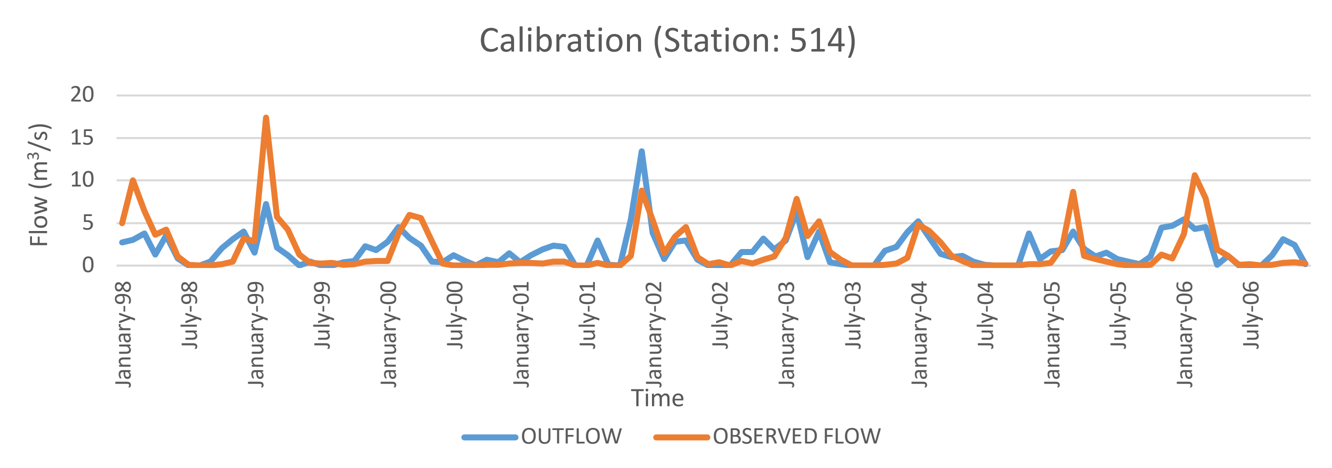

Figure 19 Station 514 Calibration Period Result.

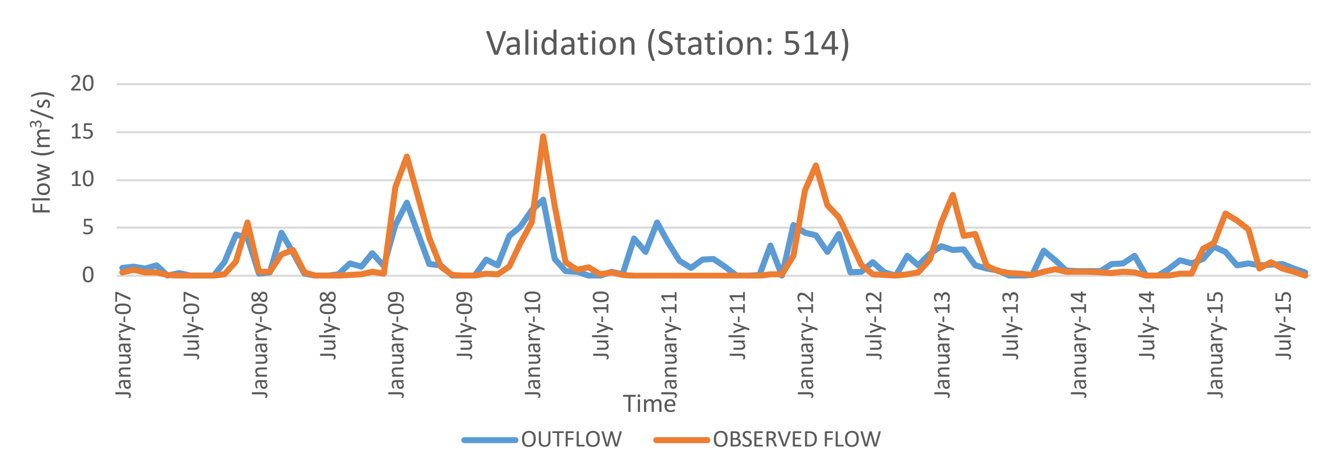

Figure 20 Station 514 Validation Period Result.

Table 5 Statistical indicators at Station 514 for Hydrological Modeling Results.

Calibration				Validation			
ME	-0.02	MNSE	0.34	ME	-0.14	MNSE	0.35
MAE	1.38	D	0.79	MAE	1.43	D	0.77
MSE	4.50	MD	0.62	MSE	4.85	MD	0.60
RMSE	2.12	CP	0.44	RMSE	2.20	CP	0.08
NRMSE%	73.40	R	0.68	NRMSE%	73.00	R	0.69
PBIAS%	-1.00	r^2	0.46	PBIAS%	-8.10	r^2	0.47
RSR	0.73	Br^2	0.28	RSR	0.73	Br^2	0.26
rSD	0.70	KGE	0.56	Rsd	0.59	KGE	0.48
NSE	0.46	VE	0.25	NSE	0.46	VE	0.19

According to Table 5, the NSE value calculated for the calibration phase at station 514 was 0.46 and the KGE value was 0.56. In the validation phase, the NSE value was 0.46 and the KGE value was 0.48. These results show that the model effectively simulates the hydrological processes at the station.

Figure 21 and Figure 22 show the results of calibration and validation processes for station number 515.

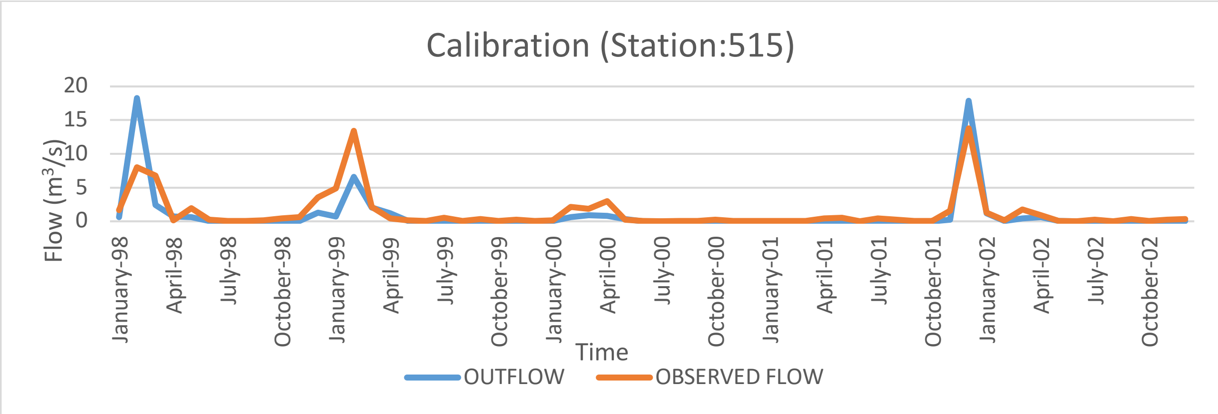

Figure 21 Station 515 Calibration Period Result.

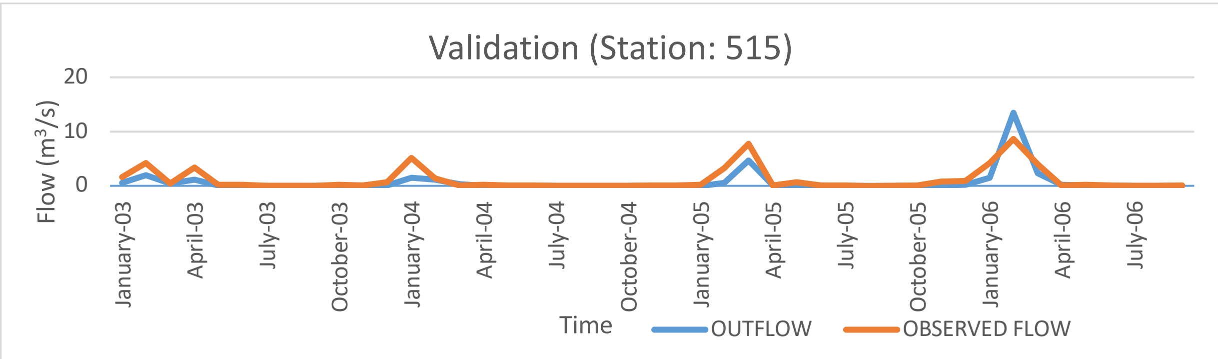

Figure 22 Station 515 Validation Period Result.

Table 6 indicates statistical indicators of calibration and validation of the model for the station 515.

Table 6 Statistical indicators at Station 515 for Hydrological Modeling Results.

Calibration				Validation			
ME	-0.30	MNSE	0.49	ME	-0.41	MNSE	0.56
MAE	0.83	D	0.89	MAE	0.64	D	0.89
MSE	3.77	MD	0.75	MSE	1.72	MD	0.76
RMSE	1.94	CP	0.95	RMSE	1.31	CP	0.68
NRMSE%	69.60	R	0.82	NRMSE%	63.30	R	0.82
PBIAS%	-23.90	r^2	0.67	PBIAS%	-37.60	r^2	0.67
RSR	0.70	Br^2	0.63	RSR	0.63	Br^2	0.54
rSD	0.511.20	KGE	0.64	Rsd	1.03	KGE	0.58
NSE	0.51	VE	0.35	NSE	0.59	VE	0.40

In Table 6, the calibration results obtained for station 515 are NSE value 0.51 and KGE value 0.64. In the validation phase, the NSE value was 0.59 and the KGE value was 0.58. These results show that the model performs reliably at this station as well.

Figure 23 and Figure 24 show the results of calibration and validation processes for station number 523.

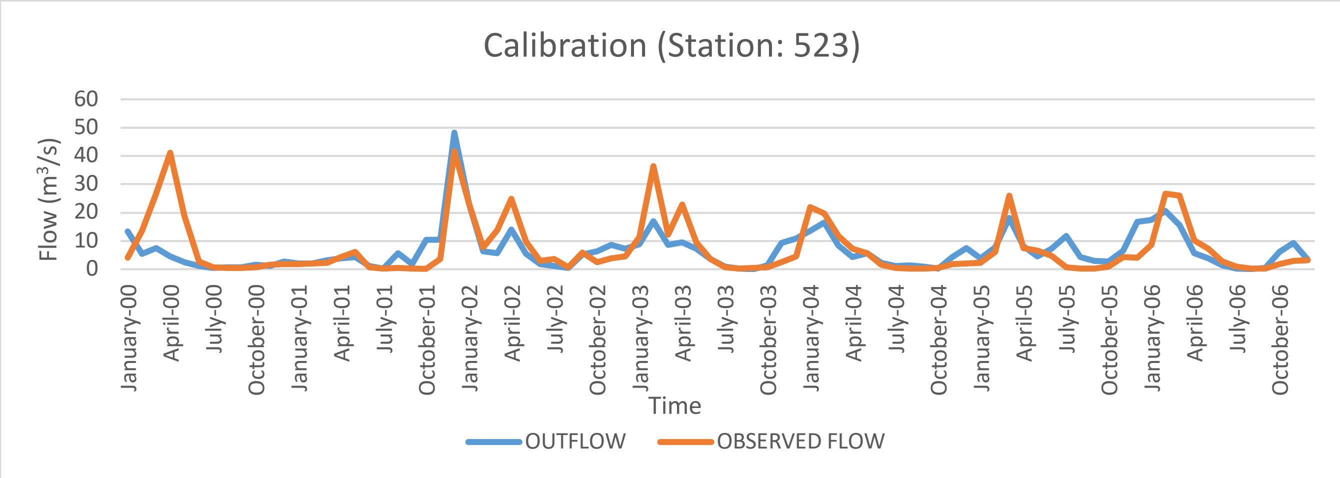

Figure 23 Station 523 Calibration Period Result.

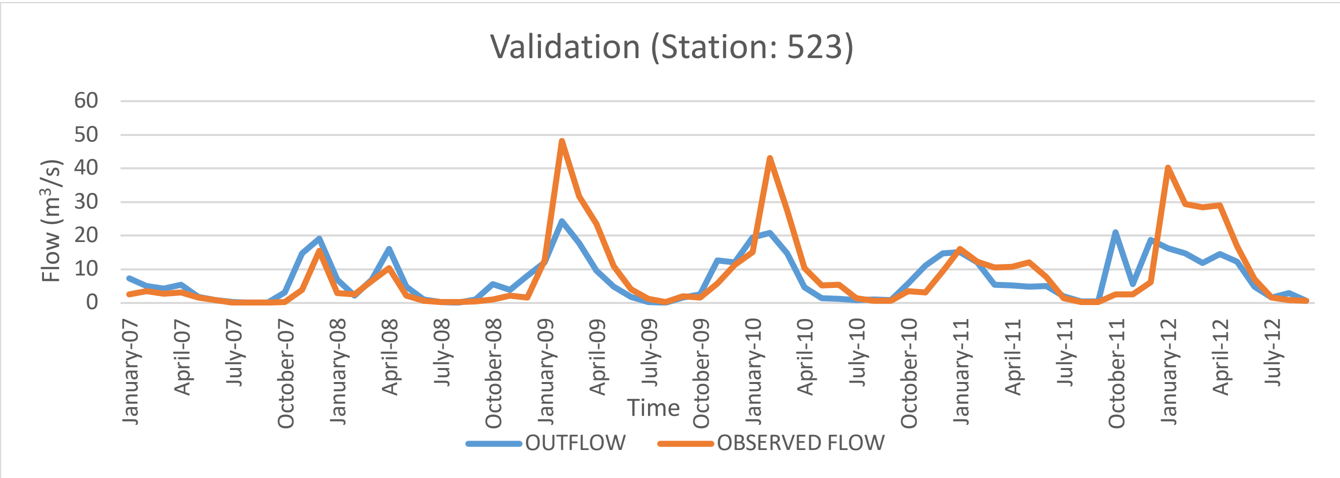

Figure 24 Station 523 Validation Period Result.

Statistical indicators of calibration and validation of the model for station number 523 were presented in Table 7.

Table 7 Statistical indicators at Station 523 for Hydrological Modeling Results.

Calibration				Validation			
ME	-0.82	MNSE	0.41	ME	-1.31	MNSE	0.41
MAE	4.18	D	0.80	MAE	4.80	D	0.79
MSE	49.15	MD	0.65	MSE	59.70	MD	0.66
RMSE	7.01	CP	0.44	RMSE	7.73	CP	0.26
NRMSE%	72.30	R	0.69	NRMSE%	69.40	R	0.74
PBIAS%	-11.20	r^2	0.48	PBIAS%	7.73	r^2	0.55
RSR	0.72	Br^2	0.31	RSR	0.69	Br^2	0.32
rSD	0.73	KGE	0.57	Rsd	0.59	KGE	0.49
NSE	0.47	VE	0.42	NSE	0.51	VE	0.43

According to the results of station 523 in Table 7, the NSE value computed for the calibration phase is 0.47 and the KGE value is 0.57. In the validation phase, the NSE value is 0.51 and the KGE value is 0.49. These results show that the model performs satisfactorily at this station, as well. In addition, when the calibration and validation graphs are analysed, it is seen that the observation records and model outputs fit well.

In general, the results obtained for these three stations in the Gediz Basin show that the developed hydrological models have worked successfully in both calibration and validation phases and are reliable tools for predicting future hydrological events.

6.1.3. Guadalquivir Basin, Doñana National Park Area (ES)

For the Doñana case study in Spain, two separate models were created (Figure 25 a-b). The graphs of the three stations used for the first tributary, namely Guadalquivir, are given in Figure 26-28. Since the observed streamflow data set for the stations in the Doñana region was not available for a sufficiently long period, the calibration was carried out on the full dataset. Studies on this subject show that calibrating the entire dataset is the most suitable approach, yielding robust parameter sets, optimizing model accuracy during an independent test period, and obviating the need for the modeler to make assumptions (Arsenault et al., 2018).

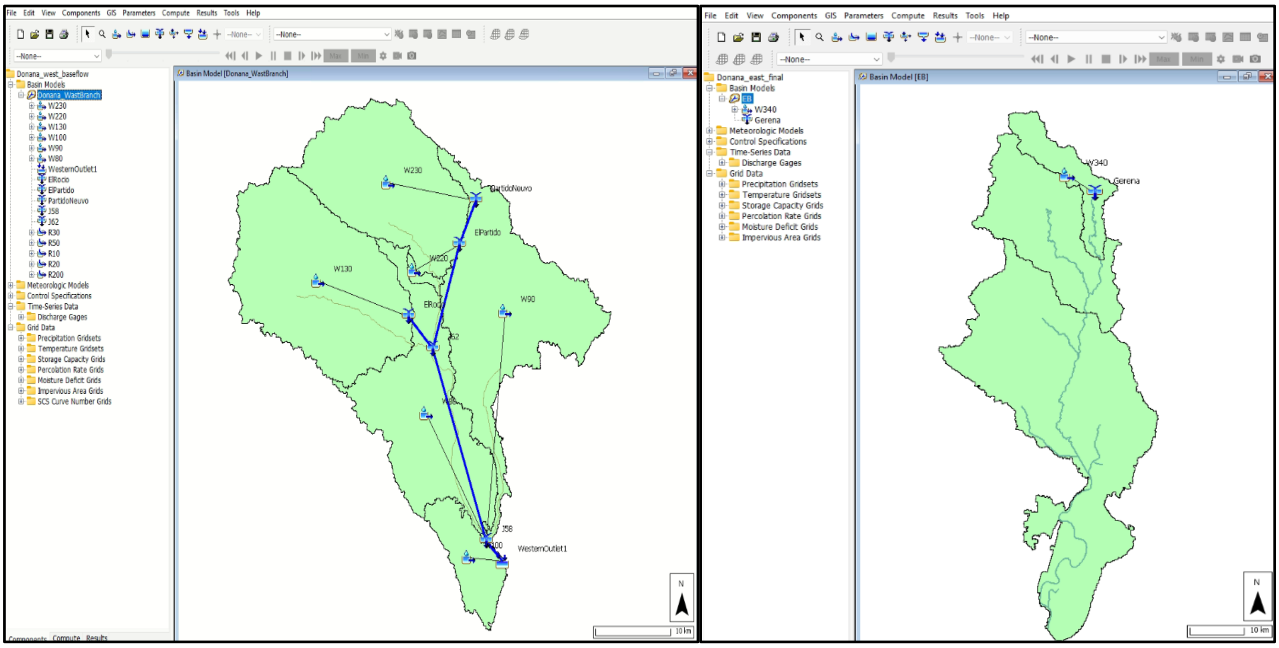

Figure 25 HEC-HMS schematic diagram for Doñana case study (a. Guadalquivar, b.Guadimar).

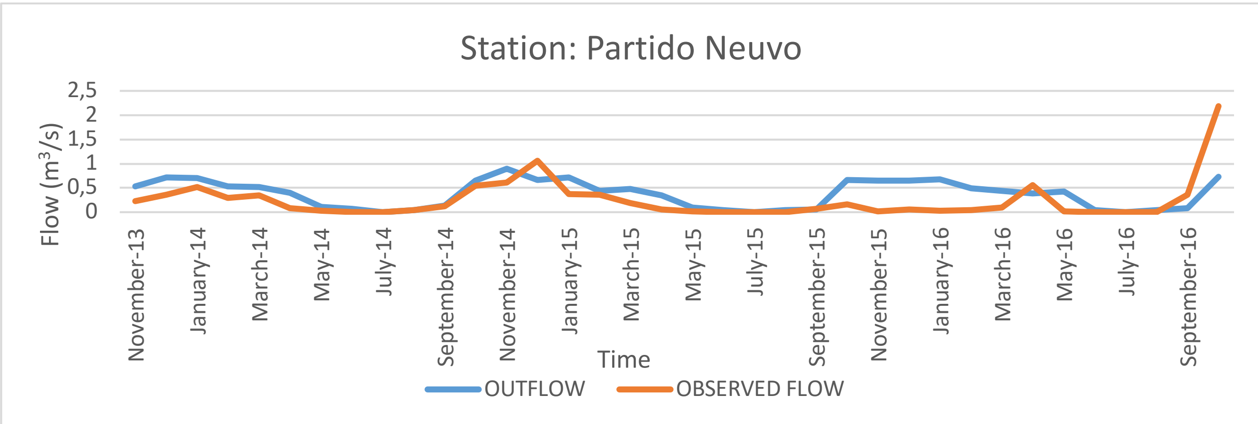

Figure 26 Partido Nuevo Result.

Statistical results of the models are presented in Table 9-10.

Table 8 Statistical indicators at Partido Nuevo for Hydrological Modeling Results.

Results			
ME	0.13	MNSE	0.01
MAE	0.26	D	0.67
MSE	0.14	MD	0.52
RMSE	0.38	CP	0.01
NRMSE%	92.00	R	0.51
PBIAS%	52.10	r^2	0.26
RSR	0.92	Br^2	0.17
rSD	0.69	KGE	0.22
NSE	0.13	VE	-0.04

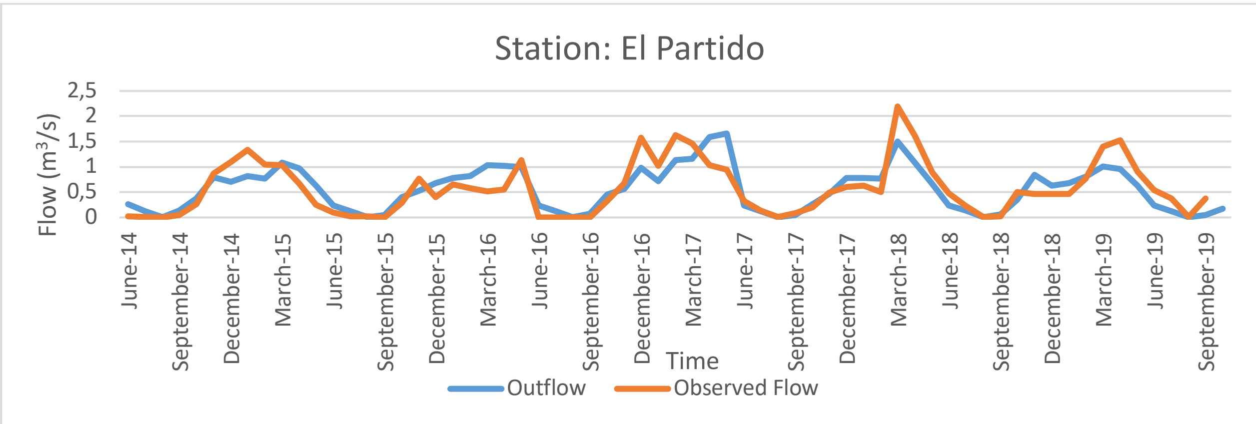

Figure 27 El Partido Calibration Period Result.

Table 9 Statistical indicators at El Partido for Hydrological Modeling Results.

Results			
ME	-0.02	MNSE	0.45
MAE	0.23	D	0.90
MSE	0.08	MD	0.71
RMSE	0.29	CP	0.52
NRMSE%	56.00	R	0.83
PBIAS%	-2.90	r^2	0.68
RSR	0.56	Br^2	0.57
rSD	0.83	KGE	0.75
NSE	0.68	VE	0.61

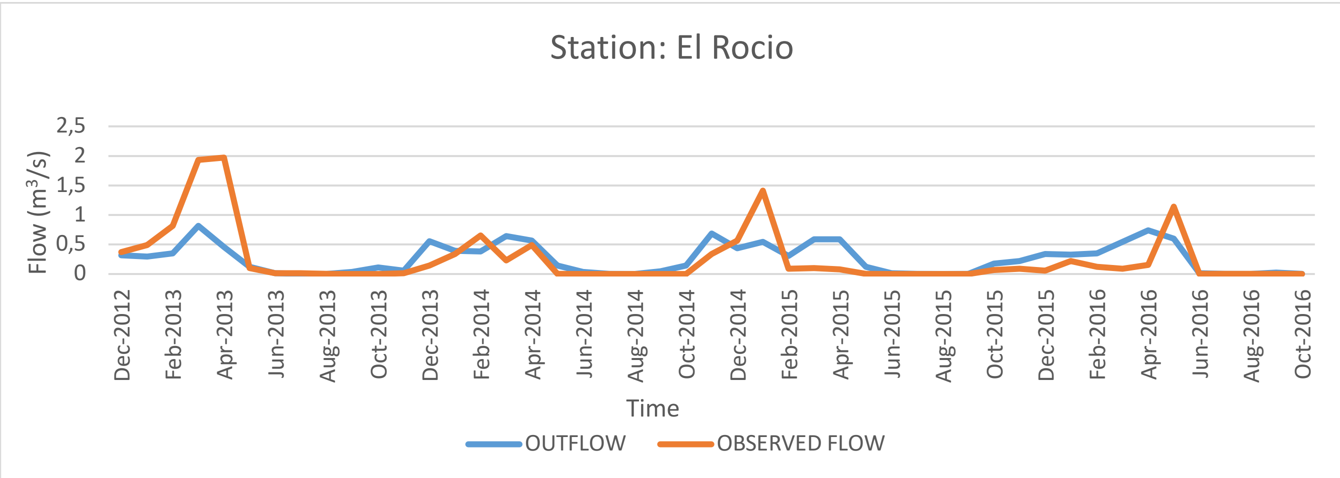

Figure 28 El Partido Calibration Period Result.

Table 10 Statistical indicators at El Rocio for Hydrological Modeling Results.

Results			
ME	0.00	MNSE	0.30
MAE	0.22	D	0.67
MSE	0.14	MD	0.59
RMSE	0.38	CP	0.36
NRMSE%	80.10	R	0.59
PBIAS%	-0.10	r^2	0.35
RSR	0.80	Br^2	0.16
rSD	0.53	KGE	0.37
NSE	0.34	VE	0.15

The second branch, the Guadimar branch, was modelled based on a single station. While Figure 29 indicates the calibration results, Table 11 shows statistical indicators of observed and calibrated streamflow for Guadimar branch.

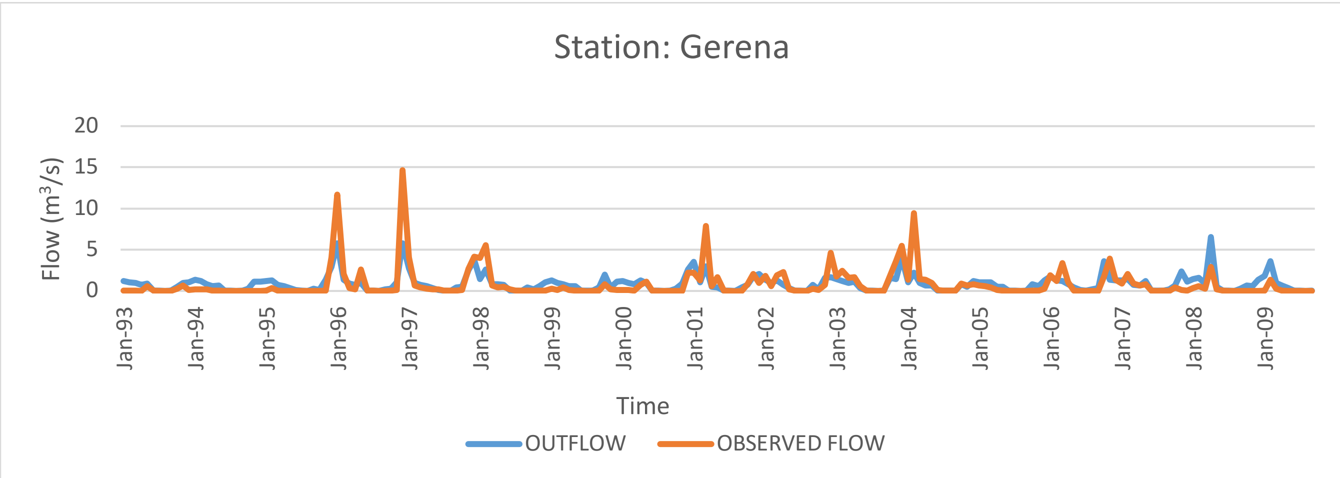

Figure 29 Gerena Calibration Period Result.

Table 11 Statistical indicators at Gerena for Hydrological Modeling Results.

Results			
ME	0.04	MNSE	0.38
MAE	0.64	D	0.78
MSE	1.59	MD	0.62
RMSE	1.26	CP	0.65
NRMSE%	68.80	R	0.75
PBIAS%	4.80	r^2	0.56
RSR	0.69	Br^2	0.29
rSD	0.56	KGE	0.49
NSE	0.52	VE	0.22

The hydrological modeling study for the Doñana region of Spain was performed at four different water stations. The modeling results of each station were evaluated using various performance metrics.

For the Partido Nuevo station, the NSE value was 0.13 and the KGE value was 0.22. These results indicate that the model simulates hydrological processes with limited success.

At El Partido station, the NSE value was 0.68 and the KGE value was 0.75. These results indicate that the model captures the hydrological variables in this region successfully.

In the results obtained for El Rocio station, the NSE value was 0.52 and the KGE value was 0.49. It is seen that the model performs satisfactorily in this tributary region as well.

Finally, for the Gerena station, the NSE value is 0.52 and the KGE value is 0.49. These results show that the model in the Guadimar branch performs well in general.

These results for each station show that the model can effectively simulate hydrological processes in specific regions. The obtained NSE and KGE values provide vital information to comprehensively evaluate the performance of the model.

This project is part of the PRIMA programme supported by the European Union.
GA n° [2041] [LENSES] [Call 2020 Section 1 Nexus IA]

6.1.4. International Long-Term Ecological Research Network Sites (Pinios-GR)

Hydrological modeling was applied for the two watersheds of Pinios River basin that constitute the LENSES project pilot areas namely, Agia (Figure 30) and Pinios River Deltaic plain (PRDP, Figure 31) watersheds. The hydrological models' application aims to simulate the relevant processes and the impact of water resources management on water budget, focusing on groundwater recharge, since water provision in both watersheds, especially for agriculture, is highly dependent on groundwater. The Soil & Water Assessment Tool (SWAT) model was applied for both watersheds. Regarding PDP, the model developed in the study of Pisinaras et al. (2021) was used. SWAT model was selected because:

a. it can simulate actual crop growth and subsequently crop water needs by incorporating the local-specific cultivation practices,
b. the land phase of the hydrologic cycle is simulated by incorporating all the related components and therefore groundwater recharge from the vadose zone can be calculated and
c. it incorporates the estimation of capillary rise from the shallow aquifers to the soil profile for which there is strong evidence that it constitutes a significant component of the PRDP phreatic aquifer budget (Pisinaras et al., 2021).

PRDP was divided into 20 sub-watersheds which include in total 384 hydrologic response units (HRUs). As mentioned above, SWAT model was also applied for the Agia watershed, which was divided into 15 sub-basins and furthermore into 563 HRUs. It must be mentioned that Agia watershed is the pilot watershed in which the Pinios Hydrologic Observatory (Pisinaras et al., 2018) has been established since 2016 and therefore the existing data and infrastructure was used for the SWAT model application. Regarding soil data, a hybrid map was compiled which combined soil analysis data collected from 100 points in the plain part of Agia watershed and soil properties from the European Soil Database (ESDB) (Panagos, 2006) and provided by the European Soil Data Centre (ESDAC) (Panagos et al., 2012) for the remaining part of the watershed. Concerning land use, a hybrid approach was implemented, as resulted from the combination of CORINE2018 land cover data and crop spatial distribution data provided by the Hellenic Payment and Control Agency for Guidance and Guarantee Community Aid. Even though the crop spatial distribution provides spatial data on the agricultural field level, the degree of detail in crop type did not allow to distinguish between the diverse types of orchards. Therefore, all the orchards included in the watershed were assumed to be apple trees, which is the dominant crop of the watershed. Climate data constitutes one of the major inputs of SWAT model and therefore, data from the 3 meteorological stations were used (Figure 30). Regarding irrigation practices and aiming to approach the applied irrigation practices more realistically, irrigation water amounts as recorded with telemetric water meters from 4 pilot orchards were used for the cultivation periods of year 2021 and 2022. According to this data, the average irrigation amount of 665 mm per cultivation period was calculated, which according to the irrigation practices applied in the watershed it was distributed to weekly irrigation events between mid-May and late September when the model was applied for the references (1971-2000) and projected period (2011-2100).

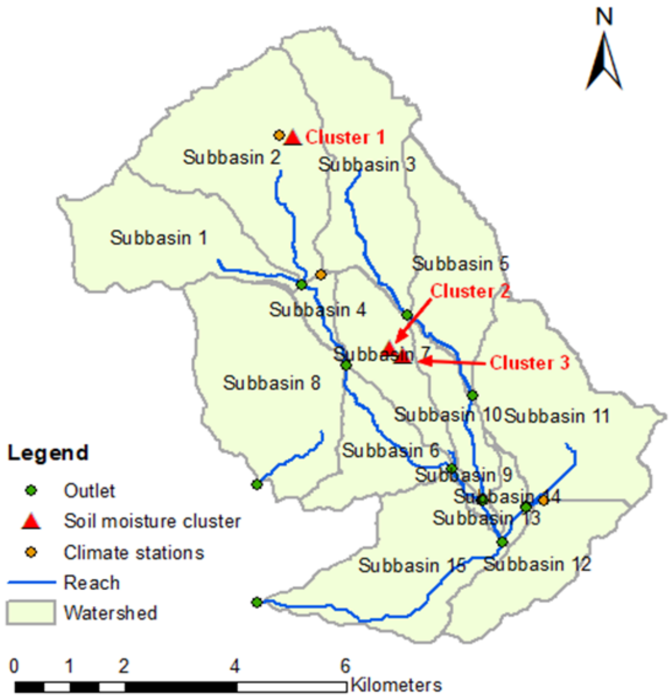

Figure 30 Location map of Agia watershed including the sub-basins, as modelled with SWAT model. The soil moisture cluster that provided data for calibration and validation of the model and the climate station used are also presented.

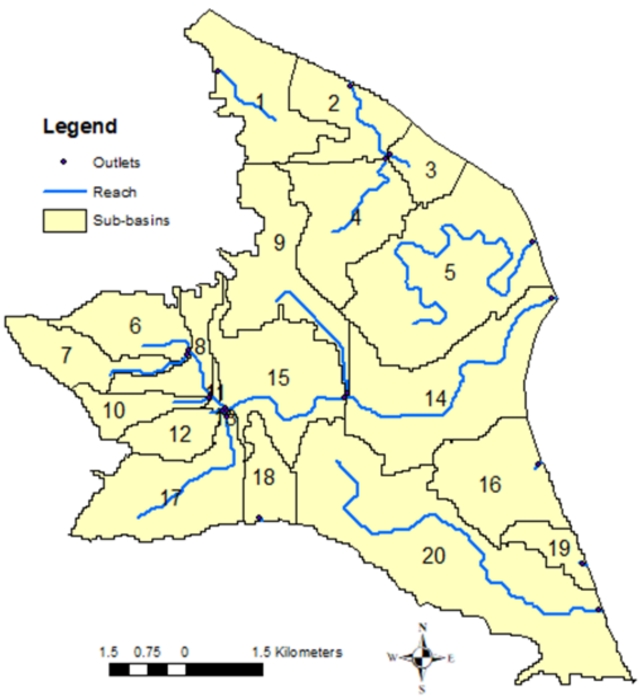

Figure 31 Location map of Pinios River Delta plain watershed including the sub-basins, as modelled with SWAT model.

This project is part of the PRIMA programme supported by the European Union.
GA n° [2041] [LENSES] [Call 2020 Section 1 Nexus IA]

The most usual procedure for hydrological models' calibration is the following: satisfactory match between observed and simulated river discharge must be achieved after adjustment of relevant model parameters in ranges restricted by the physical boundaries of each. Since only ephemeral river water discharge is observed in Agia watershed and reliable river discharge data was not available, the calibration and validation of SWAT model following the above approach was not feasible. Therefore, SWAT model calibration and validation in Agia watershed was performed based on soil moisture data obtained from 3 cluster of FDR soil moisture sensors (6 sensors for each cluster, installed in pairs at 3 depths, 5, 20 and 50 cms) located in the mountainous area of the watershed (Cluster 1, Figure 30) and 24 similar clusters installed in 2 pilot apple orchards (Clusters 2 and 3, Figure 30), which are presented in detail by Brogi et al. (2023). The above-mentioned soil moisture clusters are representative of the 2 most significant land uses of the watershed, namely forests and apple orchards. Therefore, soil water content was the model calibration variable for the SWAT model application in Agia. Soil water content has been introduced in the calibration procedure of SWAT model by several studies (de Andrade et al., 2019; Kundu et al., 2017; Musyoka et al., 2021; Zare et al., 2022). The total simulation period ranged between year 2017 and 2022, while years 2017 and 2018 were used as the model warm-up period. The temporal evolution of simulated and observed soil water content for the calibration and validation periods are presented in Figures 32 and 33, respectively. The model results are also analysed statistically using a wide range of indices, and the results are presented in Table 12.

Regarding cluster 1, Figure 32 indicates that simulated soil water content captures satisfactorily the temporal evolution of the observed values, apart from some of the high observed values. The satisfactory performance of the model in simulating soil water content is also proved by the statistical indices presented in Table 12, since the majority of the indices reached values that are representative of very efficient model performance (r^2=0.93, NSE=0.92 and PBIAS=1.2%). KGE measures the interaction between the model's mean, variance and observation error. In this context, the obtained KGE value (0.96) indicate that the model successfully captures the soil water dynamics. Similarly satisfactory results were achieved for the validation period, as proved by the temporal evolution of the observed and simulated soil water content presented in Figure 33 and the statistical indices presented in Table 12.

Concerning cluster 2, Figure 32 indicates that the model satisfactory simulates the winter and spring temporal evolution of soil water content. The model simulates very efficiently the rapid decrement of soil water content from early April to late May when apple trees growth has started. Nevertheless, considerable discrepancies between the observed and simulated soil water content were observed during the irrigation period which can be attributed the fact that irrigation is not applied in a completely uniform way, thus affecting soil moisture and consequently soil water content. Moreover, the model overestimated soil water content after October, which can be attributed to the fact that considerable evapotranspiration is observed after the harvesting period. Despite the above, the statistical indices presented in Table 12 demonstrate satisfactory performance between observed and simulated soil water content and thus the model can be considered as capable to simulate the effects of irrigation practices in soil water content. Regarding validation of clusters 2 and 3, it was not feasible, since there were significant gaps in precipitation data of the adjacent meteorological station.

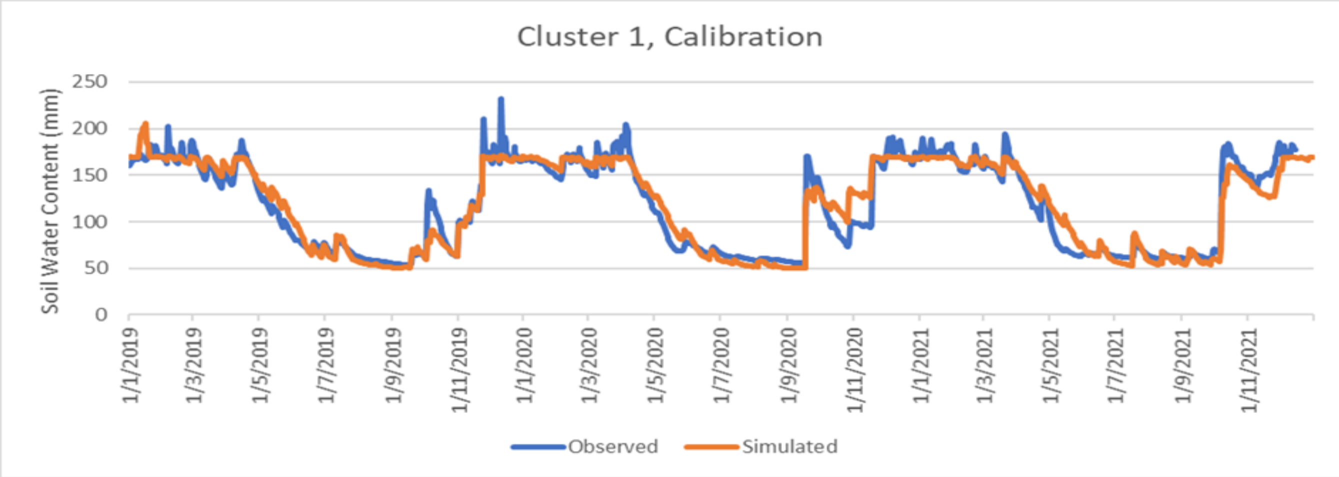

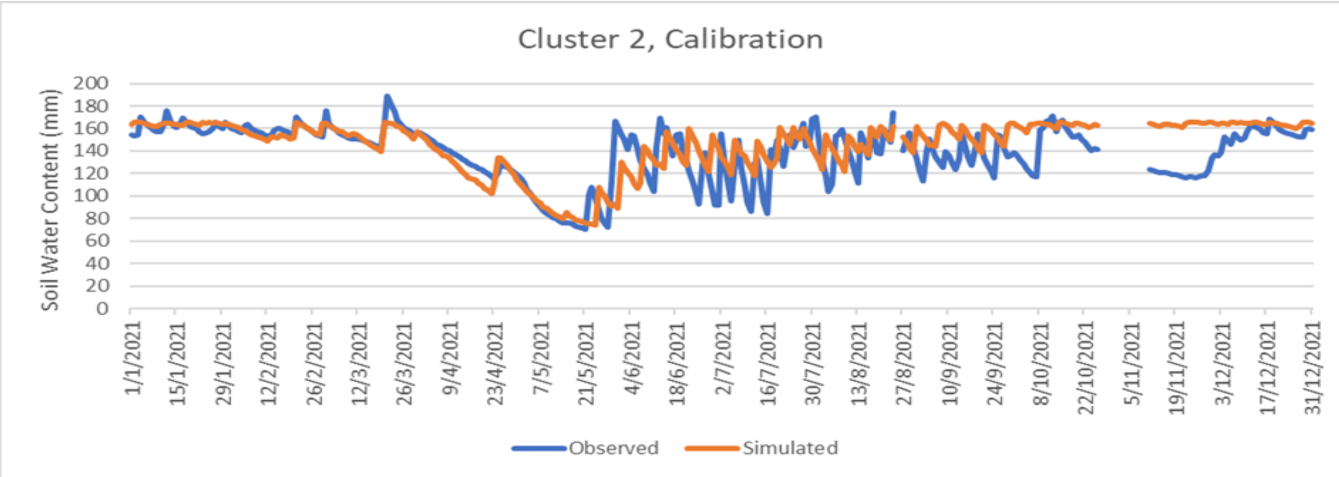

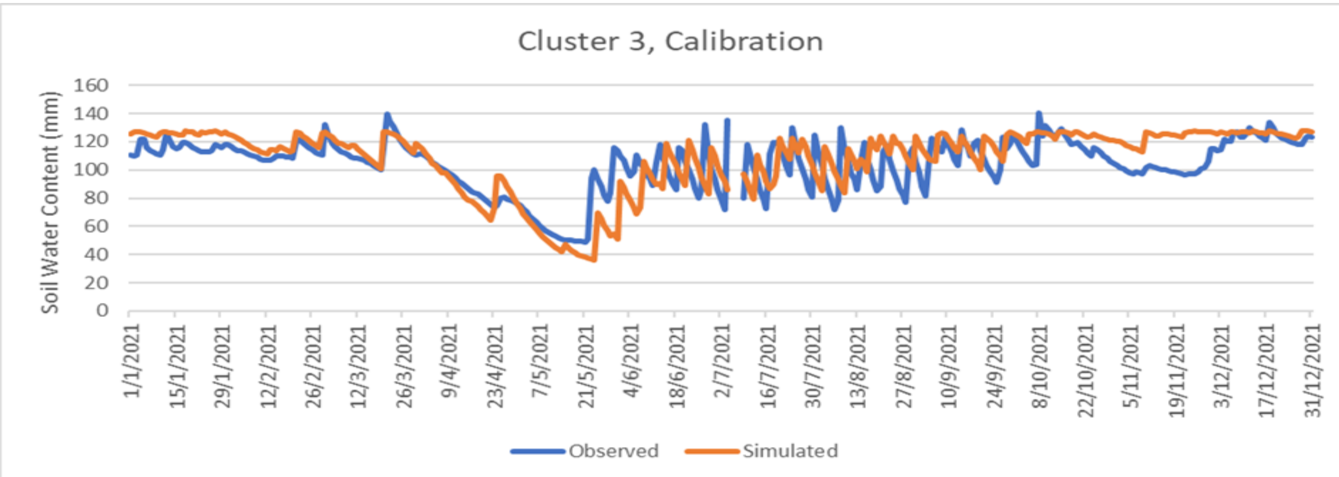

Figure 32 Temporal evolution of daily observed and simulated soil water content for the 3 soil clusters during the calibration period (2020-2021 for Cluster 1 and 2021 for Clusters 2 and 3).

This project is part of the PRIMA programme supported by the European Union.
GA n° [2041] [LENSES] [Call 2020 Section 1 Nexus IA]

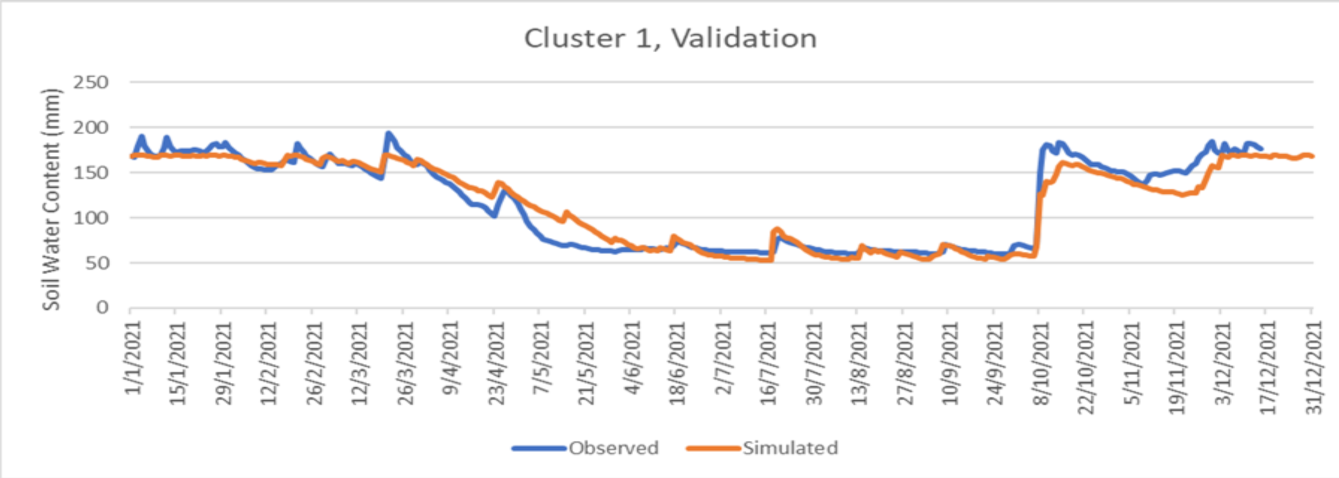

Figure 33 Temporal evolution of daily observed and simulated soil water content for the cluster 1 during the validation period.

Regarding cluster 3 and similarly to cluster 3, Figure 32 indicates that the model satisfactory simulates the winter and spring temporal evolution of soil water content. Interestingly enough, the model simulates very efficiently the rapid decrement of soil water content from early April to late May, when apple trees growth has started. Nevertheless, considerable discrepancies between the observed and simulated soil water content during the irrigation period were also observed in the field monitored by cluster 3. Similarly, to the field monitored by cluster 2, these discrepancies can be attributed to the fact that irrigation is not applied in a completely uniform way, thus affecting soil moisture and consequently soil water content. Once again, the model overestimated soil water content after October, which enforces the evidence that considerable evapotranspiration may be observed after the harvesting period. Despite the above, the statistical indices presented in Table 12 demonstrate the worst of all the 3 clusters but still satisfactory matching between observed and simulated soil water content and thus the model can be considered as capable to simulate the effects of irrigation practices in soil water content.

Table 12 Statistical indices used for the assessment of SWAT model calibration and validation in Agia watershed.

Cluster 1	Calibration				Validation			
	ME	1.44	MNSE	0.79	ME	-1.83	MNSE	0.8
	MAE	9.23	D	0.98	MAE	9.42	D	0.98
	MSE	167.8	MD	0.89	MSE	166.99	MD	0.89
	RMSE	12.95	CP	-1.77	RMSE	12.92	CP	-3.65
	NRMSE%	27.7	R	0.96	NRMSE%	26.5	R	0.97
	PBIAS%	1.2	r2	0.93	PBIAS%	-1.6	r2	0.93
	RSR	0.28	Br2	0.92	RSR	0.27	Br2	0.91
	rSD	1.01	KGE	0.96	rSD	0.93	KGE	0.92
	NSE	0.92	VE	0.92	NSE	0.93	VE	0.92
Cluster 2	**Calibration**							
	ME	-1.7	MNSE	0.58				
	MAE	9.84	D	0.91				
	MSE	258	MD	0.79				
	RMSE	16.06	CP	-1.92				
	NRMSE%	56.4	R	0.84				
	PBIAS%	-1.2	r2	0.7				
	RSR	0.56	Br2	0.69				
	rSD	0.96	KGE	0.83				
	NSE	0.68	VE	0.93				
Cluster 3	**Calibration**							
	ME	-0.75	MNSE	0.36				
	MAE	10.58	D	0.9				
	MSE	224.57	MD	0.73				
	RMSE	14.99	CP	-2.9				
	NRMSE%	72.2	R	0.84				
	PBIAS%	-0.7	r2	0.71				
	RSR	0.72	Br2	0.71				
	rSD	1.32	KGE	0.64				
	NSE	0.48	VE	0.89				

6.1.5. International Long-Term Ecological Research Network Sites (Koiliaris and Keritis – GR)

For the Koiliaris River Basin, data is available from 2004 to the present day (Figure 34). Figures 35-40 depict the simulation of modelled and observed flow. The simulation results indicate that the model can accurately represent the hydrology of the watershed. The goodness of fit during calibration was evaluated using three statistical metrics proposed by Moriasi et al.: the Nash Sutcliffe Efficiency (NSE), Percent Bias (PBias), and Root Mean Square Error Standard Deviation Ratio (RSR). A simulation is considered satisfactory if NSE < 0.5, PBias < 25%, and RSR < 0.7. For the validation period of 2010-2020, the NSE was 0.82, PBias was 12.6%, and RSR was 0.42, indicating a "very good" fit.

For the Keritis River Basin, and more specifically for the Meskla spring, monthly data are available from 1978 to 2004, while for the Agyia springs, data are available from 1978 to 1985. Data for the Keritis River is available for 2012-2013 and 2014-2015.

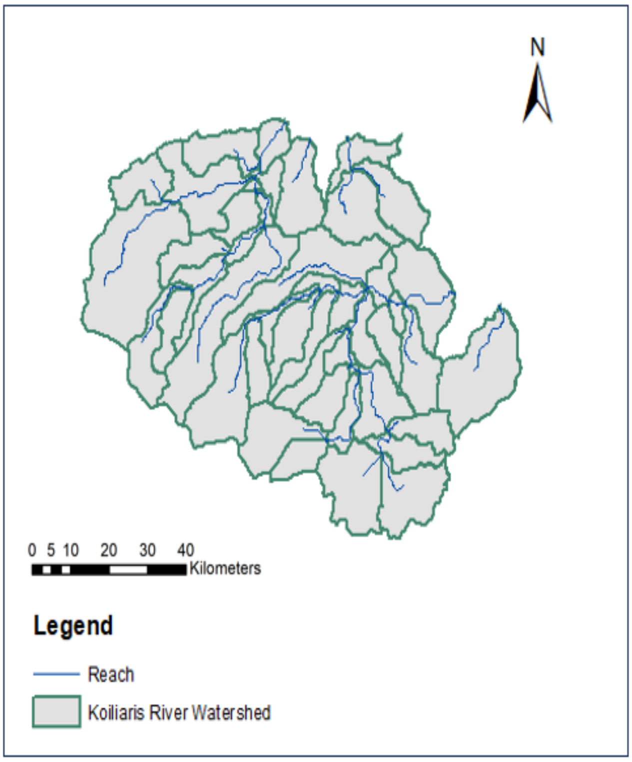

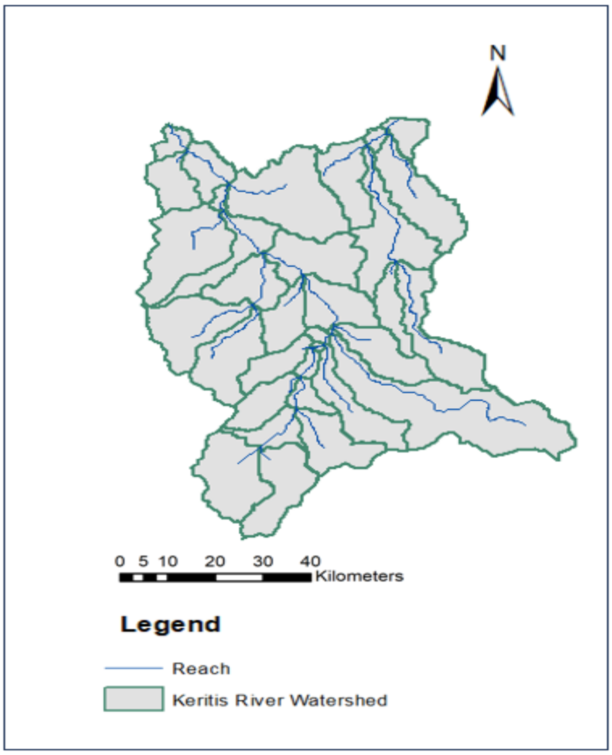

Figure 34 SWAT Model of Keritis and Koiliaris Case Study Area.

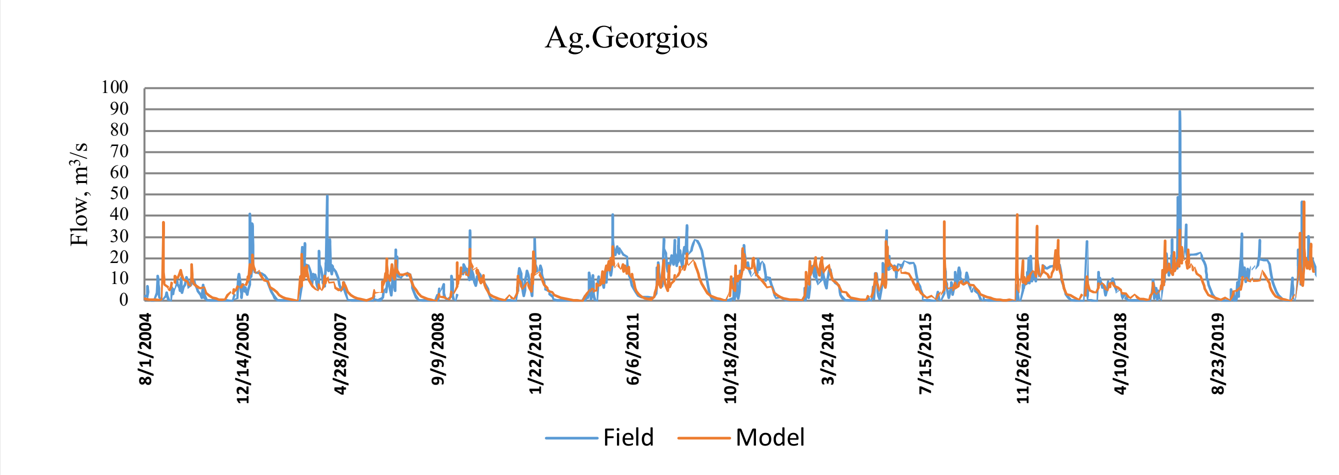

Figure 35 Hydrologic Simulation at St. Georgios station for the 2004-2021 period.

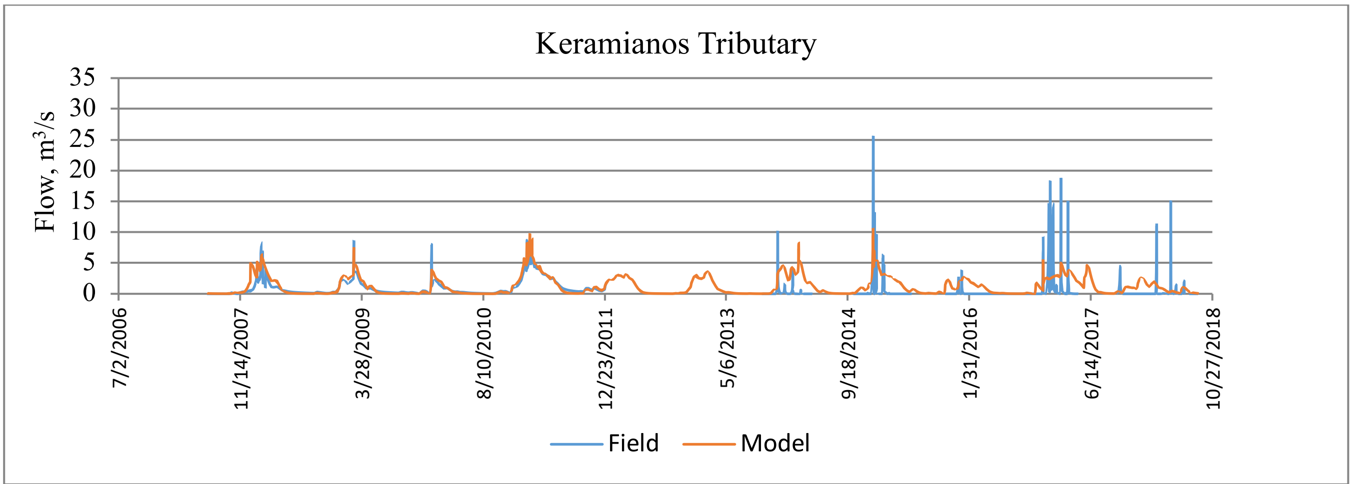

Figure 36 Hydrologic Simulation at St, Keramianos Gorge Entrance.

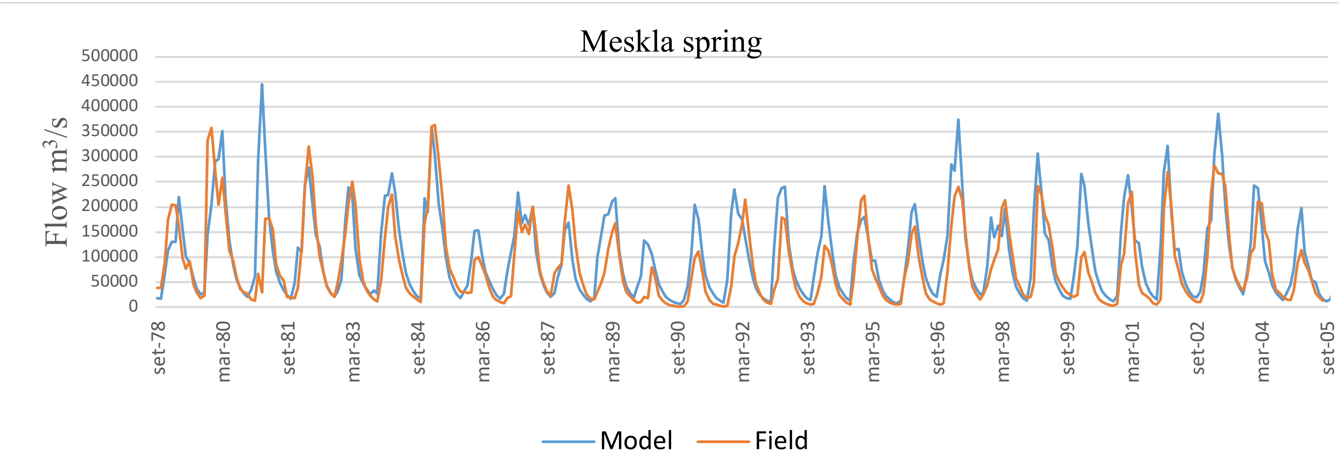

Figure 37 Hydrologic Simulation at Meskla springs for the 1978-2005 period.

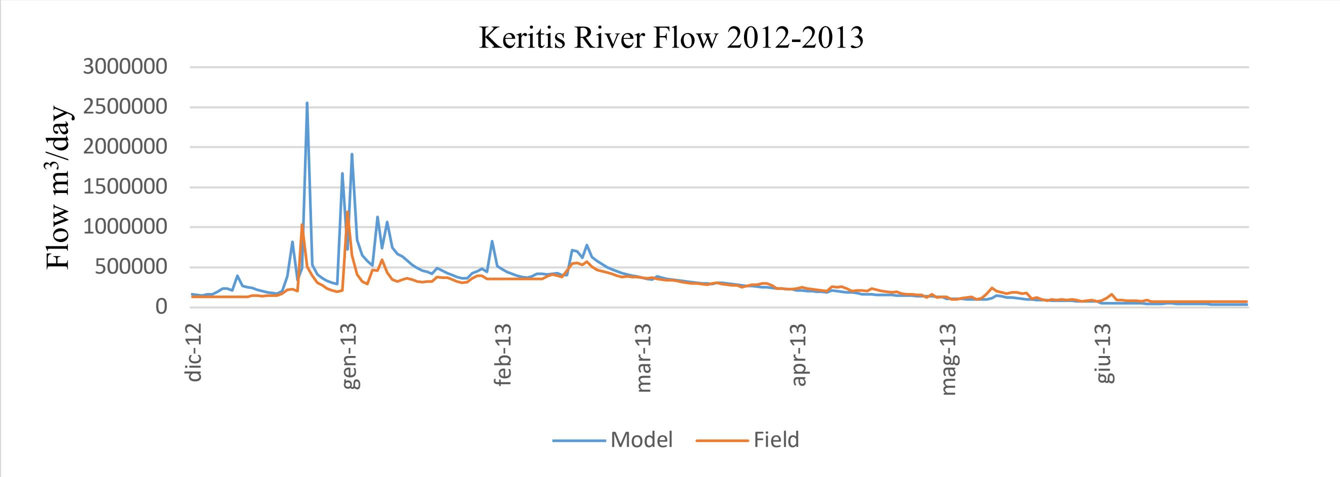

Figure 38 Hydrologic Simulation at Keritis river for the 2012-2013 period.

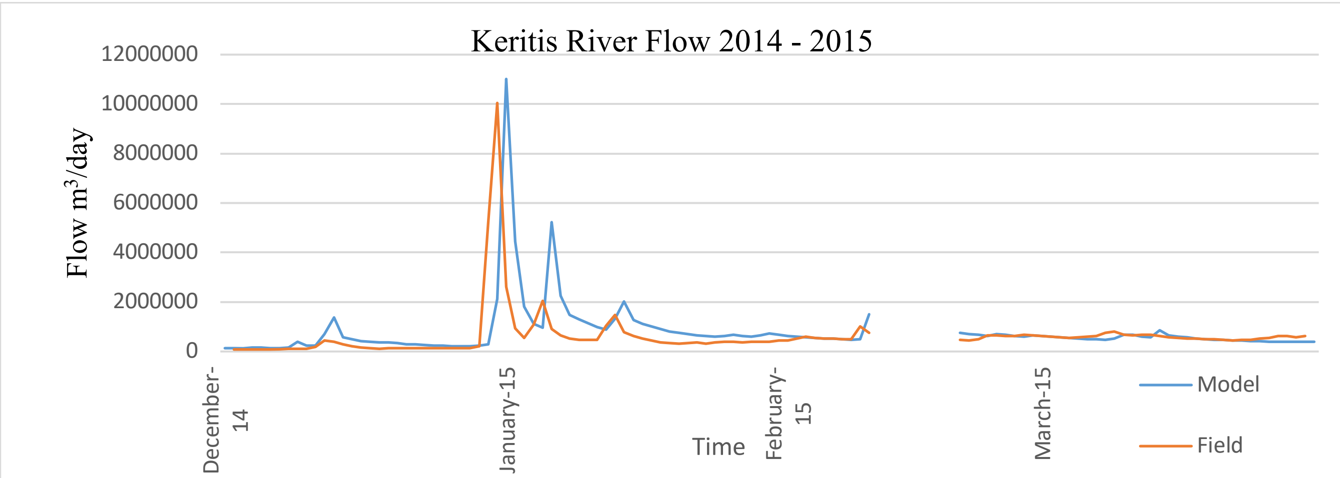

Figure 39 Hydrologic Simulation at Keritis river for the 2014-2015 period.

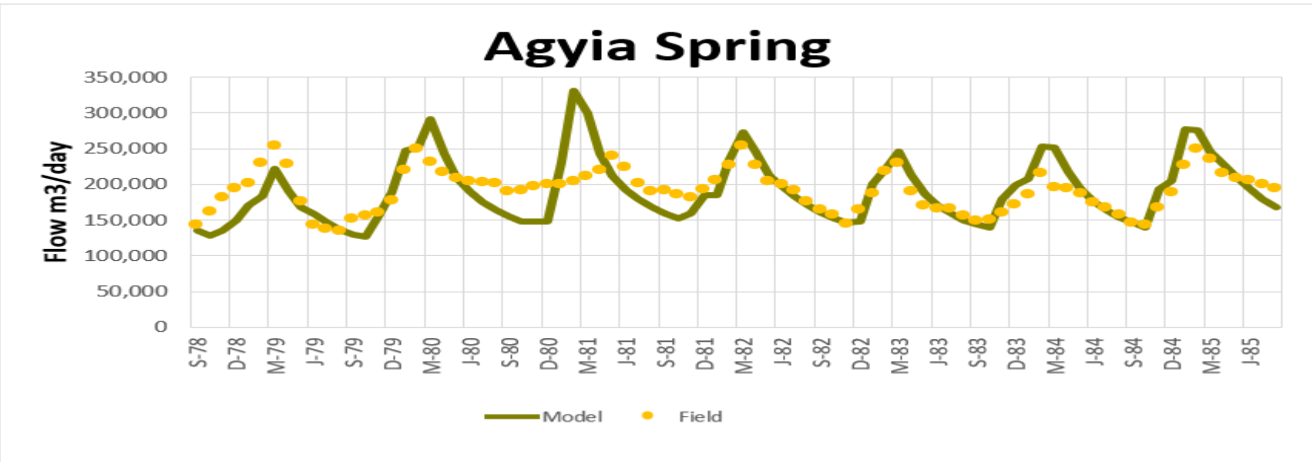

Figure 40 Hydrologic Simulation at Agia springs for the 1978-1985 period.

6.1.6. Tarquinia Plain (IT)

Hydrological modeling process was completed for the Tarquinia plan using SWAT (Figure 41). SWAT was operated in integration with ARC-SWAT. The period 2004-2005 was used for the Warm-up period; data from 2006-2015 were used for the calibration period (5 iteration – 1000 simulation) and data from 2016-2020 were used for the validation period (1 iteration- 1000 simulation).

Automatic calibration, validation and sensitivity analysis were performed with the Sequential Uncertainty Fitting algorithm version 2 (SUFI-2). The SWAT-CUP Tool package was used for this process (Using the Output of Arc-SWAT as an Input in SWAT-CUP).

Arc-SWAT data inputs used in the study:

- Digital elevation model (DEM)
- Soil map

Arc-SWAT data outputs:

- Surface runoff
- Return flow
- Percolation
- Evapotranspiration
- Transmission losses
- Groundwater flow
- Reach routing
- Nutrient and pesticide loading
- Soil erosion
- Water transfer
- Land cover/Land use
- Meteorological data: rainfall (mm), maximum and minimum temperature (C°), wind speed (m/s), relative humidity (%).

Model calibration and validation results are given in Figures 42 and 43. The model results are also analysed statistically, and the results are presented in Table 13.

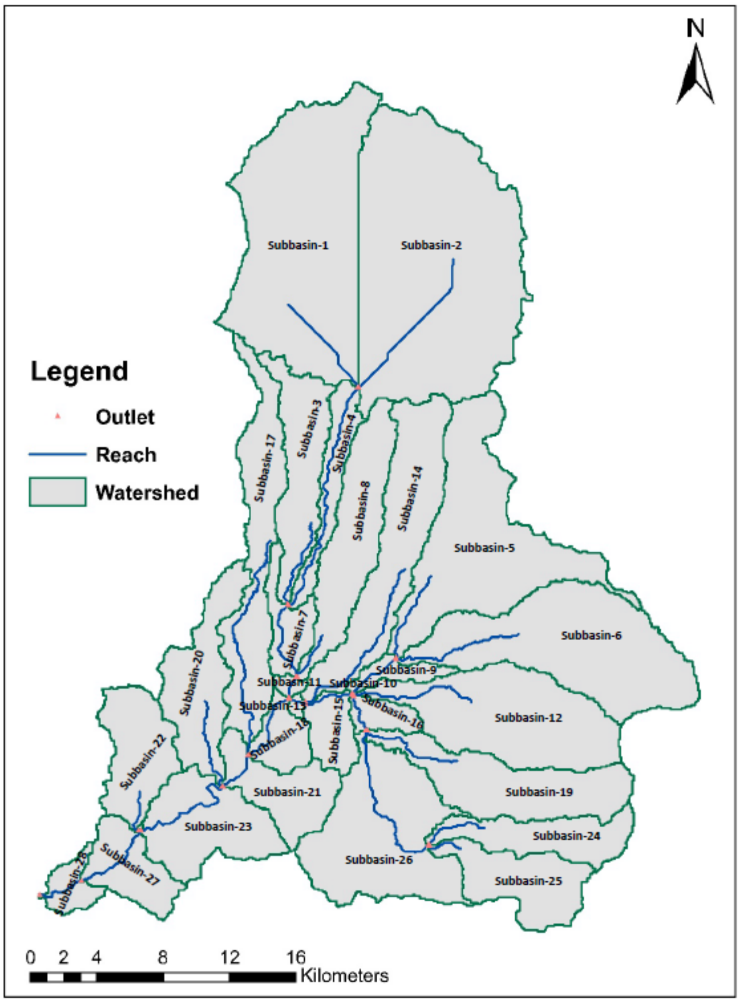

Figure 41 SWAT schematic diagram for Tarquinia.

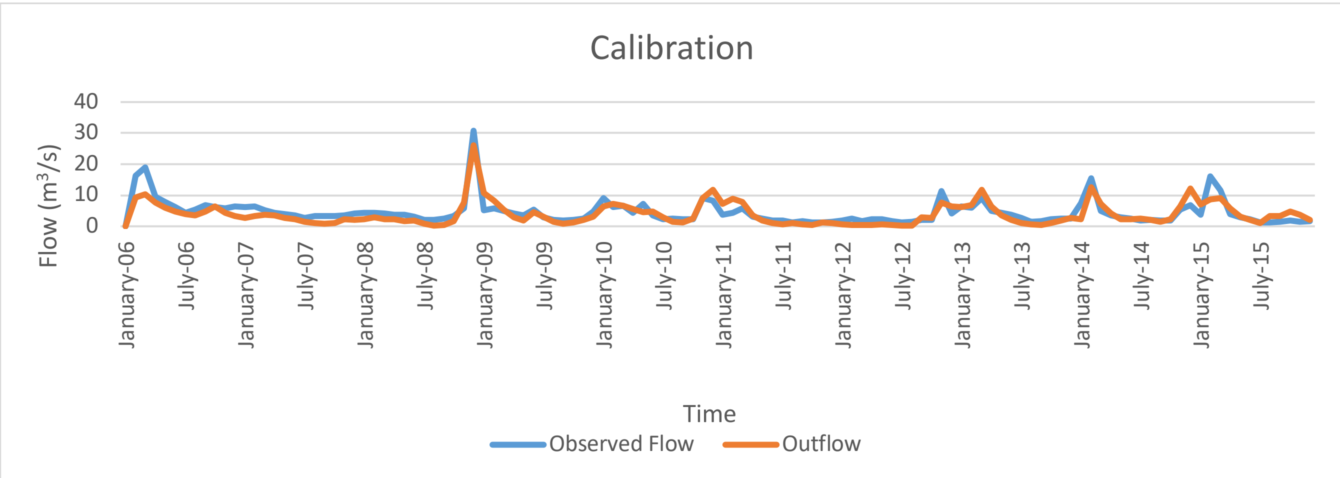

Figure 42 Tarquinia Calibration Period Result.

This project is part of the PRIMA programme supported by the European Union.
GA n° [2041] [LENSES] [Call 2020 Section 1 Nexus IA]

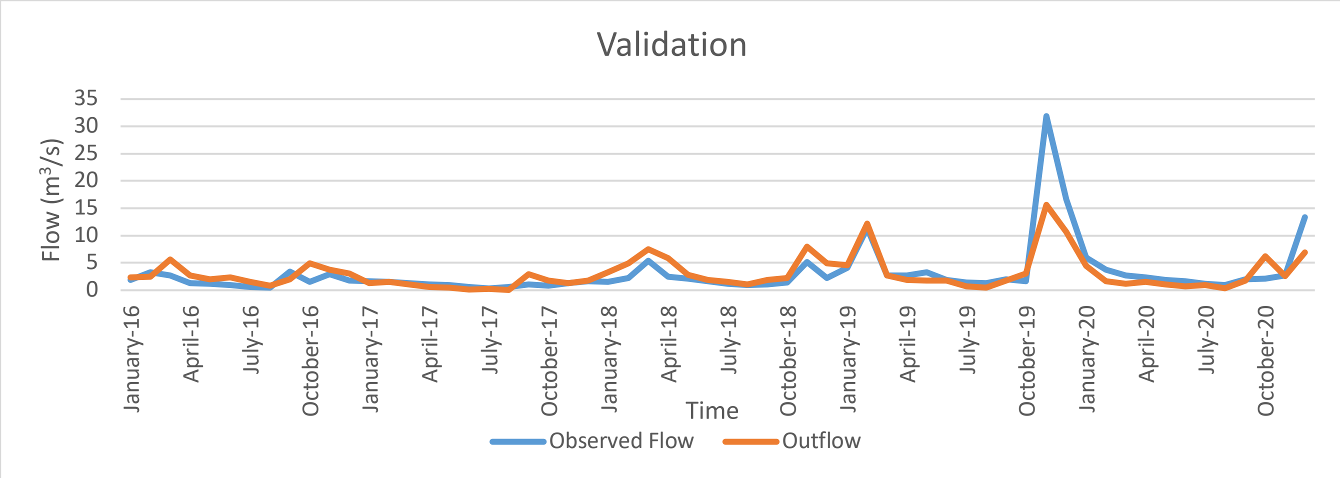

Figure 43 Tarquinia Calibration Period Result.

Table 13 Statistical indicators at Tarquinia for Hydrological Modeling Calibration Results.

Calibration				Validation			
ME	-0.65	MNSE	0.35	ME	-0.08	MNSE	0.38
MAE	1.7	D	0.91	MAE	1.47	D	0.86
MSE	5.12	MD	0.69	MSE	7.59	MD	0.67
RMSE	2.26	CP	0.89	RMSE	2.76	CP	0.71
NRMSE%	54.8	R	0.85	NRMSE%	57.8	R	0.84
PBIAS%	0.55	r^2	0.72	PBIAS%	-2.6	r^2	0.71
RSR	0.55	Br^2	0.6+	RSR	0.63	Br^2	0.47
rSD	0.9	KGE	0.77	rSD	0.63	KGE	0.6
NSE	0.71	VE	0.63	NSE	0.66	VE	0.52

The results of rainfall-runoff modeling performed within the scope of your study were evaluated using various performance metrics during the Calibration and Validation phases.

NSE values of 0.71 and 0.66 were obtained in the Calibration and Validation phases, respectively. In this context, the obtained NSE values reveal that the model performs well in terms of flow predictions. The KGE values were determined as 0.77 and 0.6 in the Calibration and Validation stages, respectively. KGE measures the interaction between the model's mean, variance and observation error. In this context, the obtained KGE values indicate that the model successfully captures the rainfall-runoff relationship. These results show that the model performs reliably and effectively in rainfall-runoff forecasting.

6.2. Climate Change Scenarios

At this stage, climate change scenarios were applied to the calibrated and validated models to examine the changes in flow values under climate change scenarios and thus to provide input to the WEAP water allocation model. In each pilot area, the hydrological models were rerun for the climate change scenarios. The period of 1971-2000 was considered as a reference period, while 2010-2100 period was scenario period for RCP 4.5 and RCP 8.5.

6.2.1. Middle Jordan Valley (JO)

For Deir Alla Case, the model results are presented in Figure 44-46.

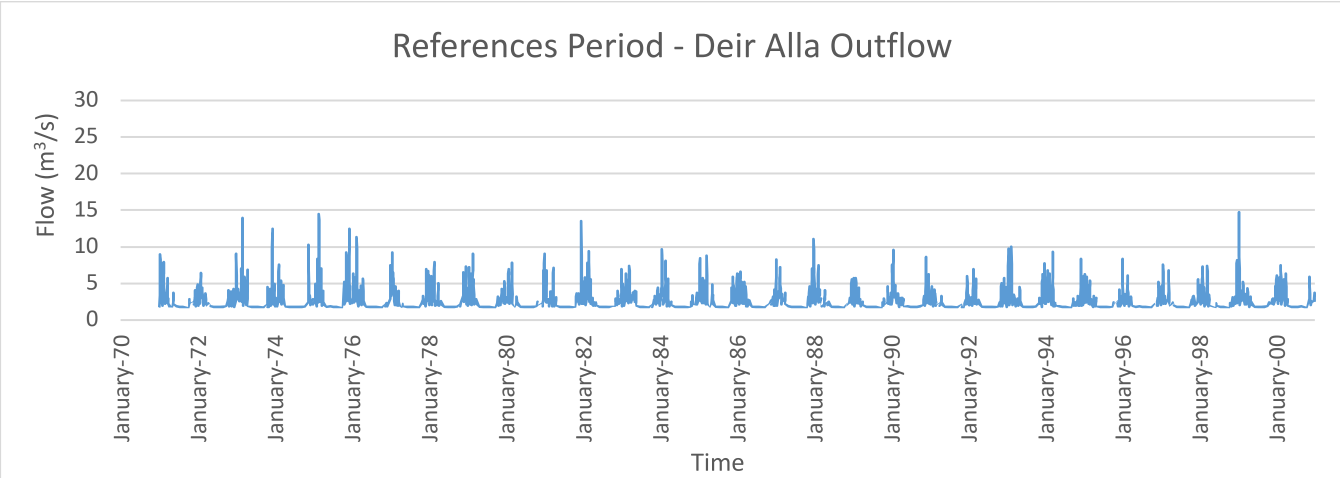

Figure 44 Jordan Reference Period Outflow (1971-2000).

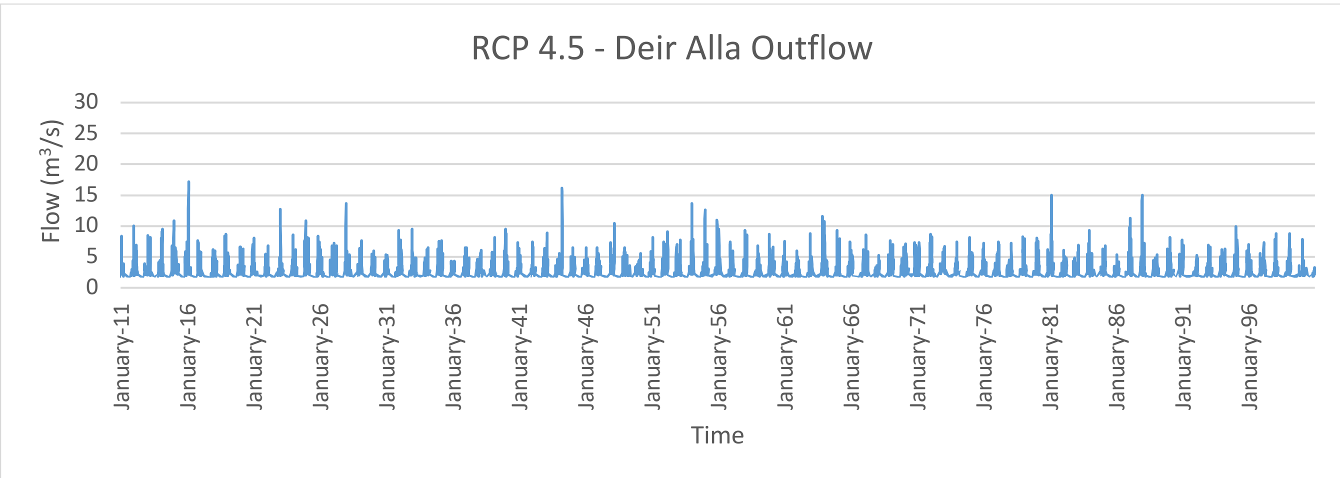

Figure 45 Jordan RCP 4.5 Scenarios Outflow (2010-2100).

This project is part of the PRIMA programme supported by the European Union.
GA n° [2041] [LENSES] [Call 2020 Section 1 Nexus IA]

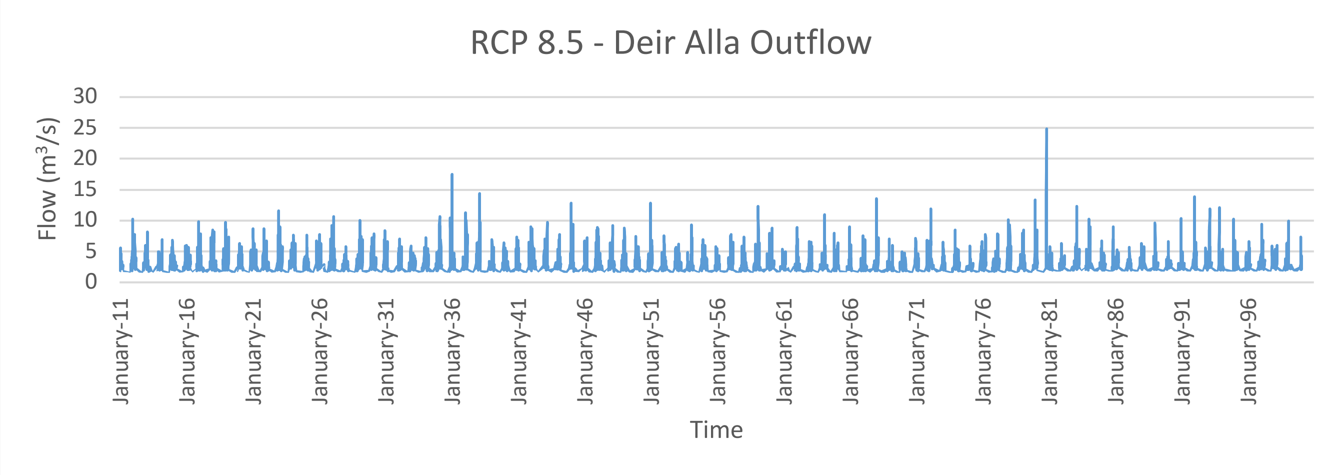

Figure 46 Jordan RCP 8.5 Scenarios Outflow (2010-2100).

Table 14 is given to show average and standard deviation values for reference and scenario periods.

Table 14 Statistical properties of climate change outcomes.

Deir Alla / Jordan	Reference Period		RCP 4.5		RCP 8.5	
	Average	St. Dev.	Average	St. Dev.	Average	Std. Dev.
Gage	2.42	1.21	1.8	1.063	2.33	1.09

This project is part of the PRIMA programme supported by the European Union.
GA n° [2041] [LENSES] [Call 2020 Section 1 Nexus IA]

6.2.2. Gediz Basin & Delta (TR)

Each station was analysed separately for Menemen Region. For each station analysed, the models were run with the reference period and RCP 4.5-8.5 data and the results obtained are given in Figure 47-49 and Table 15.

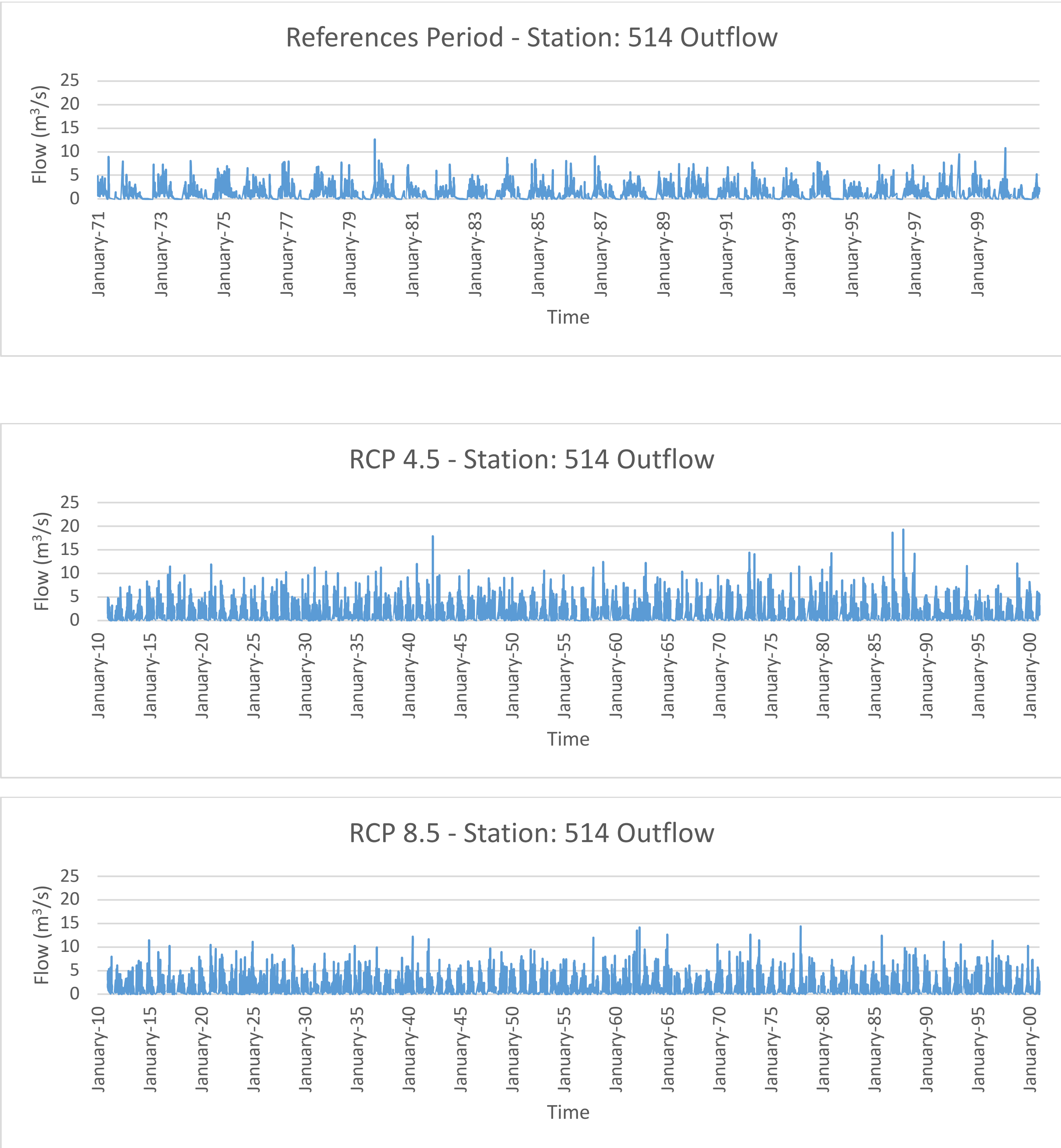

Figure 47 Stations 514 Outflow.

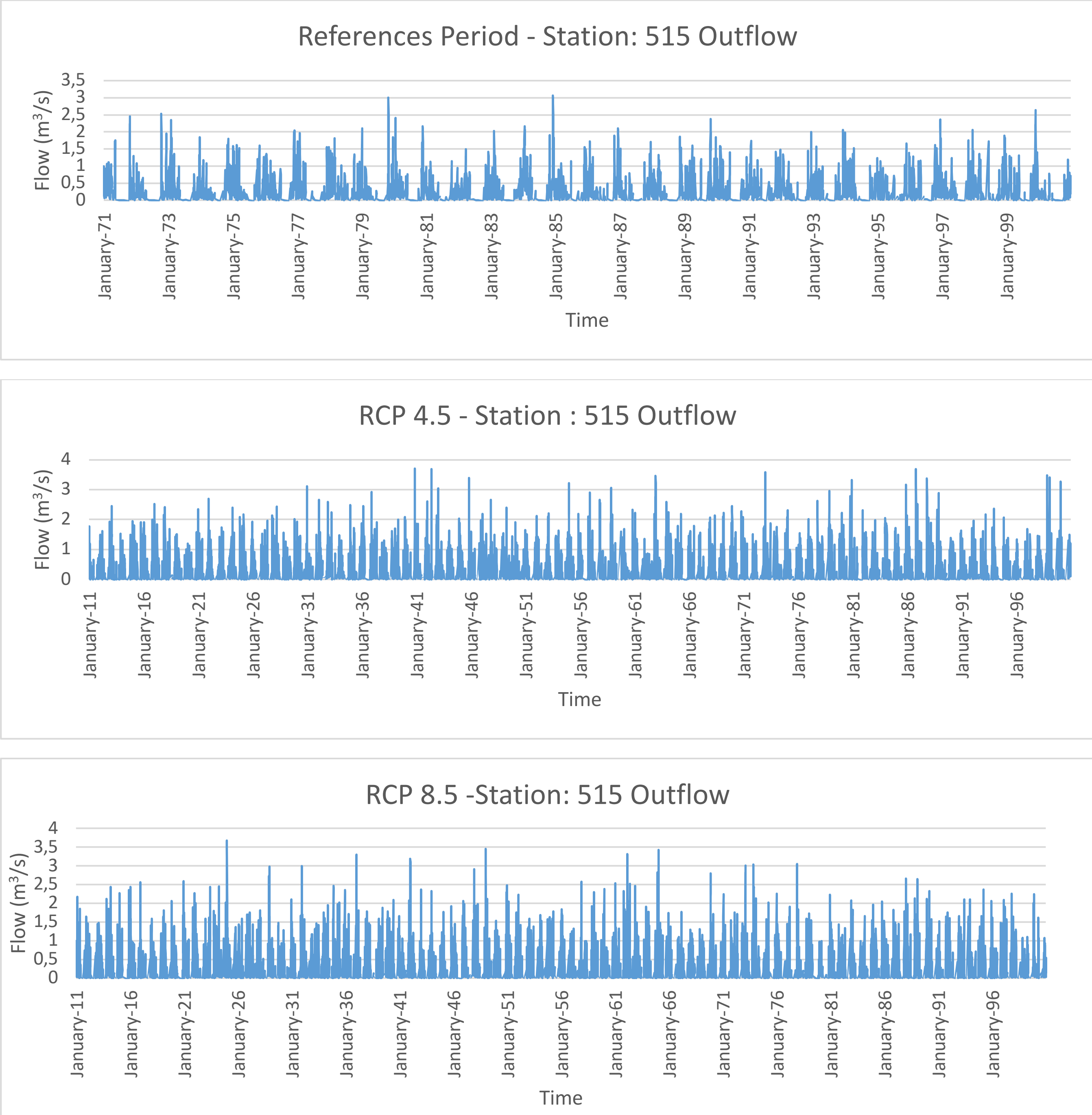

Figure 48 Stations 515 Outflow.

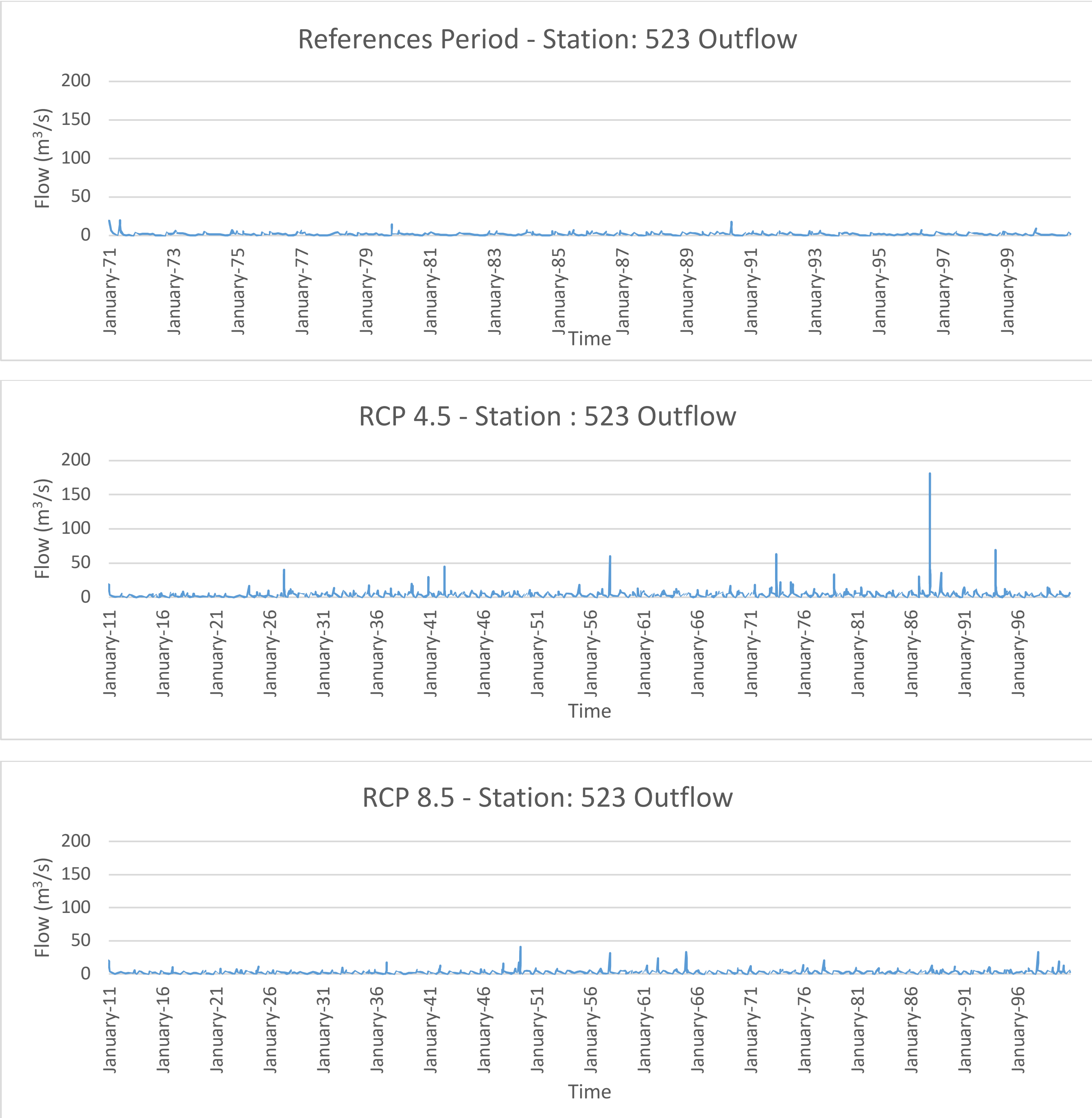

Figure 49 Stations 523 Outflow.

Table 15 Statistical properties of climate change outcomes.

Menemen /Turkey	Reference Period		RCP 4.5		RCP 8.5	
	Average	**St. Dev.**	**Average**	**St. Dev.**	**Average**	**Std. Dev.**
514	0.87	1.24	0.92	1.42	0.84	1.29
515	0.17	0.33	0.17	0.35	0.16	0.33
523	1.62	1.36	3.02	3.13	1.89	1.66

6.2.3. Guadalquivir Basin, Doñana National Park Area (ES)

Each station was analysed separately for Doñana Region. For each station analysed, the models were run with the reference period and RCP 4.5-8.5 data, and the results obtained are given in Figure 50-53 and Table 16.

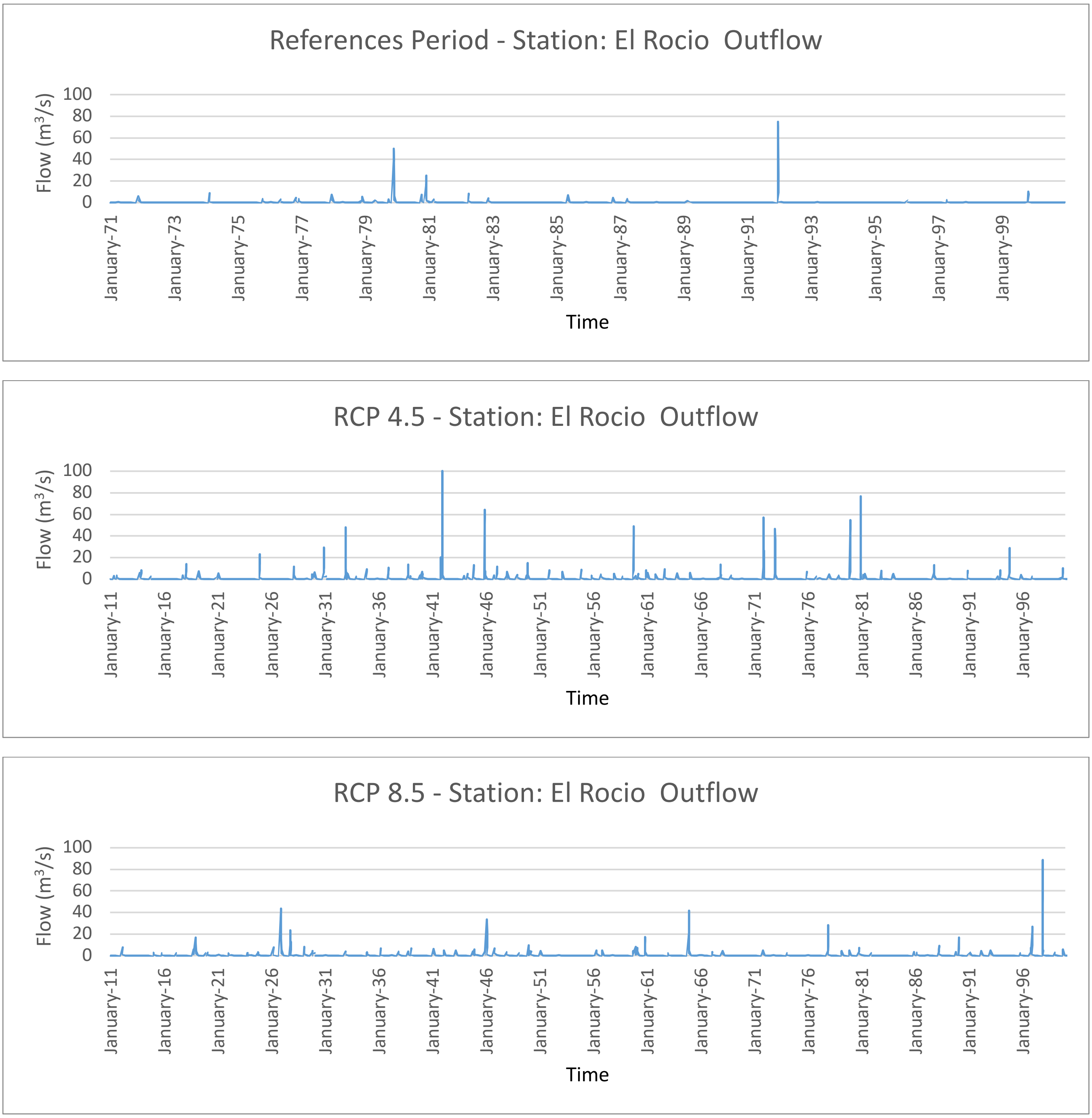

Figure 50 Stations El Rocio Outflow.

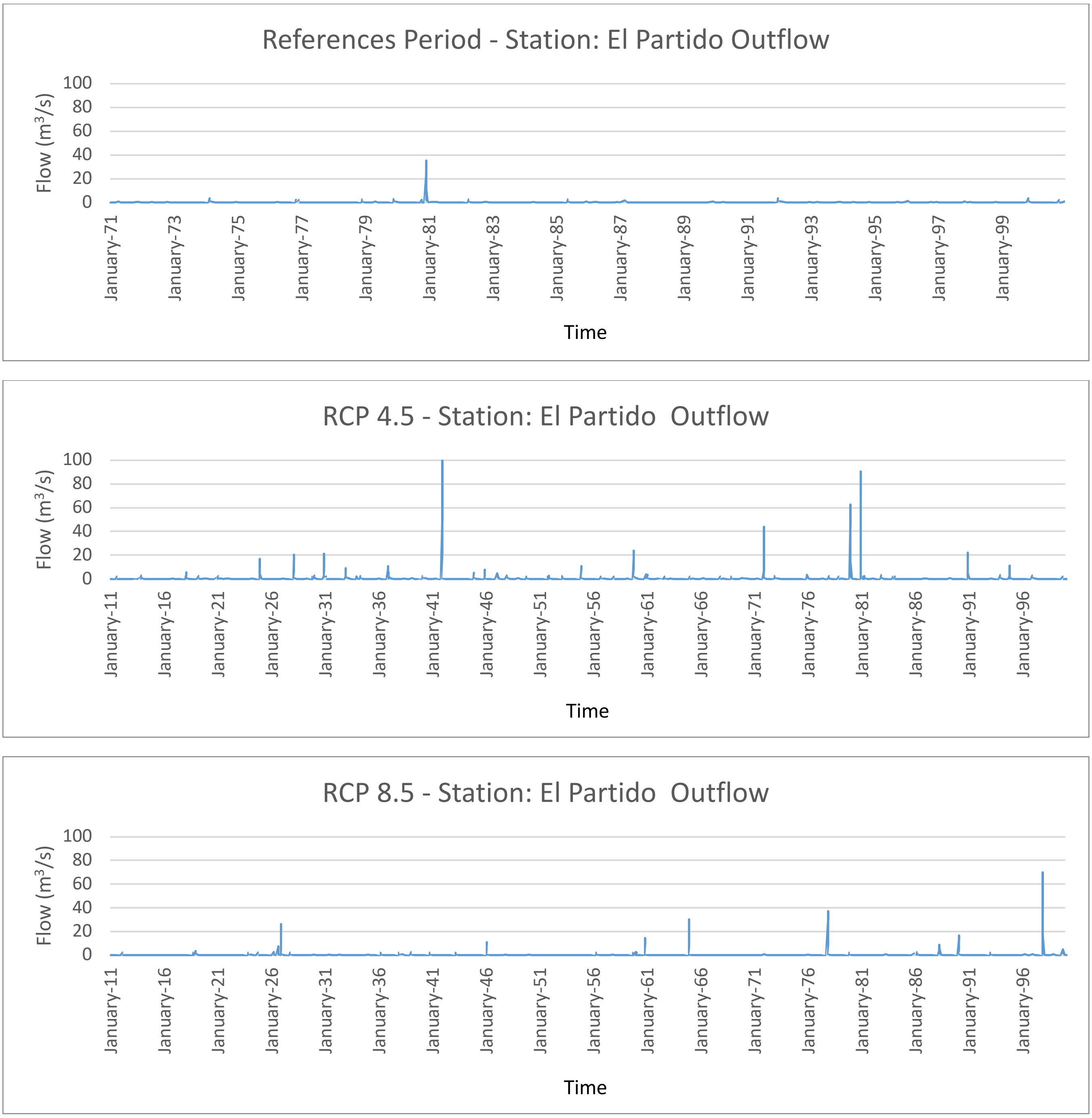

Figure 51 Station El Partido Outflow.

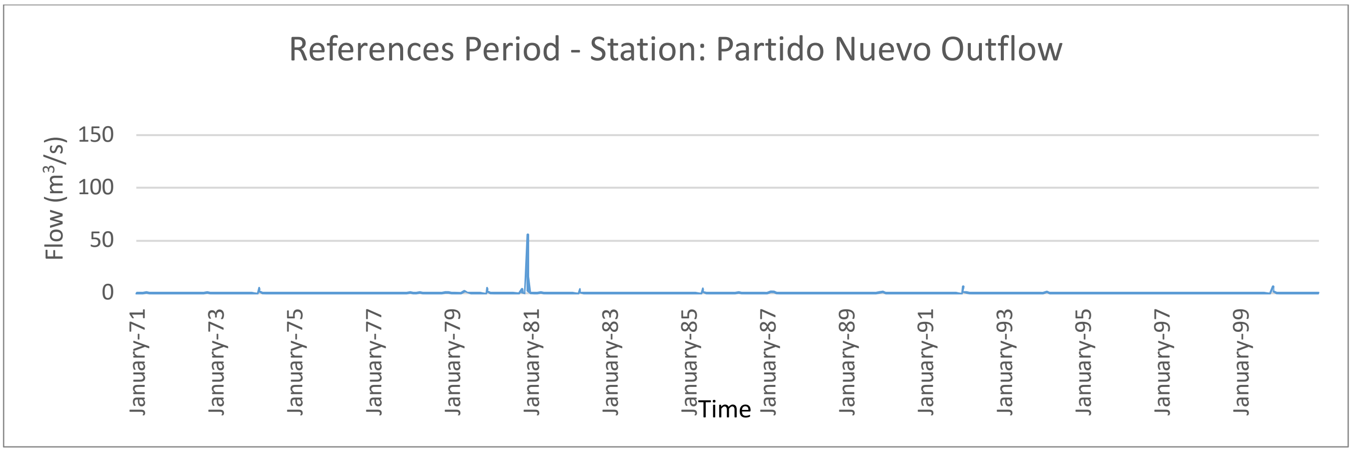

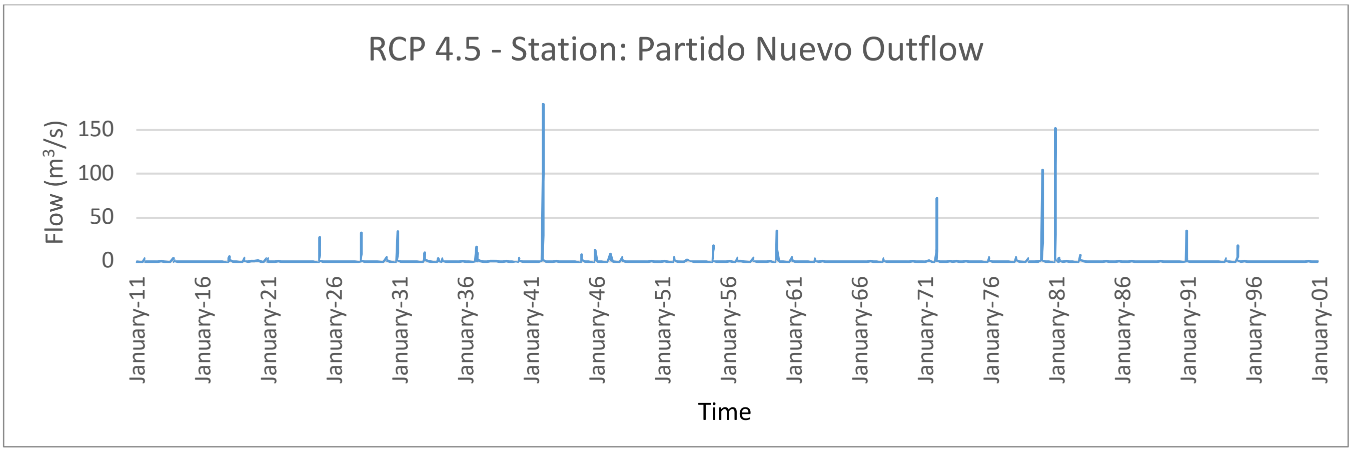

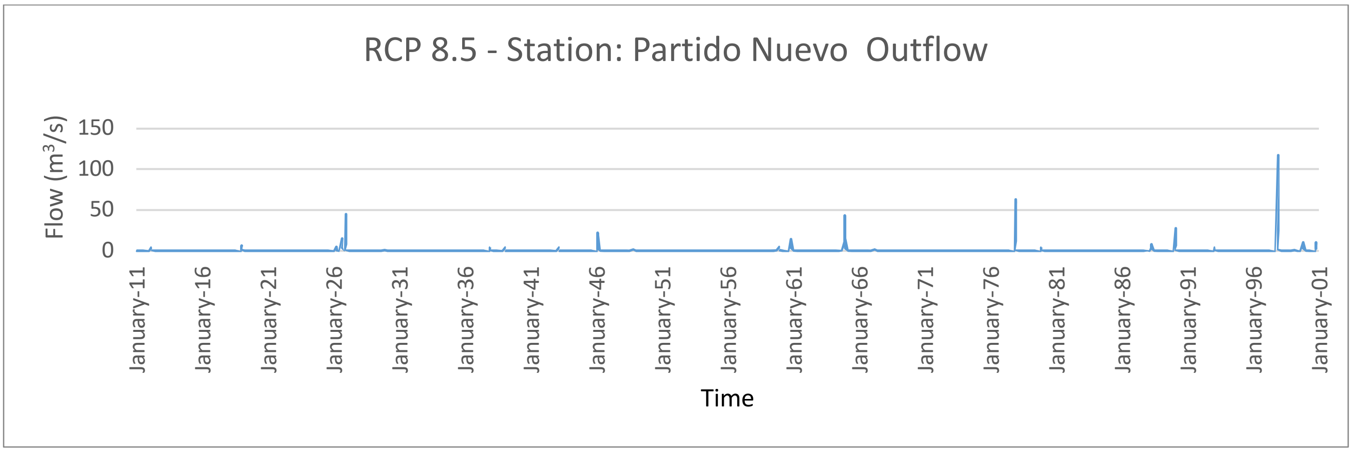

Figure 52 Station Partido Nuevo Outflow.

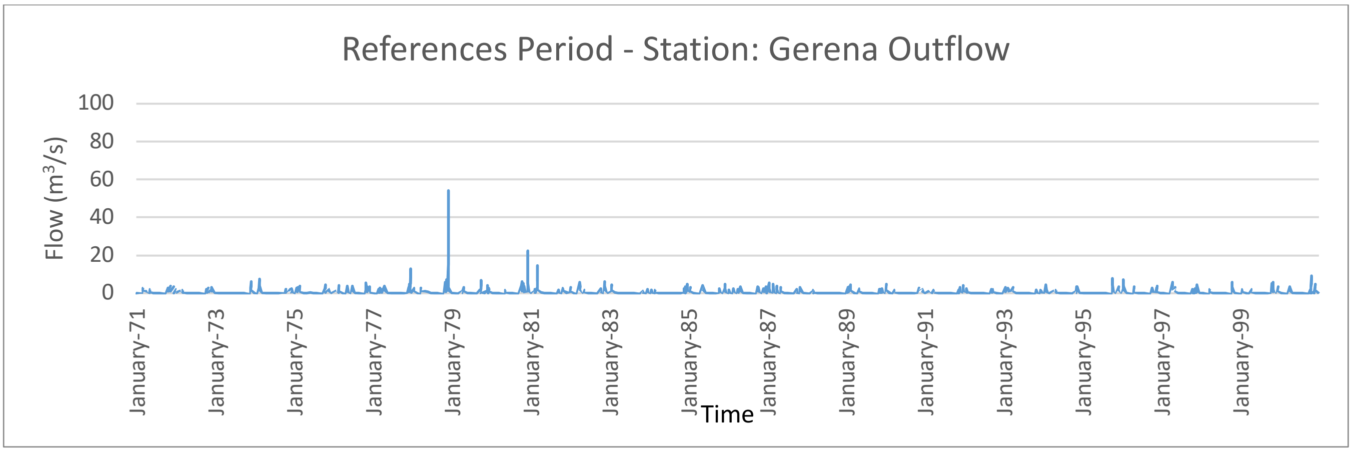

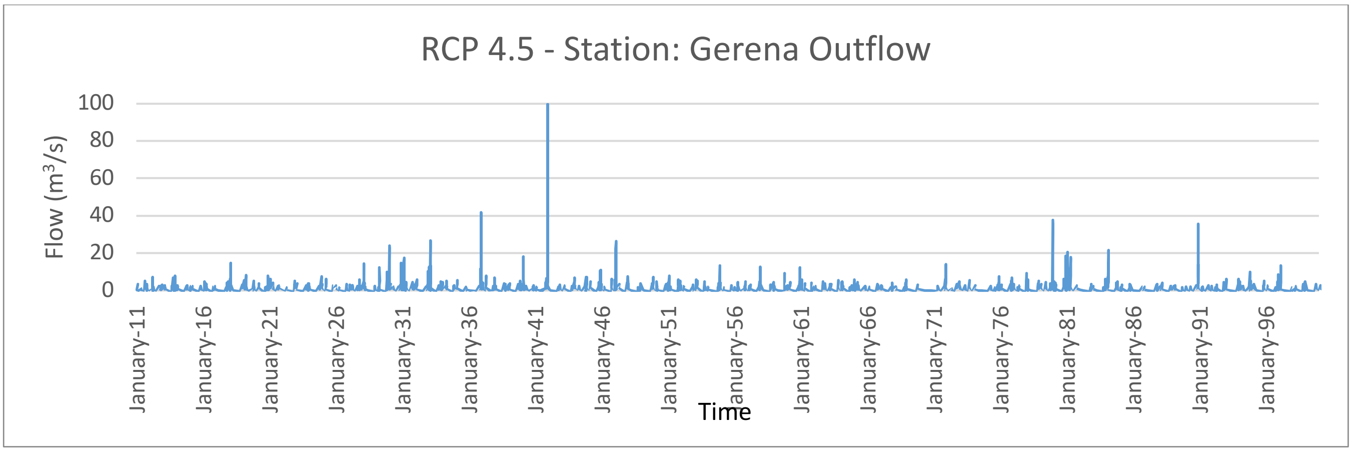

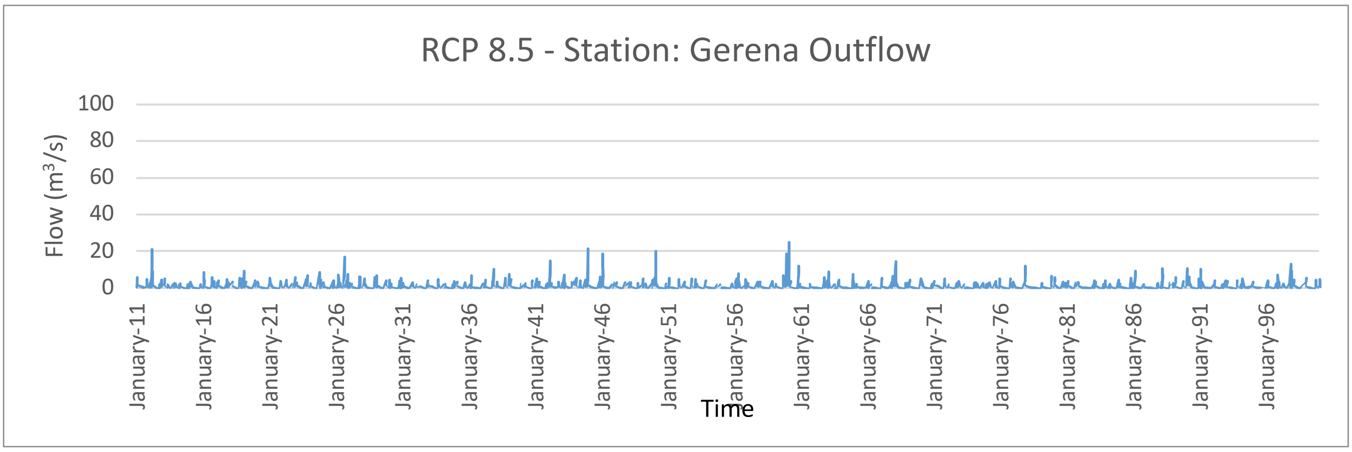

Figure 53 Station Gerena Outflow.

Table 16 Statistical properties of climate change outcomes.

Doñana /Jordan	Reference Period		RCP 4.5		RCP 8.5	
	Average	St. Dev.	Average	St. Dev.	Average	Std. Dev.
El Rocio	0.11	1.31	0.13	1.56	0.07	0.45
El Partido	0.07	0.49	0.09	1.40	0.09	0.71
Partido Nuevo	0.07	0.60	0.09	1.70	0.09	0.90
Gerena	0.23	1.03	0.24	1.30	0.19	0.77

6.2.4. International Long-Term Ecological Research Network Sites (Pinios – GR)

The climate change impact assessment for the 2 watersheds was based on the RCM data provided by DRAXIS in the context of WP3. Therefore, the reference period considered was from year 1971 to year 2000 and it constitutes the basis for comparison with the projected period (2011-2100) under RCP 4.5 and RCP 8.5 scenarios. Groundwater recharge constitutes the most critical parameter for the sustainability of the WEFE NEXUS for both areas, since it is directly connected to water provision not only for all sensors, thus affecting the interaction of the water sector with the other NEXUS sector. For this, we provide below the temporal evolution of projected annual groundwater recharge for both watersheds and both climate change scenarios (Figure 54), while the corresponding average annual groundwater recharge and standard deviation is presented in Table 17. As presented in Figure 5, higher groundwater recharge fluctuation is presented for PRDP compared to Agia and this is attributed to the direct influence of the phreatic aquifer to percolation.

Concerning the reference period (1971-2000), overall higher groundwater recharge values are observed during the first 15 year and lower values for the last. This fact indicates a decreasing trend for groundwater recharge which is also presented in both RCP4.5 and RCP8.5. It is worth to mention that there are years for which annual groundwater recharge for PRDP reaches exceptionally low values. This can be attributed to 2 or more consecutive dry years. The high standard deviation of annual groundwater recharge variation is also observed for the projected period for both climate change scenarios. In contrast, groundwater recharge in Agia demonstrates a much smoother variation.

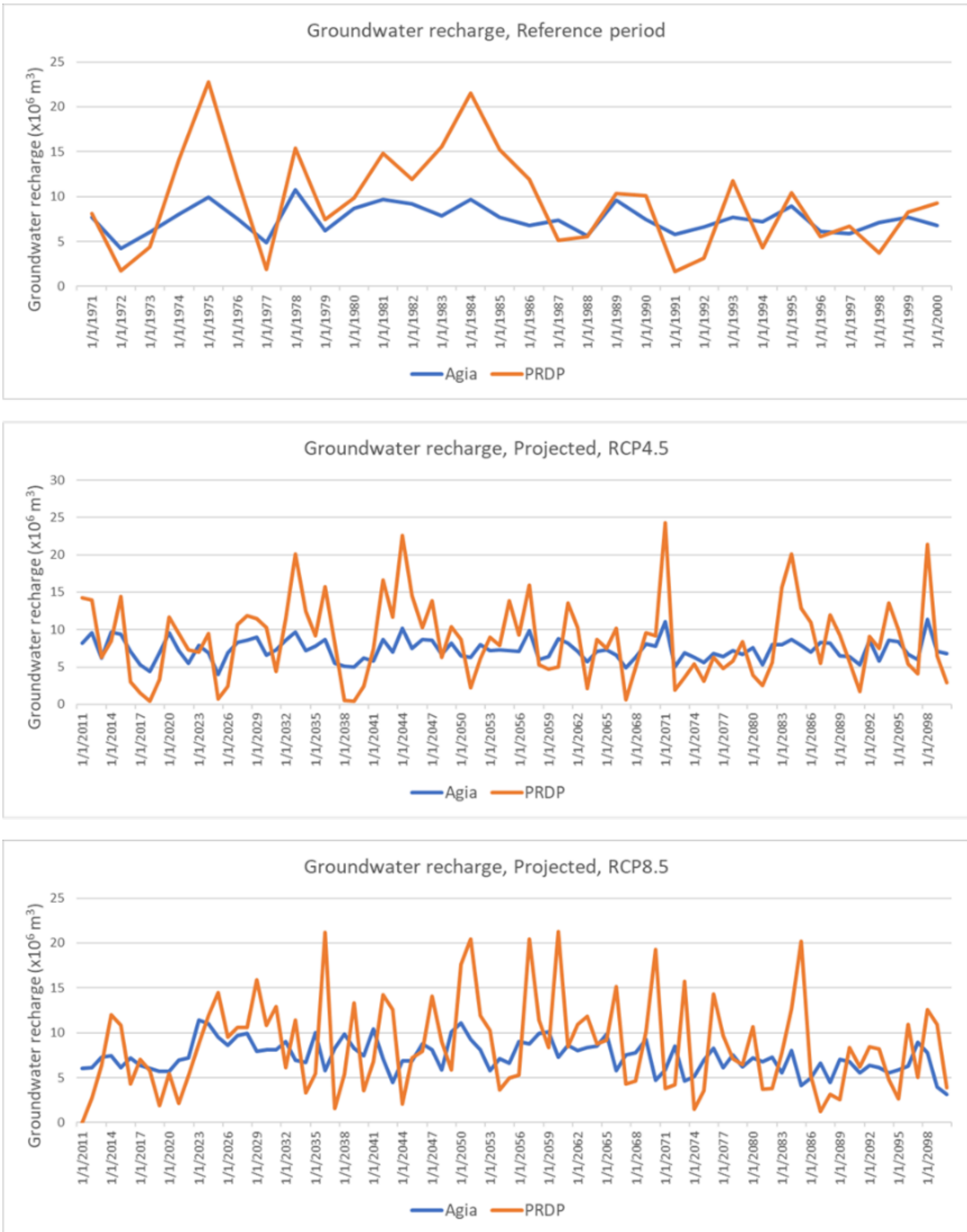

Figure 54 Temporal evolution of annual groundwater recharge in the 2 watersheds for the reference (1971-2000) and projected period (2011-2100) under RCP4.5 and RCP8.5 scenarios.

Table 17 Average annual groundwater recharge and standard deviation for the reference and projected period.

Pinios	Reference Period Groundwater recharge (x10^6 m^3)		RCP 4.5 Groundwater recharge (x10^6 m^3)		RCP 8.5 Groundwater recharge (x10^6 m^3)	
	Average	St. Dev.	Average	St. Dev.	Average	Std. Dev.
Agia	7.48	1.57	7.30	1.45	7.36	1.75
Delta	9.48	5.49	8.57	5.27	8..71	5.02

Table 18 Annual precipitation and groundwater recharge change for the projected periods compared to the reference period.

Watershed	Scenario	Period	Precipitation change (%)	Groundwater Recharge change (%)
Agia	**RCP45**	2011-2040	-1.88	-2.91
		2041-2070	2.26	-1.50
		2071-2100	1.12	-2.78
		2011-2100	0.50	-2.40
	RCP85	2011-2040	5.59	4.55
		2041-2070	10.43	7.02
		2071-2100	-1.04	-16.43
		2011-2100	4.99	-1.62
Delta	**RCP45**	2011-2040	-6.71	-14.47
		2041-2070	-2.07	-2.10
		2071-2100	-4.94	-12.09
		2011-2100	-4.57	-9.55
	RCP85	2011-2040	-0.73	-13.00
		2041-2070	3.18	10.74
		2071-2100	-7.26	-22.03
		2011-2100	-1.60	-8.10

As presented in Table 18, for the period 2011-2100 and climate scenario RCP4.5 in Agia, annual precipitation was found to be slightly increase by 0.5% compared to the reference period (1971-2000), while the annual groundwater recharge was found to be decreased by 2.4%. The corresponding changes for RCP8.5 were found to be 4.99 and -1.62%, respectively. Similarly, for PRDBP, the annual precipitation changes for the period 2011-2100 and scenario RCP4.5 was -4.57% and the corresponding groundwater recharge change was -9.55. The corresponding changes for annual precipitation and groundwater recharges for RCP8.5 were -1.6 and 8.1%, respectively. Therefore, groundwater recharge was found to be decreased during the projected period for both climate change scenarios, even though precipitation was found to be increased by 5% in the case of Agia watershed under RCP8.5 scenario. This fact reflects the influence of projected precipitation and evapotranspiration patterns in groundwater recharge. Apart from the changes for the whole projected period, the changes for the periods 2011-2040, 2041-2070 and 2071-2100 are also presented in Table 3 to further investigated groundwater recharge variation trends. Groundwater recharges decrease up to 16.43% was presented for Agia watershed (period 2071-200, RCP8.5) and up to 22.03% for PRDP watershed (period 2071-200, RCP8.5). This is a critical outcome since water availability in both watersheds is highly dependent on groundwater availability.

6.2.5. International Long-Term Ecological Research Network Sites (Koiliaris and Keritis – GR)

Climate projections are generated using two types of models: Global Climate Models (GCMs), which simulate the climate globally, and Regional Climate Models (RCMs), designed to simulate the climate for specific regions (Mc Sweeney & Hausfather, 2018). GCMs typically operate at a spatial resolution ranging from 50 to 250 km and demand significant computational power and time. RCMs were primarily developed to refine climate data produced by coarse-resolution GCMs, offering detailed information at finer, sub-GCM grid scales more suitable for studying regional phenomena and conducting climate risk assessments. The disparities between the results of RCMs and GCMs arise from the former depicting global circulation, considering large-scale factors like greenhouse gases (GHGs) or solar radiation fluctuations. In contrast, the latter enhances this information both spatially and temporally, incorporating finer-scale details such as topography, coastlines, inland water bodies, land cover, or mid-range dynamic processes (Giorgi, 2019).

The spatial resolution of GCM simulations is deemed appropriate for climate analysis on a larger geographic scale (European, Mediterranean, etc.) but not at the local level. This limitation arises because the average climatic conditions in broader areas significantly differ from those specific to smaller regions. Consequently, a thorough analysis at the local scale was deemed necessary, employing RCM simulations based on the RCPs. Among the four RCPs outlined by the IPCC (2013), RCP4.5 and RCP8.5 were chosen. The former serves to examine a more realistic mitigation scenario as an intermediate option according to emissions, while the latter represents a scenario capturing GHG emissions in the absence of mitigation measures (IPCC, 2013). Specifically, RCP4.5 envisions the stabilization of radiative forcing at 4.5 W/m² by the year 2100 without surpassing that value (Thomson et al., 2011), whereas RCP8.5 anticipates that radiative forcing will exceed 8.5 W/m² by 2100 and continue to rise for a certain duration (Riahi et al., 2011).

In our study, we utilized the new data for scenarios (precipitation, temperature) to operate the SWAT-Karst model. This led to the calculation of new flows for rivers and springs, which were then incorporated into the WEAP model. The meteorological stations included in the SWAT model for simulating the two study areas until today contain observed data from the stations Alikianos, Meskla, Askifou, Kalives, Samonas, Psichro Pigadi, and Agrokipio.

Before utilizing the new precipitation and temperature data, it was necessary to compare them with the data from local meteorological stations for the same time period (1971-2000) to determine if there was a deviation from the field data. As shown in Figure 55-56, we concluded that the RCM data does not coincide with the observed values of the local stations. Consequently, the application of corrective parameters was necessary.

Initially, we calculated the average monthly precipitation/temperature for the period 1971-2000 for both scenarios and the local stations. Subsequently, we determined their respective ratios, which were applied to the new daily data. The correction factors applied to each station for each scenario in the daily precipitation and temperature data are depicted in Tables 19-20.

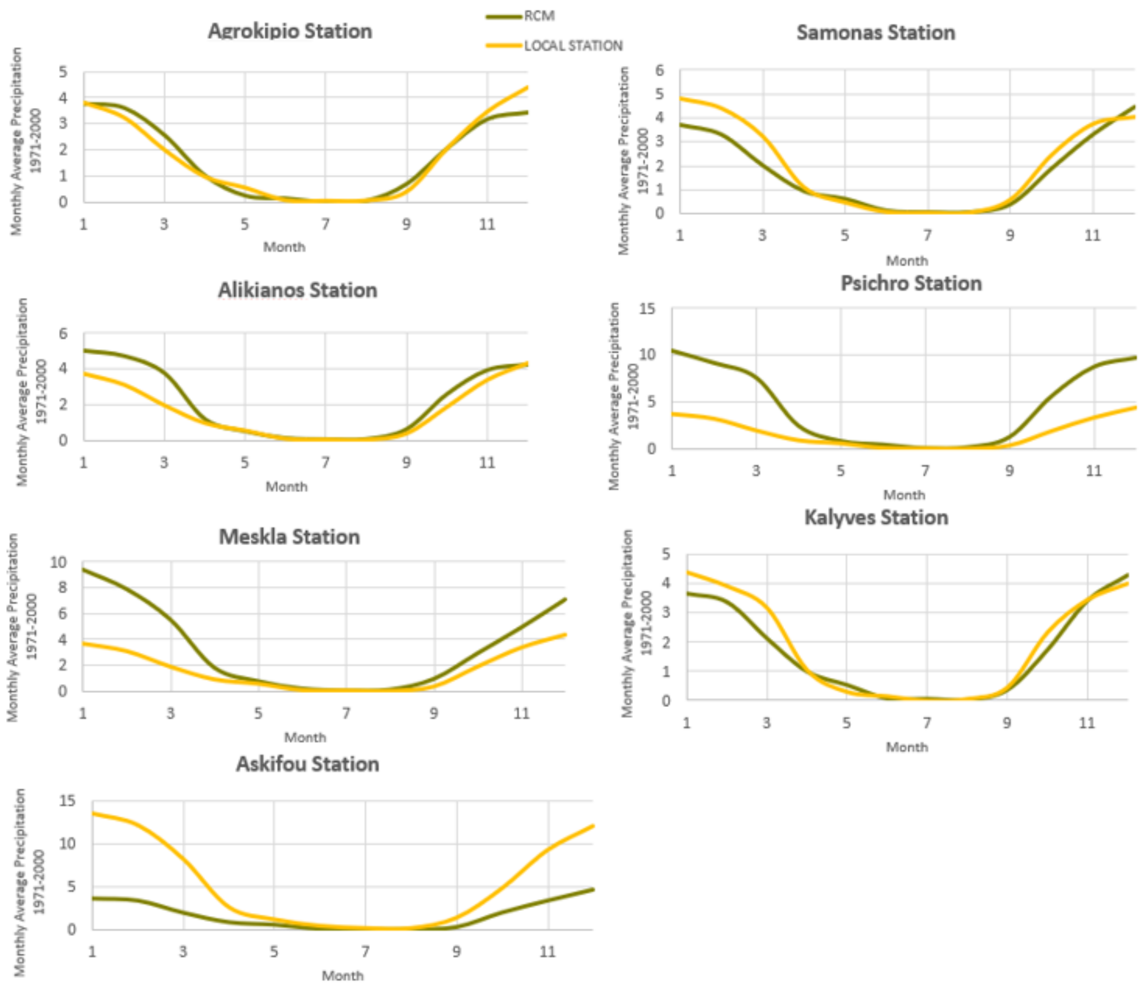

Figure 55 Comparison of precipitation data from the model with local weather stations.

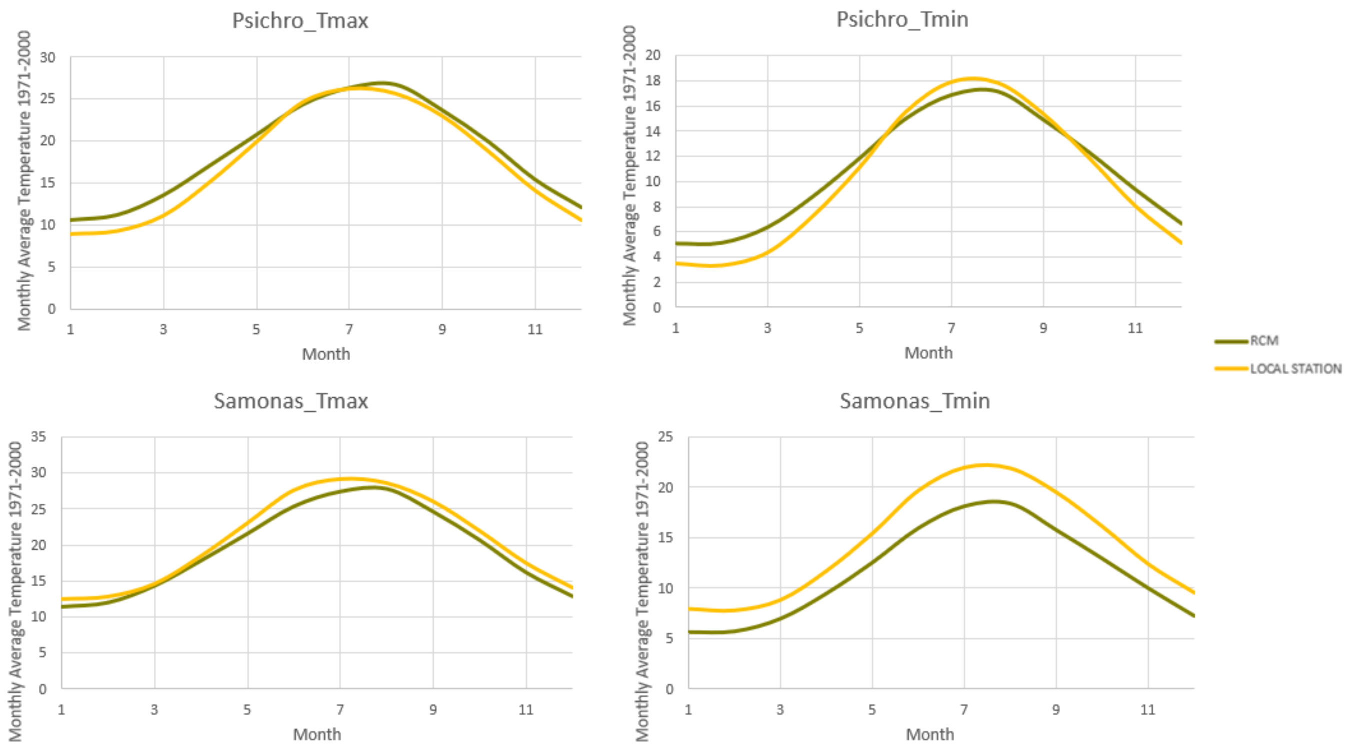

Figure 56 Comparison of temperature data from the model with local weather stations.

Table 19 Correction factor for each station for precipitation.

Month	Agrokipio	Alikianos	Meskla	Psichro Pigadi	Samonas	Kalyves	Askifou
Jan	1.01	0.75	0.40	0.35	1.30	1.20	3.74
Feb	0.89	0.67	0.40	0.35	1.34	1.17	3.61
Mar	0.78	0.53	0.35	0.26	1.62	1.50	4.19
Apr	0.95	0.84	0.51	0.38	1.20	1.05	3.01
May	2.15	1.13	0.76	0.77	0.81	0.57	2.02
Jun	0.47	0.94	0.50	0.28	0.81	1.85	4.50
Jul	5.01	1.17	0.91	4.20	1.07	0.10	7.01
Aug	1.04	0.86	0.34	0.40	1.30	1.50	4.43
Sep	0.57	0.66	0.40	0.31	1.58	1.21	4.66
Oct	0.99	0.74	0.65	0.34	1.31	1.34	2.41
Nov	1.09	0.87	0.69	0.38	1.13	1.01	2.74
Dec	1.28	1.03	0.62	0.45	0.91	0.94	2.59

Table 20 Correction factor for each station for temperature.

Month	Psichro_Tmax	Psichro_Tmin	Samonas_Tmax	Samonas_Tmin
Jan	0.84	0.69	1.09	1.41
Feb	0.83	0.66	1.07	1.36
Mar	0.82	0.69	1.02	1.27
Apr	0.88	0.83	1.03	1.23
May	0.96	0.94	1.07	1.23
Jun	1.01	1.03	1.09	1.23
Jul	1.00	1.06	1.06	1.21
Aug	0.96	1.03	1.03	1.19
Sep	0.97	1.03	1.05	1.23
Oct	0.94	0.96	1.06	1.24
Nov	0.91	0.86	1.08	1.24
Dec	0.87	0.77	1.09	1.32

The monthly average surface flow in cubic meters per second (cms) of the two main rivers, 'Koiliaris' and 'Keritis,' under two scenarios (RCP4.5, RCP8.5) for the years 2022-2100, is depicted in Figure 57 and Figure 58. Tables 21 present the statistical properties of the river Basins.

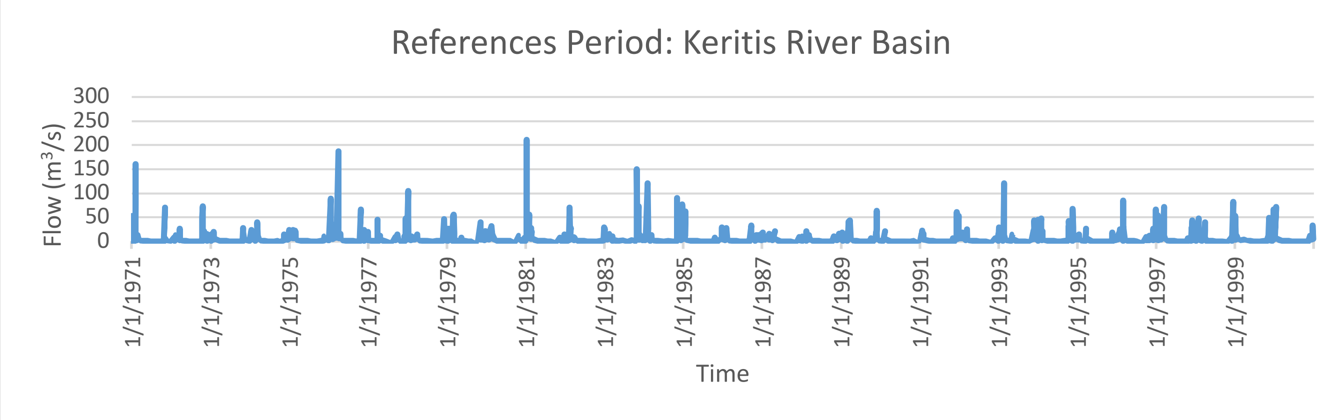

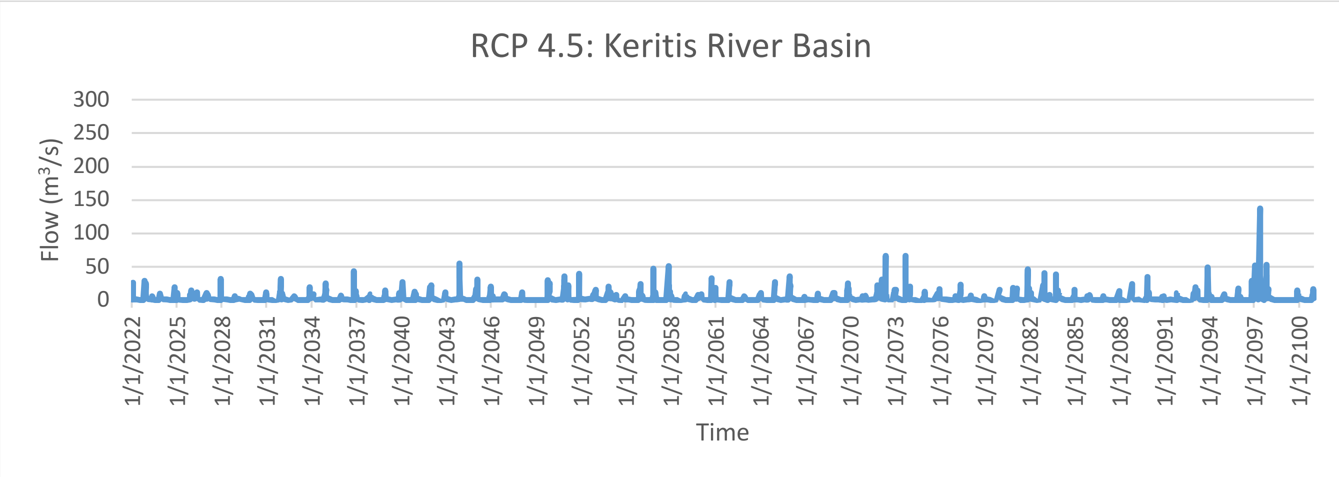

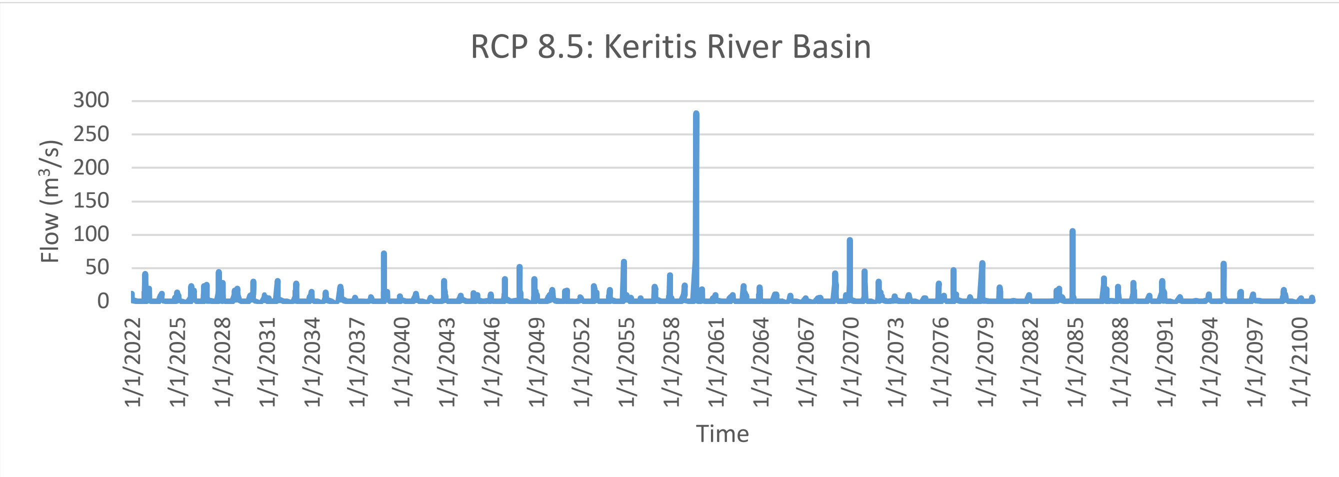

Figure 57 Surface flow of Keritis river for each scenario.

This project is part of the PRIMA programme supported by the European Union.
GA n° [2041] [LENSES] [Call 2020 Section 1 Nexus IA]

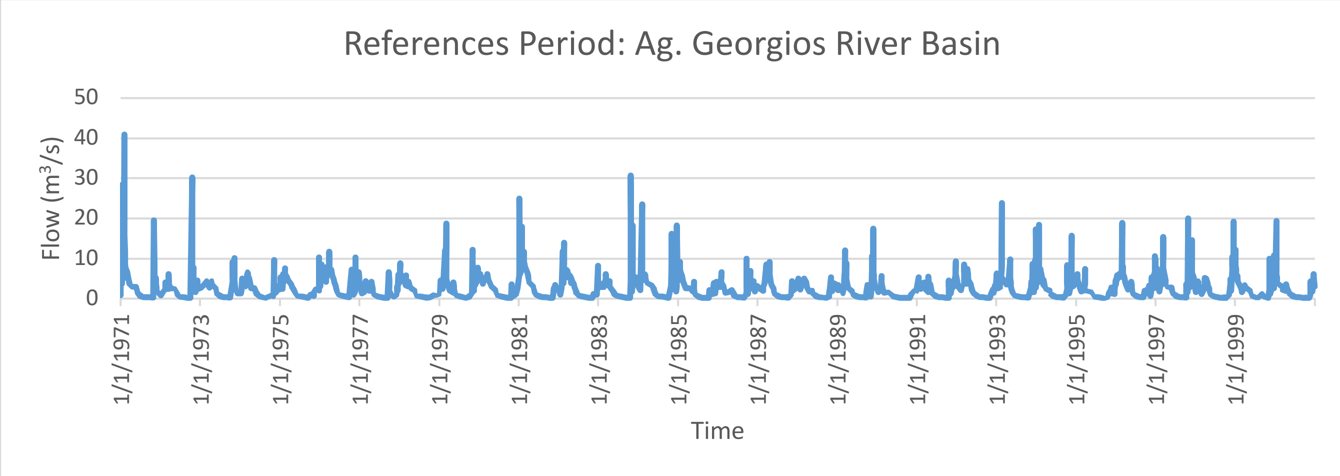

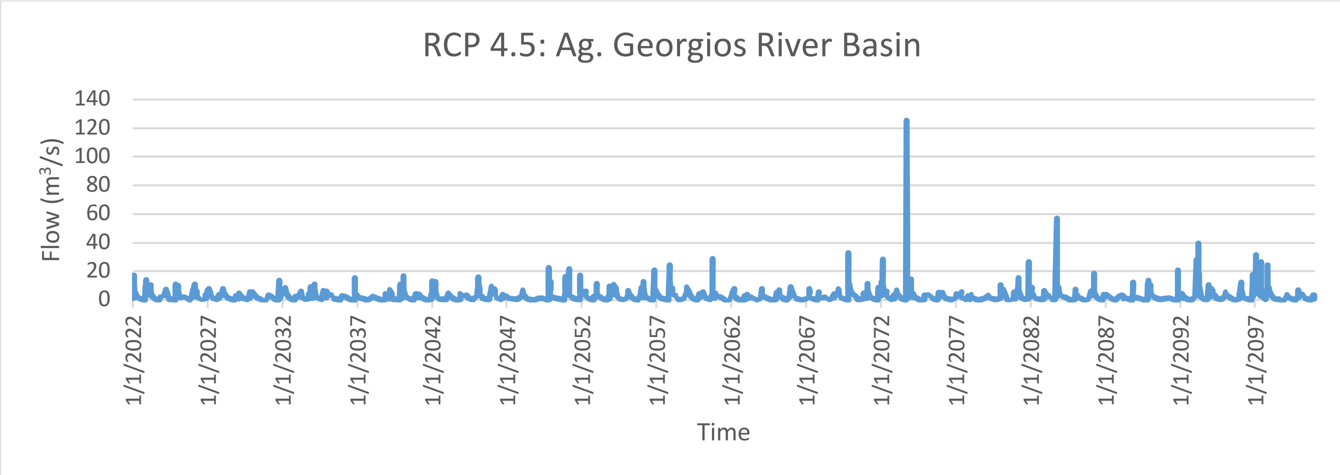

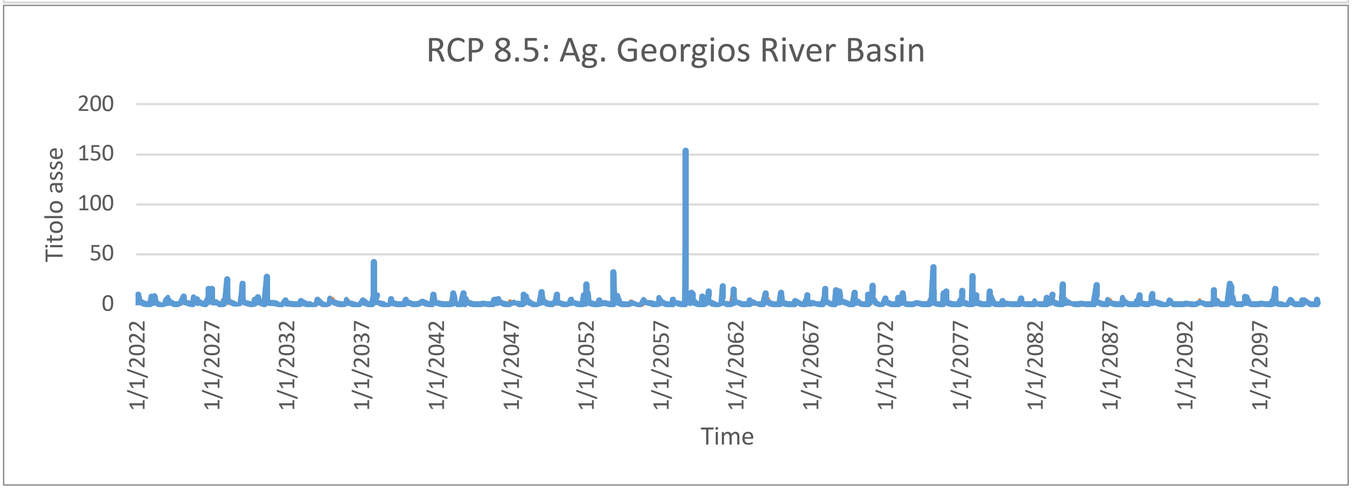

Figure 58 Surface flow of Koiliaris river for each scenario.

Table 21 Statistical properties of climate change outcomes in Keritis River Basin.

	Reference Period		RCP4.5		RCP 8.5	
	Average	St.Dev.	Average	St.Dev.	Average	St.Dev.
Keritis River Basin	1.99	6.32	1.27	0.96	0.75	1.16
Koiliaris River Basin	2.04	2.02	1.38	1.17	1.10	1.11

6.2.6. Tarquinia Plain (IT)

The model reference period for the Tarquinia Region was created for the RCP 4.5 scenario and the RCP 8.5 scenario. The graphs of the obtained results are shown in Figures 59-61. In addition, statistical results for the values obtained from the model results are given in Table 23.

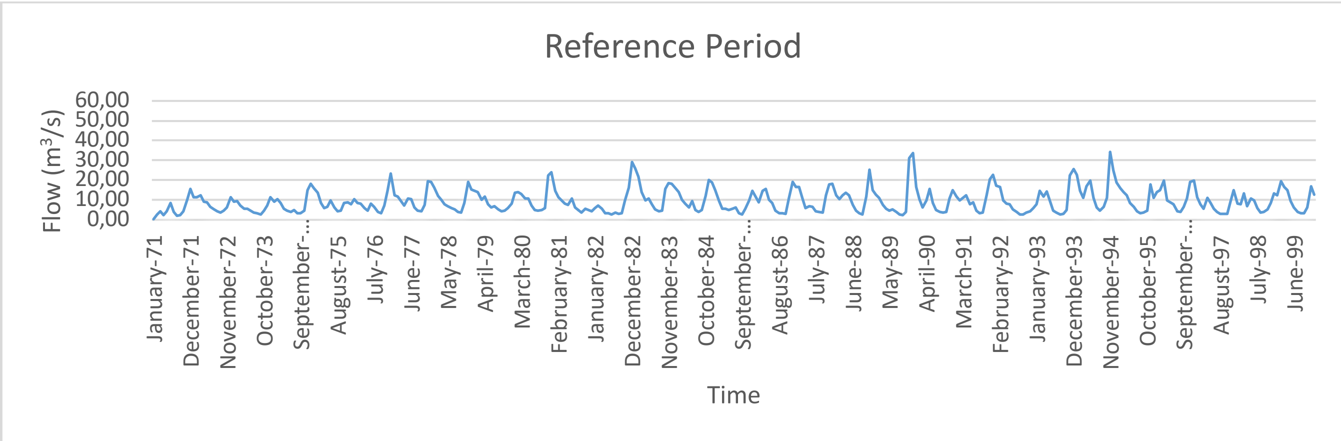

Figure 59 Tarquinia References Period Outflow (1971-2000).

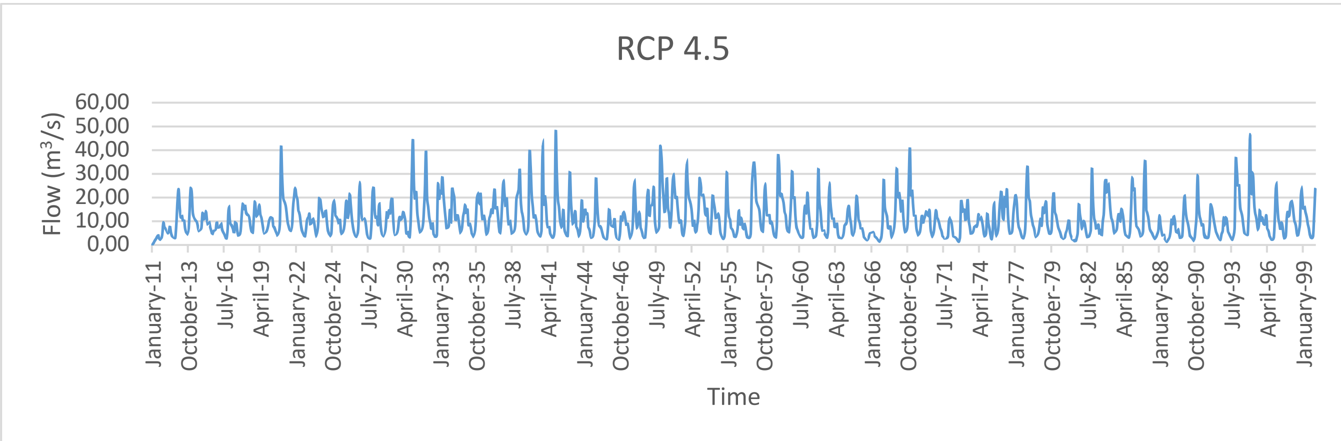

Figure 60 Tarquinia RCP 4.5. Scenarios Outflow (2011-2100).

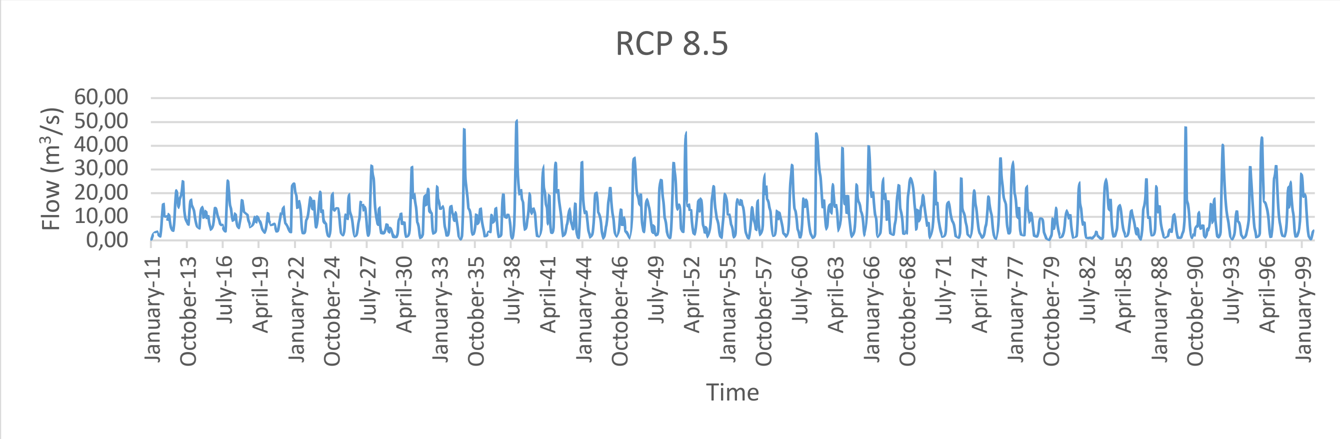

Figure 61 Tarquinia RCP 8.5. Scenarios Outflow (2011-2100).

Table 22 Statistical properties of climate change outcomes.

Tarquinia	Reference Period		RCP 4.5		RCP 8.5	
	Average	**St. Dev.**	**Average**	**St. Dev.**	**Average**	**Std. Dev.**
	9.35	5.85	10.80	7.66	9.90	8.19

6.3. Water Accounting Modeling

6.3.1. Middle Jordan Valley (JO)

The water accounting model of Deir Alla, the same as the rest of the pilot areas, has been developed on WEAP software. Since the pilot area was relatively small, the demand sites of the pilot have been represented as the sectors as; agriculture, domestic, and industry (Figure 62). As water sources, Wadi Rajib represents the surface flow, and Zarqa and Kurnub represent the groundwater flow contribution to the pilot. According to the stakeholder expert opinions and official reports of Jordan's water resources (Jordan Ministry of Water Irrigation, 2023), the modelled HEC-HMS outflow has been divided and defined as the inflow for the surface water and recharge for the groundwater sources. As there were no stream gauges on downstream of the pilot, the model has been validated according to the stakeholder expert opinions.

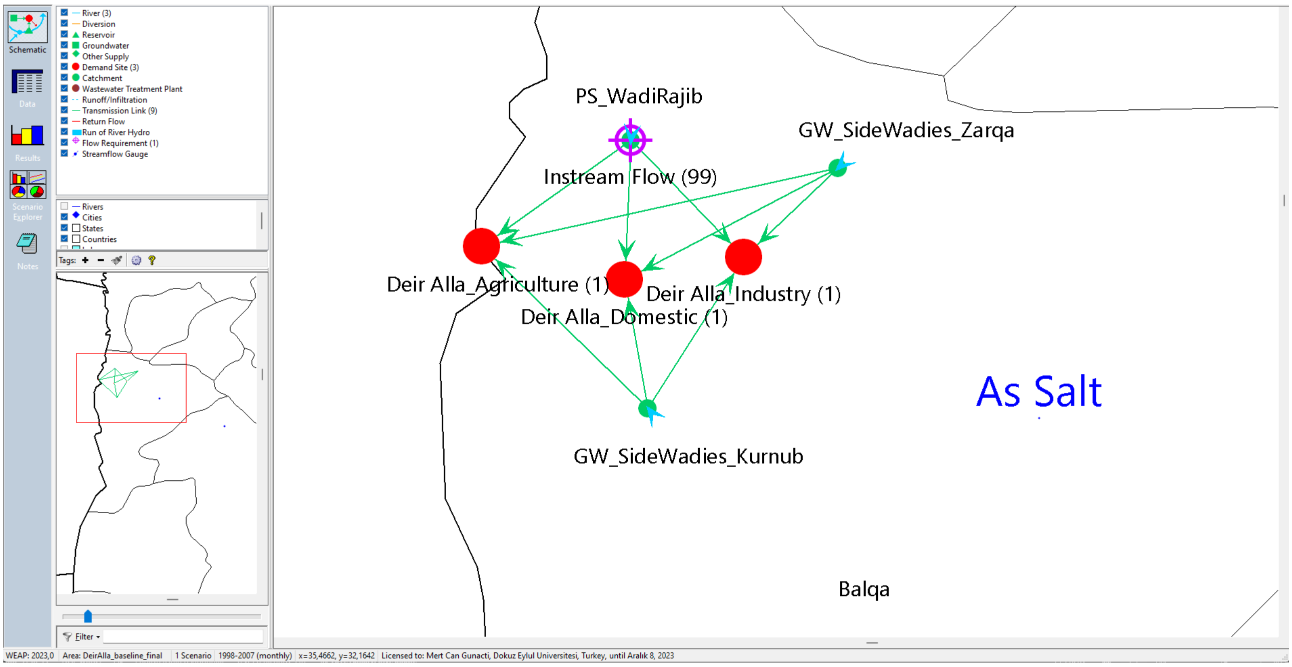

Figure 62 Deir Alla WEAP Schematic.

Based on the developed model, water accounting indicators of Nexus (sectoral water use, total amount of supply, total amount of demand, supply demand ratio, unmet demand, reliability of source, coverage of demand, unmet instream flow requirement, water exploitation index, and groundwater exploitation index) have been determined for the baseline and RCP4.5 and RCP8.5 scenarios for each sector and overall average. Average irrigation productivity and unit gross revenues have been calculated according to the crop pattern, crop yields, and crop unit gross revenues that the pilot reported (Figures 63-74).

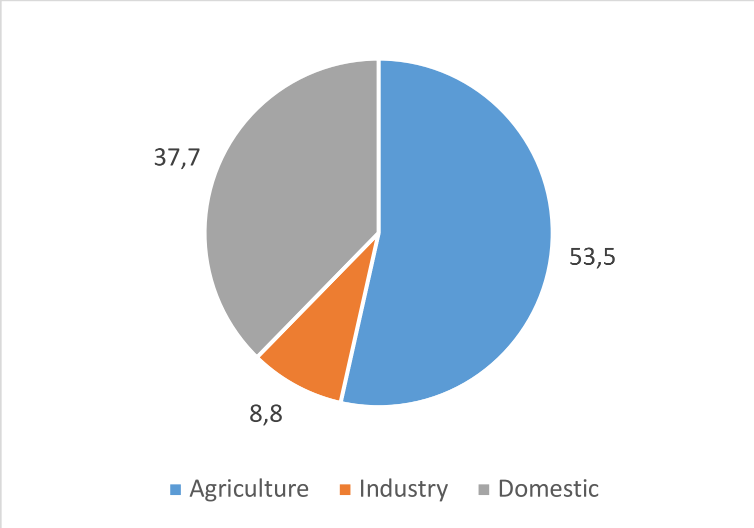

Figure 63 Deir Alla sectoral water use.

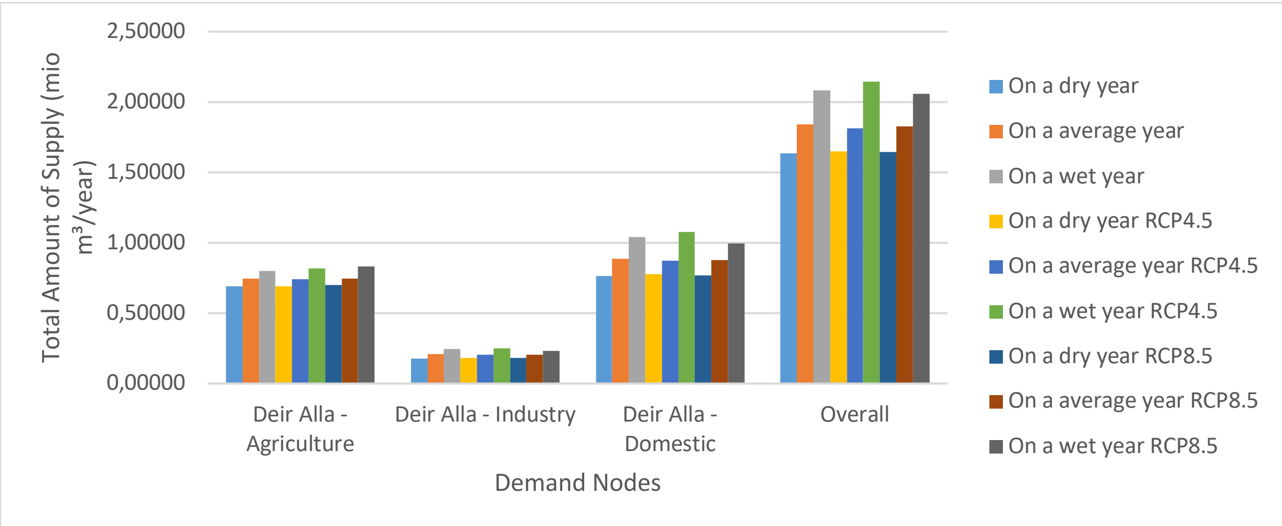

Figure 64 Deir Alla total amount of supply.

This project is part of the PRIMA programme supported by the European Union.
GA n° [2041] [LENSES] [Call 2020 Section 1 Nexus IA]

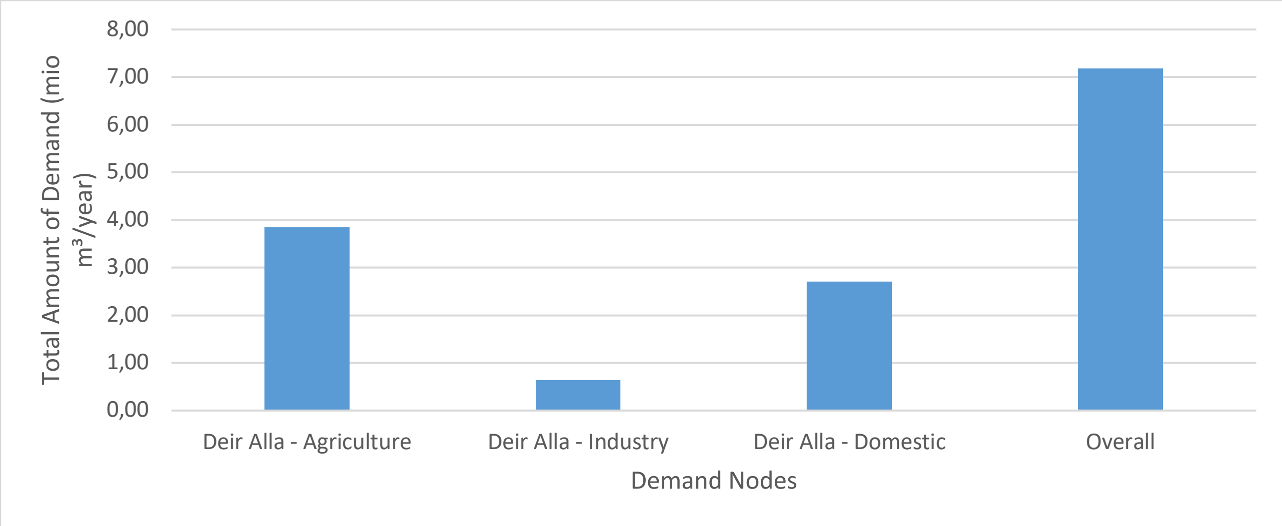

Figure 65 Deir Alla total amount of demand.

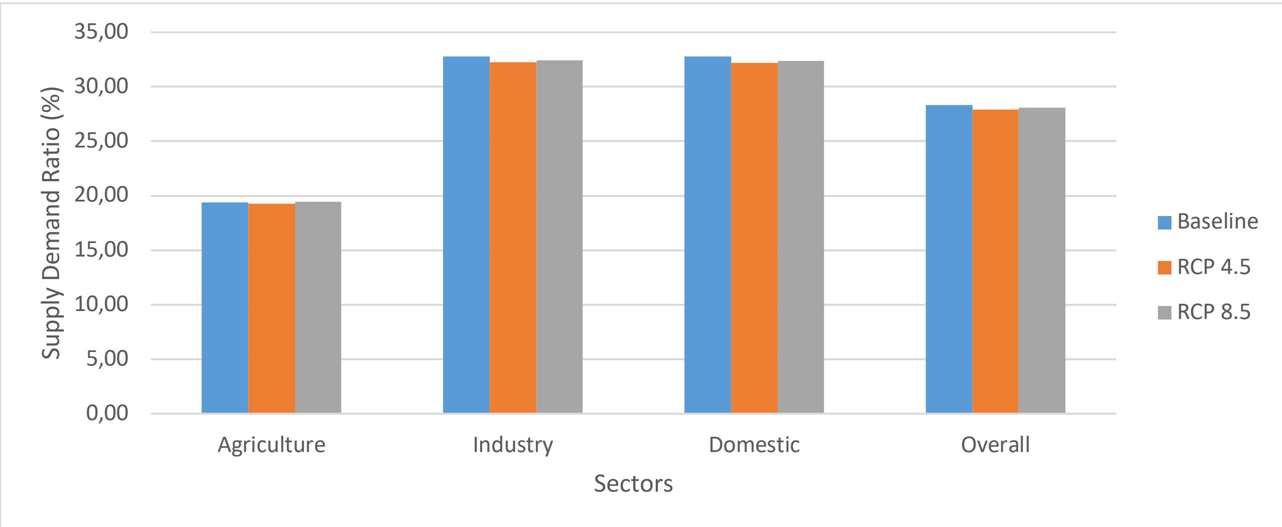

Figure 66 Deir Alla total supply demand ratio.

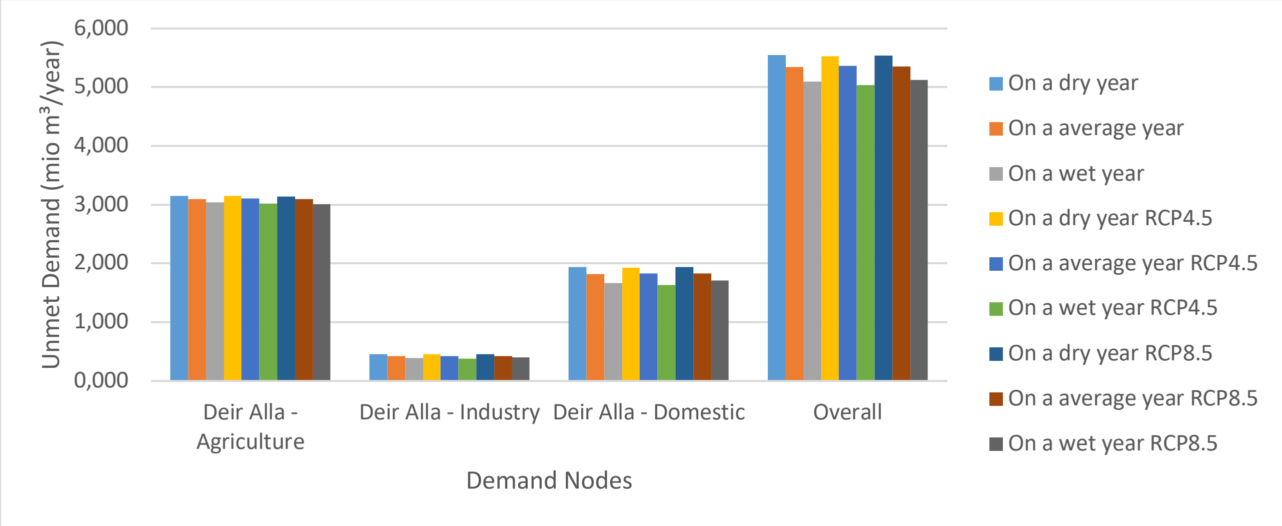

Figure 67 Deir Alla unmet demand.

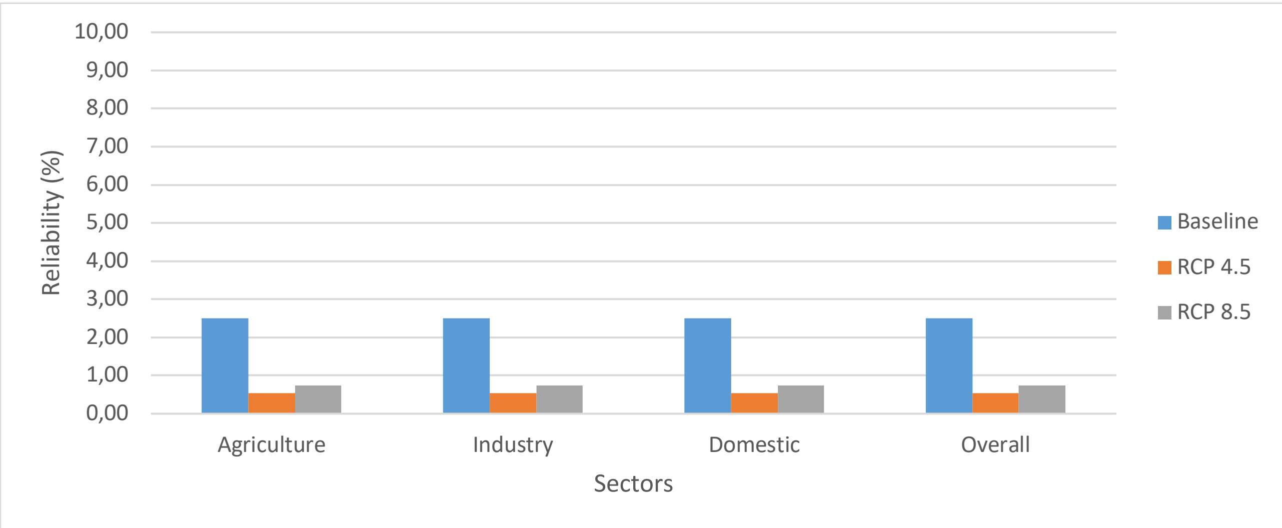

Figure 68 Deir Alla reliability of source.

This project is part of the PRIMA programme supported by the European Union.
GA n° [2041] [LENSES] [Call 2020 Section 1 Nexus IA]

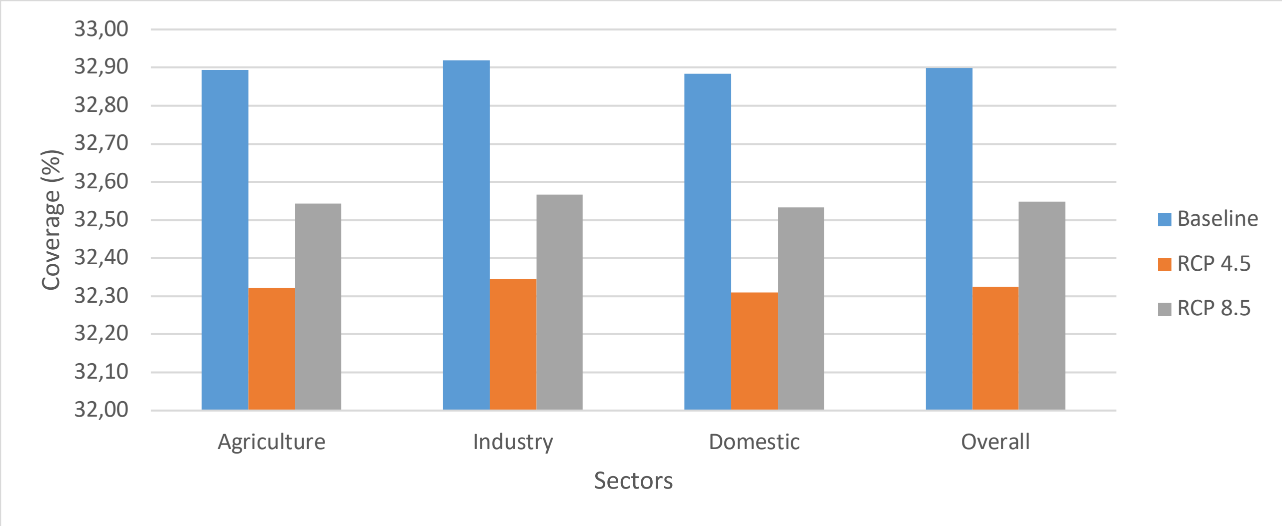

Figure 69 Deir Alla coverage of demand.

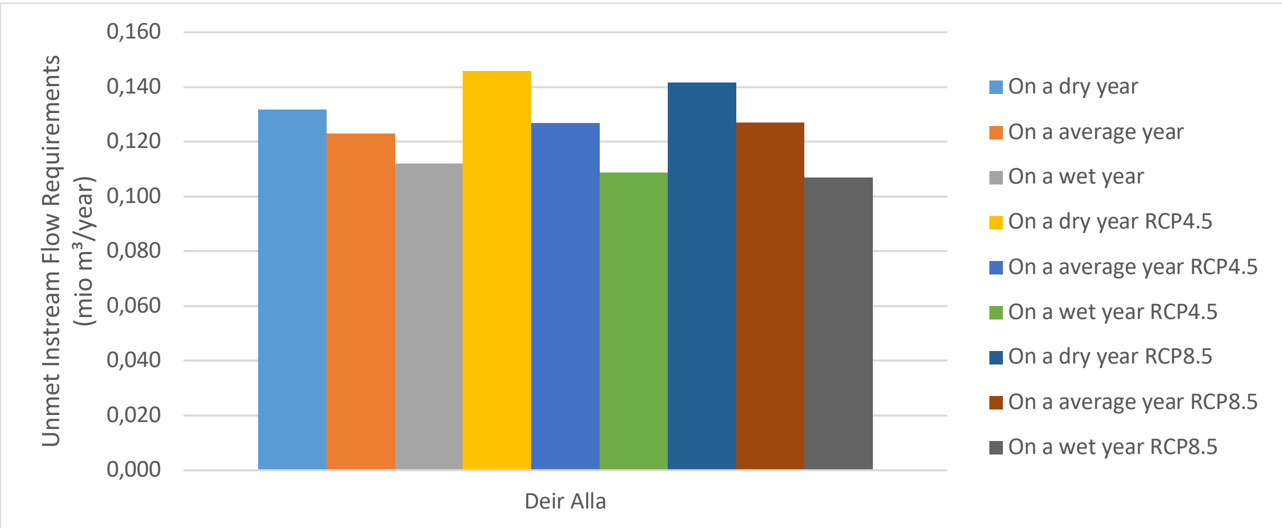

Figure 70 Deir Alla unmet instream flow requirements.

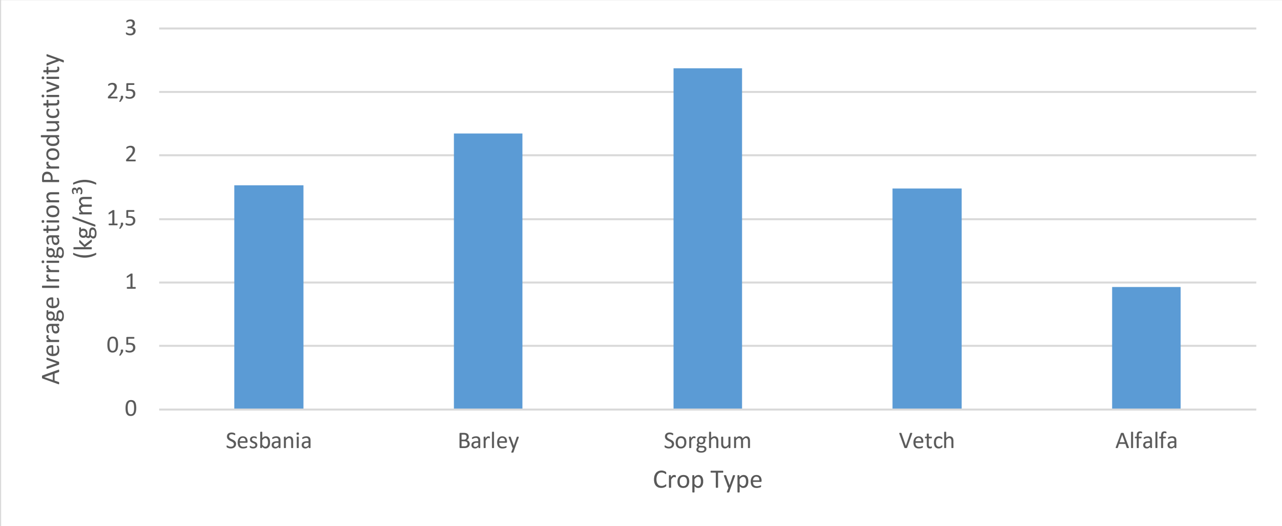

Figure 71 Deir Alla average irrigation productivity.

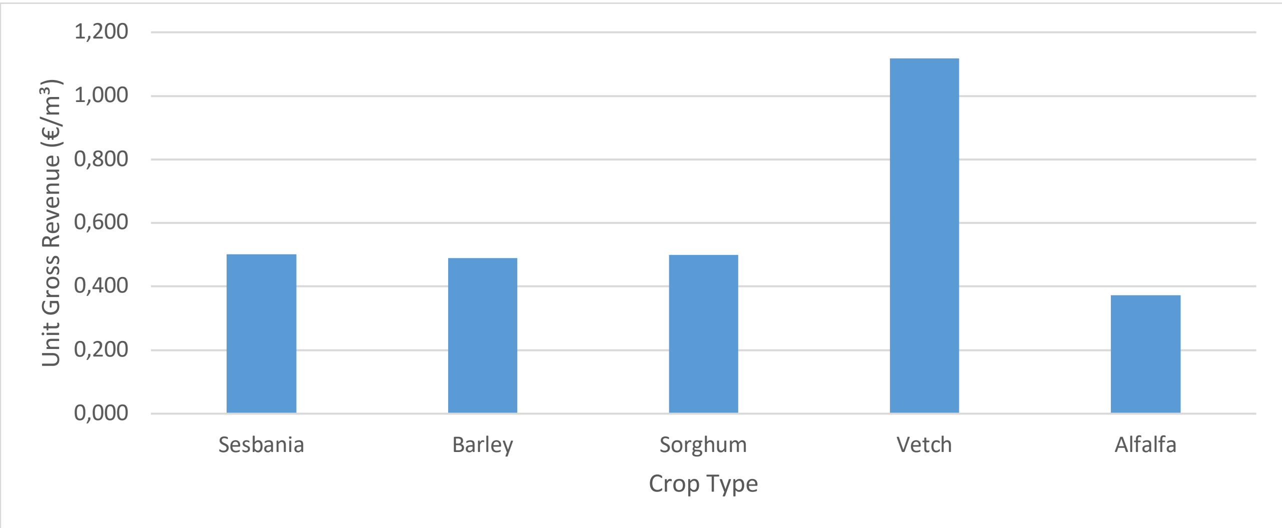

Figure 72 Deir Alla crop unit gross revenue.

This project is part of the PRIMA programme supported by the European Union.
GA n° [2041] [LENSES] [Call 2020 Section 1 Nexus IA]

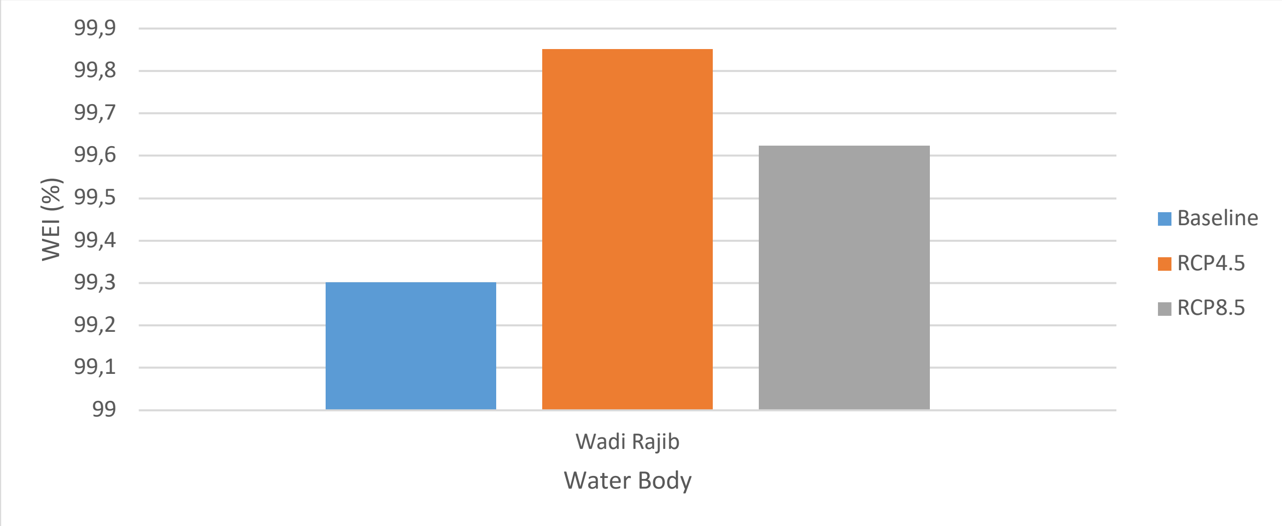

Figure 73 Deir Alla water exploitation index

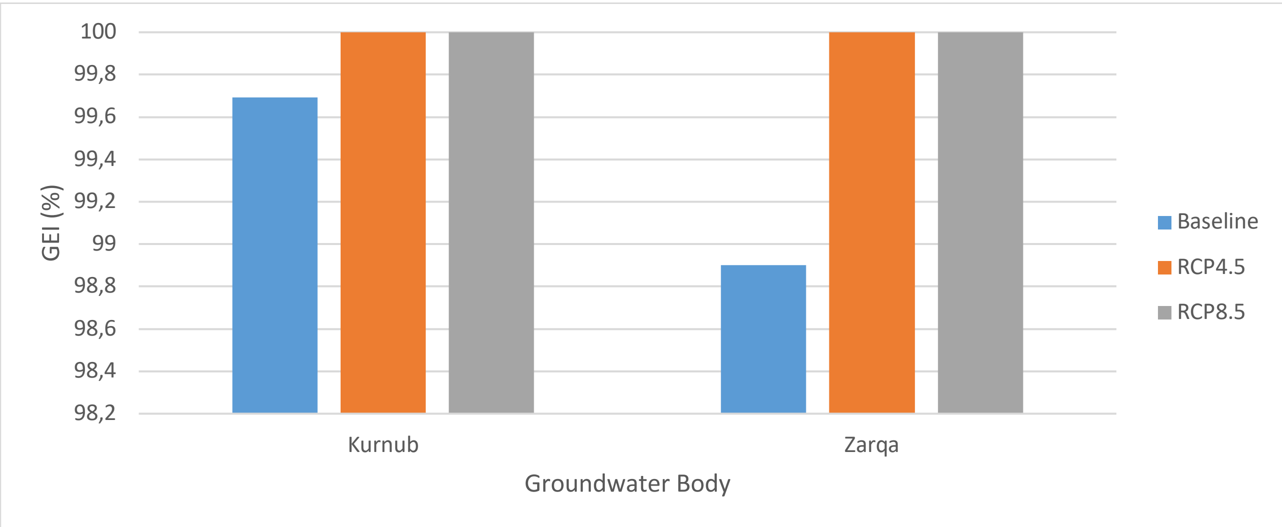

Figure 74 Deir Alla groundwater exploitation index

6.3.2. Gediz Basin & Delta (TR)

To assess the water accounting of Menemen pilot area, whole Gediz River Basin has been included in the WEAP model since the Menemen plain is located on the outlet of Gediz River Basin. There are 16 agricultural and 1 environmental demand node defined in the model. Although there seem to be only 2 sectors defined (agriculture and environment), the industry sector is represented by the industrial crops (cotton) that are cultivated in the basin (Figure 75). The Demirköprü Dam and the Marmara Lake are the major water resources of the basin. The stream gauge available on downstream of the main river is utilized in the comparison of observed-modelled results of the model (Figure 76) (Table 24).

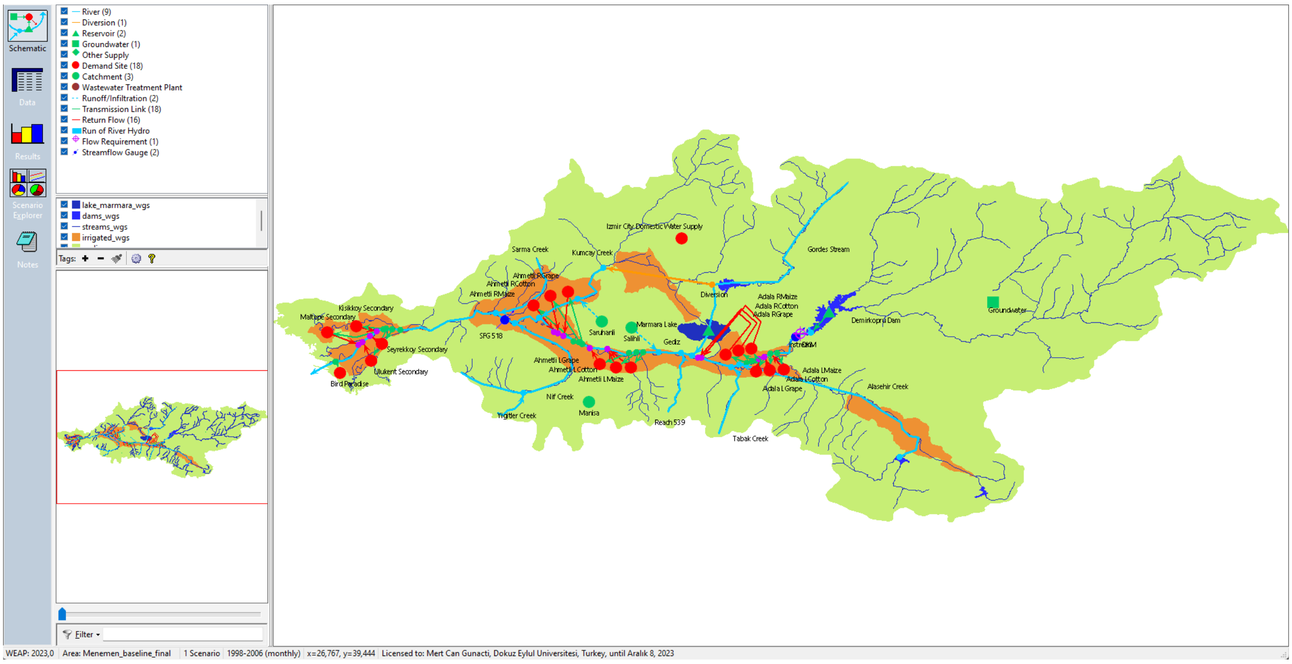

Figure 75 Gediz WEAP Schematic.

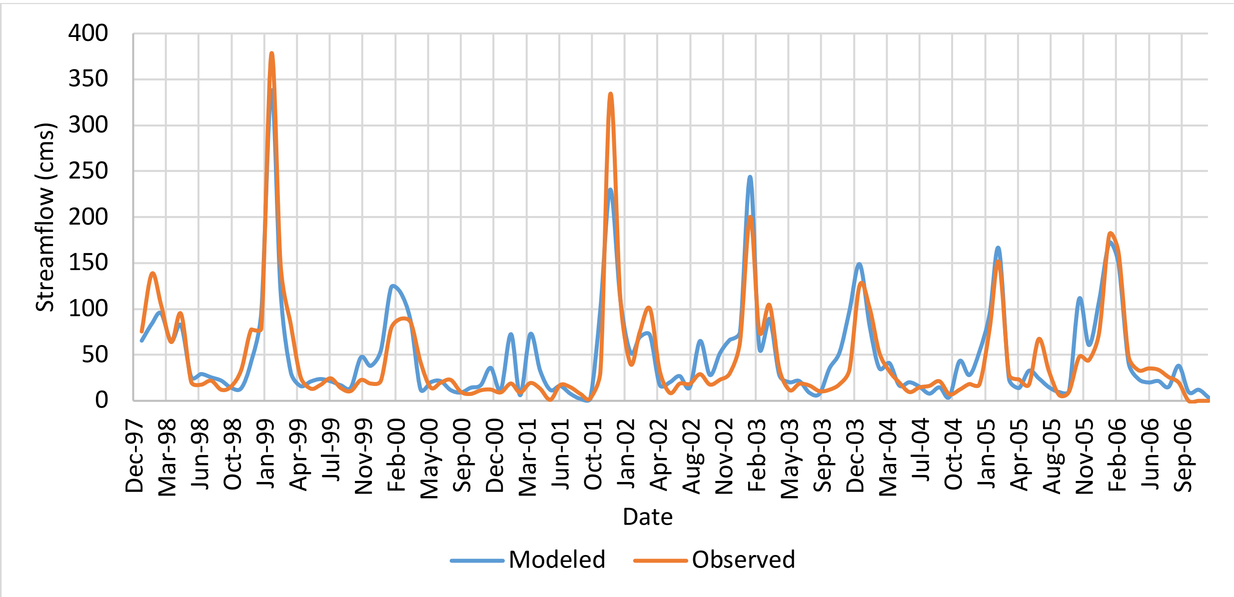

Figure 76 Gediz WEAP model observed-modelled streamflow comparison.

Table 23 Goodness of fit statistics of Gediz WEAP model.

Goodness-of-fit statistics	
NSE	0.82
KGE	0.85
NRMSE %	53
PBIAS%	7.5
RSR	0.43
R^2	0.82

Based on the developed model, water accounting indicators of Nexus (sectoral water use, total amount of supply, total amount of demand, supply demand ratio, unmet demand, reliability of source, coverage of demand, unmet instream flow requirement, water exploitation index, and groundwater exploitation index) have been determined for the baseline and the climate change scenarios of RCP4.5 and RCP8.5 for each sector and overall average. Average irrigation productivity and unit gross revenues have been calculated according to the crop pattern, crop yields, and crop unit gross revenues that the pilot reported (Figures 77-97).

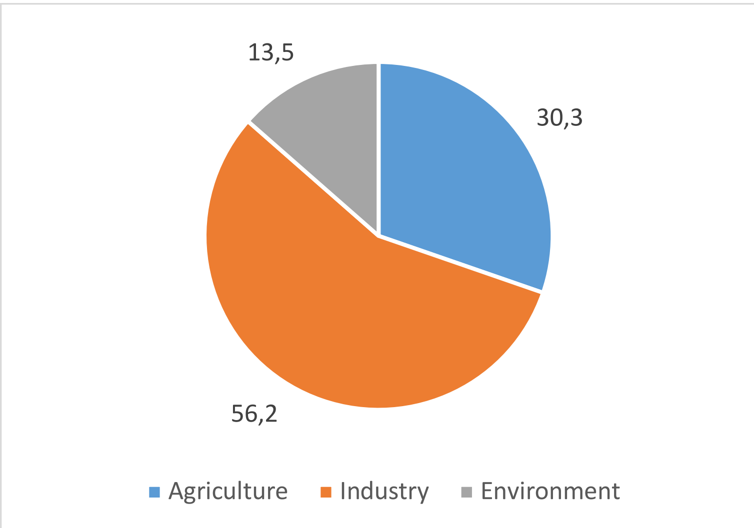

Figure 77 Gediz sectoral water use.

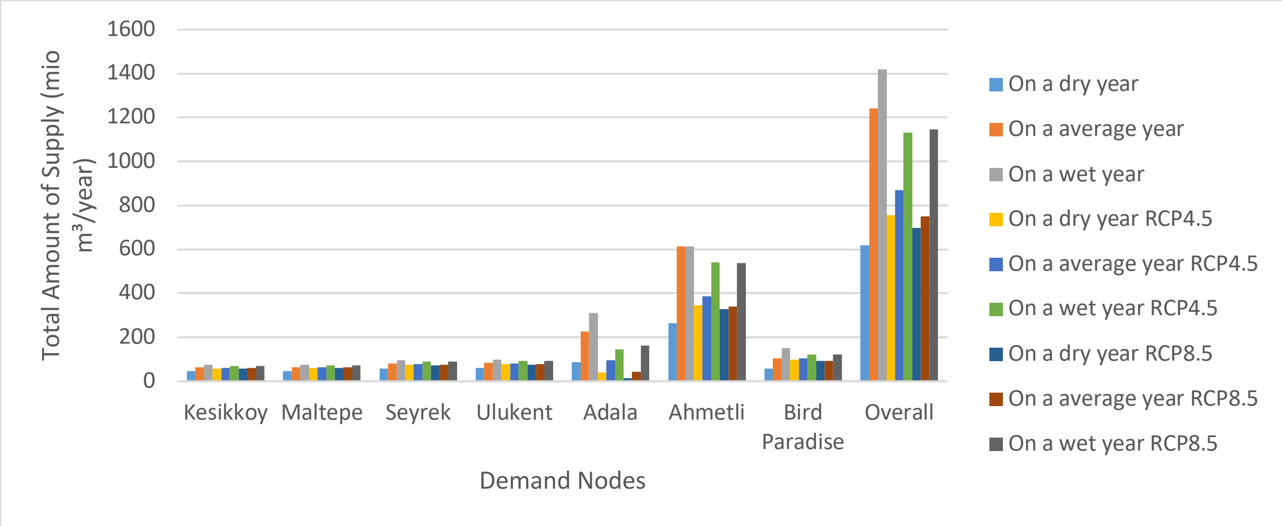

Figure 78 Gediz total amount of supply.

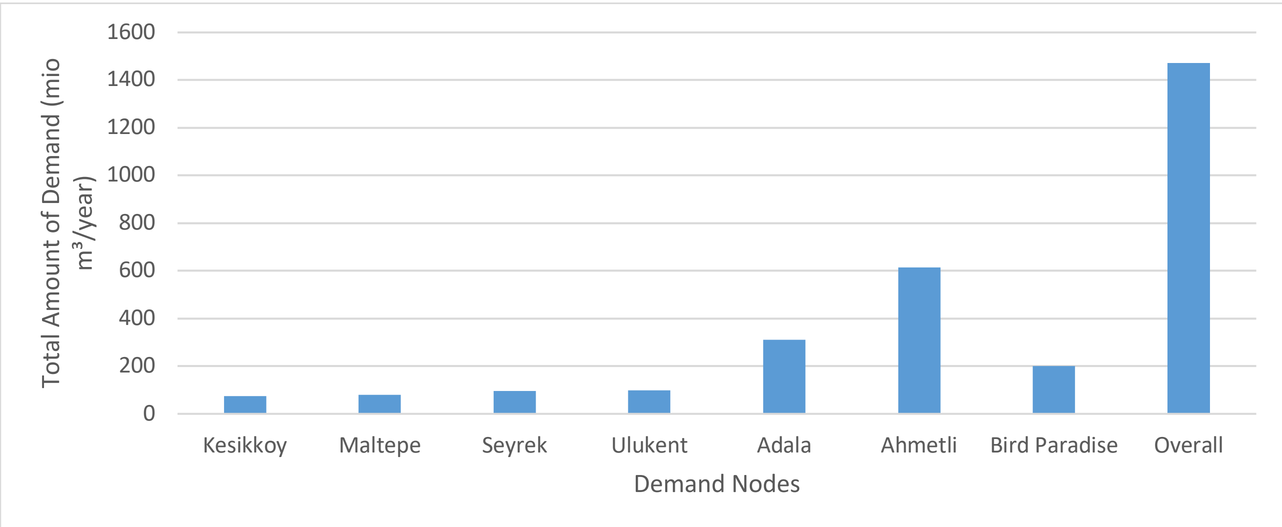

Figure 79 Gediz total amount of demand.

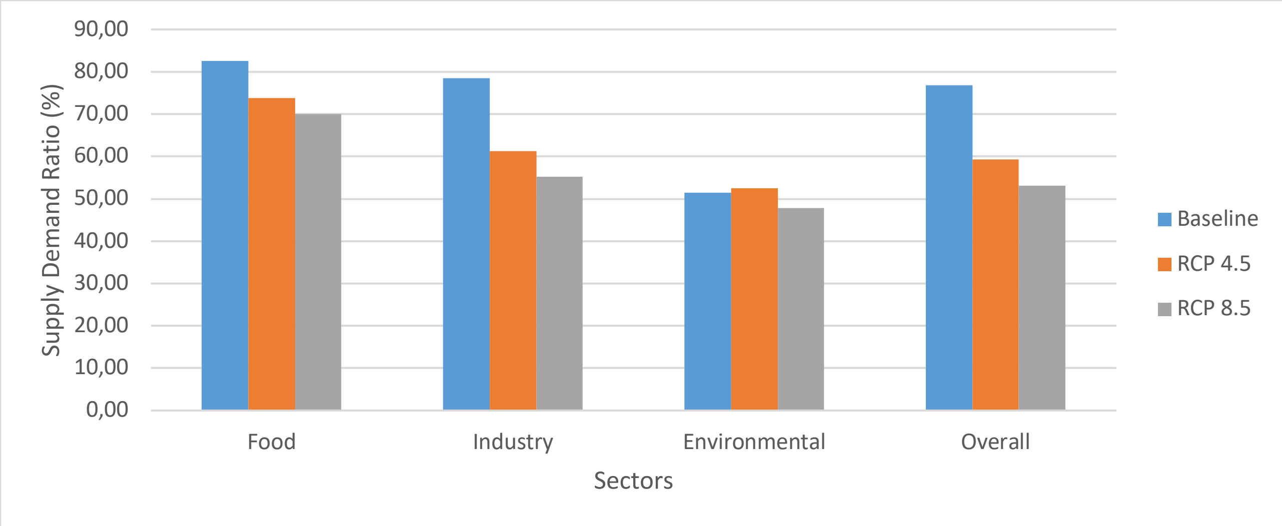

Figure 80 Gediz supply demand ratio.

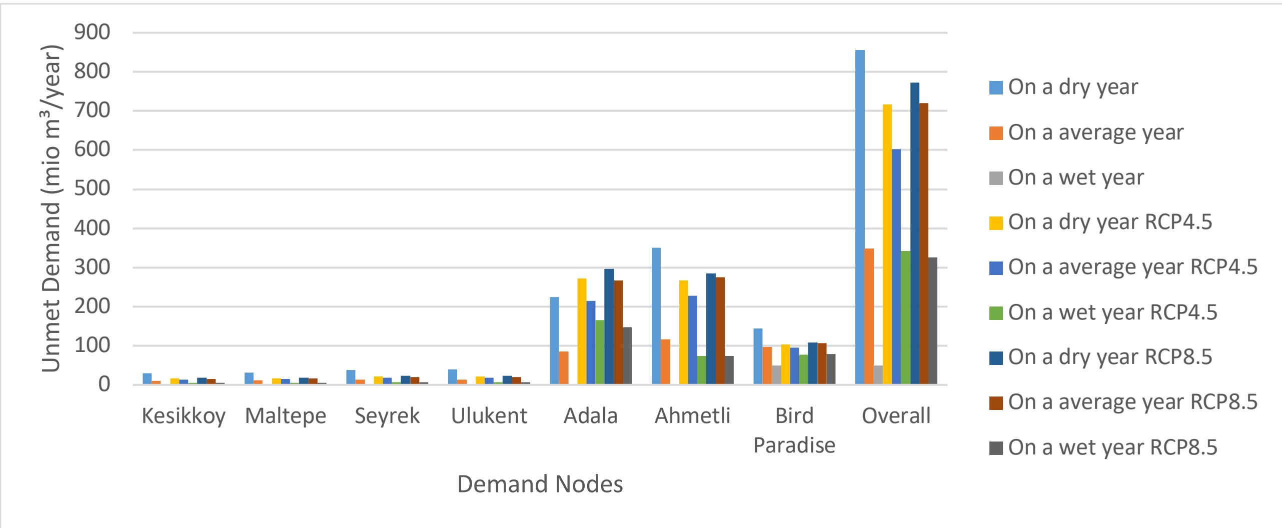

Figure 81 Gediz unmet demand.

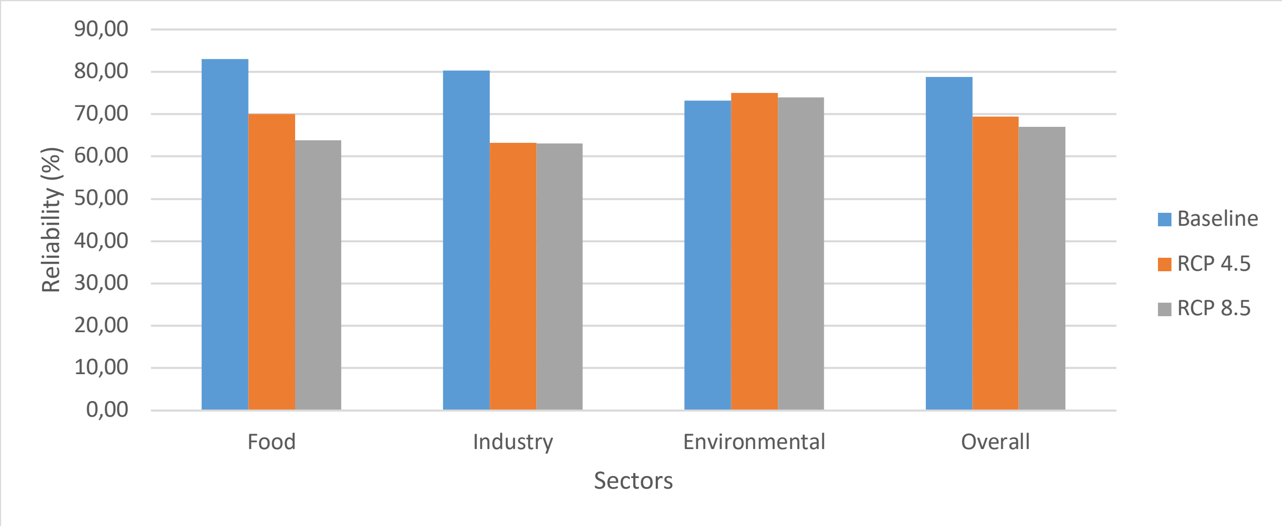

Figure 82 Gediz reliability of source.

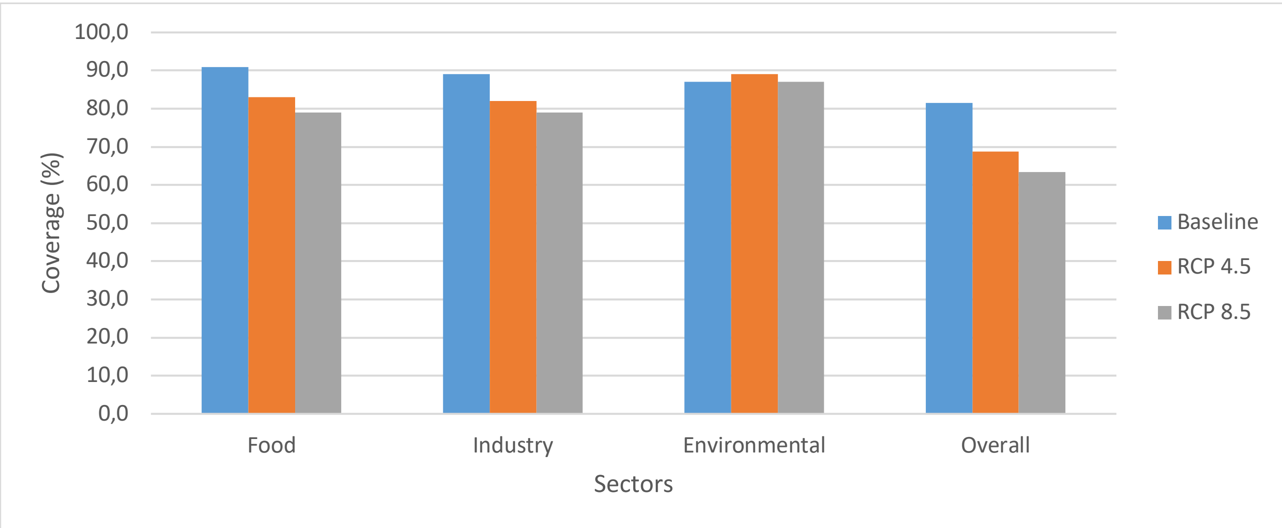

Figure 83 Gediz coverage of demand.

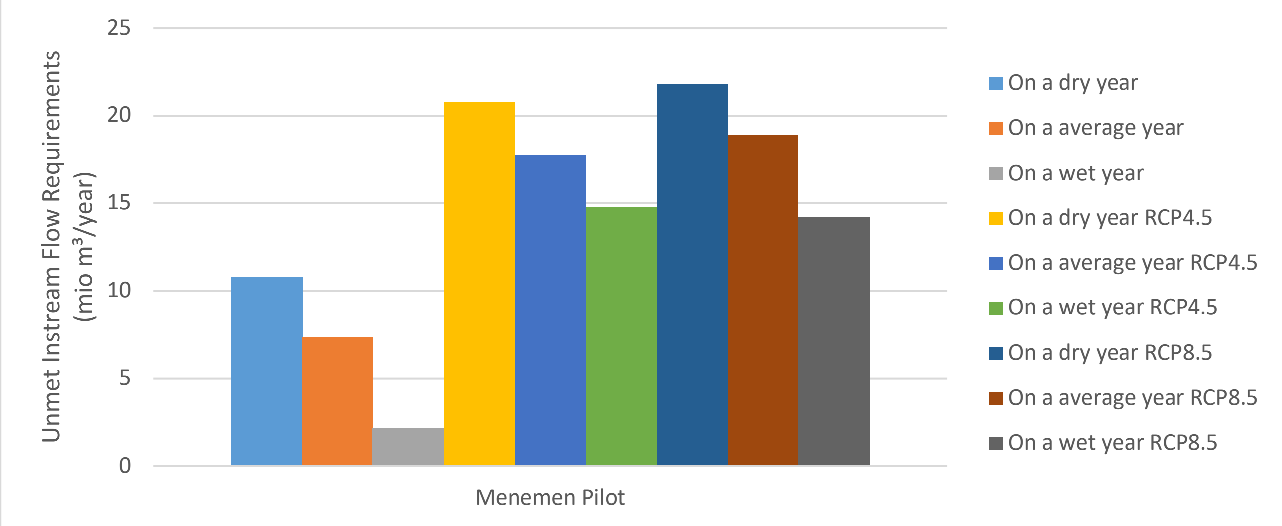

Figure 84 Gediz unmet instream flow requirements.

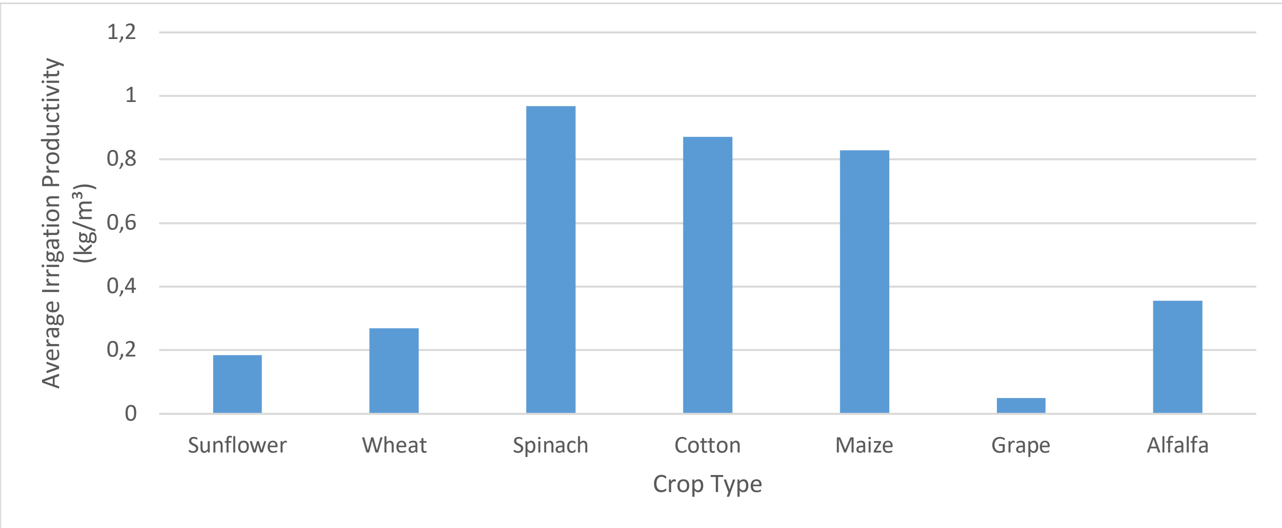

Figure 85 Average irrigation productivity of Kesikkoy demand node.

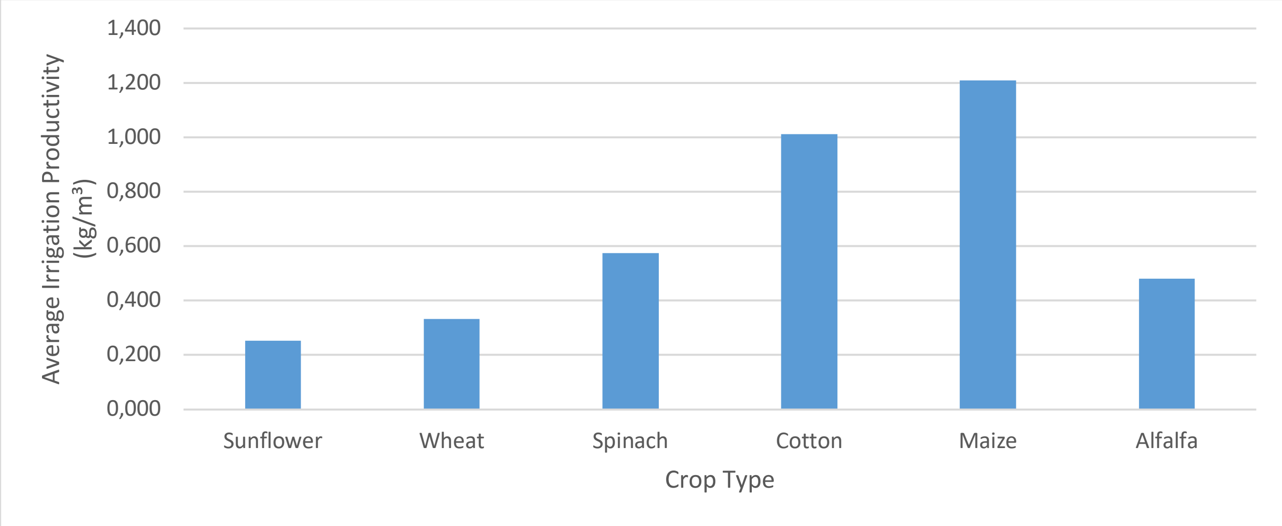

Figure 86 Average irrigation productivity of Maltepe demand node.

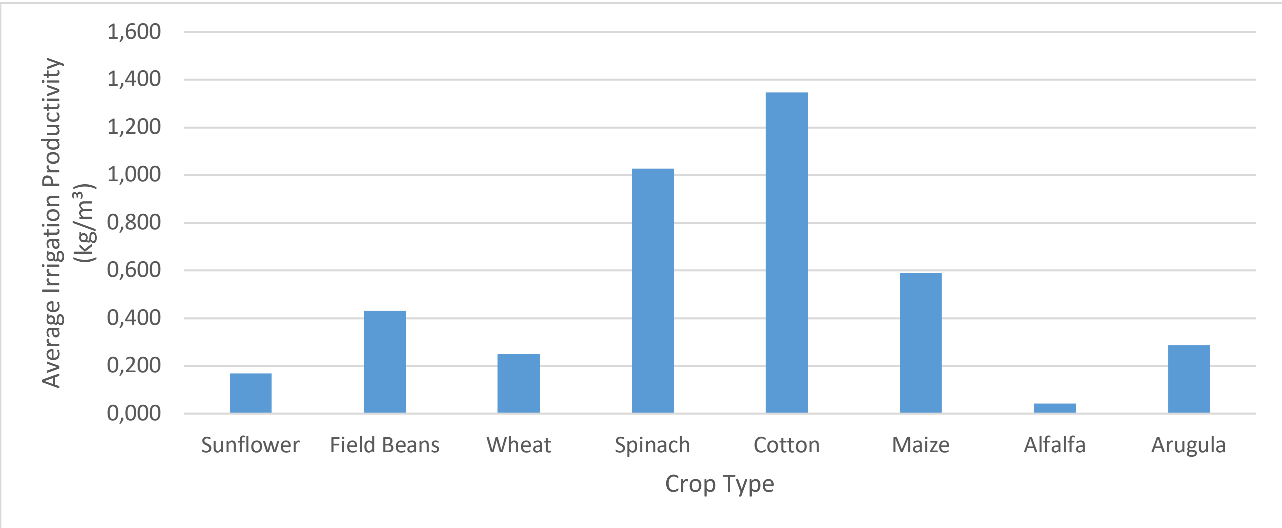

Figure 87 Average irrigation productivity of Seyrekkoy demand node.

This project is part of the PRIMA programme supported by the European Union.
GA n° [2041] [LENSES] [Call 2020 Section 1 Nexus IA]

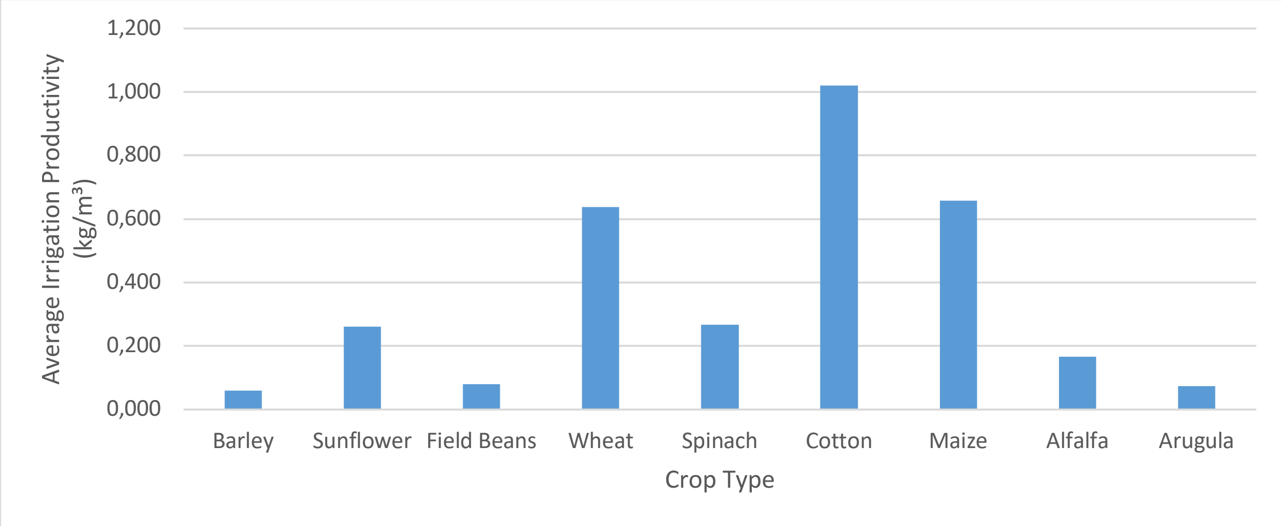

Figure 88 Average irrigation productivity of Ulukent demand node.

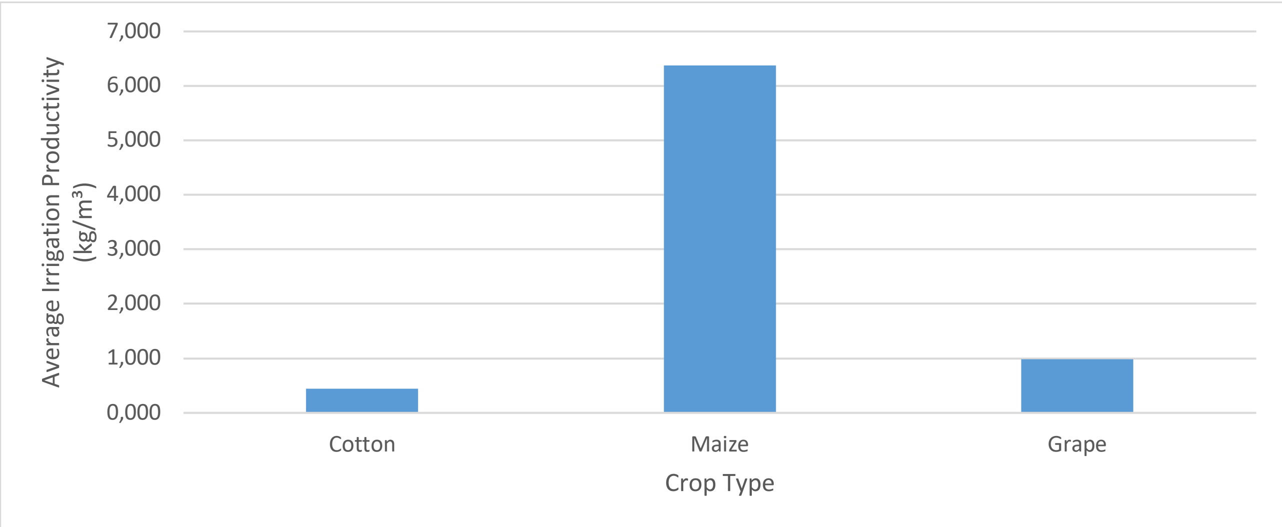

Figure 89 Average irrigation productivity of Adala demand node.

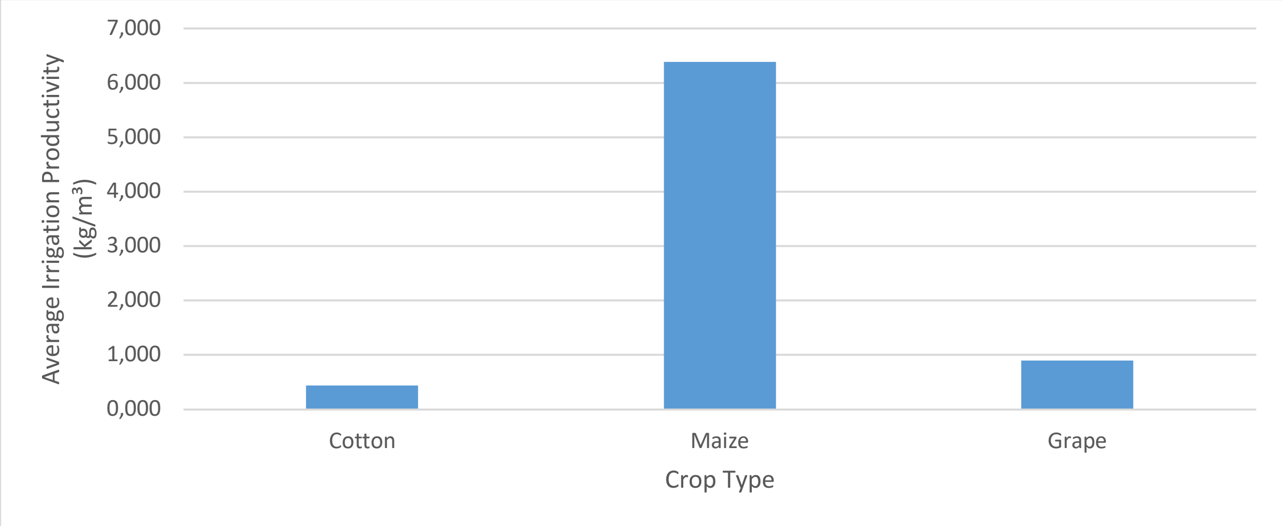

Figure 90 Average irrigation productivity of Ahmetli demand node.

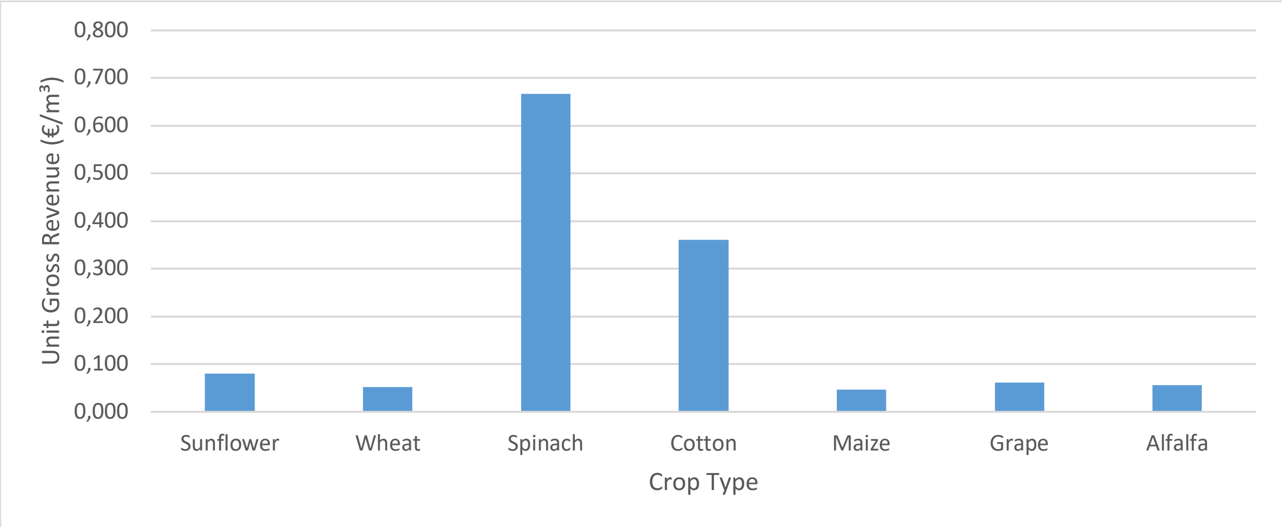

Figure 91 Unit Gross Revenue of Kesikkoy demand node.

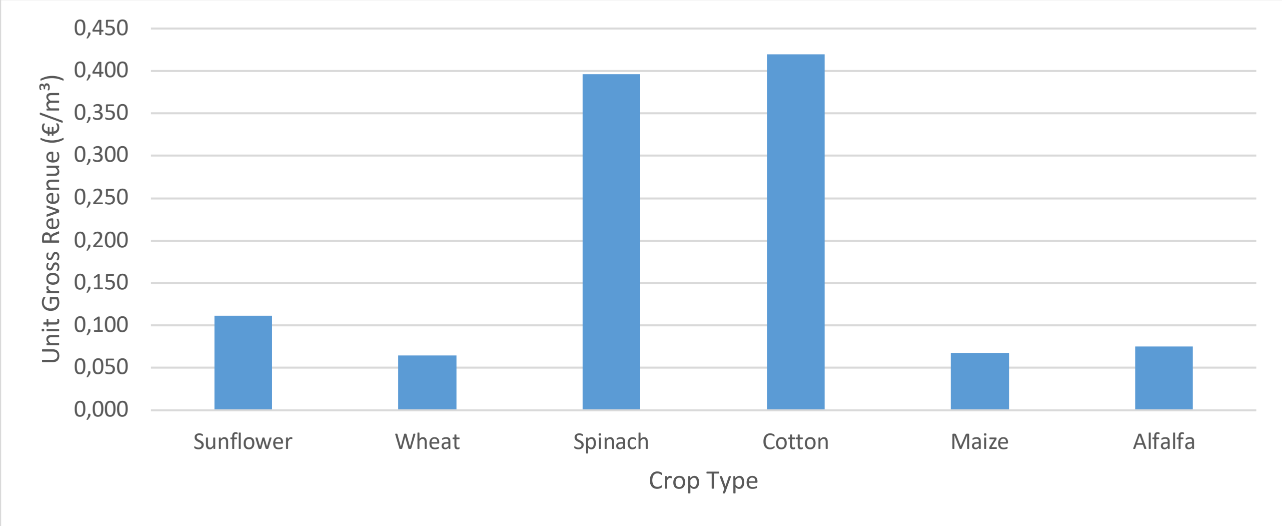

Figure 92 Unit Gross Revenue of Maltepe demand node.

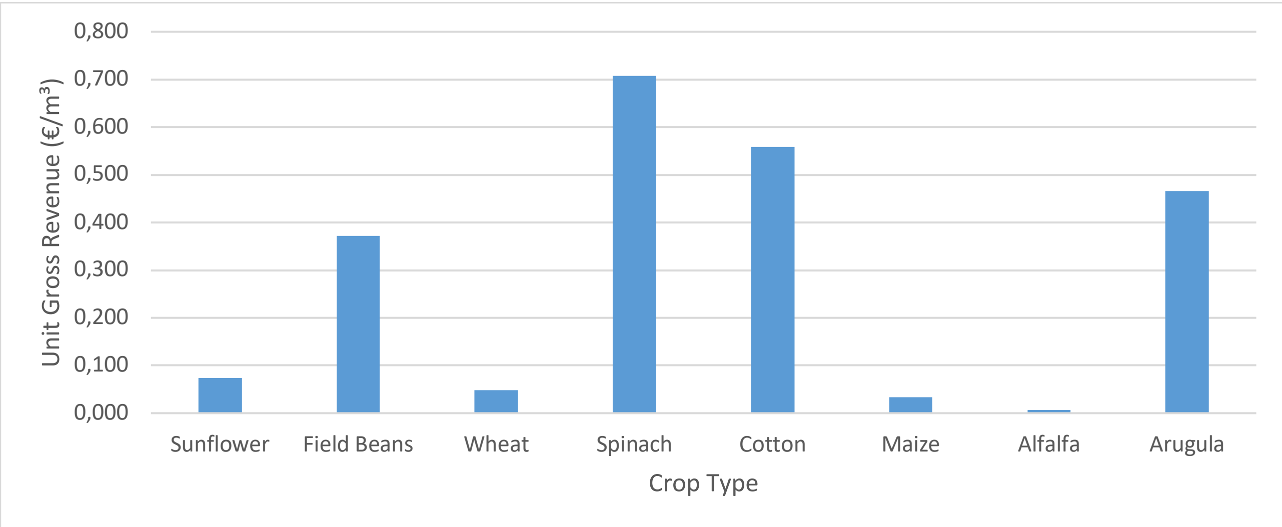

Figure 93 Unit Gross Revenue of Seyrekkoy demand node.

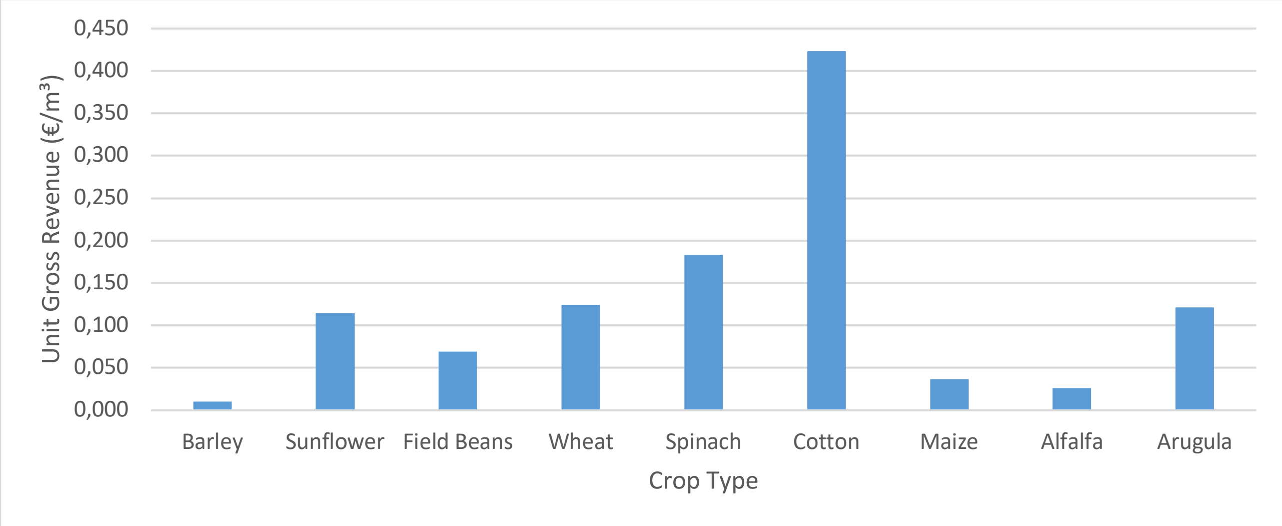

Figure 94 Unit Gross Revenue of Ulukent demand node.

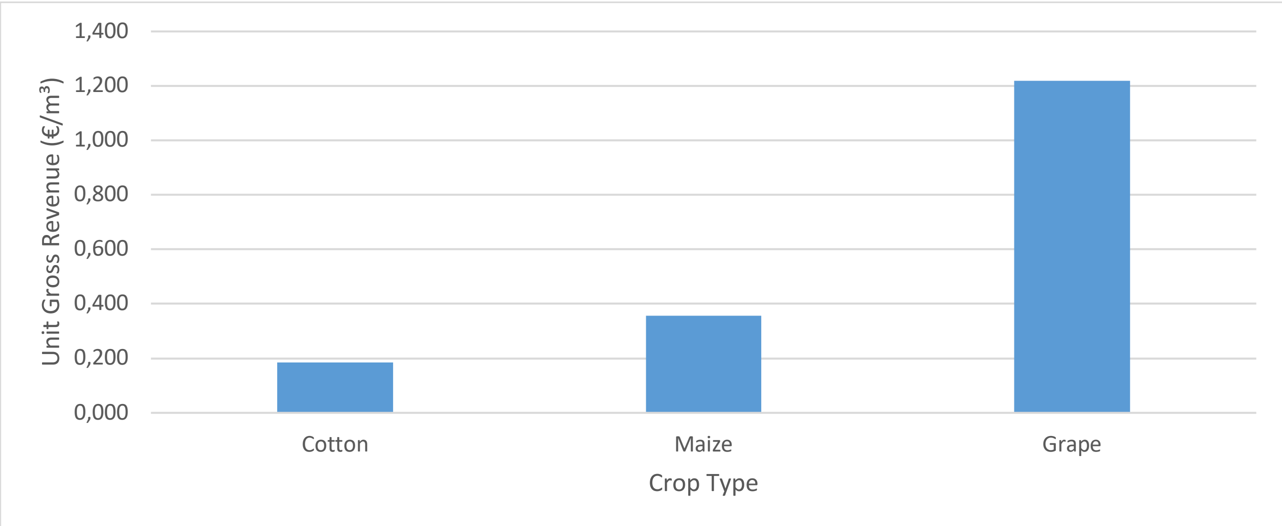

Figure 95 Unit Gross Revenue of Adala demand node.

This project is part of the PRIMA programme supported by the European Union.
GA n° [2041] [LENSES] [Call 2020 Section 1 Nexus IA]

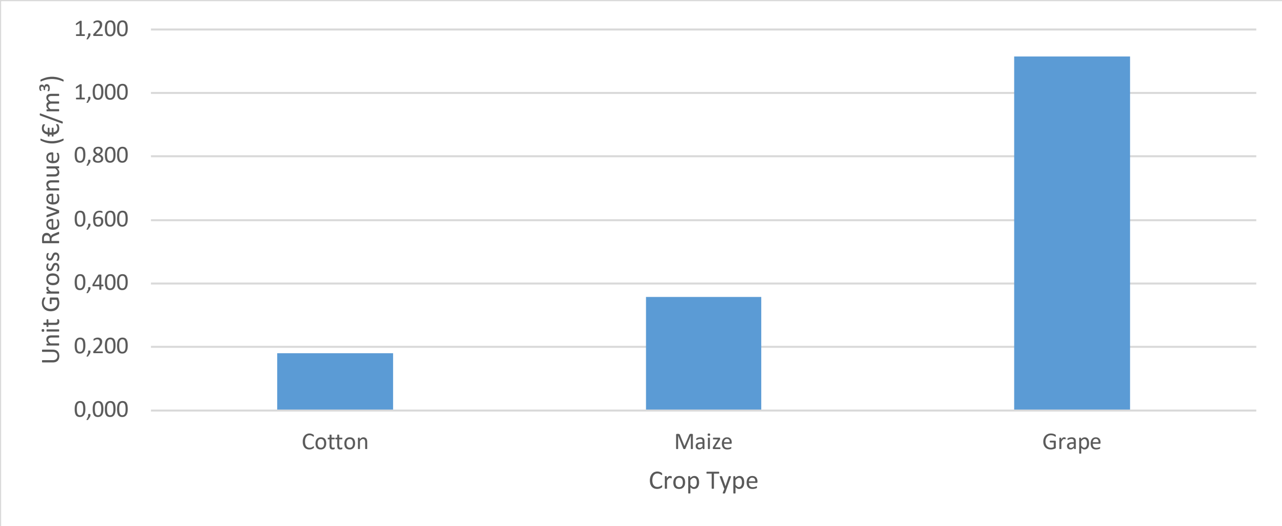

Figure 96 Unit Gross Revenue of Ahmetli demand node.

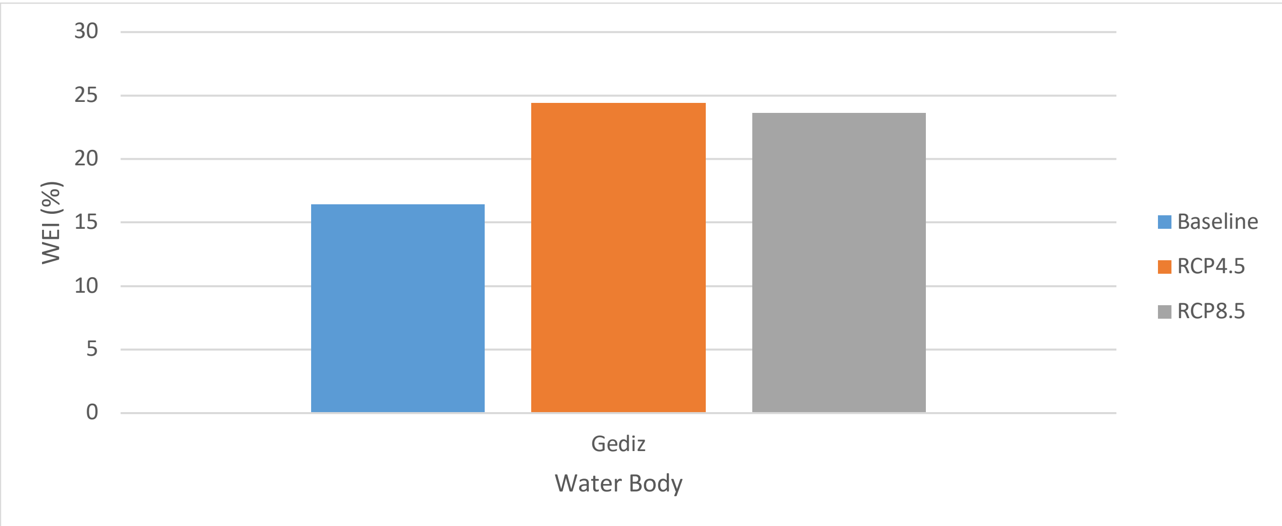

Figure 97 Gediz water exploitation index.

6.3.3. Guadalquvir Basin, Doñana National Park Area (ES)

As the Spanish pilot area, Doñana National Park and its urban/agricultural land on the upstream part have been selected, which is at the outlet of the Guadalquivir River Basin (Figure 98). Since there were streamflow gauges available on the Doñana sub-basin to represent the upstream sections of the basin, the entire Guadalquivir River Basin was not modelled. While the Guadiamar, Madre de la Marismas and El Rocio rivers are the main surface water resources, which are also utilized as the observed-modelled results comparison of the WEAP model (Figure 99-101) (Table 25), the entire area has also an interconnected groundwater source system. There are intensive agricultural and industrial activities in the pilot as well as there are urban and environmental demands. However, the main focus of the pilot is the Marshlands. The marshlands of Doñana which also represents the National Park, struggle with water scarcity and water quality degradation.

On the scope of water accounting efforts, the unmet demands of the Marshlands point out this problem to be further discussed on the other WPs of the project.

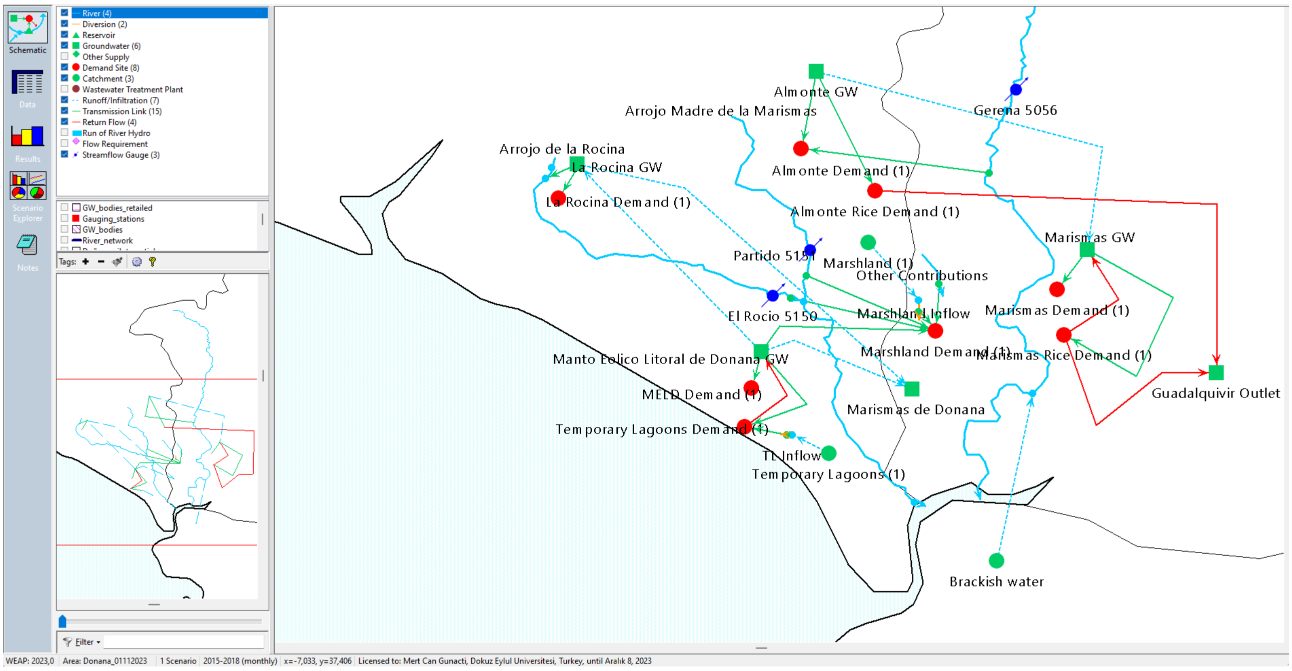

Figure 98 Doñana WEAP Schematic.

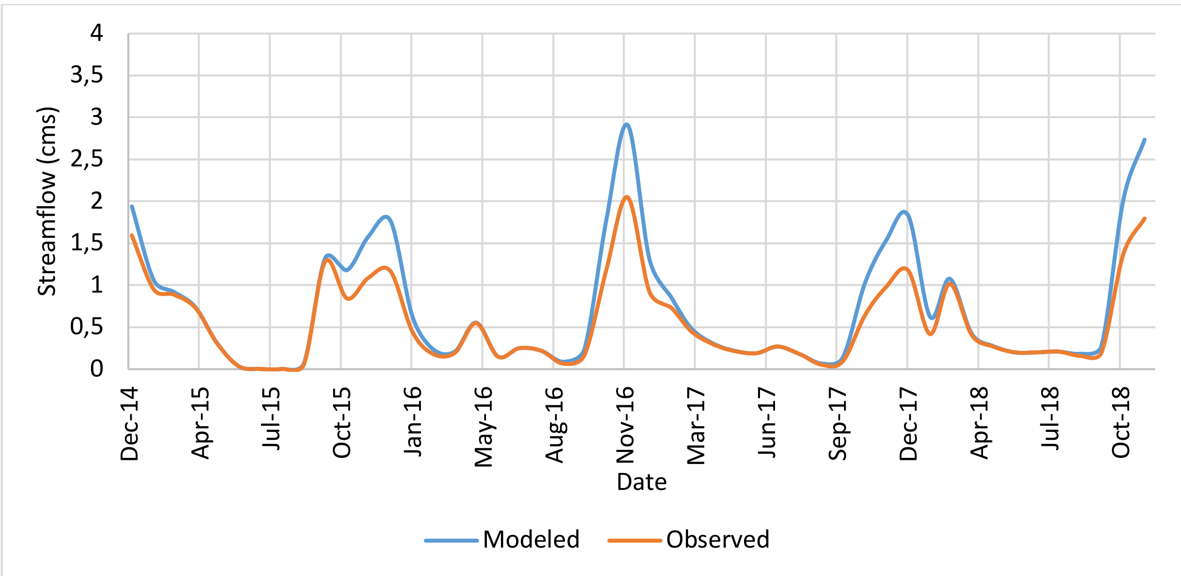

Figure 99 Garena reach WEAP model observed-modelled streamflow comparison.

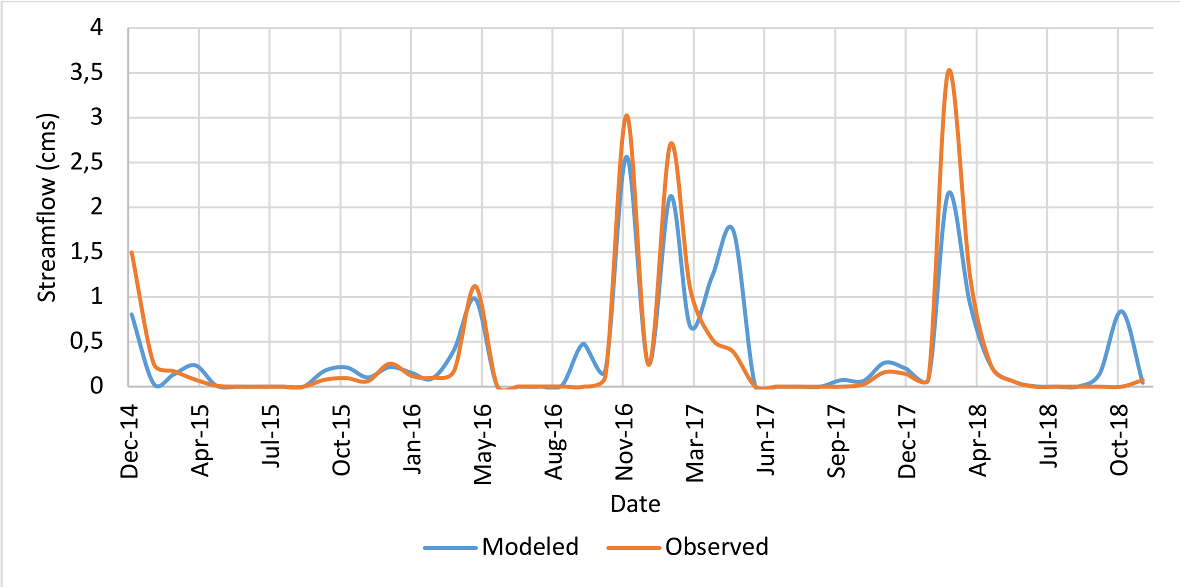

Figure 100 El Rocio reach WEAP model observed-modelled streamflow comparison.

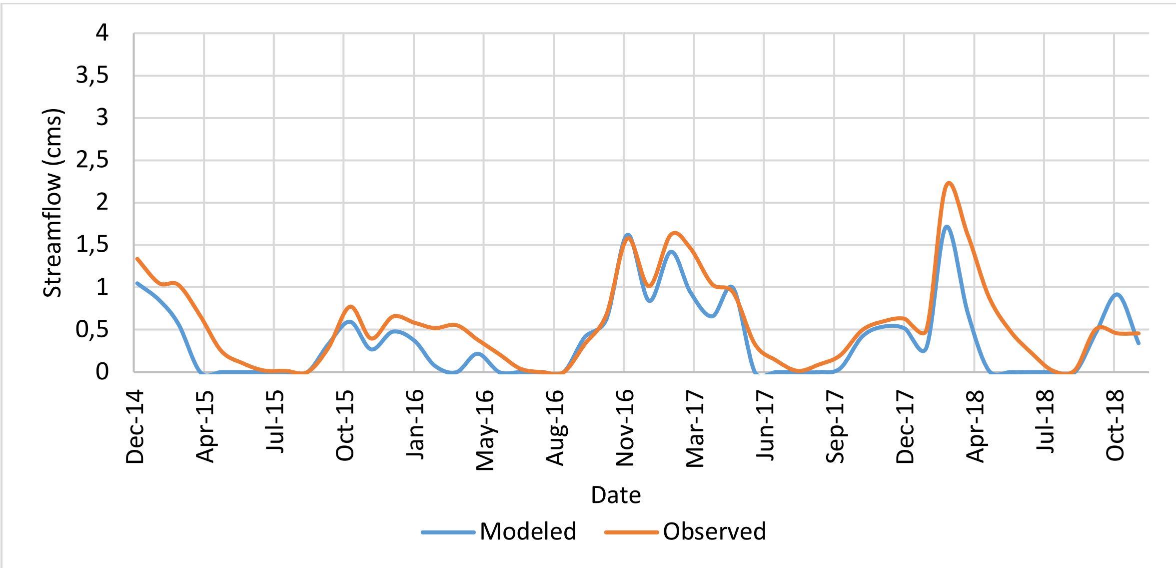

Figure 101 Partido reach WEAP model observed-modelled streamflow comparison.

This project is part of the PRIMA programme supported by the European Union.
GA n° [2041] [LENSES] [Call 2020 Section 1 Nexus IA]

Table 24 Goodness of fit statistics of Doñana WEAP model.

Goodness-of-fit statistics					
Garena reach		**El Rocio reach**		**Partido reach**	
NSE	0.65	NSE	0.77	NSE	0.63
KGE	0.47	KGE	0.76	KGE	0.63
NRMSE%	54	NRMSE%	100	NRMSE%	55
PBIAS%	30	PBIAS%	1.4	PBIAS%	-33
RSR	0.59	RSR	0.47	RSR	0.6
R^2	0.96	R^2	0.78	R^2	0.77

Based on the developed model, water accounting indicators of Nexus (sectoral water use, total amount of supply, total amount of demand, supply demand ratio, unmet demand, reliability of source, coverage of demand, unmet instream flow requirement, water exploitation index, and groundwater exploitation index) have been determined for the baseline and the climate change scenarios of RCP4.5 and RCP8.5 for each sector and overall average (Figure 102-111). Average irrigation productivity and unit gross revenues have been calculated according to the crop pattern, crop yields, and crop unit gross revenues that the pilot reported.

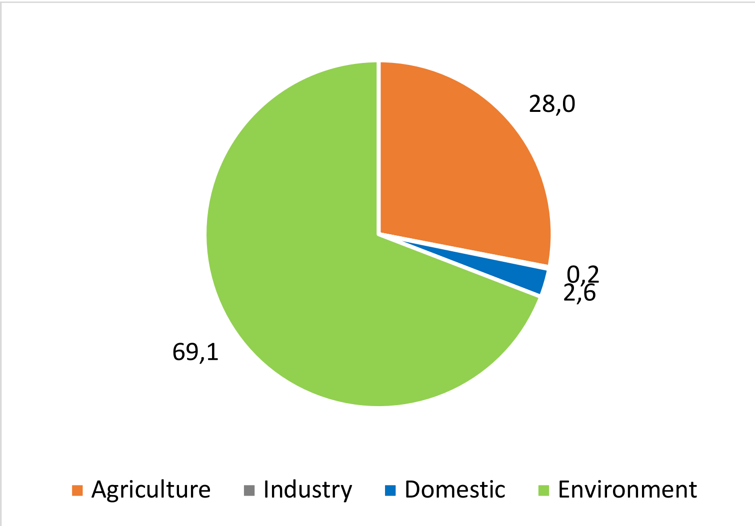

Figure 102 Doñana sectoral water use.

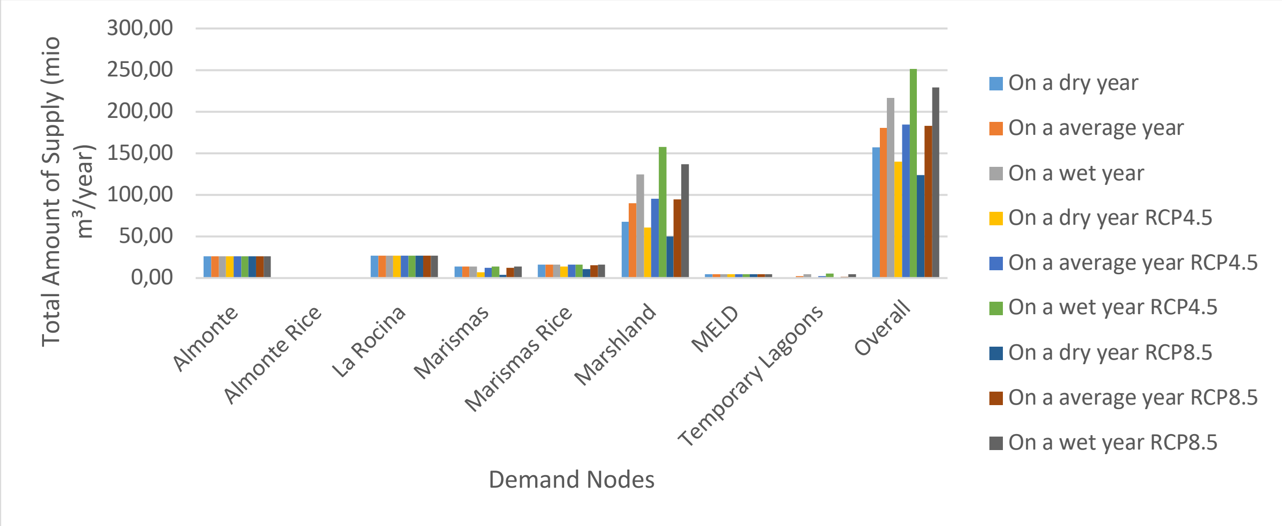

Figure 103 Doñana total amount of supply.

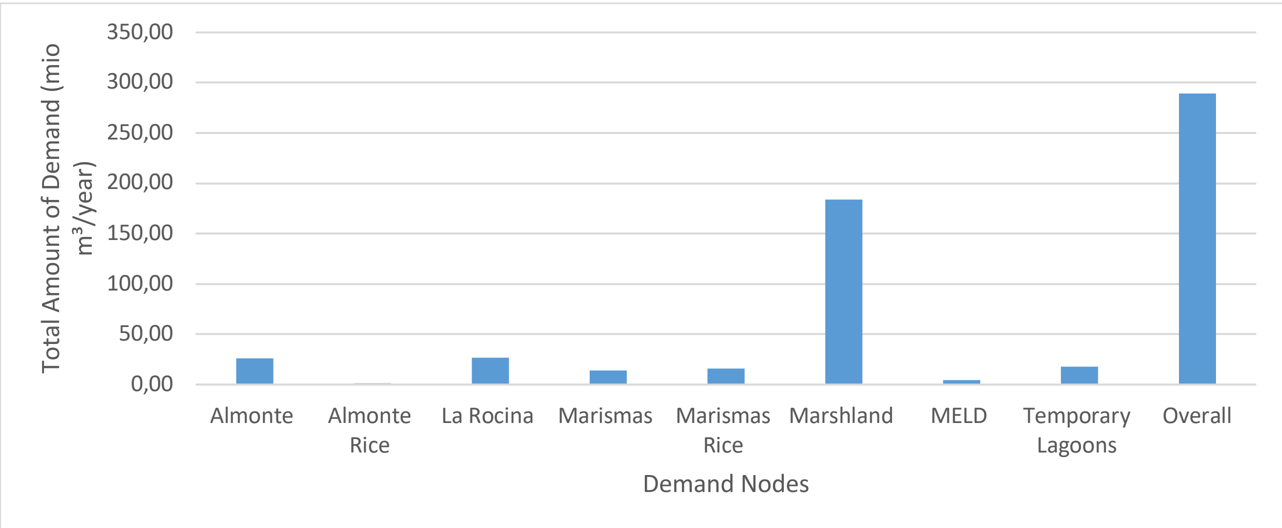

Figure 104 Doñana total amount of demand.

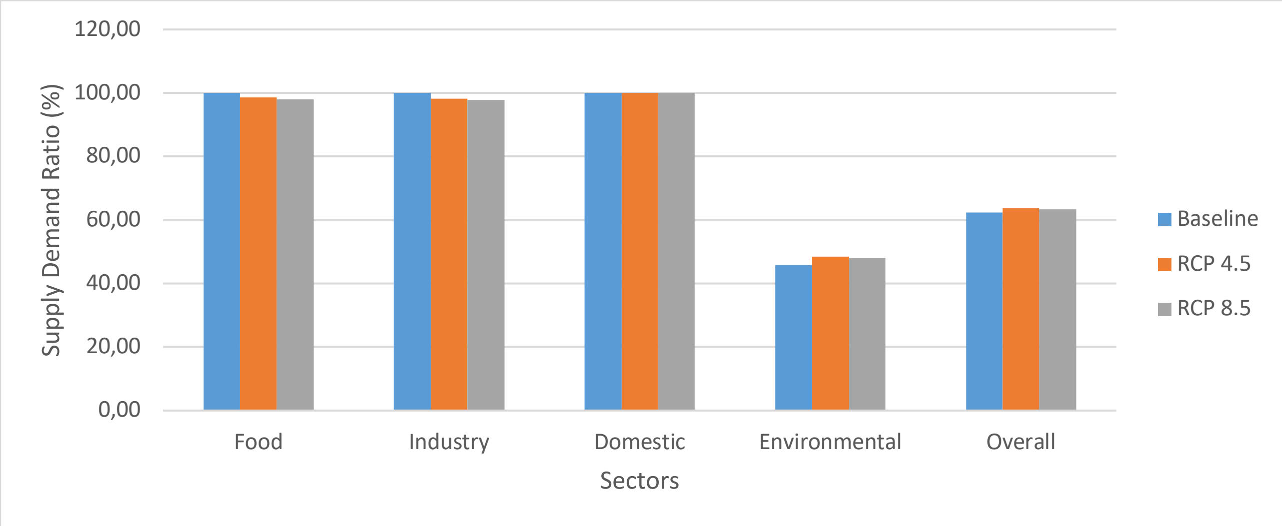

Figure 105 Doñana supply demand ratio.

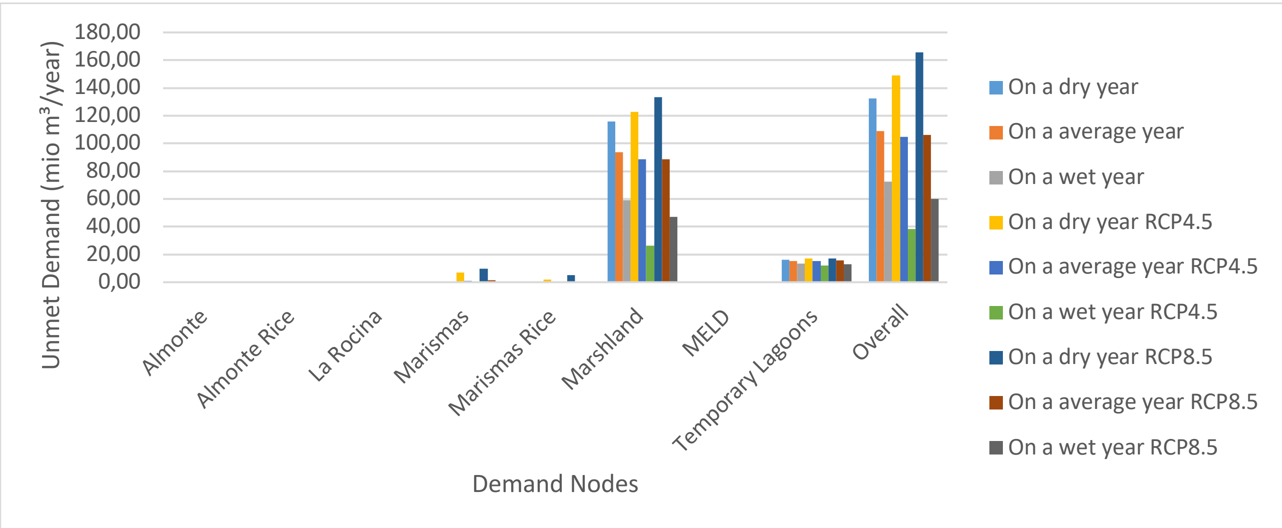

Figure 106 Doñana unmet demand.

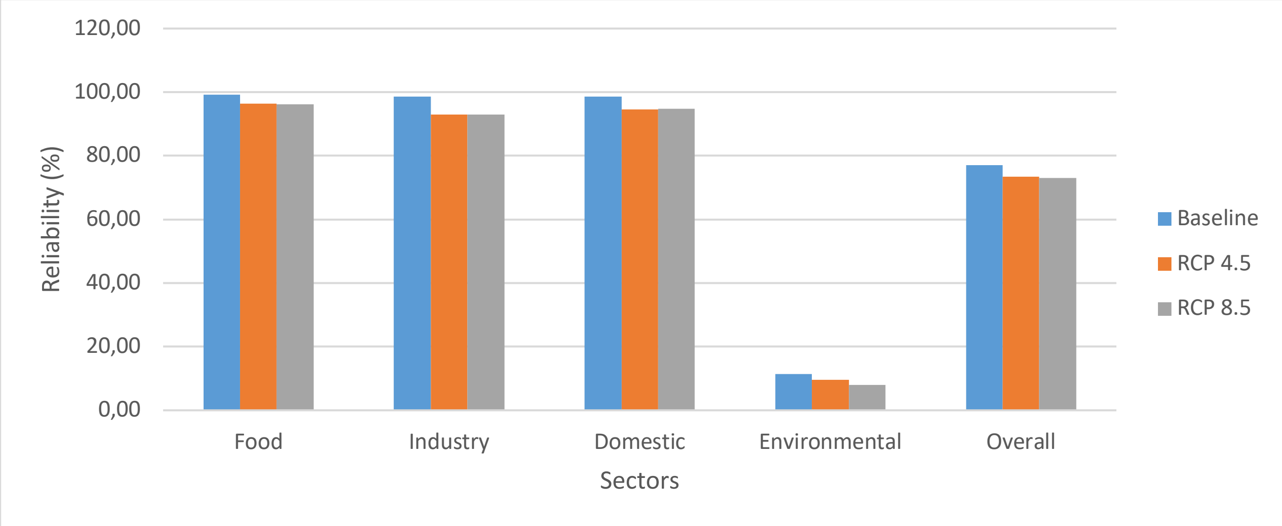

Figure 107 Doñana reliability of source.

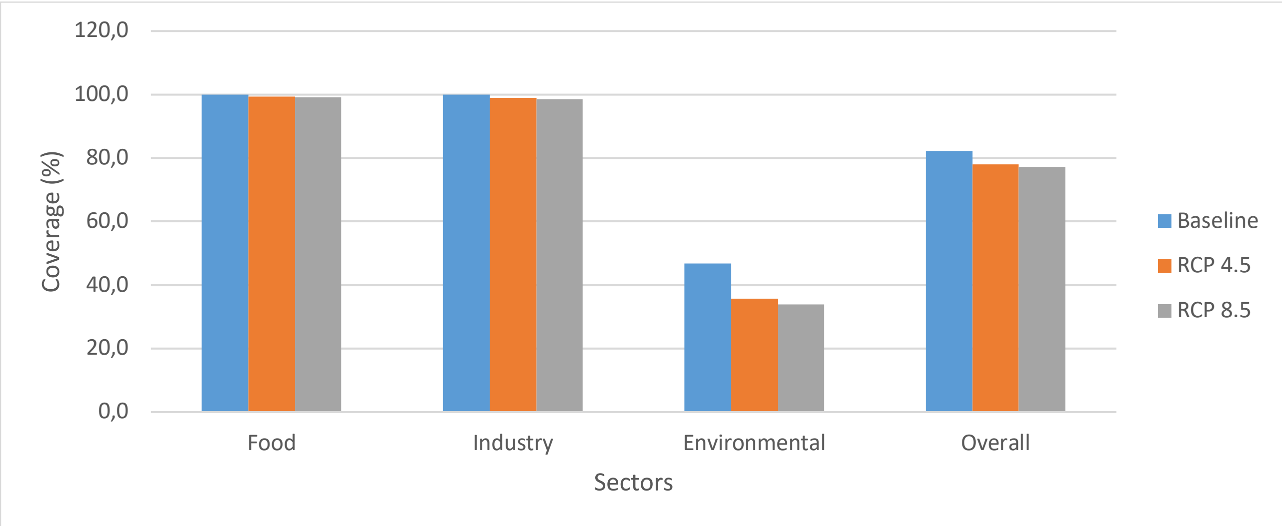

Figure 108 Doñana coverage of demand.

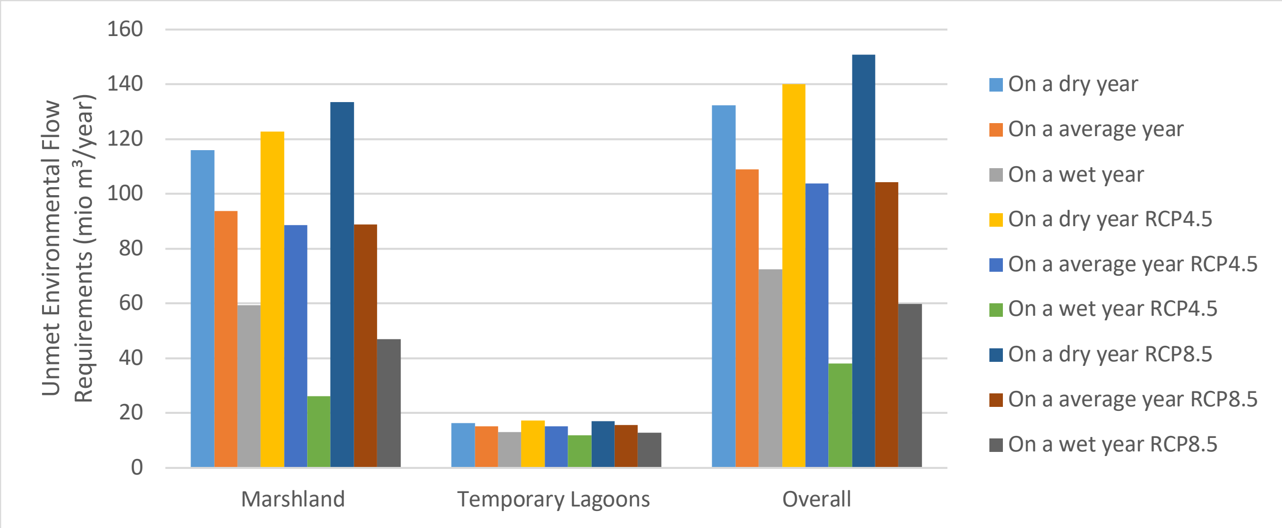

Figure 109 Doñana unmet environmental flow.

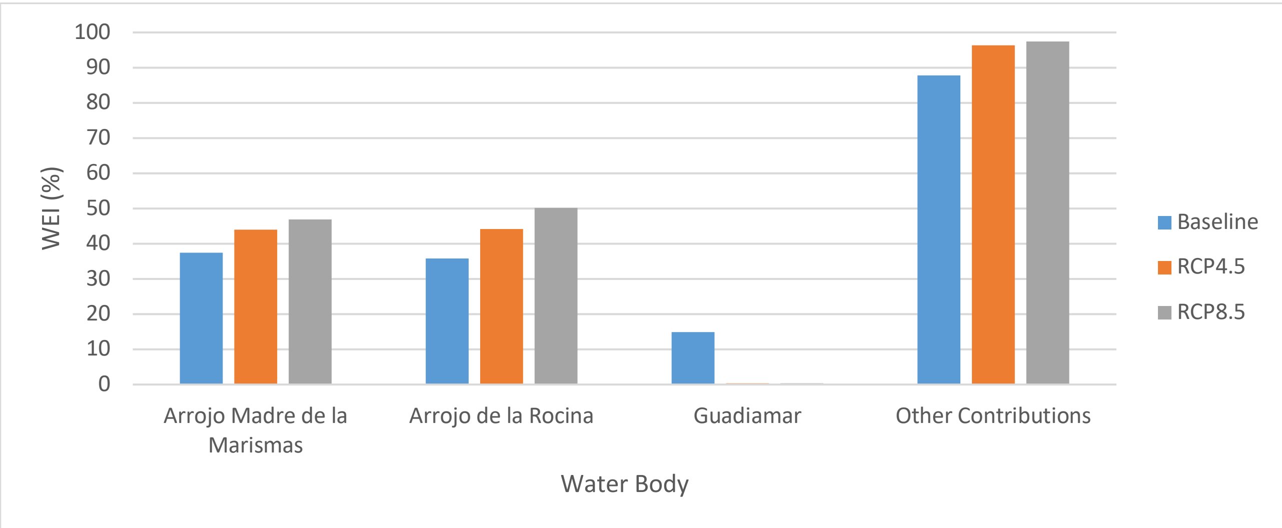

Figure 110 Doñana water exploitation index

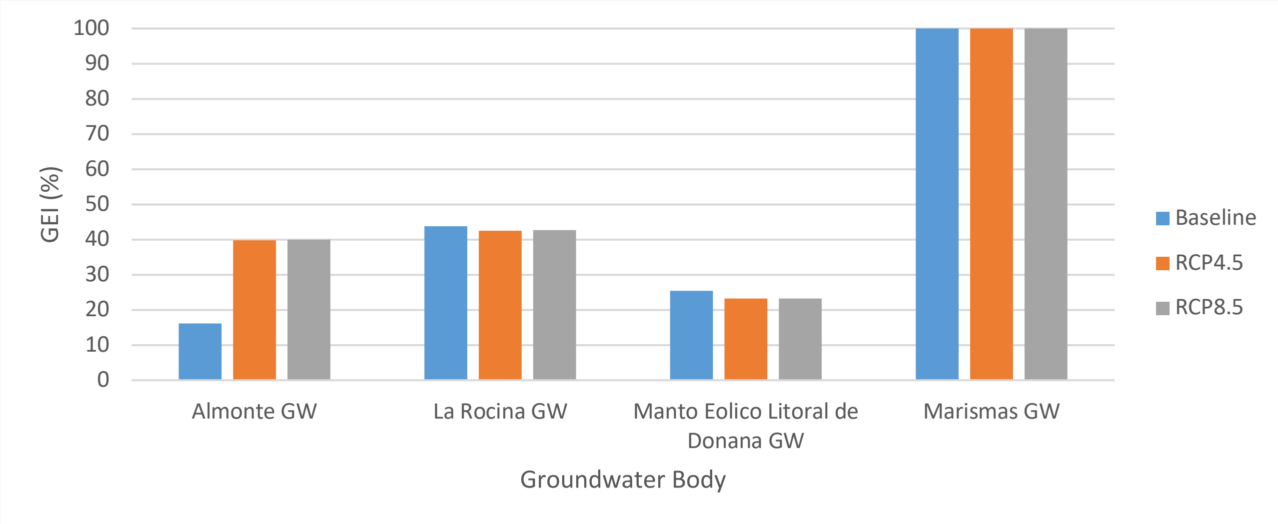

Figure 111 Doñana groundwater exploitation index.

6.3.4. International Long-Term Ecological Research Network Sites (Pinios – GR)

Pinios pilot consists of two sub-areas, which are Pinios Delta and Agia Region (Figure 112, 113). While there are intensive agricultural activities in both of the sub-areas, industry, and domestic water uses also take a significant share of the total available water in the pilot. Pinios River and the available groundwater are the main sources of water. For the model validation, the expert opinion of the pilot leader of Pinios, SWRI, and their previous study of the Delta area has been considered (Pisinaras, Paraskevas, and Panagopoulos, 2021). For the Agia Region, again the expert opinion of SWRI and the SWAT model results have been considered.

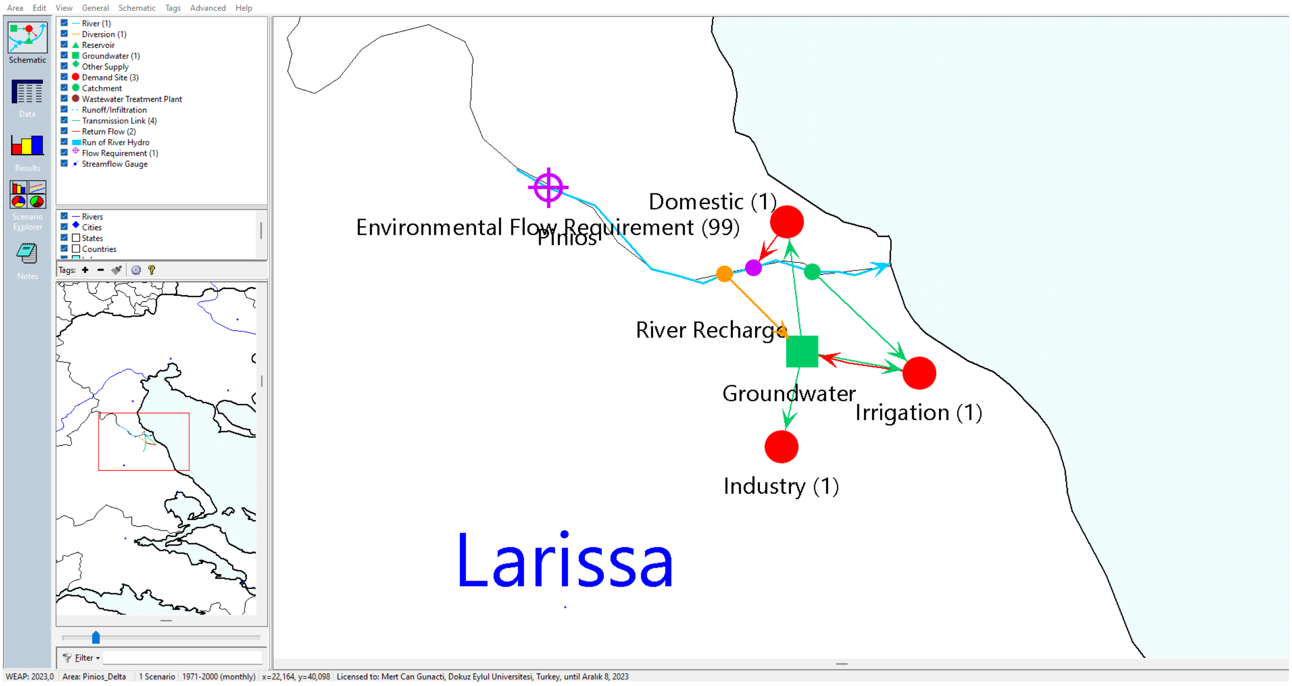

Figure 112 Pinios Delta WEAP Schematic.

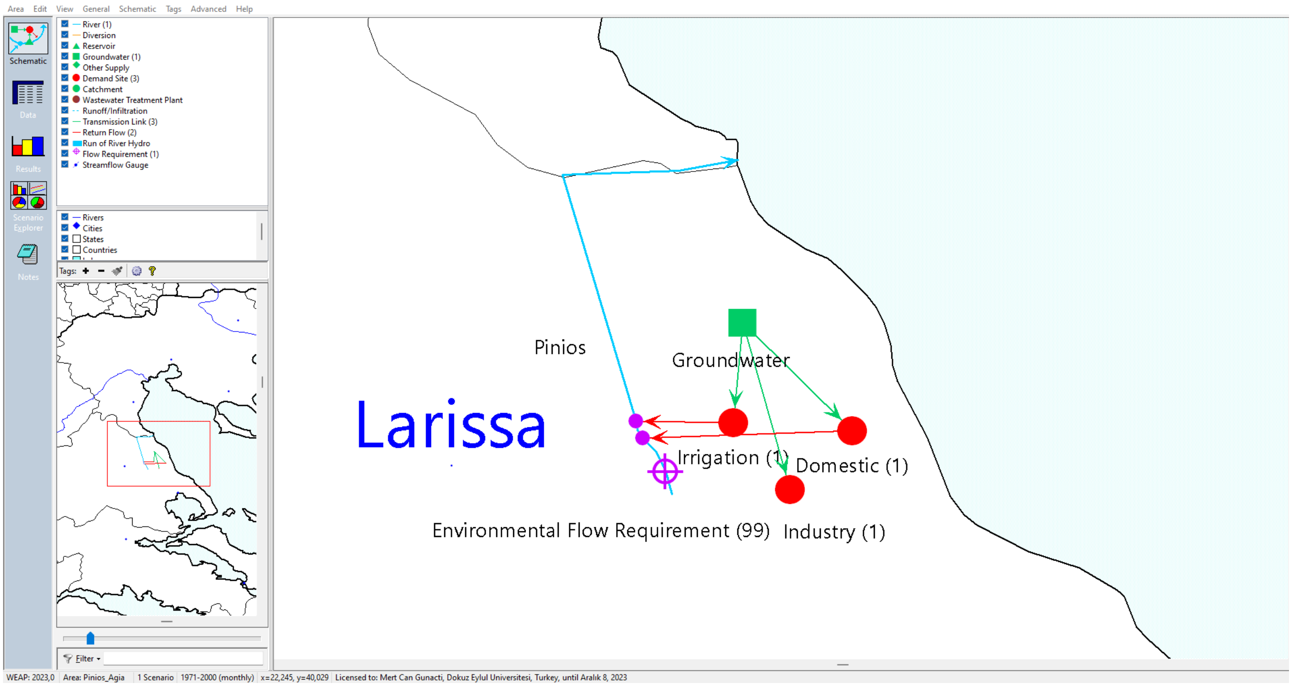

Figure 113 Pinios - Agia region WEAP Schematic.

Based on the developed model, water accounting indicators of Nexus (sectoral water use, total amount of supply, total amount of demand, supply demand ratio, unmet demand, reliability of source, coverage of demand, unmet instream flow requirement, water exploitation index, and groundwater exploitation index) have been determined for the baseline and the climate change scenarios of RCP4.5 and RCP8.5 for each sector and overall (Figures 114-128). Average irrigation productivity and unit gross revenues have been calculated according to the crop pattern, crop yields, and crop unit gross revenues that pilots reported.

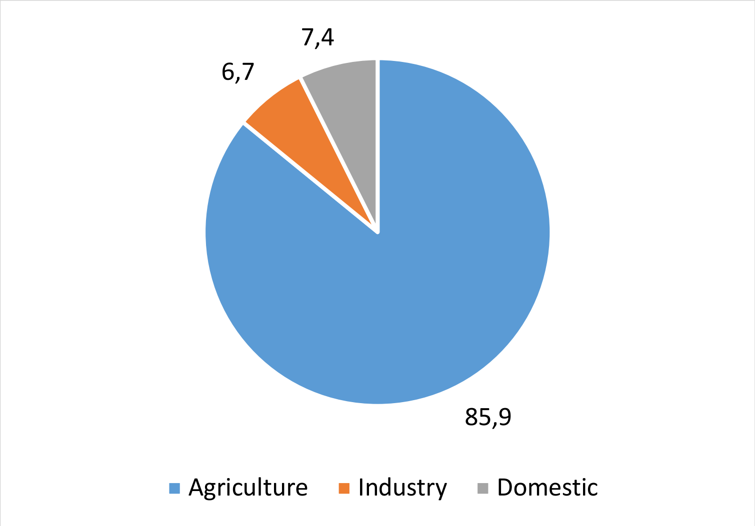

Figure 114 Pinios sectoral water use.

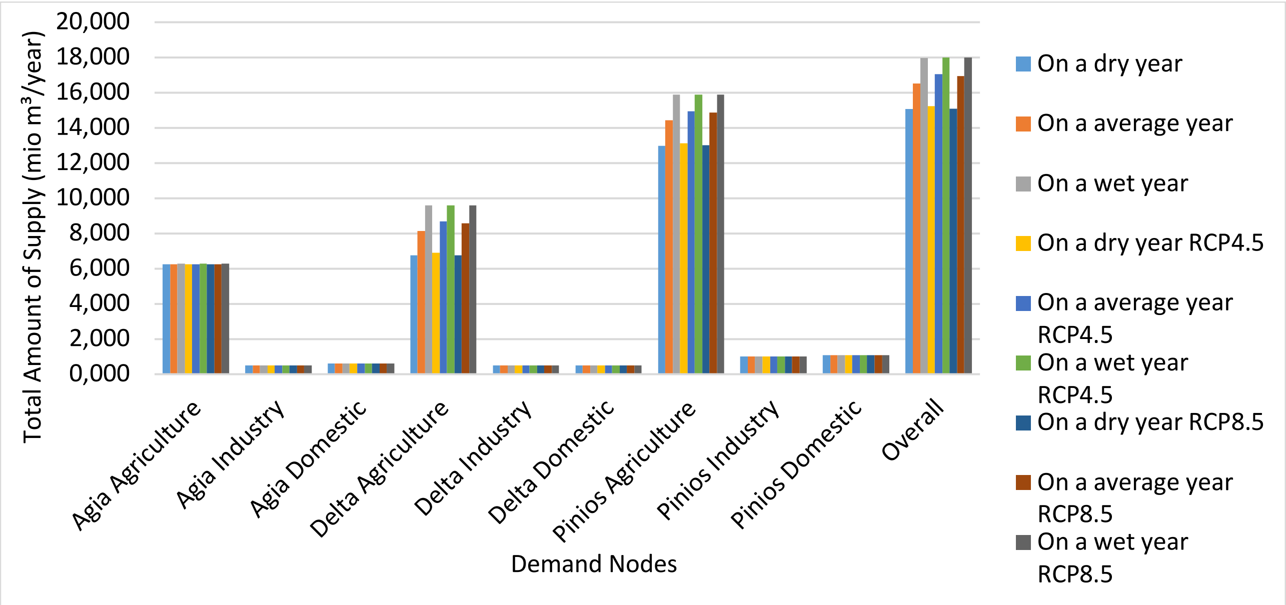

Figure 115 Pinios total amount of supply.

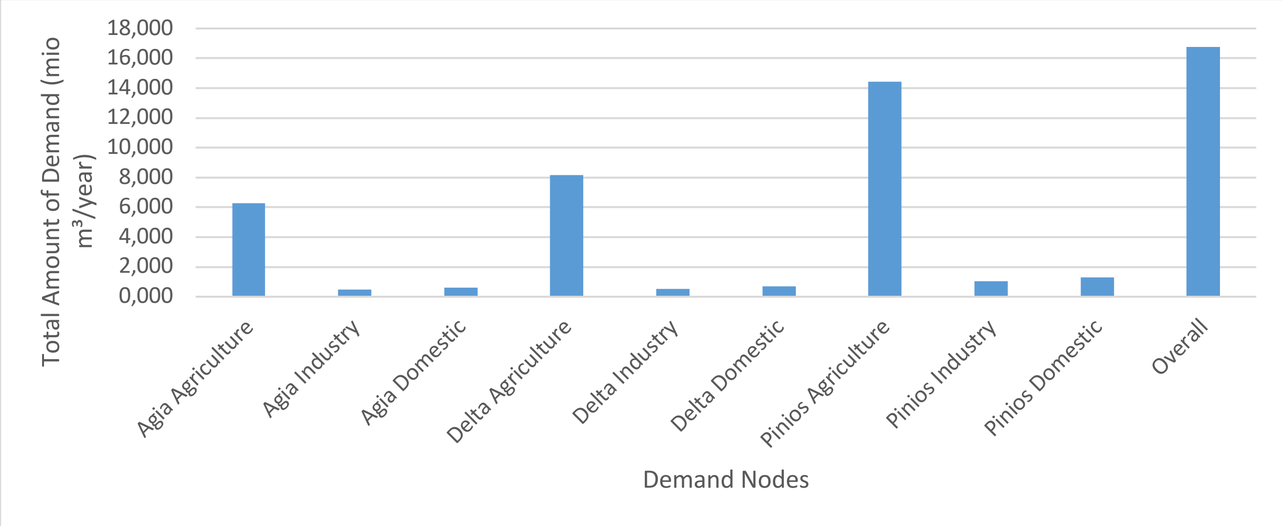

Figure 116 Pinios total amount of demand.

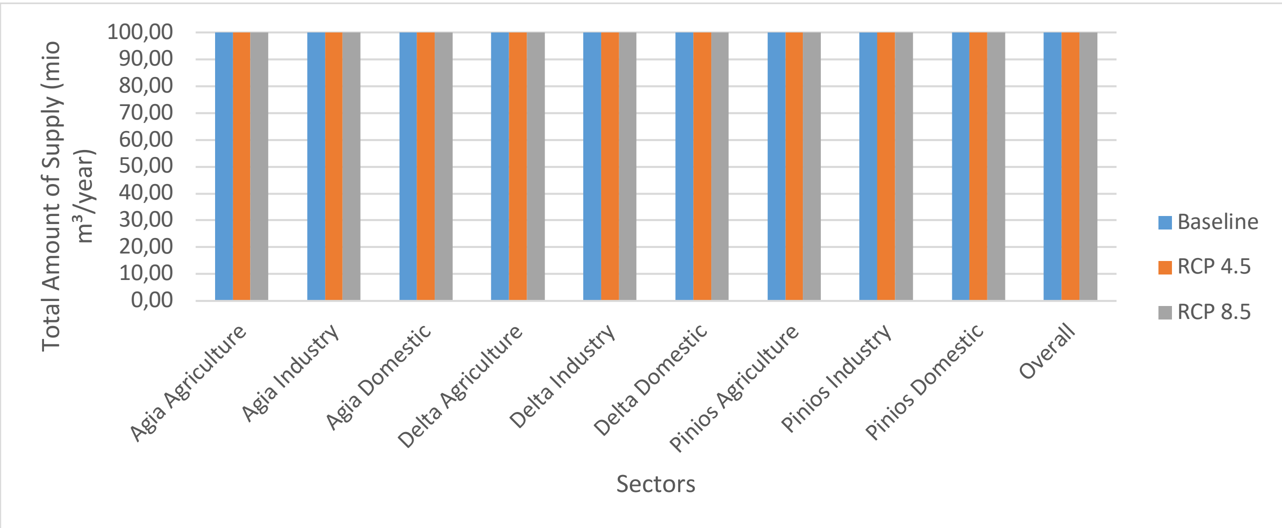

Figure 117 Pinios supply demand ratio.

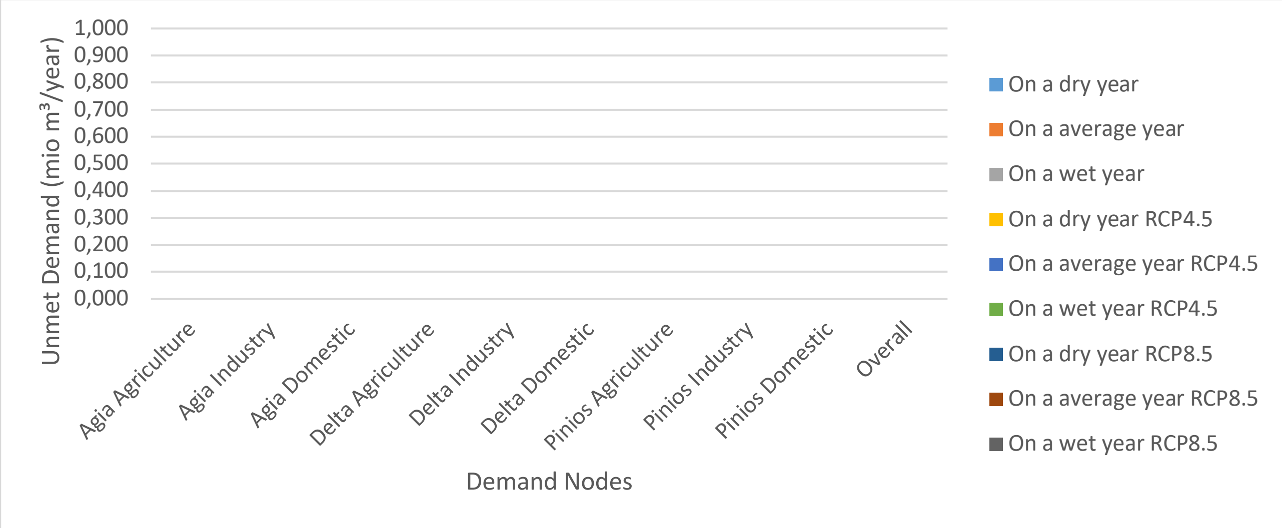

Figure 118 Pinios unmet demand.

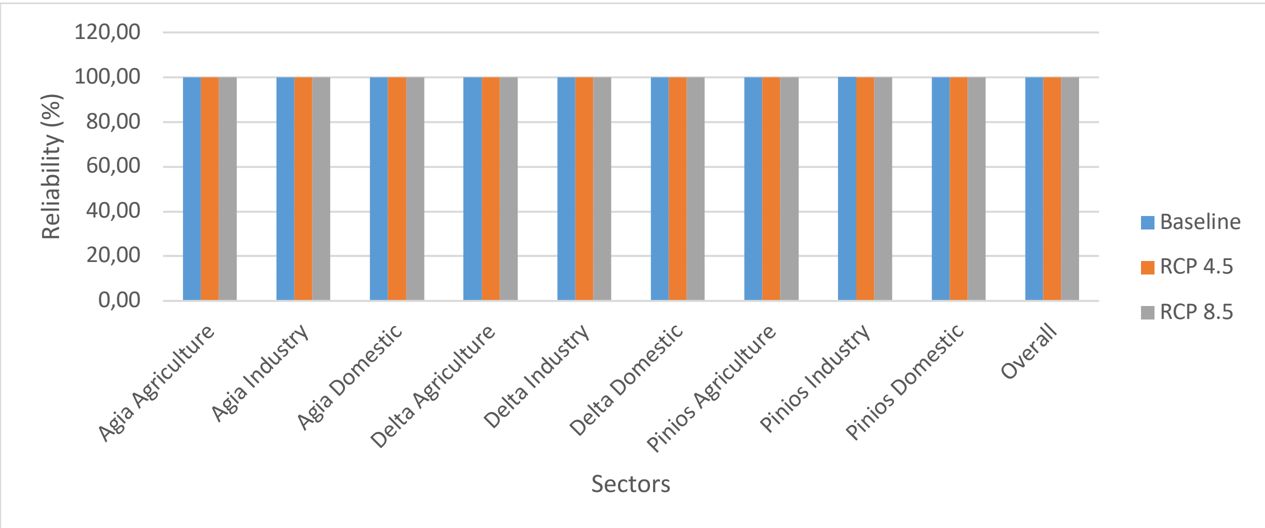

Figure 119 Pinios reliability of source.

This project is part of the PRIMA programme supported by the European Union.
GA n° [2041] [LENSES] [Call 2020 Section 1 Nexus IA]

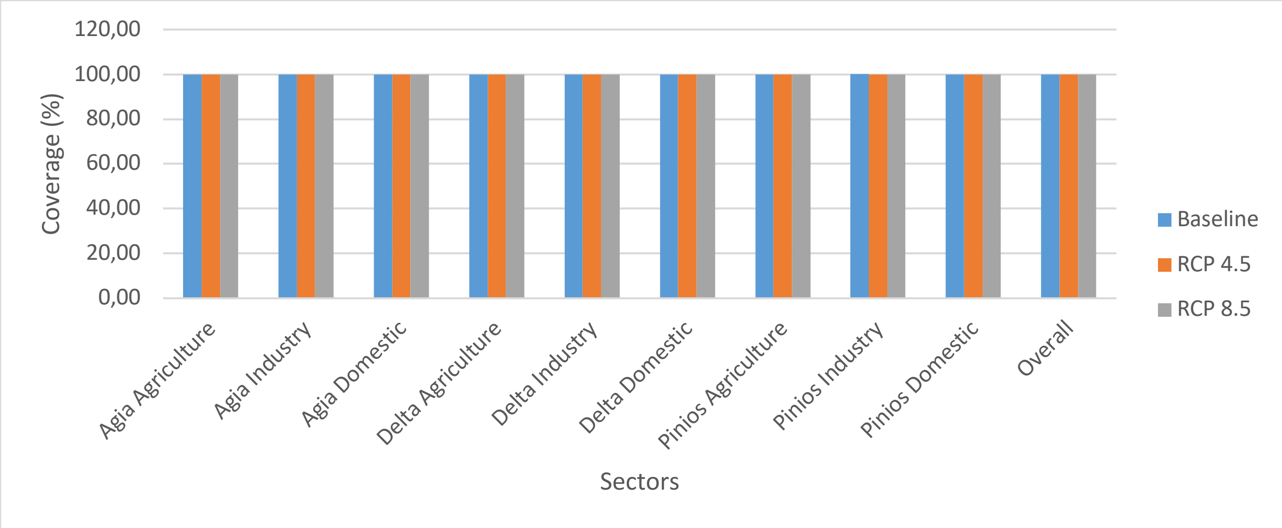

Figure 120 Pinios coverage of demand.

Figure 121 Pinios unmet instream flow requirements.

This project is part of the PRIMA programme supported by the European Union.
GA n° [2041] [LENSES] [Call 2020 Section 1 Nexus IA]

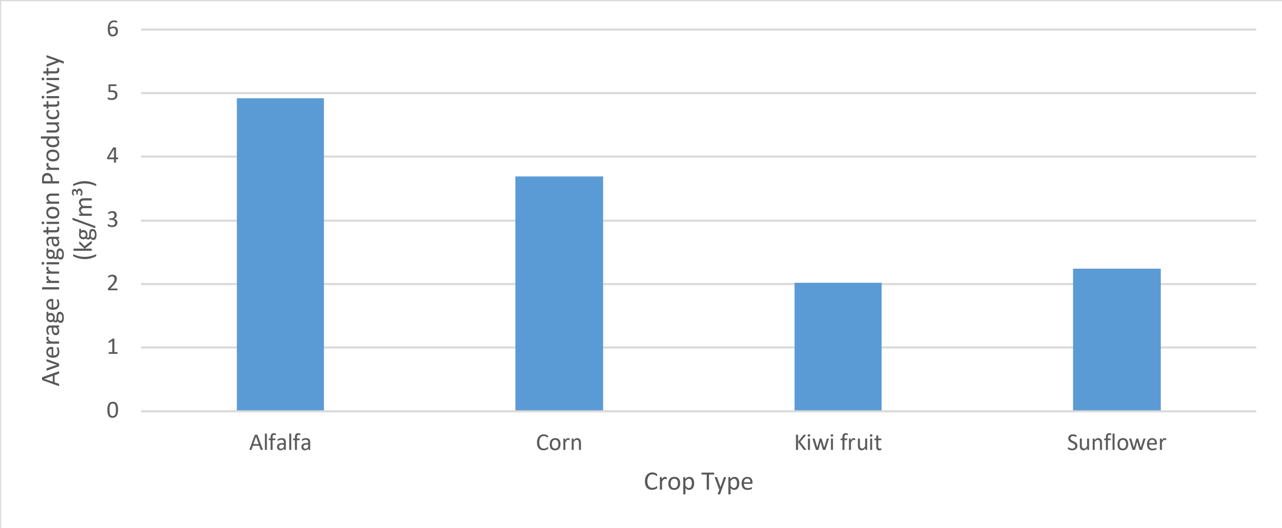

Figure 122 Pinios Delta average irrigation productivity

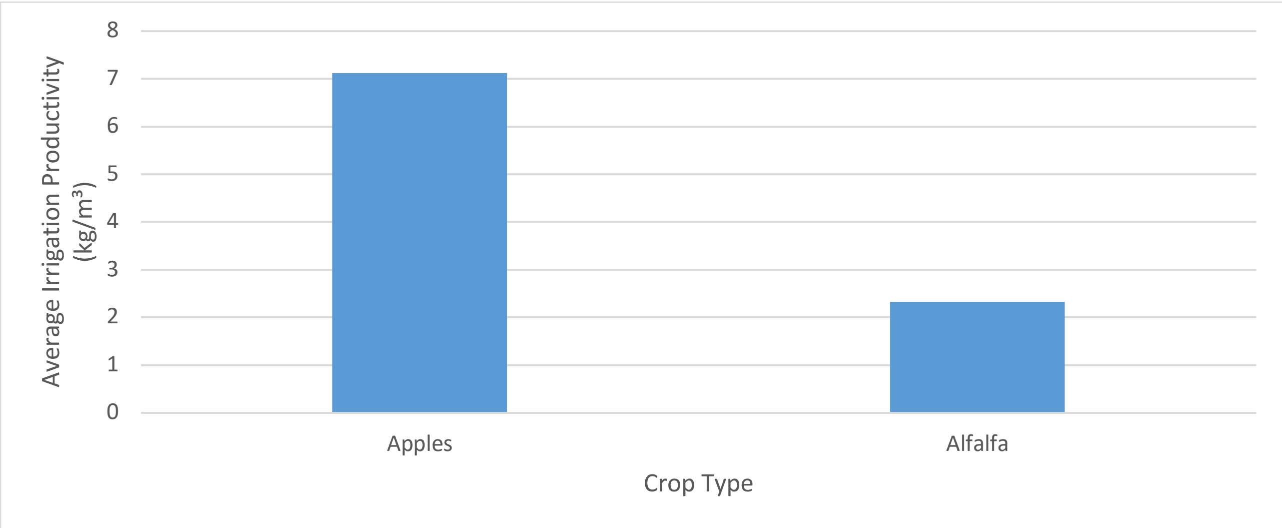

Figure 123 Pinios – Agia average irrigation productivity

This project is part of the PRIMA programme supported by the European Union.
GA n° [2041] [LENSES] [Call 2020 Section 1 Nexus IA]

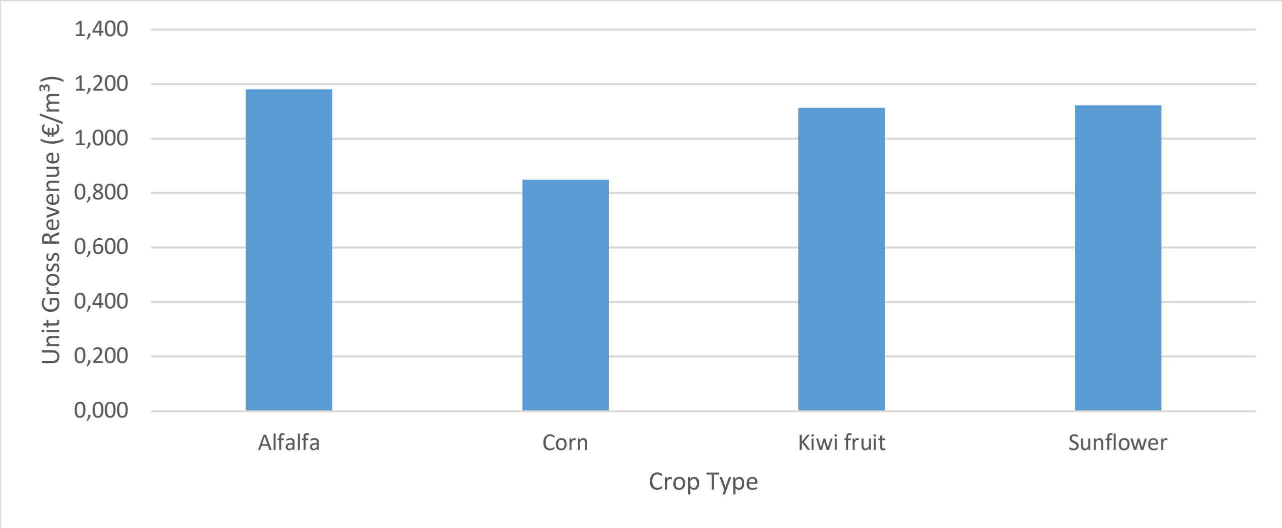

Figure 124 Pinios Delta crop unit gross revenue

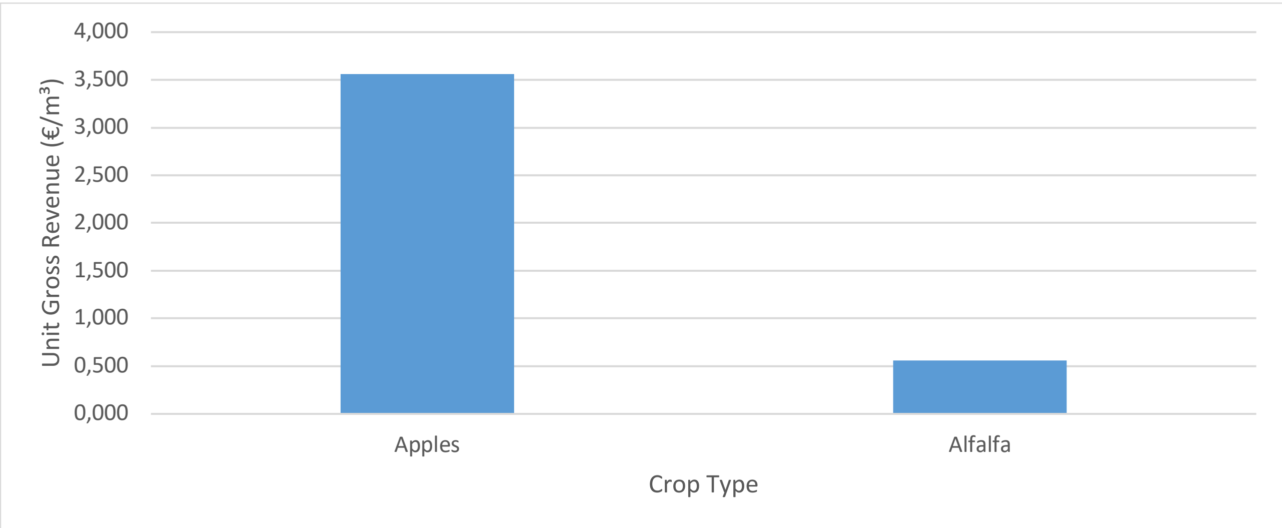

Figure 125 Pinios – Agia crop unit gross revenue

This project is part of the PRIMA programme supported by the European Union.
GA n° [2041] [LENSES] [Call 2020 Section 1 Nexus IA]

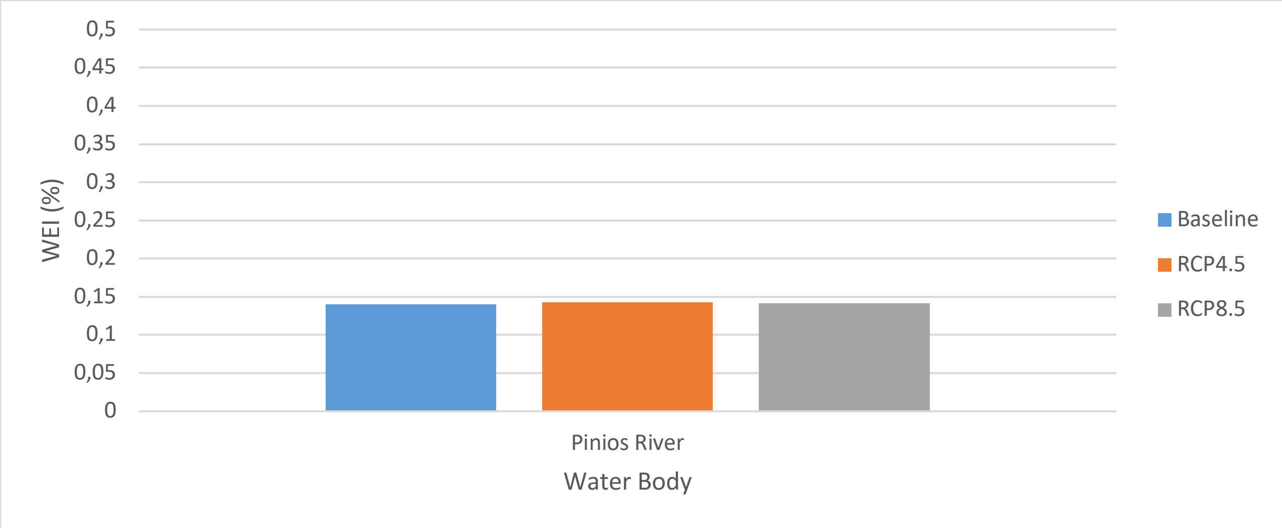

Figure 126 Pinios Delta water exploitation index

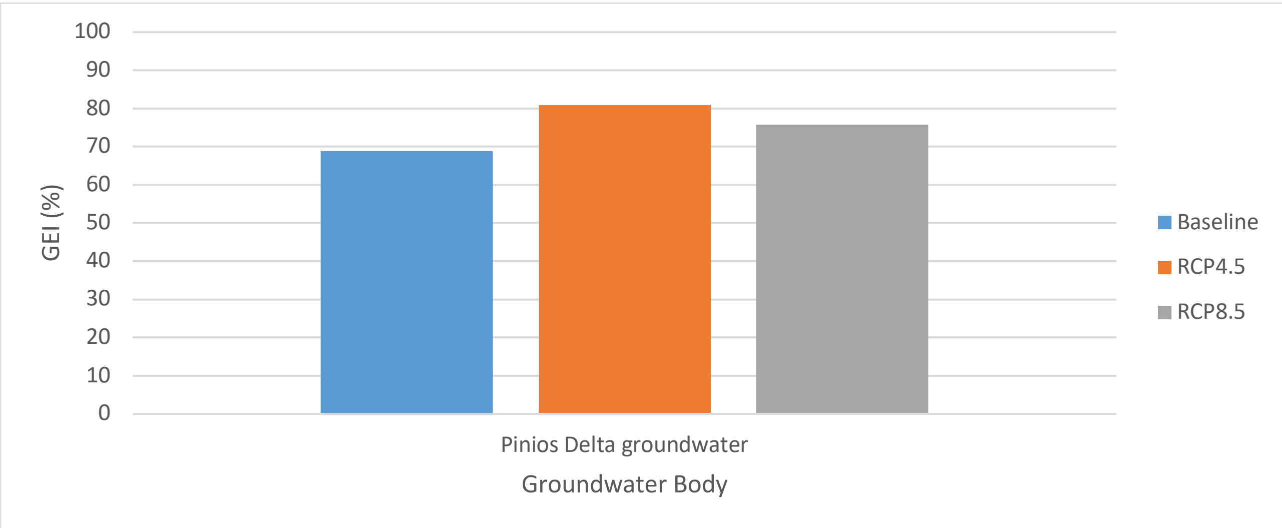

Figure 127 Pinios Delta groundwater exploitation index.

This project is part of the PRIMA programme supported by the European Union.
GA n° [2041] [LENSES] [Call 2020 Section 1 Nexus IA]

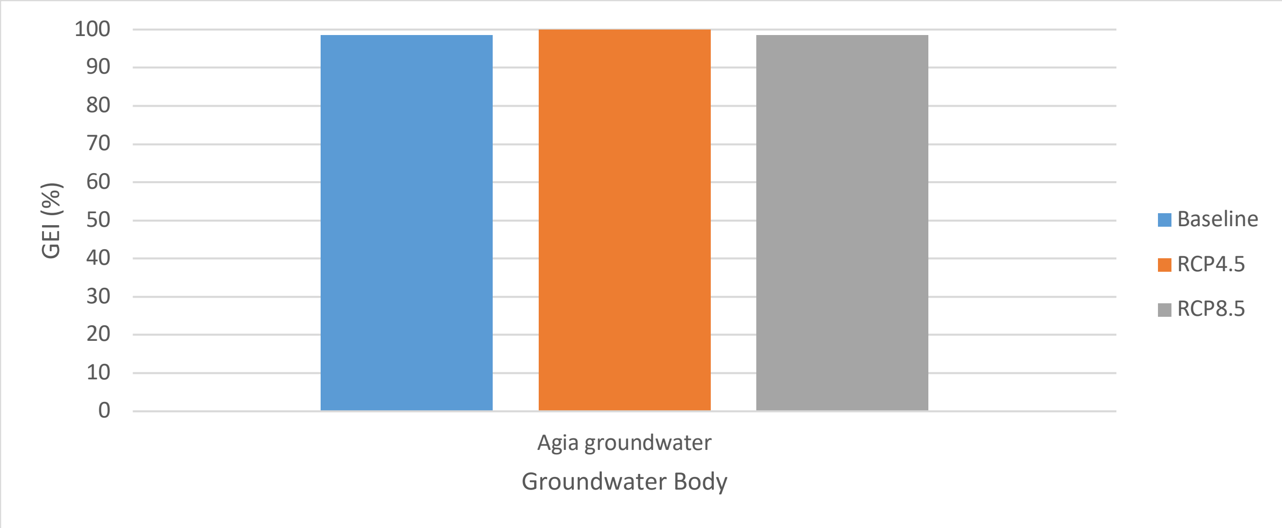

Figure 128 Pinios - Agia groundwater exploitation index.

6.3.5. International Long-Term Ecological Research Network Sites (Koiliaris – GR)

Koiliaris Critical Zone of the island of Crete is home to intensive avocado cultivations (Figure 129). Although the island's water resources are plentiful, water quality, salination in particular is the main concern of the avocado farmers because of its harmful effects on the yield and the quality of avocado production. Rich groundwater sources have led the farmers to exploit them via wells. Besides agricultural water use, domestic use of water also takes a significant share of the available water sources. Streamflow gauges on the outlet of the two main reaches have been utilized for the comparison of the modelled-observed values of the WEAP model (Figure 130, 131) (Table 26).

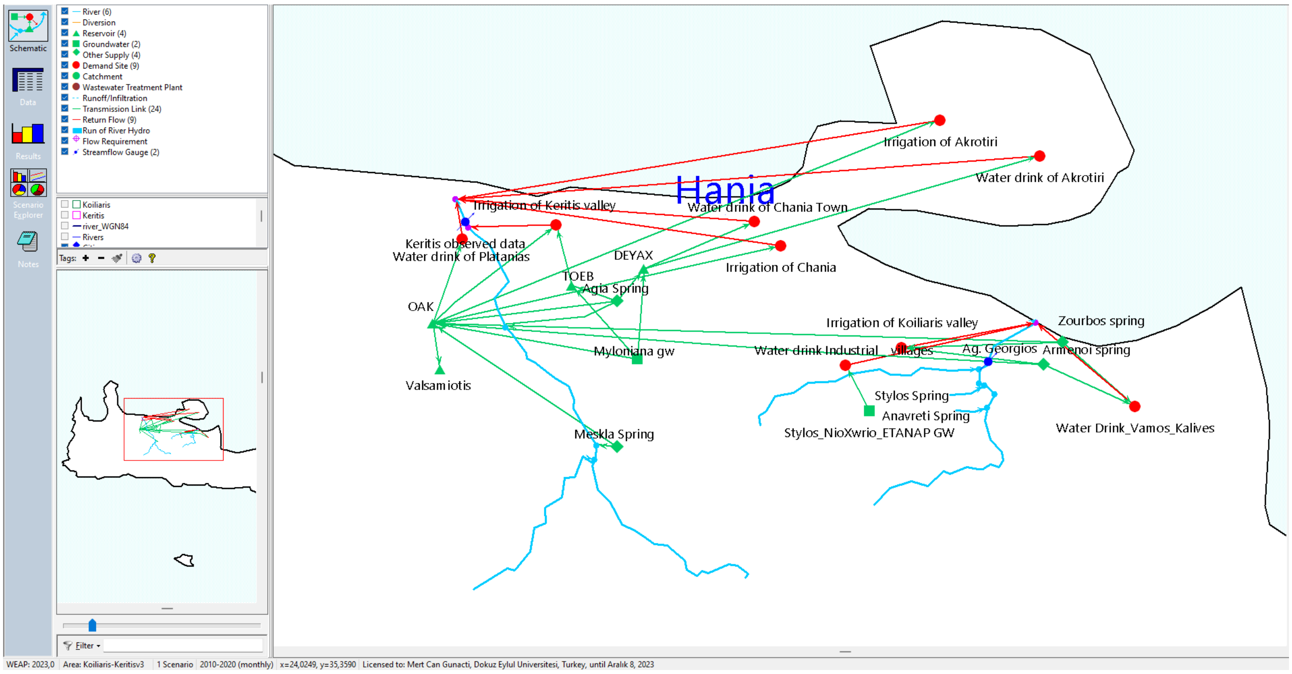

Figure 129 Koiliaris WEAP Schematic.

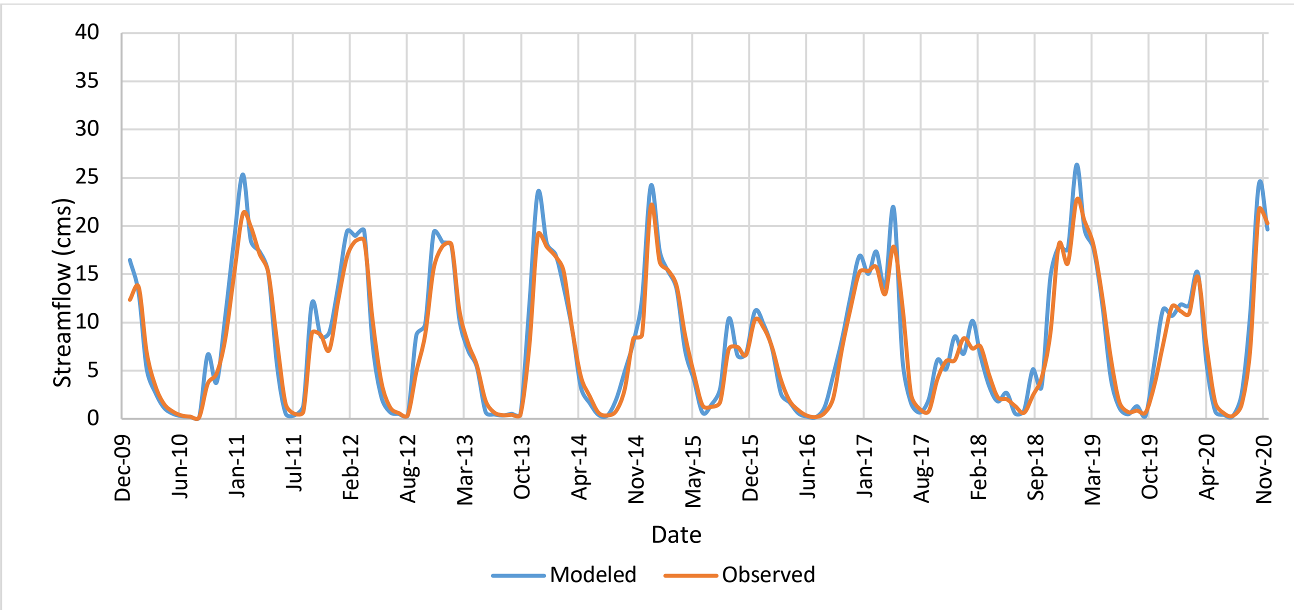

Figure 130 Ag. Georgios reach WEAP model observed-modelled streamflow comparison.

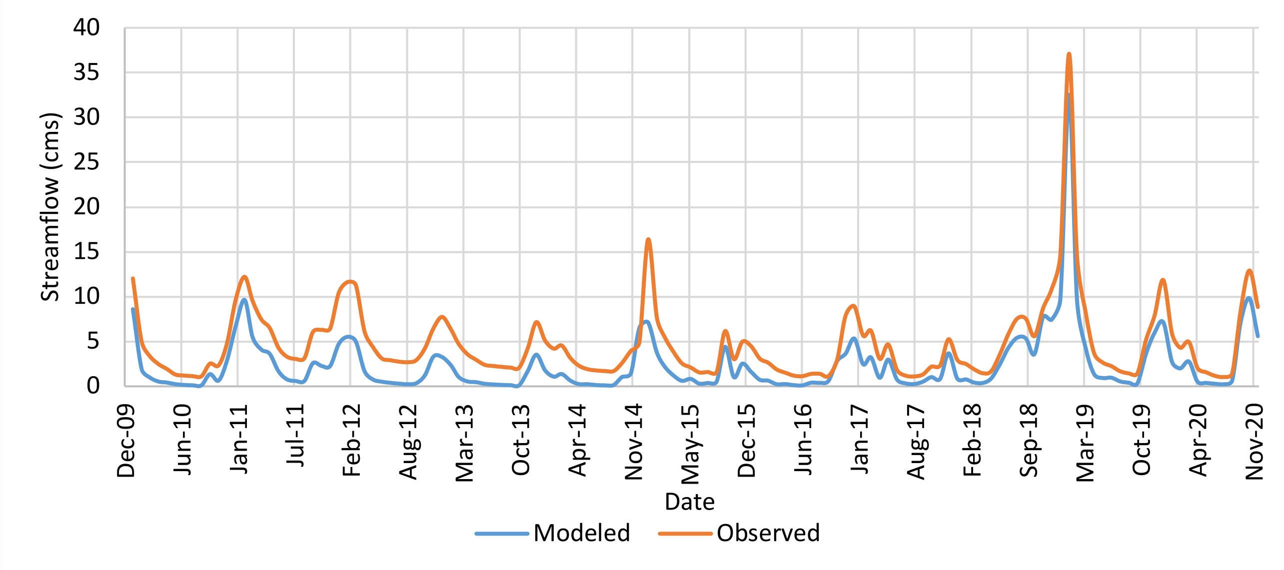

Figure 131 Keritis reach WEAP model observed-modelled streamflow comparison.

Table 25 Goodness of fit statistics of Koiliaris WEAP model.

Goodness-of-fit statistics			
Ag. Georgios reach		**Keritis reach**	
NSE	0.92	NSE	0.61
KGE	0.89	KGE	0.48
NRMSE%	23	NRMSE%	57
PBIAS%	6.1	PBIAS%	-49
RSR	0.27	RSR	0.62
R^2	0.94	R^2	0.92

Based on the developed model, water accounting indicators of Nexus (sectoral water use, total amount of supply, total amount of demand, supply demand ratio, unmet demand, reliability of source, coverage of demand, unmet instream flow requirement, water exploitation index, and groundwater exploitation index) have been determined for the baseline and the climate change scenarios of RCP4.5 and RCP8.5 for each sector and overall average (Figure 132-142). Average irrigation productivity and unit gross revenues have been calculated according to the crop pattern, crop yields, and crop unit gross revenues that the pilot reported.

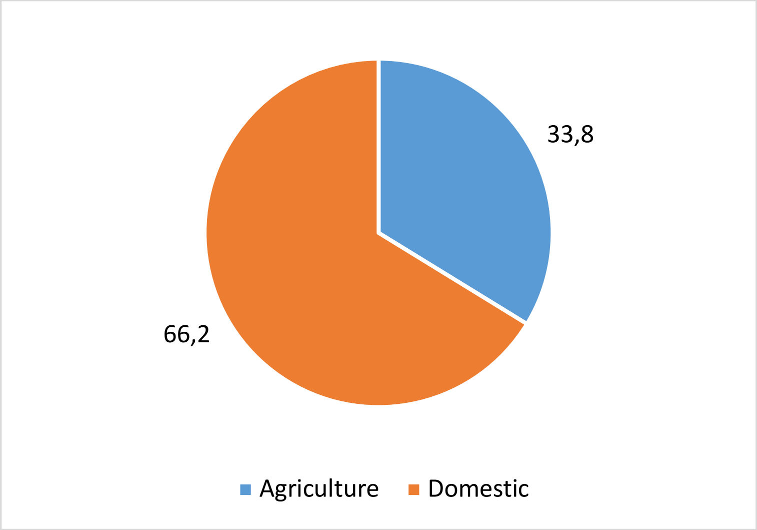

Figure 132 Koiliaris sectoral water use.

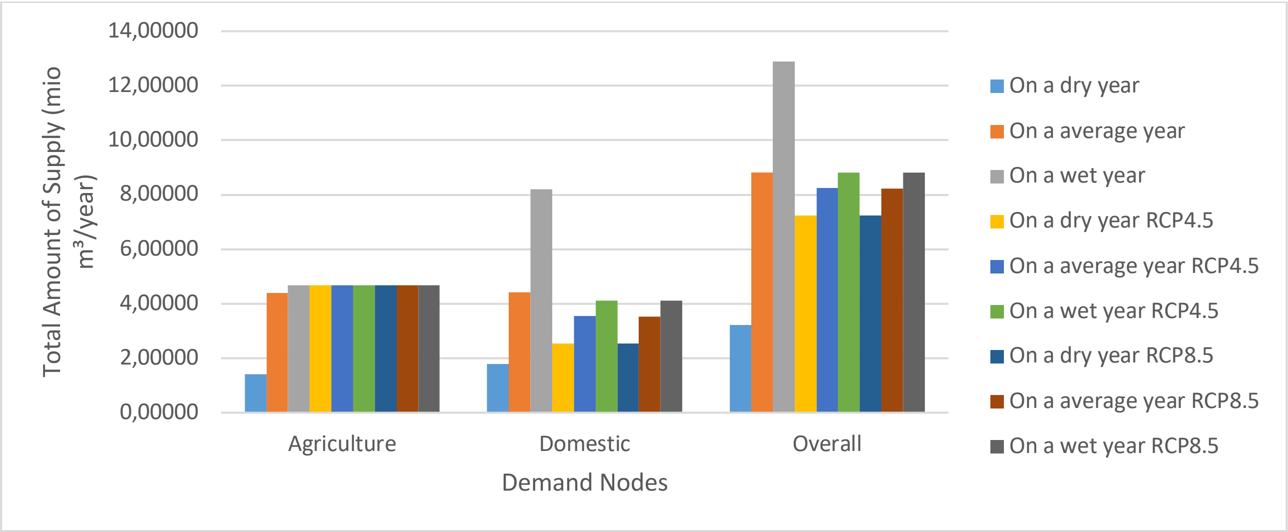

Figure 133 Koiliaris total amount of supply.

This project is part of the PRIMA programme supported by the European Union.
GA n° [2041] [LENSES] [Call 2020 Section 1 Nexus IA]

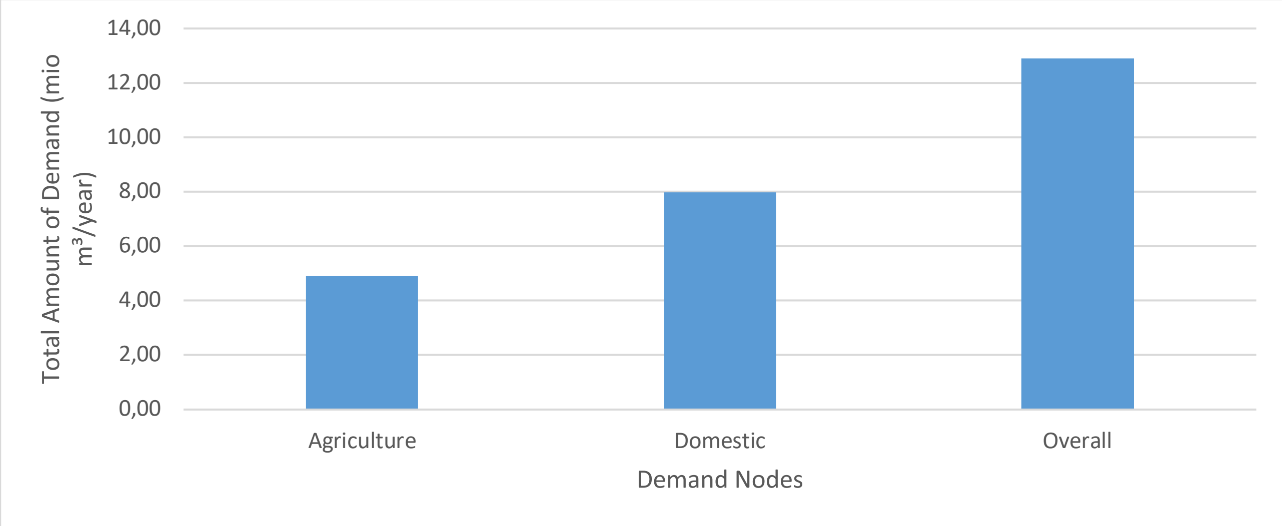

Figure 134 Koiliaris total amount of demand.

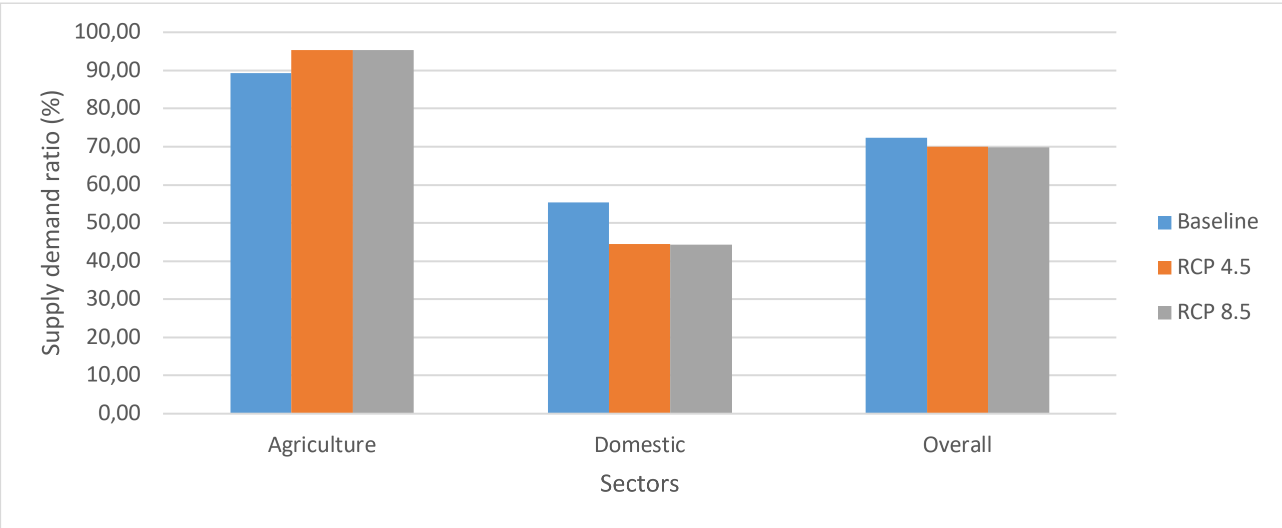

Figure 135 Koiliaris supply demand ratio.

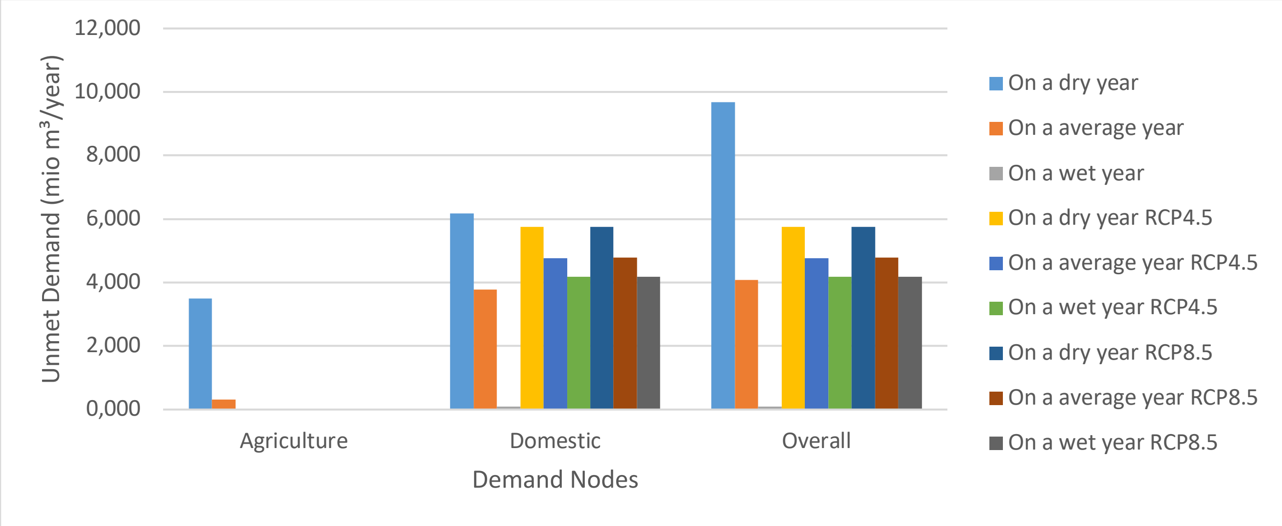

Figure 136 Koiliaris unmet demand.

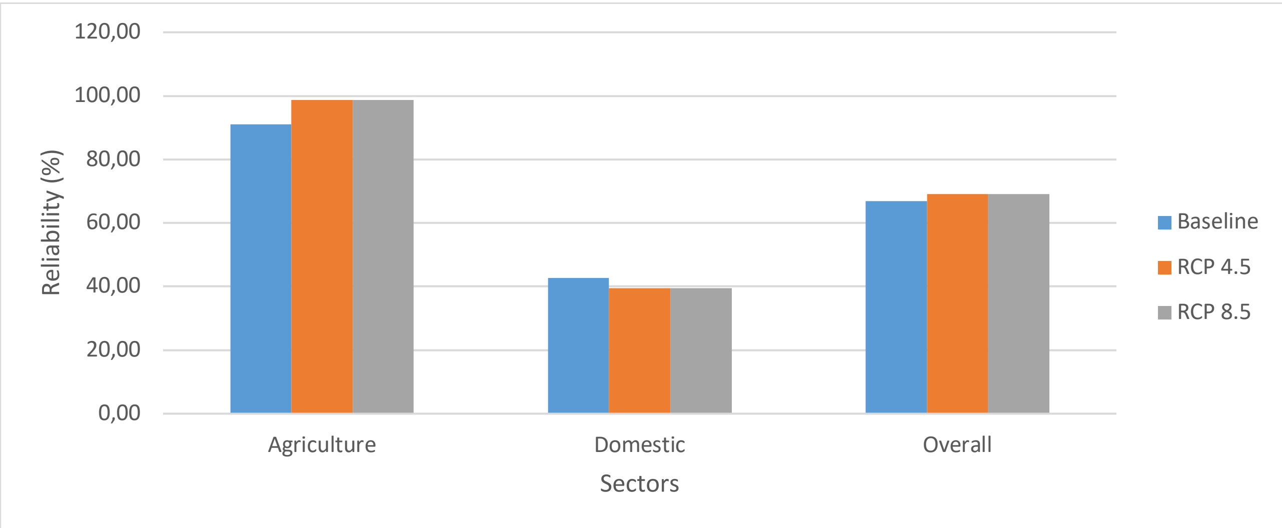

Figure 137 Koiliaris reliability of source.

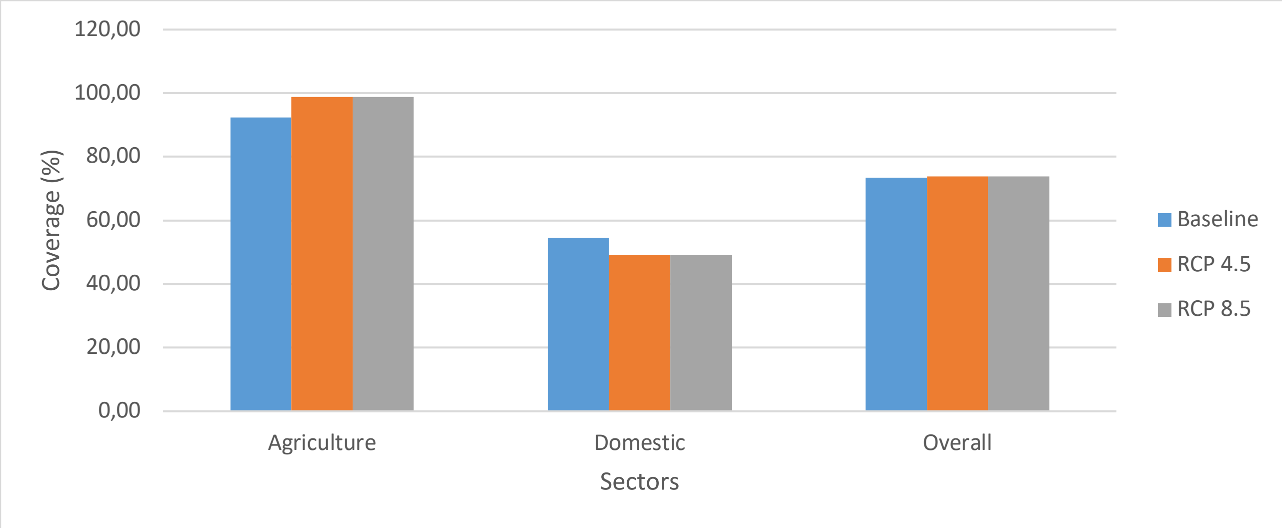

Figure 138 Koiliaris coverage of demand.

Figure 139 Koiliaris unmet instream flow requirements.

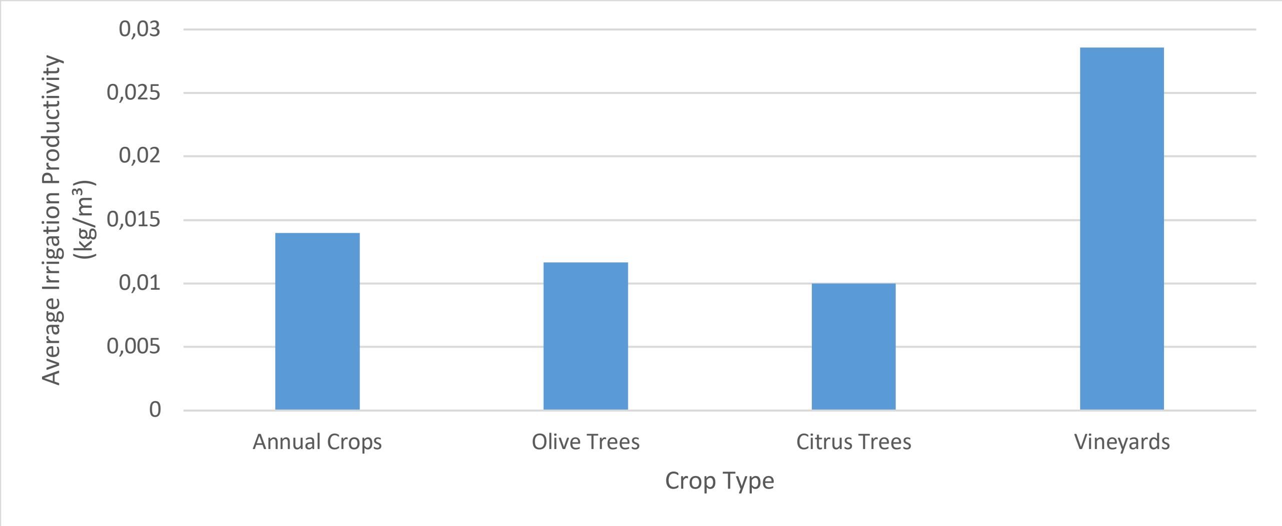

Figure 140 Koiliaris average irrigation productivity.

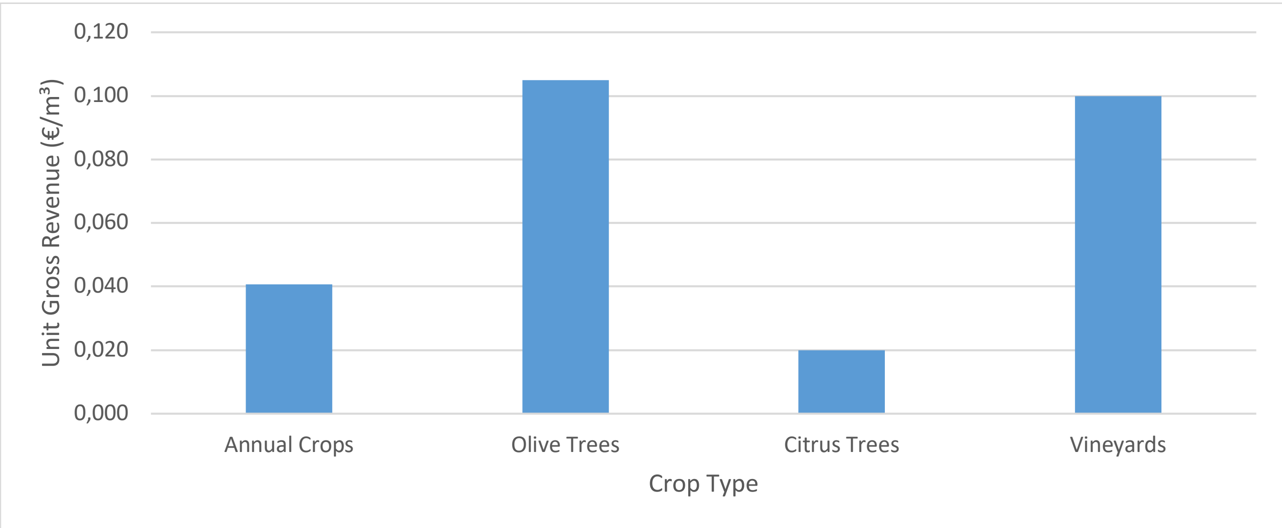

Figure 141 Koiliaris crop unit gross revenue.

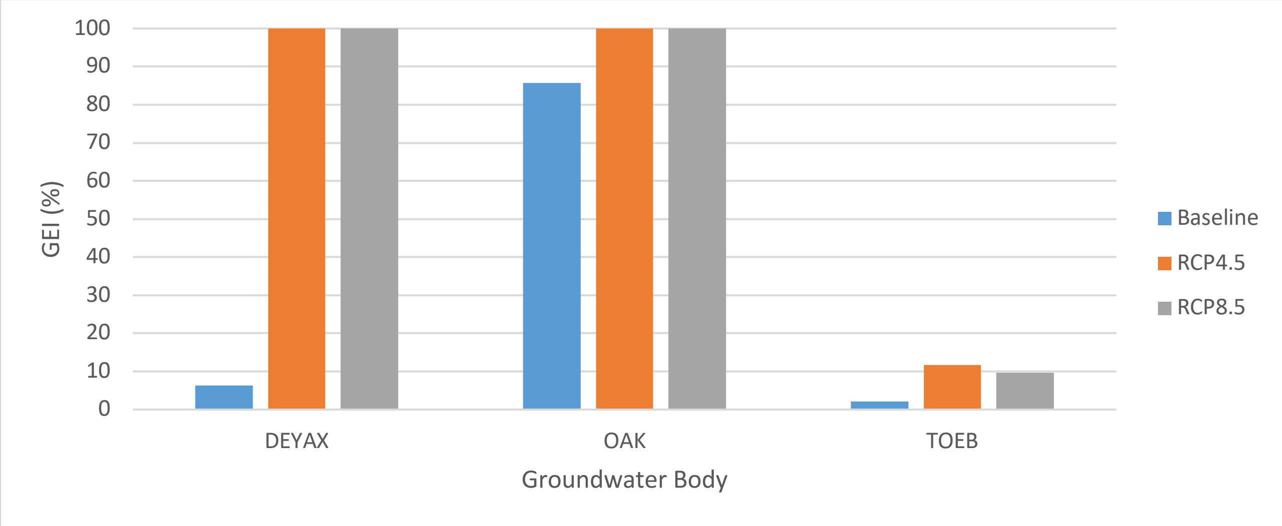

Figure 142 Koiliaris groundwater exploitation index.

6.3.6. Tarquinia Plain (IT)

The Italian pilot has been represented by the Tarquinia region of Lazio state. The main water source in the pilot is the Bolsena Lake. The Marta River allocates its water to the downstream regions of the pilot Tarquinia (Figure 143). While intensive agricultural activities dominate the region, other sectors such as industry or domestic use are negligible concerning the share of water use. Although the stakeholder meetings indicate that water scarcity is not the main problem of Tarquinia's agricultural community, they also agree that the water accounting of the pilot will be helpful in the way of solving other issues related to water. Modelled-observed streamflow values have been compared according to the streamflow gauge, which is located at the outlet of the pilot (Figure 144) (Table 28).

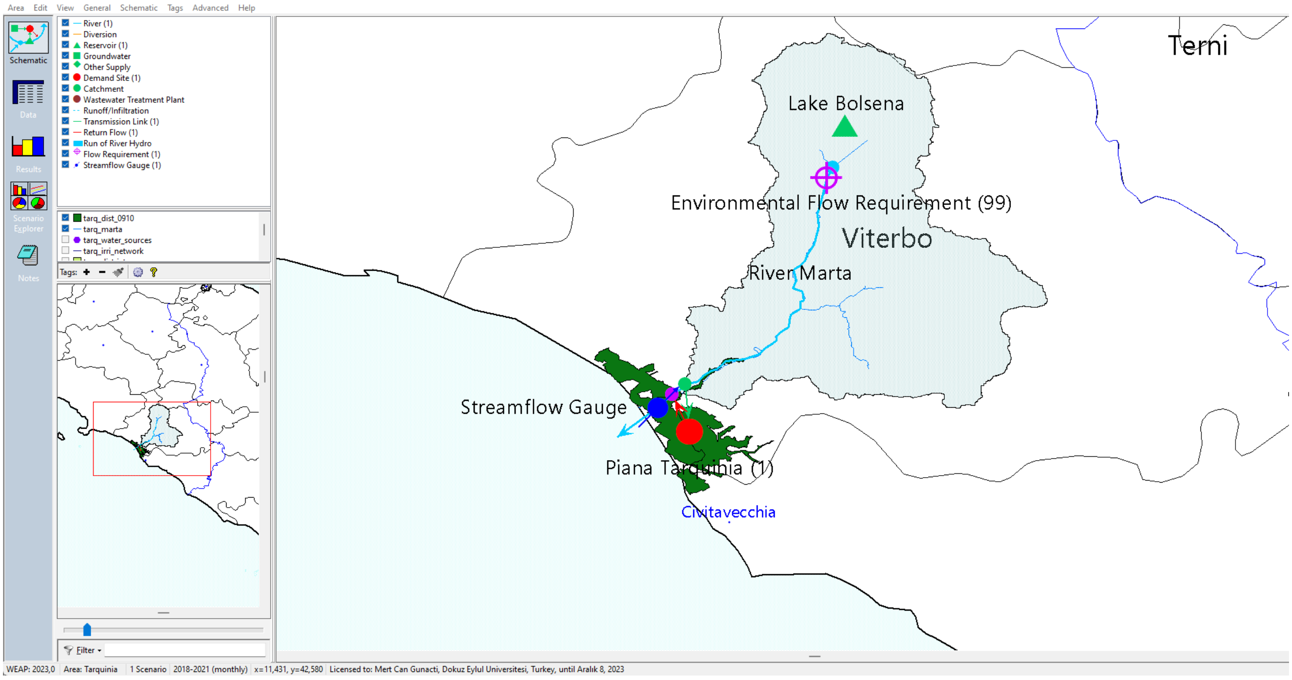

Figure 143 Tarquinia WEAP Schematic.

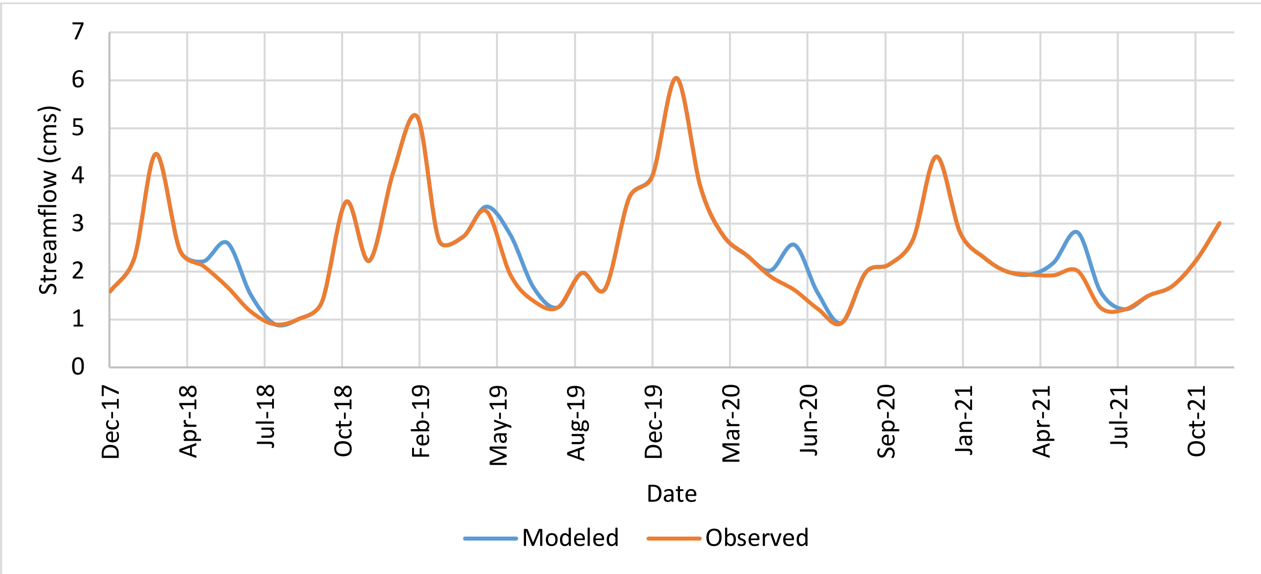

Figure 144 WEAP model observed-modelled streamflow comparison.

This project is part of the PRIMA programme supported by the European Union.
GA n° [2041] [LENSES] [Call 2020 Section 1 Nexus IA]

Table 26 Goodness of fit statistics of Gediz WEAP model.

Goodness-of-fit statistics	
NSE	0.94
KGE	0.94
NRMSE %	12
PBIAS%	4.7
RSR	0.24
R^2	0.95

Based on the developed model, water accounting indicators of Nexus (sectoral water use, total amount of supply, total amount of demand, supply demand ratio, unmet demand, reliability of source, coverage of demand, unmet instream flow requirement, water exploitation index, and groundwater exploitation index) have been determined for the baseline and the climate change scenarios of RCP4.5 and RCP8.5 for each sector and overall average. Average irrigation productivity and unit gross revenues have been calculated according to the crop pattern, crop yields, and crop unit gross revenues that the pilot reported (Figures 145-155).

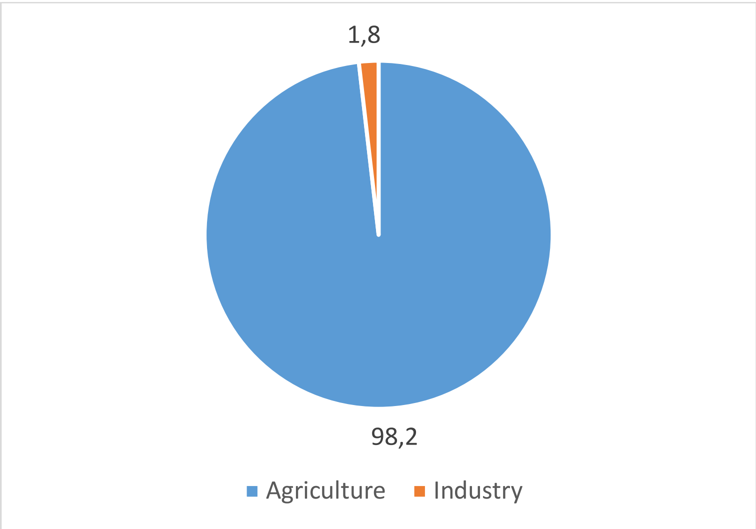

Figure 145 Tarquinia sectoral water use.

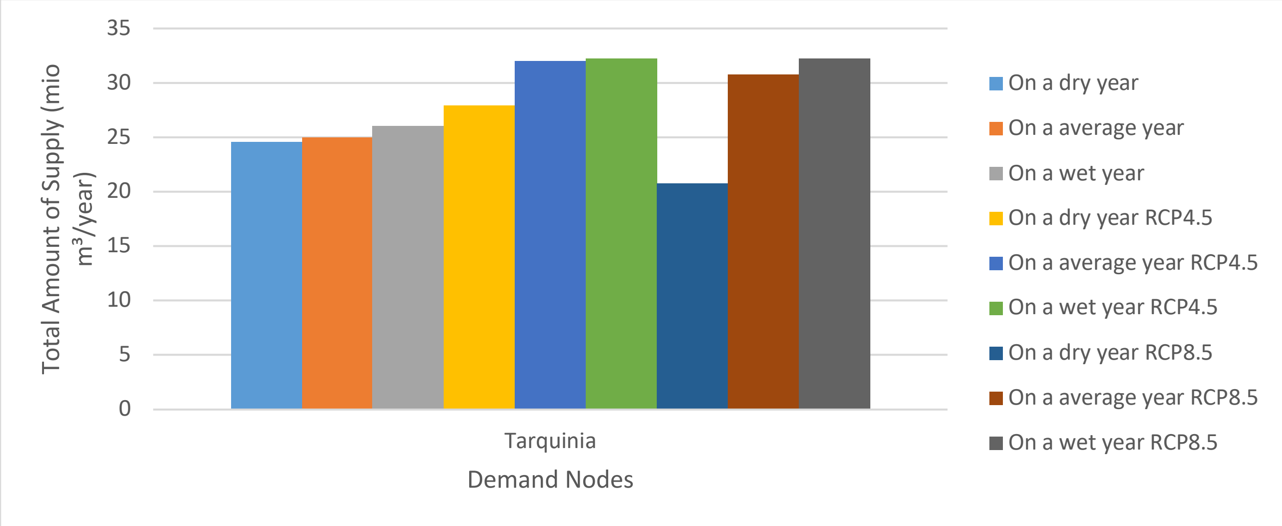

Figure 146 Tarquinia total amount of supply.

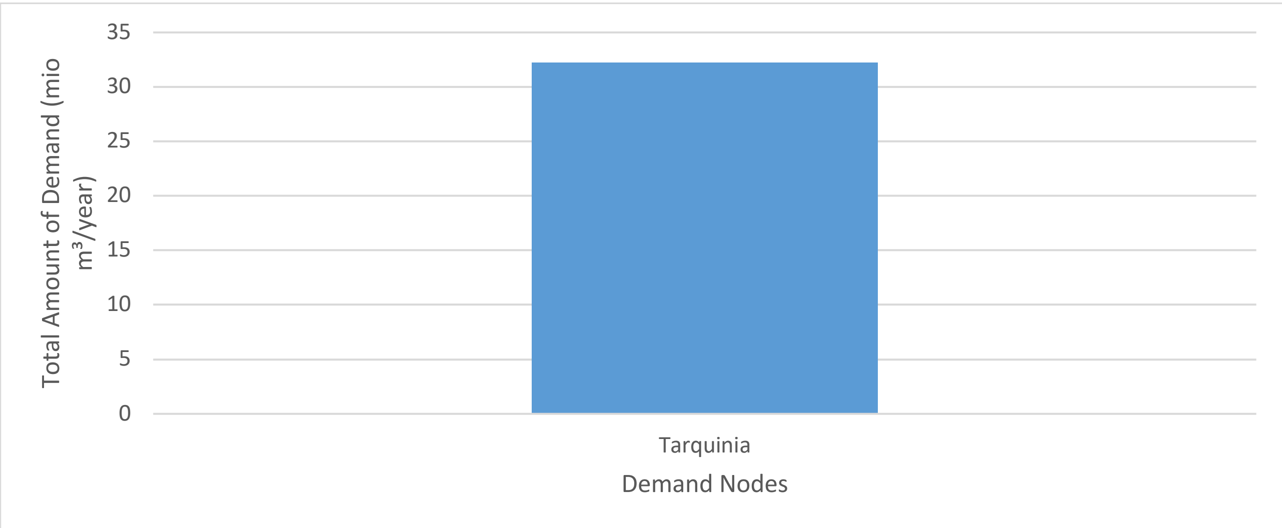

Figure 147 Tarquinia total amount of demand.

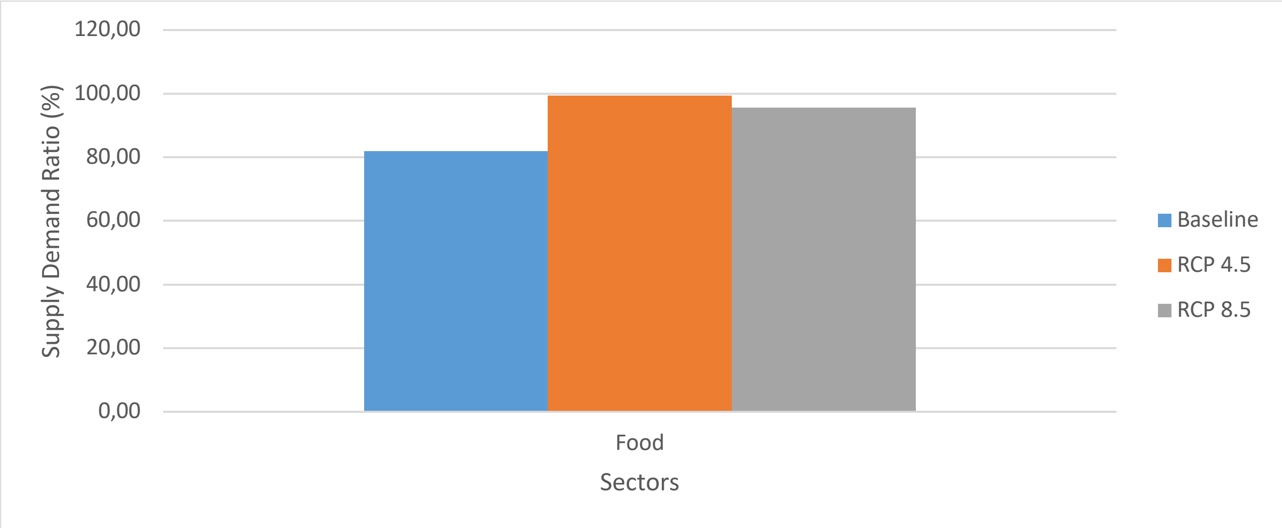

Figure 148 Tarquinia supply demand ratio.

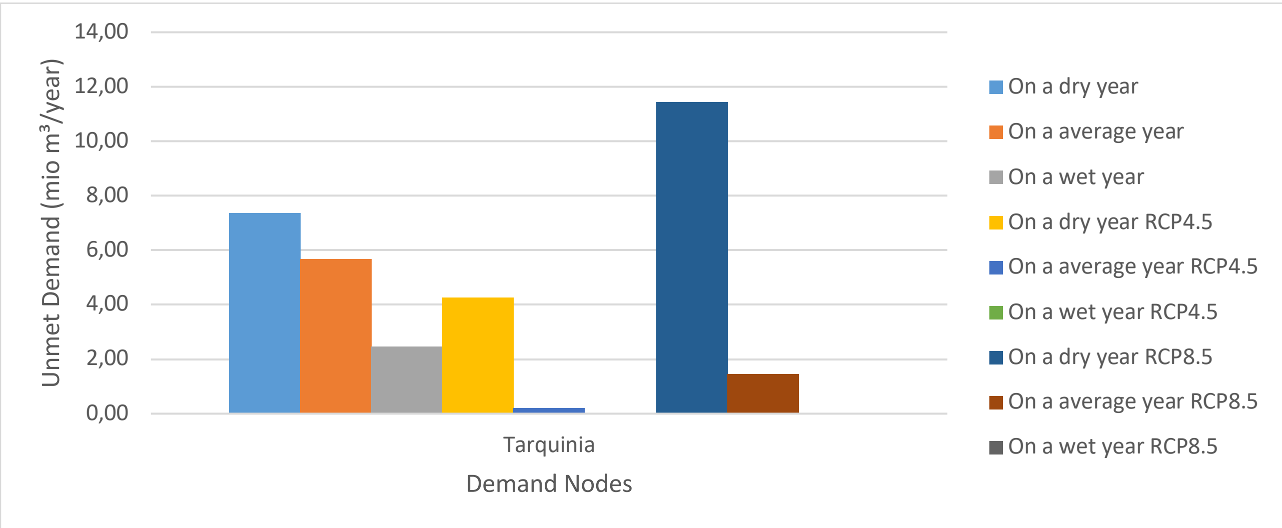

Figure 149 Tarquinia unmet demand.

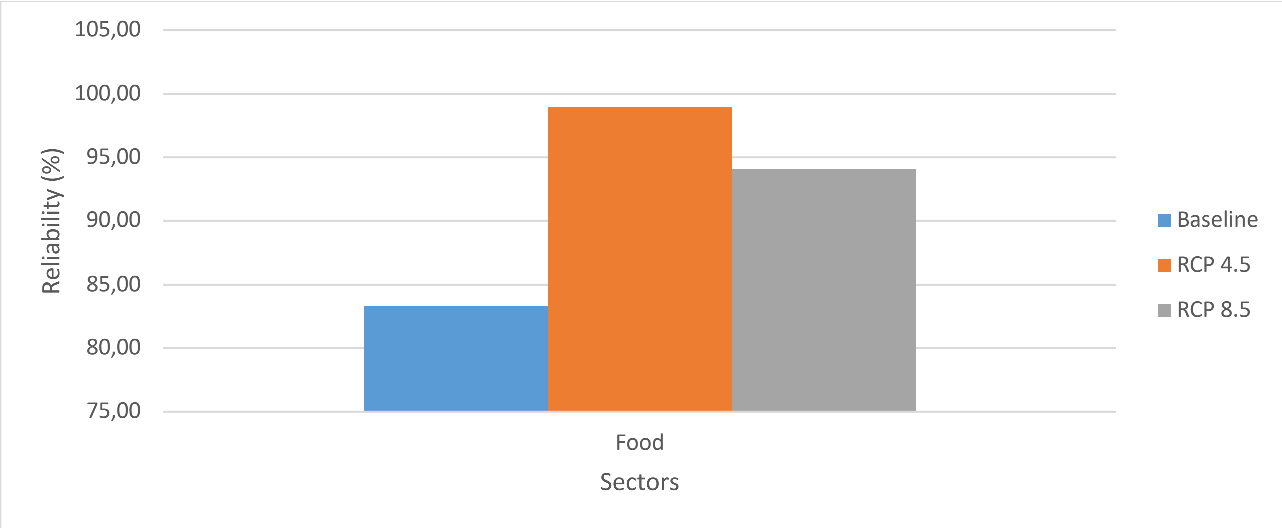

Figure 150 Tarquinia reliability of source.

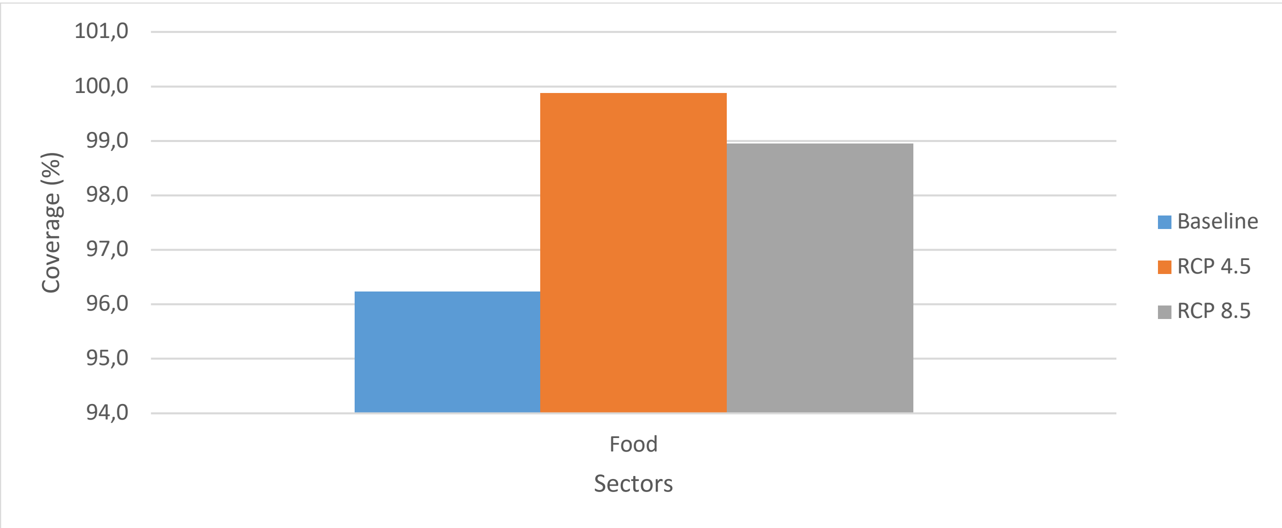

Figure 151 Tarquinia coverage of demand.

This project is part of the PRIMA programme supported by the European Union.
GA n° [2041] [LENSES] [Call 2020 Section 1 Nexus IA]

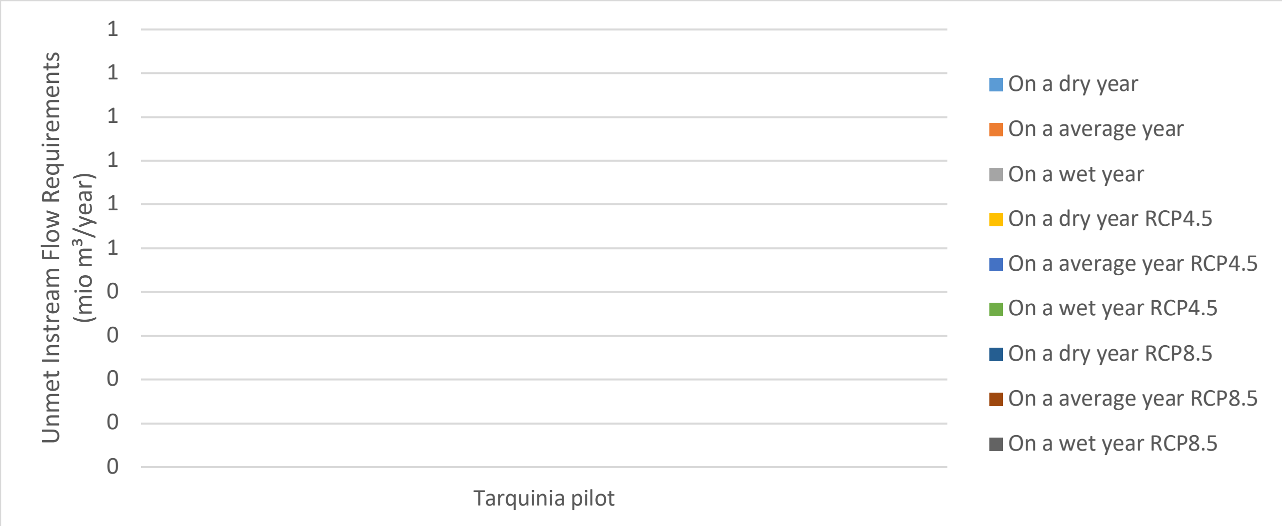

Figure 152 Tarquinia unmet instream flow requirements.

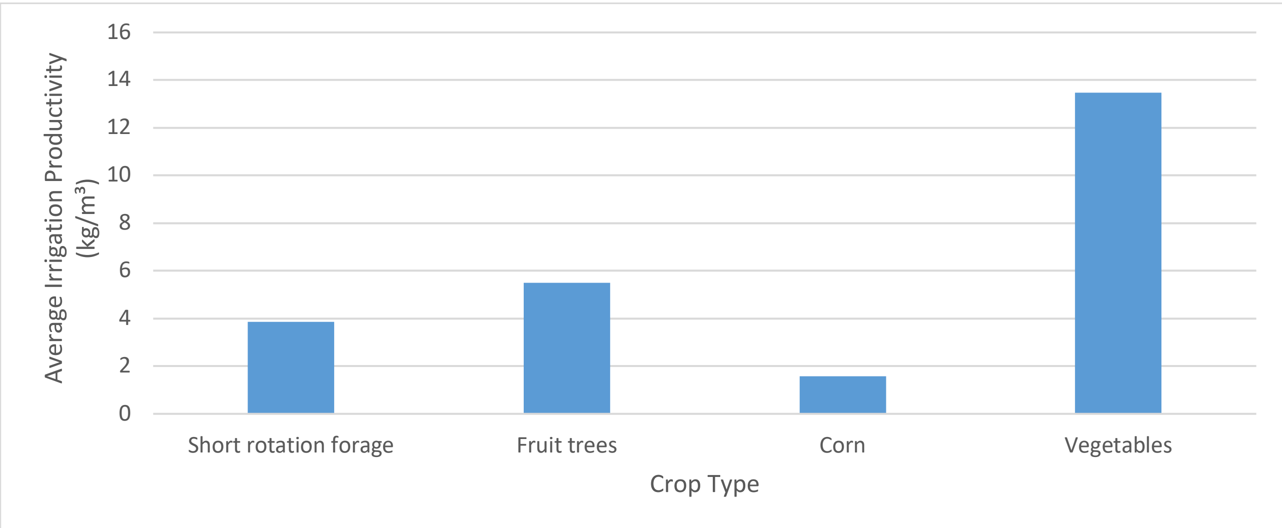

Figure 153 Average irrigation productivity of Tarquinia.

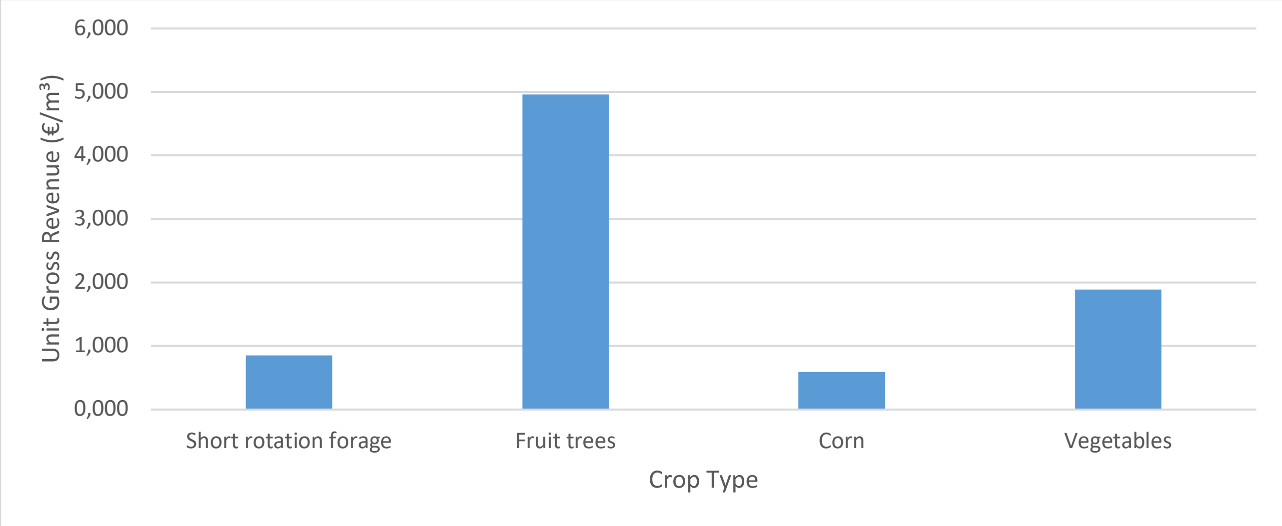

Figure 154 Crop unit gross revenue of Tarquinia.

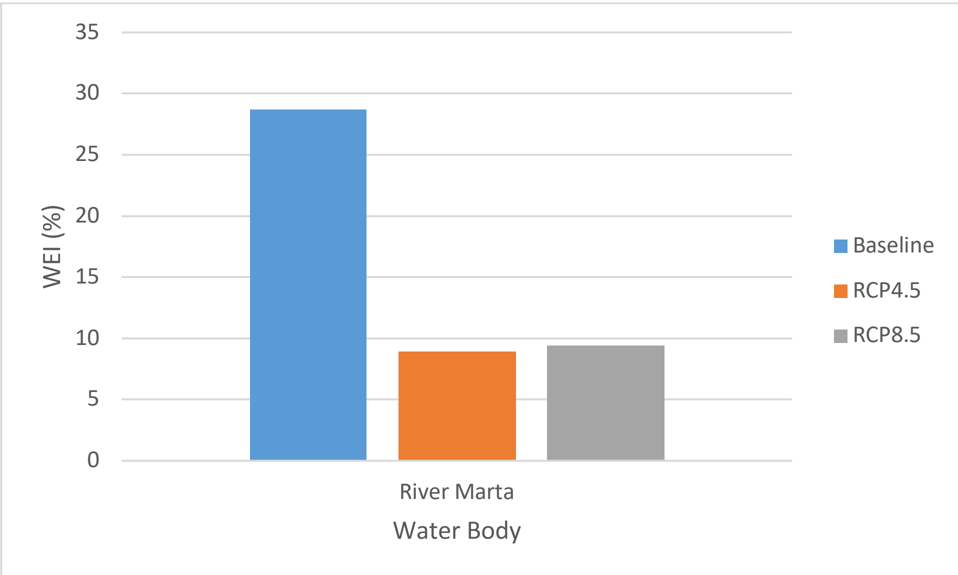

Figure 155 Tarquinia water exploitation index.

This project is part of the PRIMA programme supported by the European Union.
GA n° [2041] [LENSES] [Call 2020 Section 1 Nexus IA]

7. Conclusions

Within the context of this deliverable, six different pilot areas (Deir Alla, Gediz, Tarquinia, Doñana, Koliaris and Pinios) of LENSES project has been evaluated in the scope of Water which is one of the domains of WEF Nexus. These pilots are extending from most western to eastern regions of Mediterranean Basin, and representing the variability of meteorological and hydrologic conditions, ranging from most arid areas (deir Alla) to rich biodiversity sites maintained by environmental protection zones (Tarquinia, Gediz, Doñana etc..) with different challenges for Nexus domains. Therefore, the studies represented in this deliverable also aid for a stride towards augmenting our understanding of hydrological systems, their intricate responses to climate change and ecosystem. This initiative aligns with a holistic perspective on managing water resources in an integrated manner regarding the various water demands of different water sectors and also environment and eco-system. The Nexus indicators derived from modeling results also enable the understanding of possible changes under climate change conditions. As explained above, the impact of NBS will be measured in Deliverable 5.4, so this effort also established a set of tools that constitute the baseline situation for all pilots towards the evaluation of actions, implementation of NBSs and policy recommendations.

Within each designated pilot area, thorough and detailed hydrological models have been developed to ascertain future water quantities, providing crucial input to water allocation models. These models play a pivotal role as essential inputs for subsequent water allocation models. In this phase, hydrological definitions have been established for pilot regions situated in diverse geographical areas across Mediterranean Region which is expected to be harshly affected by the changing climate. The projection of future flow patterns has been achieved by integrating climate change model outputs into the established hydrological models. This approach facilitates the discernment of basin responses under various climate change scenarios, shedding light on the dynamic behaviour of these regions amidst evolving environmental conditions.

The water accounting approach undertaken at different scales, considering both spatial and temporal dimensions acknowledged the extension of ecosystems beyond the confines of individual irrigated farms. This step laid the foundation for a holistic comprehension of the interplay between water resources and the broader environment, establishing a comprehensive understanding of the complex dynamics involved. Especially, any change in sectoral water demands and in available water supplies directly affects the Nexus and this understanding reveals the impact of current policies while entailing the creation and implementation of new policies.

CONDOLENCES AND COMMEMORATION:

On the date of December 3, 2023, based on news we received, we have learned with deep sorrow that our colleague, former Ph. D. student of Ea-Tek team members, Mohamed NAJAR, one of the authors of this report, passed away as a result of an airstrike in the Gaza Strip. In the sadness of losing a young and successful scientist and a beloved father in this senseless and brutal war, we extend our heartfelt condolences to his family and express our hope for the return of peaceful days in the Levant and the rest of the world.

8. References

Al-Kharabsheh, A. (2000). Ground-water modeling and long-term management of the Azraq basin as an example of arid area conditions (Jordan). Journal of Arid Environments, 44(2), 143-153.

Al-Weshah, R. A. (2000). Optimal use of irrigation water in the Jordan Valley: A case study. Water Resources Management, 14, 327-338.

Arampatzis, G., Panagopoulos, A., Pisinaras, V., Tziritis, E., & Wendland, F. (2018). Identifying potential effects of climate change on the development of water resources in Pinios River Basin, Central Greece. Applied water science, 8(2), 51.

Arnold, J.G., Srinivasan, R., Muttiah, R.S., and Williams, J.R. (1998). Large area hydrologic modeling and assessment: Part I. Model development. Journal of the American Water Resources Association, 34(1), 73-89.

Arsenault, R., Brissette, F., & Martel, J. L. (2018). The hazards of split-sample validation in hydrological model calibration. Journal of hydrology, 566, 346-362.

Brogi, C., Pisinaras, V., Köhli, M., Dombrowski, O., Hendricks Franssen, H. J., Babakos, K., ... & Bogena, H. R. (2023). Monitoring Irrigation in Small Orchards with Cosmic-Ray Neutron Sensors. Sensors, 23(5), 2378.

Casulli, V. (2009). A high-resolution wetting and drying algorithm for free-surface hydrodynamics. International Journal for Numerical Methods in Fluids, 60(4), 391-408.

Cetinkaya C.P., Fistikoglu O., Fedra K., Harmancioglu N. B., (2008) Optimization Methods Applied for Sustainable Management of Water Scarce Basins, Journal of Hydroinformatics, 10/1/69-95/2008

Cetinkaya C.P., Gunacti M.C., (2017) Multi-Criteria Analysis of Water Allocation Scenarios in a Water Scarce Basin, Water Resources Management, Volume 32 Issue 8 Pages 2867-2884

Dahamsheh, A., & Aksoy, H. (2007). Structural characteristics of annual precipitation data in Jordan. Theoretical and Applied Climatology, 88, 201-212.

de Andrade, C. W., Montenegro, S. M., Montenegro, A. A., Lima, J. R. D. S., Srinivasan, R., & Jones, C. A. (2019). Soil moisture and discharge modeling in a representative watershed in northeastern Brazil using SWAT. Ecohydrology & Hydrobiology, 19(2), 238-251.

Duncan, J., & Cogan, J. J. (2022). Decolonizing water governance: A critical perspective on water justice and indigenous rights. Water Alternatives, 15(1), 1-17.

Gallart, F., Benito, G., Martín-Vide, J. P., Benito, A., Prió, J. M., & Regüés, D. (1999). Fluvial geomorphology and hydrology in the dispersal and fate of pyrite mud particles released by the Aznalcóllar mine tailings spill. Science of the total environment, 242(1-3), 13-26.

Gassman, P. W., Reyes, M. R., Green, C. H., & Arnold, J. G. (2007). The soil and water assessment tool: historical development, applications, and future research directions. Transactions of the ASABE, 50(4), 1211-1250.

Gleick, P. H. (1993). Closing the loop: Depletion and pollution of freshwater resources. Science, 261(5120), 785-788.

Gleick, P. H., Rosegrant, M. W., Bierman, J., Famiglietti, J. N., Gelbman, K., Heraghty, J., Holm, B. K., & Willis, R. B. (2013). The global water system: A critical infrastructure for humanity. Environmental Science & Technology, 47(12), 575-586.

Gül, G. O., Gül, A., Baran, T., Barbaros, F., Yumuk, H., & Ceylan, J. (2018). Assessing environmental conditions for the Gediz Delta through estimated flows at the ungauged Delta Inlet. pp. 255-261. In Gastescu, P., Bretcan, P. (edit, 2018), Water resources and wetlands, 4th International Conference Water resources and wetlands, 5-9 September 2018, Tulcea (Romania), p.312

Gül, G. O., Rosbjerg, D., Gül, A., Ondracek, M., & Dikgola, K. (2010). Assessing climate change impacts on river flows and environmental flow requirements at catchment scale. Ecohydrology: Ecosystems, Land and Water Process Interactions, Ecohydrogeomorphology, 3(1), 28-40.

Harmancioglu N.B, Barbaros F., Cetinkaya C.P., (2013) Sustainability Issues in Water Management, Water Resources Management, Volume 27, Issue 6 (2013), Page 1867-1891

Harmancioglu N.B, Cetinkaya C.P., Barbaros F., (2020) "Sustainability Issues in Water Management in the Context of Water Security", Water Resources of Turkey, Edt: Nilgun B. Harmancioglu, Dogan Altinbilek, Springer International Publishing, ISBN: 978-3-030-11728-3

Hoeffler, O., & Crook, D. A. (2022). Water governance and justice: The case of the Mekong River Basin. Water Policy, 24(5), 1245-1261.

Hydrologic Modeling System HEC-HMS (2008), Applications Guide. https://www.hec.usace.army.mil/software/hec-hms/documentation/HECHMS_Applications_Guide_March2008.pdf

Jordan Ministry of Water and Irrigation, Jordan. (2023). National Water Strategy 2023–2040. Amman, Jordan. https://www.mwi.gov.jo/EBV4.0/Root_Storage/AR/EB_List_Page/national_water_strategy_2023-2040.pdf

Kundu, D., Vervoort, R. W., & van Ogtrop, F. F. (2017). The value of remotely sensed surface soil moisture for model calibration using SWAT. Hydrological Processes, 31(15), 2764-2780.

Meadows, D. H., Meadows, D. L., Randers, J., & Behrens III, W. W. (2004). The limits to growth: Revisiting the 1972 report. New York: Chelsea Green Publishing.

Merwade, V., & Rajib, A. (2014). Setting up a SWAT Model with ArcSWAT. Purdue University: School of Civil Engineering, Purdue University.

Minshall, N. E. (1960). Predicting storm runoff on small experimental watersheds. Journal of the Hydraulics Division, 86(8), 17-38.

Moriasi, D.N., Arnold, J.G., Van Liew, M.W., Bingner, R.L., Harmel, R.D., Veith, T.L., 2007. Model evaluation guidelines for systematic quantification of accuracy in watershed simulations. Trans. ASABE 50, 885–900

Musyoka, F. K., Strauss, P., Zhao, G., Srinivasan, R., & Klik, A. (2021). Multi-step calibration approach for SWAT model using soil moisture and crop yields in a small agricultural catchment. Water, 13(16), 2238.

Neitsch, S.L., Arnold, J.G., Kiniry, J.R. and Williams, J.R. (2011a). Soil and Water Assessment Tool Theoretical Documentation. Temple, Texas 76502: USDA-153 ARS Grassland Soil and Water Research Laboratory, and Texas A&M University, Blackland Research and Extension Center.

Neitsch, S.L., Arnold, J.G., Kiniry, J.R., and Williams, J.R. (2011b). Soil and Water Assessment Tool Theoretical Documentation Version 2009. Texas Water Resources Institute, College Station, Texas

Onuşluel Gül, G. Ü. L. A. Y., & Rosbjerg, D. (2010). Modeling of hydrologic processes and potential response to climate change through the use of a multisite SWAT. Water and environment journal, 24(1), 21-31.

Panagos, P. (2006). The European soil database. GEO: connexion, 5(7), 32-33.

Panagos, P., Van Liedekerke, M., Jones, A., & Montanarella, L. (2012). European Soil Data Centre: Response to European policy support and public data requirements. Land use policy, 29(2), 329-338.

Pisinaras, V., Herrmann, F., Panagopoulos, A., Tziritis, E., McNamara, I., & Wendland, F. (2023). Fully Distributed Water Balance Modeling in Large Agricultural Areas—The Pinios River Basin (Greece) Case Study. Sustainability, 15(5), 4343.

Pisinaras, V., Panagopoulos, A., Herrmann, F., Bogena, H. R., Doulgeris, C., Ilias, A., ... & Wendland, F. (2018). Hydrologic and geochemical research at Pinios Hydrologic Observatory: Initial results. Vadose zone journal, 17(1), 1-16.

Pisinaras, V., Paraskevas, C., & Panagopoulos, A. (2021). Investigating the effects of agricultural water management in a Mediterranean coastal aquifer under current and projected climate conditions. Water, 13(1), 108.

Rawls, W. J., Brakensiek, D. L., & Saxtonn, K. E. (1982). Estimation of soil water properties. Transactions of the ASAE, 25(5), 1316-1320.

Stephenson, D. (2003). Water resources management. CRC Press.

Thiemig, V., Gomes, G. N., Skøien, J. O., Ziese, M., Rauthe-Schöch, A., Rustemeier, E., Rehfeldt, K., Walawender, J. P., Kolbe, C., Pichon, D., Schweim, C., and Salamon, P.: EMO-5: a high-resolution multi-variable gridded meteorological dataset for Europe, Earth Syst. Sci. Data, 14, 3249–3272, https://doi.org/10.5194/essd-14-3249-2022, 2022.

Tortajada, C., & Lin, J. (2022). The social dimensions of water scarcity: A critical review. Water Resources Research, 58(7), e2022WR026310.

Trick, T., & Custodio, E. (2004). Hydrodynamic characteristics of the western Doñana region (area of El Abalario), Huelva, Spain. Hydrogeology Journal, 12, 321-335.

Waterbury, J. (2002). Scarcity and security: The challenges of sustainable water development. World Politics, 54(2), 327-356.

Welle, P., D. Woodward, and H. Moody. (1980). A Dimensionless Unit Hydrograph for the Delmarva Peninsula, American Society of Agricultural Engineers Paper 80-2013, St. Joseph, Michigan.

World Water Assessment Programme. (2015). The future of water: A new framework for action. United Nations Educational, Scientific and Cultural Organization.

Zagana, E., Kuells, C., Udluft, P., & Constantinou, C. (2007). Methods of groundwater recharge estimation in eastern Mediterranean—a water balance model application in Greece, Cyprus and Jordan. Hydrological Processes: An International Journal, 21(18), 2405-2414.

Zare, M., Azam, S., & Sauchyn, D. (2022). Evaluation of Soil Water Content Using SWAT for Southern Saskatchewan, Canada. Water, 14(2), 249.

Annex 1

LENSES Topology Guide

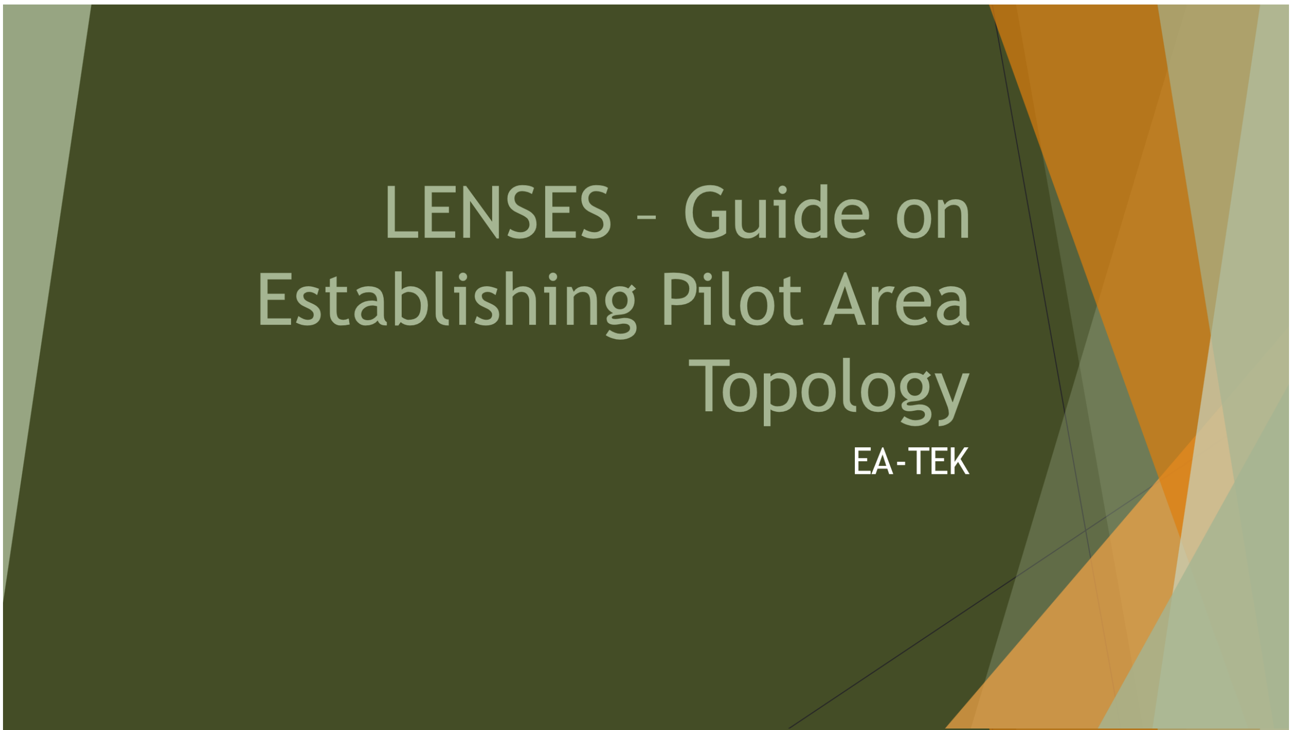

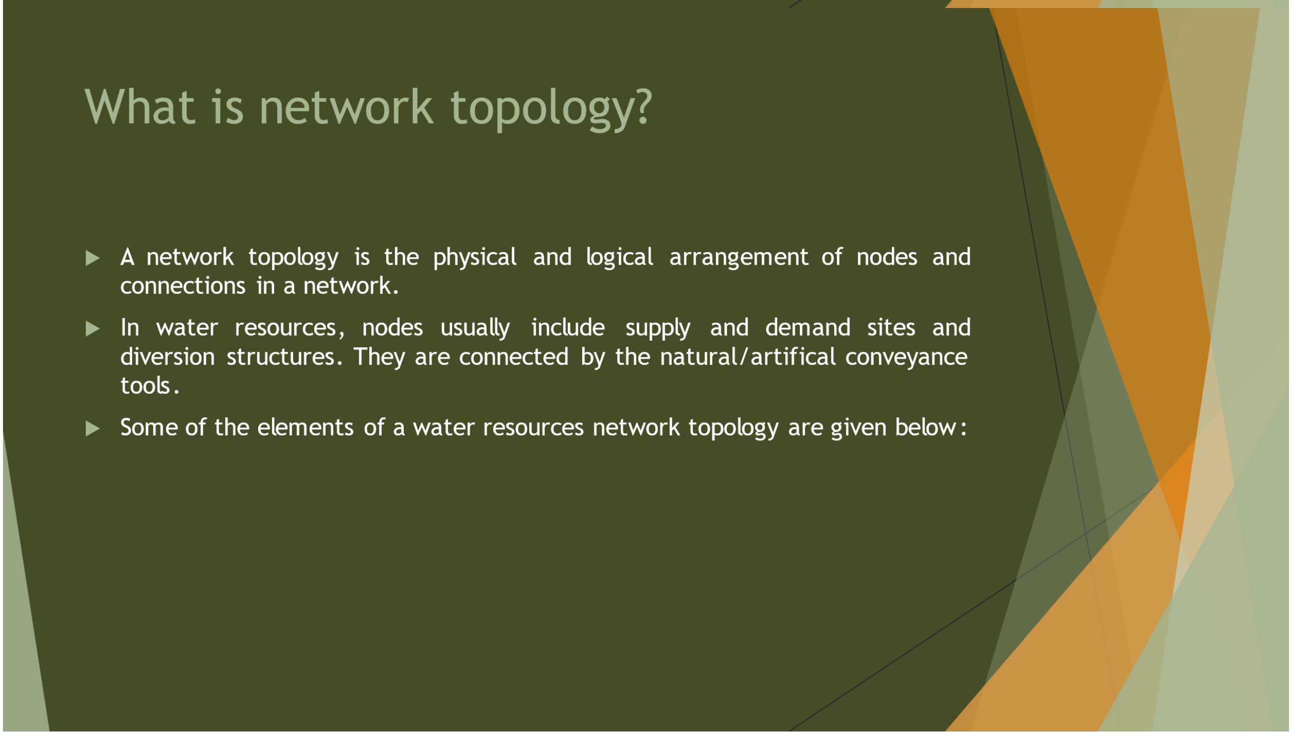

This project is part of the PRIMA programme supported by the European Union.
GA n° [2041] [LENSES] [Call 2020 Section 1 Nexus IA]

Elements of water resources network topology

Network Element	Description	Examples
Supply Node	Supply nodes provide water to the network.	• Reservoirs (Dams, Lakes), • Groundwater (Wells), • Basins (network could be allocating water from another basin or an upper sub-basin)
Demand Node	Demand nodes are where the water is partially consumed (consumptive use, e.g agriculture) or not consumed but demanded (non-consumptive use, e.g cooling water demand in industry).	• Domestic, • Agricultural, • Industrial, • Environmental, • Fishery, • Energy
Gauge Node	Gauge nodes are where the gauging stations are established for collecting quality/quantity data.	• Streamflow gauges
End Node	End node is used to represent the physical outlet of the network.	• Sea, lake, groundwater, another basin, sub-basin, etc.

Elements of water resources network topology

Network Element	Description	Examples
Supply Node	Supply nodes provide water to the network.	• Reservoirs (Dams, Lakes), • Groundwater (Wells), • Basins (network could be allocating water from another basin or an upper sub-basin)
Demand Node	Demand nodes are where the water is partially consumed (consumptive use, e.g agriculture) or not consumed but demanded (non-consumptive use, e.g cooling water demand in industry).	• Domestic, • Agricultural, • Industrial, • Environmental, • Fishery, • Energy
Gauge Node	Gauge nodes are where the gauging stations are established for collecting quality/quantity data.	• Streamflow gauges
End Node	End node is used to represent the physical outlet of the network.	• Sea, lake, groundwater, another basin, sub-basin, etc.

Elements of water resources network topology

Network Element	Description	Examples
Diversion Node	Diversion nodes are the structures where the water is regulated according to the needs of the network, e.g flow regulation, diversion, etc.	• Weirs
Conveyance Links (Reaches)	Conveyance links connect all nodes to each other.	• Pressure flow in pipes, • Open channel flow (natural or artifical).
Return Flow Links/Nodes	Return Flow is the treated (e.g industrial discharge) or non-treated (e.g agricultural irrigation) water coming from a demand node back to the network. Non-treated return flows can connect to the network directly from a demand node, while the treated return flows are firstly processed on a return flow node (e.g treatment plant).	Return Flows • Treated water (e.g industrial discharges), • Non-treated water (e.g irrigation), Return Flow Node • Treatment Plant

How to connect them?

- The network usually has one start and one finish, start being the supply node(s) and finish being the end node(s).

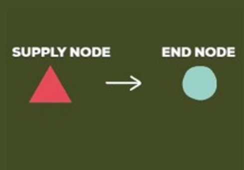

- Between the supply and end nodes; demand, diversion and/or return flows should be placed, through connections by the conveyance and/or return flow links.

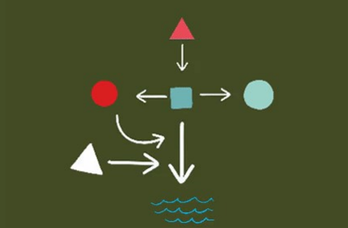

How to connect them?

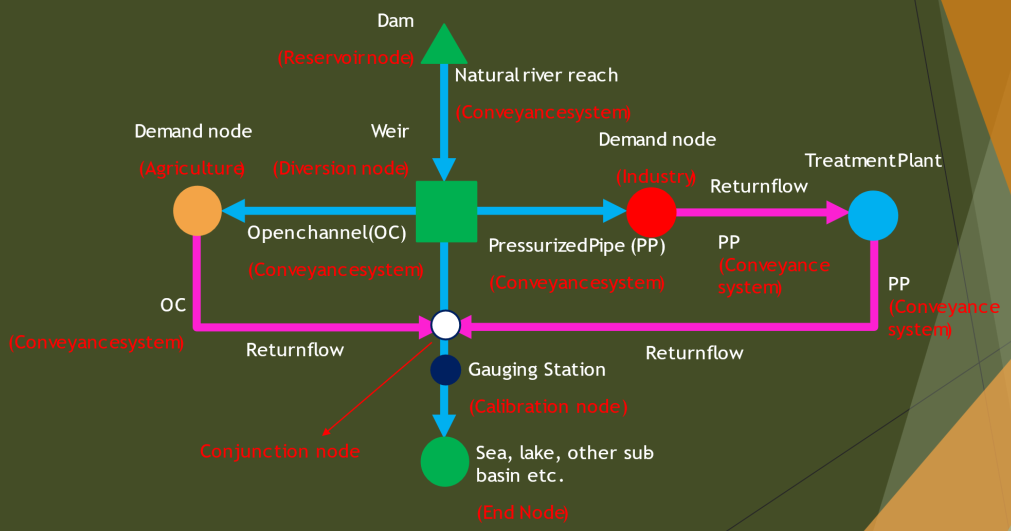

Data Requirements

- Once the network is complete, data required to model these systems become clear. According to the elements in your network, below listed data are required for each element.

Network Element	Required Data
Reservoir	• Inflow data series (daily/monthly), • Initial and total storage capacity (hm³), • Volume-area-elevation curve, • Evaporation rate (Daily/monthly), • Levels of reservoir storage (inactive zone, buffer zone, conservation zone, flood control zone), • (If available) Hydropower: max and min turbine flows, tailwater elevation, efficiency. • Operational rules (Storage/Release policy)

Data Requirements

Network Element	Required Data

Demand site	• Withdrawal
	  • for domestic use; per person m^3/s,
	  • for agriculture; per hectare m^3/s,
	  • for industry total m^3/s,
	• Consumption (% of withdrawal not returned) and routing of any return flow,
	• Loss Rate,
	• Reuse Rate,
	• (If available) Regional/sectoral priorities for water supply (Among demand sites, what is the order of claim on water resources)

Data Requirements

Network Element	Required Data
Gauging Stations	• River gauge flows as daily/monthly time series data • Meteorological data (Rainfall - Precipitation, Temperature, solar radiation, humidity, wind speed/direction, evapotranspiration (ET), etc.)
Diversion Nodes	• Weir flows as daily/monthly time series data

Conveyance Links	• Maximum flow m^3/s,
	• Losses,
	  • Loss from System (%)
	  • Loss to Groundwater (%)
	  • Evaporation
	• Routing Method parameters,
	  • Reach length,
	  • Slope,
	  • Manning's n
	  • Channel cross-section geometry (natural/artifical)
	  • Etc.

PRIMA PARTNERSHIP FOR RESEARCH AND INNOVATION IN THE MEDITERRANEAN AREA
This project is part of the PRIMA programme supported by the European Union.
GA n° [2041] [LENSES] [Call 2020 Section 1 Nexus IA]

Data Requirements

- Additionally, Land Use / Land Cover (LULC) map and soil data of the network are also necessary for the inclusion of LULC change impacts in the model.

Data type	Resolution
LULC map of the network	• 10-30-60 meters (Landsat, Sentinel 2, etc.)
Soil map	• 10-30-60 meters (Soilgrids, national data sets)

An example

- You can create the topology network by several softwares, e.g https://app.diagrams.net/

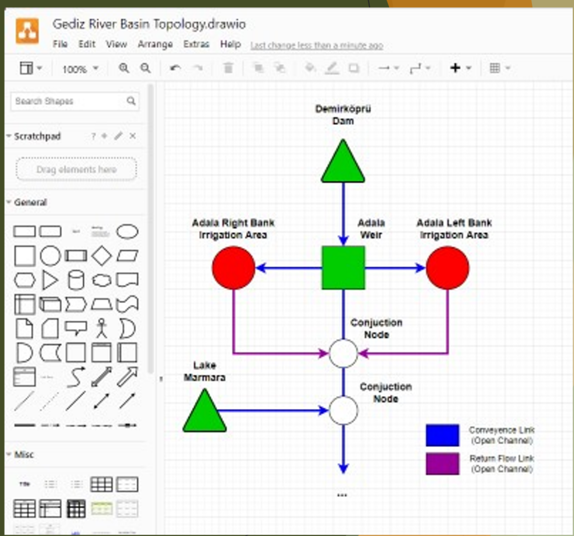

Annex 2

Water Accounting Indicators

Table A2.1 Deir Alla sectoral water use

Sector	Amount (hm^3/year)	Percentage
Agriculture	3.84	53.50
Industry	0.63	8.80
Domestic	2.71	37.70
Overall	7.18	100.00

Table A2.2 Gediz sectoral water use

Sector	Amount (hm^3/year)	Percentage
Agriculture	179.17	30.30
Industry	332.02	56.20
Environment	80.00	13.50
Overall	591.19	100.00

Table A2.3 Doñana sectoral water use

Sector	Amount (hm^3/year)	Percentage
Agriculture	81.58	28.00
Industry	0.50	0.20
Domestic	7.70	2.60
Environment	201.15	69.10
Overall	290.93	100.00

This project is part of the PRIMA programme supported by the European Union.
GA n° [2041] [LENSES] [Call 2020 Section 1 Nexus IA]

Table A2.4 Pinios sectoral water use

	Sector	Amount (hm^3/year)	Percentage
AGIA	Agriculture	6.26	42.0
	Industry	0.50	3.40
	Domestic	0.60	4.10
DELTA	Agriculture	6.52	43.90
	Industry	0.50	3.40
	Domestic	0.49	3.30
PINIOS	Agriculture	12.78	85.90
	Industry	1.00	6.70
	Domestic	1.10	7.40
	Overall	14.88	100.0

Table A2.5 Koiliaris sectoral water use

Sector	Amount (hm^3/year)	Percentage
Agriculture	3.66	33.80
Domestic	7.18	66.20
Overall	10.84	100.00

Table A2.6 Tarquinia sectoral water use

Sector	Amount (hm^3/year)	Percentage
Agriculture	10.63	98.20
Industry	0.20	1.80
Overall	10.82	100.00

This project is part of the PRIMA programme supported by the European Union.
GA n° [2041] [LENSES] [Call 2020 Section 1 Nexus IA]

Table A2.7 Deir Alla total amount of supply (hm^3/y)

	Baseline			RCP4.5			RCP8.5		
Demand Node	On a dry year	On a average year	On a wet year	On a dry year RCP4.5	On a average year RCP4.5	On a wet year RCP4.5	On a dry year RCP8.5	On a average year RCP8.5	On a wet year RCP8.5
Deir Alla - Agriculture	0.69	0.74	0.79	0.69	0.74	0.81	0.69	0.74	0.83
Deir Alla - Industry	0.17	0.20	0.24	0.18	0.20	0.25	0.17	0.20	0.23
Deir Alla - Domestic	0.76	0.88	1.04	0.77	0.87	1.07	0.76	0.87	0.99
Overall	1.63	1.83	2.08	1.64	1.81	2.14	1.64	1.82	2.05

Table A2.8 Gediz total amount of supply (hm^3/y)

	Baseline			RCP4.5			RCP8.5		
Demand Node	On a dry year	On a average year	On a wet year	On a dry year RCP4.5	On a average year RCP4.5	On a wet year RCP4.5	On a dry year RCP8.5	On a average year RCP8.5	On a wet year RCP8.5
Kesikkoy	46.00	65.00	75.00	58.70	61.20	70.10	57.30	59.70	70.00
Maltepe	46.00	65.00	75.00	61.30	63.90	73.20	59.80	62.30	73.10
Seyrek	58.00	82.00	96.00	74.50	77.60	88.90	72.70	75.80	88.90
Ulukent	60.00	85.00	98.00	76.70	80.00	91.60	74.90	78.10	91.60
Adala	86.00	227.00	310.00	39.30	96.10	144.50	14.50	42.80	162.20
Ahmetli	266.00	613.00	613.00	347.00	385.80	539.30	327.80	338.40	538.80
Bird Paradise	57.00	103.00	150.00	97.00	104.10	122.60	92.00	93.50	121.00
Overall	617.00	1240.00	1418.00	754.00	869.00	1130.00	699.00	751.00	1146.00

This project is part of the PRIMA programme supported by the European Union.
GA n° [2041] [LENSES] [Call 2020 Section 1 Nexus IA]

Table A2.9 Doñana total amount of supply (hm^3/y)

	Baseline			RCP4.5			RCP8.5		
Demand Node	On a dry year	On a average year	On a wet year	On a dry year RCP4.5	On a average year RCP4.5	On a wet year RCP4.5	On a dry year RCP8.5	On a average year RCP8.5	On a wet year RCP8.5
Almonte	26.09	26.12	26.13	26.09	26.09	26.11	26.10	26.10	26.10
Almonte Rice	0.95	0.95	0.95	0.95	0.95	0.95	0.90	0.90	0.90
La Rocina	26.87	26.87	26.87	26.87	26.87	26.87	26.90	26.90	26.90
Marismas	13.76	13.76	13.76	6.68	12.67	13.76	4.10	12.40	13.80
Marismas Rice	16.06	16.06	16.06	14.06	15.93	16.06	11.00	15.70	16.10
Marshland	67.76	89.91	124.37	60.87	95.18	157.46	50.10	94.90	136.70
MELD	4.28	4.28	4.28	4.28	4.28	4.28	4.30	4.30	4.30
Temporary Lagoons	1.04	2.25	4.26	0.19	2.26	5.59	0.30	1.90	4.60
Overall	156.81	180.20	216.69	139.99	184.23	251.08	123.78	183.10	229.27

Table A2.10 Pinios total amount of supply (hm^3/y)

		Baseline			RCP4.5			RCP8.5		
	Demand Node	On a dry year	On a average year	On a wet year	On a dry year RCP4.5	On a average year RCP4.5	On a wet year RCP4.5	On a dry year RCP8.5	On a average year RCP8.5	On a wet year RCP8.5
AGIA	Agriculture	6.23	6.26	6.28	6.23	6.26	6.28	6.23	6.26	6.28
	Industry	0.50	0.50	0.50	0.50	0.50	0.50	0.50	0.50	0.50
	Domestic	0.60	0.60	0.60	0.60	0.60	0.60	0.60	0.60	0.60
DELTA	Agriculture	6.74	8.15	9.59	6.88	8.69	9.60	6.76	8.59	9.60
	Industry	0.50	0.50	0.50	0.50	0.50	0.50	0.50	0.50	0.50
	Domestic	0.49	0.49	0.49	0.49	0.49	0.49	0.49	0.49	0.49
PINIOS	Agriculture	12.97	14.41	15.87	13.12	14.95	15.88	13.00	14.85	15.88
	Industry	1.00	1.00	1.00	1.00	1.00	1.00	1.00	1.00	1.00
	Domestic	1.09	1.09	1.09	1.09	1.09	1.09	1.09	1.09	1.09
	Overall	15.07	16.51	17.97	15.22	17.05	17.98	15.10	16.95	17.99

Table A2.11 Koiliaris total amount of supply (hm³/y)

	Baseline			RCP4.5			RCP8.5		
Demand Node	On a dry year	On a average year	On a wet year	On a dry year RCP4.5	On a average year RCP4.5	On a wet year RCP4.5	On a dry year RCP8.5	On a average year RCP8.5	On a wet year RCP8.5
Agriculture	1.41	4.38	4.68	4.68	4.68	4.68	4.68	4.68	4.68
Domestic	1.79	4.42	8.21	2.54	3.55	4.12	2.54	3.53	4.12
Overall	3.21	8.81	12.90	7.24	8.24	8.81	7.23	8.22	8.81

Table A2.12 Tarquinia total amount of supply (hm³/y)

	Baseline			RCP4.5			RCP8.5		
Demand Node	On a dry year	On a average year	On a wet year	On a dry year RCP4.5	On a average year RCP4.5	On a wet year RCP4.5	On a dry year RCP8.5	On a average year RCP8.5	On a wet year RCP8.5
Tarquinia	25.00	25.00	26.00	27.90	32.00	32.20	20.80	30.80	32.20

Table A2.13 Deir Alla total amount of demand (hm^3/y)

Demand Node	On a average year
Deir Alla - Agriculture	3.84
Deir Alla - Industry	0.63
Deir Alla - Domestic	2.71
Overall	7.18

Table A2.14 Gediz total amount of demand (hm^3/y)

Demand Node	On a average year
Kesikkoy	75.00
Maltepe	79.00
Seyrek	96.00
Ulukent	98.00
Adala	310.00
Ahmetli	613.00
Bird Paradise	200.00
Overall	1471.00

Table A2.15 Doñana total amount of demand (hm^3/y)

Demand Node	On a average year
Almonte	26.13
Almonte Rice	0.95
La Rocina	26.87
Marismas	13.76
Marismas Rice	16.06
Marshland	183.69
MELD	4.28
Temporary Lagoons	17.46
Overall	289.00

Table A2.16 Pinios total amount of demand (hm³/y)

	Demand Node	On a average year
AGIA	Agia Agriculture	6.26
	Agia Industry	0.50
	Agia Domestic	0.60
DELTA	Delta Agriculture	8.15
	Delta Industry	0.52
	Delta Domestic	0.70
PINIOS	Pinios Agriculture	14.42
	Pinios Industry	1.03
	Pinios Domestic	1.31
	Overall	16.75

Table A2.17 Koiliaris total amount of demand (hm³/y)

Demand Node	On a average year
Agriculture	4.91
Domestic	7.98
Overall	12.89

Table A2.18 Tarquinia total amount of demand (hm³/y)

Demand Node	On a average year
Tarquinia	32.00

Table A2.19 Deir Alla supply demand ratio (%)

Sector	Baseline	RCP 4.5	RCP 8.5
Agriculture	19.40	19.27	19.43
Industry	32.80	32.23	32.41
Domestic	32.77	32.20	32.37
Overall	28.32	27.90	28.07

Table A2.20 Gediz supply demand ratio (%)

Sector	Baseline	RCP 4.5	RCP 8.5
Food	82.60	73.82	70.05
Industry	78.44	61.34	55.26
Environmental	51.52	52.51	47.76
Overall	76.77	59.36	53.15

PRIMA PARTNERSHIP FOR RESEARCH AND INNOVATION IN THE MEDITERRANEAN AREA
This project is part of the PRIMA programme supported by the European Union.
GA n° [2041] [LENSES] [Call 2020 Section 1 Nexus IA]

Table A2.21 Doñana supply demand ratio (%)

Sector	Baseline	RCP 4.5	RCP 8.5
Food	99.99	98.57	98.01
Industry	99.99	98.30	97.86
Domestic	99.99	99.92	99.93
Environmental	45.81	48.44	48.12
Overall	62.31	63.70	63.31

Table A2.22 Pinios supply demand ratio (%)

	Sector	Baseline	RCP 4.5	RCP 8.5
AGIA	Agia Agriculture	100.00	100.00	100.00
	Agia Industry	100.00	100.00	100.00
	Agia Domestic	100.00	100.00	100.00
DELTA	Delta Agriculture	100.00	100.00	100.00
	Delta Industry	100.00	100.00	100.00
	Delta Domestic	100.00	100.00	100.00
PINIOS	Pinios Agriculture	100.00	100.00	100.00
	Pinios Industry	100.00	100.00	100.00
	Pinios Domestic	100.00	100.00	100.00
	Overall	100.00	100.00	100.00

Table A2.23 Koiliaris supply demand ratio (%)

Sector	Baseline	RCP 4.5	RCP 8.5
Agriculture	89.31	95.36	95.36
Domestic	55.42	44.54	44.32
Overall	72.37	69.95	69.84

Table A2.24 Tarquinia supply demand ratio (%)

Sector	Baseline	RCP 4.5	RCP 8.5
Food	81.83	99.36	95.53

This project is part of the PRIMA programme supported by the European Union.
GA n° [2041] [LENSES] [Call 2020 Section 1 Nexus IA]

Table A2.25 Deir Alla reliability of source (%)

Sector	Baseline	RCP 4.5	RCP 8.5
Agriculture	2.50	0.53	0.74
Industry	2.50	0.53	0.74
Domestic	2.50	0.53	0.74
Overall	2.50	0.53	0.74

Table A2.26 Gediz reliability of source (%)

Sector	Baseline	RCP 4.5	RCP 8.5
Food	83.02	70.08	63.91
Industry	80.32	63.21	63.11
Environmental	73.15	75.00	74.00
Overall	78.83	69.43	67.00

Table A2.27 Doñana reliability of source (%)

Sector	Baseline	RCP 4.5	RCP 8.5
Food	99.31	96.38	96.20
Industry	98.61	93.00	92.90
Domestic	98.61	94.66	94.73
Environmental	11.46	9.55	8.07
Overall	77.00	73.40	72.97

This project is part of the PRIMA programme supported by the European Union.
GA n° [2041] [LENSES] [Call 2020 Section 1 Nexus IA]

Table A2.28 Pinios reliability of source (%)

	Sector	Baseline	RCP 4.5	RCP 8.5
AGIA	Agia Agriculture	100.00	100.00	100.00
	Agia Industry	100.00	100.00	100.00
	Agia Domestic	100.00	100.00	100.00
DELTA	Delta Agriculture	100.00	100.00	100.00
	Delta Industry	100.00	100.00	100.00
	Delta Domestic	100.00	100.00	100.00
PINIOS	Pinios Agriculture	100.00	100.00	100.00
	Pinios Industry	100.00	100.00	100.00
	Pinios Domestic	100.00	100.00	100.00
	Overall	100.00	100.00	100.00

Table A2.29 Koiliaris reliability of source (%)

Sector	Baseline	RCP 4.5	RCP 8.5
Agriculture	91.10	98.73	98.73
Domestic	42.73	39.49	39.49
Overall	66.91	69.11	69.11

Table A2.30 Tarquinia reliability of source (%)

Sector	Baseline	RCP 4.5	RCP 8.5
Food	83.33	98.93	94.12

Table A2.31 Deir Alla coverage of demand (%)

Sector	Baseline	RCP 4.5	RCP 8.5
Agriculture	32.89	32.32	32.54
Industry	32.92	32.35	32.57
Domestic	32.88	32.31	32.53
Overall	32.90	32.33	32.55

Table A2.32 Gediz coverage of demand (%)

Sector	Baseline	RCP 4.5	RCP 8.5
Food	91.0	83.00	79.00
Industry	89.0	82.00	79.00
Environmental	87.0	89.00	87.00
Overall	81.54	68.75	63.33

Table A2.33 Doñana coverage of demand (%)

	Baseline			RCP4.5			RCP8.5		
Demand Node	On a dry year	On a average year	On a wet year	On a dry year	On a average year	On a wet year	On a dry year	On a average year	On a wet year
Almonte	99.94	99.98	100.00	99.94	99.94	99.97	99.93	99.94	99.97
Almonte Rice	100.00	100.00	100.00	100.00	100.00	100.00	100.00	100.00	100.00
La Rocina	100.00	100.00	100.00	100.00	100.00	100.00	100.00	100.00	100.00
Marismas	100.00	100.00	100.00	79.41	96.71	100.00	72.05	95.90	100.00
Marismas Rice	100.00	100.00	100.00	95.41	99.72	100.00	88.29	99.25	100.00
Marshland	50.00	58.00	69.00	45.74	58.25	75.00	38.33	57.14	70.01
MELD	100.00	100.00	100.00	100.00	100.00	100.00	100.00	100.00	100.00
Temporary Lagoons	6.00	13.00	25.00	1.15	13.00	32.43	1.86	10.75	26.26
Overall	82.00	84.00	87.00	78.00	83.00	88.00	75.00	83.00	87.00

Table A2.34 Pinios coverage of demand (%)

	Sector	Baseline	RCP 4.5	RCP 8.5
AGIA	Agia Agriculture	100.00	100.00	100.00
	Agia Industry	100.00	100.00	100.00
	Agia Domestic	100.00	100.00	100.00
DELTA	Delta Agriculture	100.00	100.00	100.00
	Delta Industry	100.00	100.00	100.00
	Delta Domestic	100.00	100.00	100.00
PINIOS	Pinios Agriculture	100.00	100.00	100.00
	Pinios Industry	100.00	100.00	100.00
	Pinios Domestic	100.00	100.00	100.00
	Overall	100.00	100.00	100.00

Table A2.35 Koiliaris coverage of demand (%)

Sector	Baseline	RCP 4.5	RCP 8.5
Agriculture	92.34	98.78	98.78
Domestic	54.52	49.08	49.08
Overall	73.43	73.93	73.93

Table A2.36 Tarquinia coverage of demand (%)

Sector	Baseline	RCP 4.5	RCP 8.5
Food	96.2	99.88	98.96

This project is part of the PRIMA programme supported by the European Union.
GA n° [2041] [LENSES] [Call 2020 Section 1 Nexus IA]

Table A2.37 Deir Alla unmet instream flow requirement (hm^3/y)

	Baseline			RCP4.5			RCP8.5		
Demand Node	On a dry year	On a average year	On a wet year	On a dry year RCP4.5	On a average year RCP4.5	On a wet year RCP4.5	On a dry year RCP8.5	On a average year RCP8.5	On a wet year RCP8.5
Overall	0.13	0.12	0.11	0.14	0.12	0.10	0.00	0.00	0.00

Table A2.38 Gediz instream flow requirement (hm^3/y)

	Baseline			RCP4.5			RCP8.5		
Demand Node	On a dry year	On a average year	On a wet year	On a dry year RCP4.5	On a average year RCP4.5	On a wet year RCP4.5	On a dry year RCP8.5	On a average year RCP8.5	On a wet year RCP8.5
Overall	10.82	7.36	2.19	20.80	17.75	14.74	21.82	18.87	14.23

Table A2.39 Doñana environmental flow requirement (hm^3/y)

	Baseline			RCP4.5			RCP8.5		
Demand Node	On a dry year	On a average year	On a wet year	On a dry year RCP4.5	On a average year RCP4.5	On a wet year RCP4.5	On a dry year RCP8.5	On a average year RCP8.5	On a wet year RCP8.5
Marshland	115.93	93.78	59.31	122.81	88.51	26.23	133.56	88.75	47.00
Temporary Lagoons	16.42	15.21	13.20	17.27	15.20	11.87	17.16	15.59	12.91
Overall	132.35	108.99	72.51	140.09	103.71	38.10	150.72	104.35	59.92

Table A2.40 Pinios instream flow requirement (hm³/y)

	Baseline			RCP4.5			RCP8.5		
Demand Node	On a dry year	On a average year	On a wet year	On a dry year RCP4.5	On a average year RCP4.5	On a wet year RCP4.5	On a dry year RCP8.5	On a average year RCP8.5	On a wet year RCP8.5
Agia	0.00	0.00	0.00	0.00	0.00	0.00	0.00	0.00	0.00
Delta	0.00	0.00	0.00	0.00	0.00	0.00	0.00	0.00	0.00
Overall	0.00	0.00	0.00	0.00	0.00	0.00	0.00	0.00	0.00

Table A2.41 Koiliaris instream flow requirement (hm³/y)

	Baseline			RCP4.5			RCP8.5		
Demand Node	On a dry year	On a average year	On a wet year	On a dry year RCP4.5	On a average year RCP4.5	On a wet year RCP4.5	On a dry year RCP8.5	On a average year RCP8.5	On a wet year RCP8.5
Overall	0.00	0.00	0.00	0.00	0.00	0.00	0.00	0.00	0.00

Table A2.42 Tarquinia instream flow requirement (hm³/y)

	Baseline			RCP4.5			RCP8.5		
Demand Node	On a dry year	On a average year	On a wet year	On a dry year RCP4.5	On a average year RCP4.5	On a wet year RCP4.5	On a dry year RCP8.5	On a average year RCP8.5	On a wet year RCP8.5
Overall	0.00	0.00	0.00	0.00	0.00	0.00	0.00	0.00	0.00

Table A2.43 Deir Alla average irrigation productivity (kg/m³)

Reclassified crop pattern percentage (%)	Crop Type	Yield (kg/ha)	Yield (kg)	Irrigation need percentage*	Actual water demand (m³)	AIP (kg/m³)
1.20	Sesbania	13500	41472	0.612	23520	1.763
19.50	Barley	10400	519168	6.217	238875	2.173
5.90	Sorghum	18000	271872	2.633	101185	2.687
3.10	Vetch	7500	59520	0.889	34177	1.741
70.30	Alfalfa	18500	3329408	89.648	3444700	0.967
Total Area (ha):	256.00			*Calculated according to CROPWAT	3842457.50	

Table A2.44 Gediz - Kesikkoy average irrigation productivity (kg/m³)

Reclassified crop pattern percentage (%)	Crop Type	Yield (kg/ha)	Yield (kg)	Irrigation need percentage*	Actual water demand (m³)	AIP (kg/m³)
15	Sunflower	2500	655612	11.823	3558828	0.184
15	Wheat	5750	1507908	18.660	5616903	0.268
11	Spinach	18000	3461634	11.870	3573155	0.969
36	Cotton	6250	3933675	15.012	4518738	0.871
3	Maize	58000	3042042	12.184	3667714	0.829
3	Grape	3250	170459	11.451	3447078	0.049
17	Alfalfa	6850	2035895	19.000	5719341	0.356
Total Area (ha):	1748.30			*Calculated according to CROPWAT	30101760	

Table A2.45 Gediz - Maltepe average irrigation productivity (kg/m^3)

Reclassified crop pattern percentage (%)	Crop Type	Yield (kg/ha)	Yield (kg)	Irrigation need percentage*	Actual water demand (m³)	AIP (kg/m³)
19	Sunflower	2500	1056020	13.259	4167584	0.253
17	Wheat	5750	2173178	20.793	6535849	0.333
6	Spinach	18000	2401056	13.272	4171713	0.576
31	Cotton	6250	4307450	13.540	4255940	1.012
5	Maize	58000	6447280	16.947	5326944	1.210
22	Alfalfa	6850	3350362	22.190	6975151	0.480
Total Area (ha):	2223.20			*Calculated according to CROPWAT	31433184	

Table A2.46 Gediz - Seyrek average irrigation productivity (kg/m^3)

Reclassified crop pattern percentage (%)	Crop Type	Yield (kg/ha)	Yield (kg)	Irrigation need percentage*	Actual water demand (m³)	AIP (kg/m³)
13	Sunflower	2500	767162	11.898	4545748	0.169
6	Field Beans	12000	1699560	10.278	3926978	0.433
13	Wheat	5750	1764473	18.650	7125304	0.248
8	Spinach	18000	3399120	8.662	3309273	1.027
53	Cotton	6250	7819156	15.203	5808505	1.346
2	Maize	58000	2738180	12.150	4642121	0.590
2	Alfalfa	6850	323388	19.911	7607170	0.043
3	Arugula	5000	354075	3.248	1240977	0.285
Total Area (ha):	2360.5			*Calculated according to CROPWAT	38206080	

Table A2.47 Gediz - Ulukent average irrigation productivity (kg/m^3)

Reclassified crop pattern percentage (%)	Crop Type	Yield (kg/ha)	Yield (kg)	Irrigation need percentage*	Actual water demand (m³)	AIP (kg/m³)
2	Barley	5350	258501	11.053	4350740	0.059
18	Sunflower	2500	1087155	10.583	4165848	0.261
1	Field Beans	12000	289908	9.142	3598790	0.081
30	Wheat	5750	4167427	16.588	6529824	0.638
1	Spinach	18000	434862	4.147	1632456	0.266
36	Cotton	6250	5435775	13.523	5323074	1.021
2	Maize	58000	2802444	10.807	4254167	0.659
7	Alfalfa	6850	1158424	17.710	6971419	0.166
3	Arugula	5000	362385	12.441	4897368	0.074
Total Area (ha):	2415.9			*Calculated according to CROPWAT	39363840	

Table A2.48 Gediz - Adala average irrigation productivity (kg/m^3)

Reclassified crop pattern percentage (%)	Crop Type	Yield (kg/ha)	Yield (kg)	Actual water demand (m³)	AIP (kg/m³)
58	Cotton	6250	42296500	95353229	0.444
9	Maize	58000	60906960	9556092	6.374
33	Grape	5000	19252200	19467824	0.989
Total Area (ha):	11668				

Table A2.49 Gediz - Ahmetli average irrigation productivity (kg/m³)

Reclassified crop pattern percentage (%)	Crop Type	Yield (kg/ha)	Yield (kg)	Actual water demand (m³)	AIP (kg/m³)
76	Cotton	6250	94738375	216763116	0.437
3	Maize	58000	29569560	4630459	6.386
22	Grape	5000	21645200	23953407	0.904
Total Area (ha):	19997				

Table A2.50 Pinios - Agia average irrigation productivity (kg/m³)

Reclassified crop pattern percentage (%)	Crop Type	Yield (kg/ha)	Yield (kg)	Irrigation need percentage*	Actual water demand (m³)	AIP (kg/m³)
98.05	Apples	42862	43686572	98.055	6138602	7.117
1.95	Alfalfa	14000	283788	1.945	121753	2.331
Total Area (ha):	1039.52			*Calculated according to CROPWAT	6260356.713	

Table A2.51 Pinios - Delta average irrigation productivity (kg/m³)

Reclassified crop pattern percentage (%)	Crop Type	Yield (kg/ha)	Yield (kg)	Irrigation need percentage*	Actual water demand (m³)	AIP (kg/m³)
20.89	Alfalfa	14000	7606750	20.798	1544755	4.924
42.57	Corn	10496	11623879	42.388	3148315	3.692
5.88	Kiwi fruit	21165	3238612	21.552	1600734	2.023
30.66	Sunflower	3190	2544574	15.263	1133637	2.245
Total Area (ha):	2601.18			*Calculated according to CROPWAT	7427443	

Table A2.52 Koiliaris average irrigation productivity (kg/m³)

Reclassified crop pattern percentage (%)	Crop Type	Yield (kg/ha)	Yield (kg)	Irrigation need percentage*	Actual water demand (m³)	AIP (kg/m³)
10.179	Annual Crops	7000	989800	5000	70700000	0.014
79.481	Olive Trees	3500	386400 0	3000	331200000	0.011
7.235	Citrus Trees	5000	502500	5000	50250000	0.010
3.095	Vineyards	10000	430000	3500	15050000	0.028
Total Area (ha):	1389			*Calculated according to CROPWAT	467200000	

Table A2.53 Tarquinia average irrigation productivity (kg/m³)

Crop pattern percentage (%)	Crop Type	Yield (kg/ha)	Yield (kg)	Irrigation need (m³/ha)	Actual water demand (m³)	AIP (kg/m³)
4	Short rotation forage	10000	760000	2591	196916	3.859
4	Fruit trees	16500	1254000	2996	227696	5.507
2	Corn	10000	380000	6294	239172	1.588
90	Vegetables	80000	13680000 0	5942	10160820	13.463
Total Area (ha):	1900					

Table A2.54 Deir Alla crop unit gross revenue (€/m³)

Reclassified crop pattern percentage (%)	Crop Type	Yield (kg/ha)	Yield (kg)	Unit Gross Revenue of Crop (€/kg)	Total Gross Revenue (€)	Irrigation need percentage*	Actual water demand (m³)	UGR (€/m³)
1.2	Sesbania	13500	41472	0.285	11819	0.612	23520	0.503
19.5	Barley	10400	519168	0.225	116812	6.217	238875	0.489
5.9	Sorghum	18000	271872	0.186	50568	2.633	101185	0.500
3.1	Vetch	7500	59520	0.642	38211	0.889	34177.5	1.118
70.3	Alfalfa	18500	3329408	0.386	1285151	89.648	3444700	0.373
Total Area (ha):	256					*Calculated according to CROPWAT	3842457	

Table A2.55 Gediz - Kesikkoy crop unit gross revenue (€/m³)

Reclassified crop pattern percentage (%)	Crop Type	Yield (kg/ha)	Yield (kg)	Unit Gross Revenue of Crop (€/kg)	Total Gross Revenue (€)	Irrigation need percentage*	Actual water demand (m³)	UGR (€/m³)
15	Sunflower	2500	655612	0.439	287648	11.823	3558828	0.081
15	Wheat	5750	1507908	0.195	294223	18.660	5616903	0.052
11	Spinach	18000	3461634	0.688	2382404	11.870	3573155	0.667
36	Cotton	6250	3933675	0.415	1632126	15.012	4518738	0.361
3	Maize	58000	3042042	0.056	170564	12.184	3667714	0.047
3	Grape	3250	170459	1.234	210264	11.451	3447078	0.061
17	Alfalfa	6850	2035895	0.157	319622	19.000	5719341	0.056
Total Area (ha):	1748.3					*Calculated according to CROPWAT	30101760	

Table A2.56 Gediz - Maltepe crop unit gross revenue (€/m³)

Reclassified crop pattern percentage (%)	Crop Type	Yield (kg/ha)	Yield (kg)	Unit Gross Revenue of Crop (€/kg)	Total Gross Profit (€)	Irrigation need percentage*	Actual water demand (m³)	UGP (€/m³)
19	Sunflower	2500	1056020	0.439	463326	13.259	4167584	0.111
17	Wheat	5750	2173178	0.195	424031	20.793	6535849	0.065
6	Spinach	18000	2401056	0.688	1652481	13.272	4171713	0.396
31	Cotton	6250	4307450	0.415	1787210	13.540	4255940	0.420
5	Maize	58000	6447280	0.056	361493	16.947	5326944	0.068
22	Alfalfa	6850	3350362	0.157	525985	22.190	6975151	0.075
Total Area (ha):	2223.2					*Calculated according to CROPWAT	31433184	

Table A2.57 Gediz - Seyrek crop unit gross revenue (€/m³)

Reclassified crop pattern percentage (%)	Crop Type	Yield (kg/ha)	Yield (kg)	Unit Gross Revenue of Crop (€/kg)	Total Gross Profit (€)	Irrigation need percentage*	Actual water demand (m³)	UGP (€/m³)
13	Sunflower	2500	767162	0.439	336590	11.898	4545748	0.074
6	Field Beans	12000	1699560	0.860	1462112	10.278	3926978	0.372
13	Wheat	5750	1764473	0.195	344285	18.650	7125304	0.048
8	Spinach	18000	3399120	0.688	2339380	8.662	3309273	0.707
53	Cotton	6250	7819156	0.415	3244257	15.203	5808505	0.559
2	Maize	58000	2738180	0.056	153527	12.150	4642121	0.033
2	Alfalfa	6850	323388	0.157	50769	19.911	7607170	0.007
3	Arugula	5000	354075	1.635	578753	3.248	1240977	0.466
Total Area (ha):	2360.5					*Calculated according to CROPWAT	38206080	

PRIMA PARTNERSHIP FOR RESEARCH AND INNOVATION IN THE MEDITERRANEAN AREA

This project is part of the PRIMA programme supported by the European Union.
GA n° [2041] [LENSES] [Call 2020 Section 1 Nexus IA]

Table A2.58 Gediz - Ulukent crop unit gross revenue (€/m³)

Reclassified crop pattern percentage (%)	Crop Type	Yield (kg/ha)	Yield (kg)	Unit Gross Revenue of Crop (€/kg)	Total Gross Profit (€)	Irrigation need percentage*	Actual water demand (m³)	UGP (€/m³)
2	Barley	5350	258501	0.177	45800	11.053	4350740	0.011
18	Sunflower	2500	1087155	0.439	476986	10.583	4165848	0.114
1	Field Beans	12000	289908	0.860	249404	9.142	3598790	0.069
30	Wheat	5750	4167427	0.195	813150	16.588	6529824	0.125
1	Spinach	18000	434862	0.688	299285	4.147	1632456	0.183
36	Cotton	6250	5435775	0.415	2255365	13.523	5323074	0.424
2	Maize	58000	2802444	0.056	157130	10.807	4254167	0.037
7	Alfalfa	6850	1158424	0.157	181865	17.710	6971419	0.026
3	Arugula	5000	362385	1.635	592336	12.441	4897368	0.121
Total Area (ha):	2415.9					*Calculated according to CROPWAT	39363840	

Table A2.59 Gediz - Adala crop unit gross revenue (€/m³)

Reclassified crop pattern percentage (%)	Crop Type	Yield (kg/ha)	Yield (kg)	Unit Gross Revenue of Crop (€/kg)	Total Gross Profit (€)	Actual water demand (m³)	UGP (€/m³)
58	Cotton	6250	42296500	0.415	17549302	95353229	0.184
9	Maize	58000	60906960	0.056	3414999	9556092	0.357
33	Grape	5000	19252200	1.234	23747984	19467824	1.220
Total Area (ha):	11668						

Table A2.60 Gediz - Ahmetli crop unit gross revenue (€/m³)

Reclassified crop pattern percentage (%)	Crop Type	Yield (kg/ha)	Yield (kg)	Unit Gross Revenue of Crop (€/kg)	Total Gross Profit (€)	Actual water demand (m³)	UGP (€/m³)
76	Cotton	6250	94738375	0.415	39308037	216763116	0.181
3	Maize	58000	29569560	0.056	1657939	4630459	0.358
22	Grape	5000	21645200	1.234	26699798	23953407	1.115
Total Area (ha):	19997						

Table A2.61 Pinios - Agia crop unit gross revenue (€/m³)

Reclassified crop pattern percentage (%)	Crop Type	Yield (kg/ha)	Yield (kg)	Unit Gross Revenue of Crop (€/kg)	Total Gross Revenue (€)	Irrigation need percentage*	Actual water demand (m³)	UGR (€/m³)
98.05	Apples	42861	43686572	0.5	21843286	98.055	6138602	3.558
1.95	Alfalfa	14000	283788	0.24	68109	1.945	121753	0.559
Total Area (ha):	1039.52					*Calculated according to CROPWAT	6260356	

Table A2.62 Pinios - Delta crop unit gross revenue (€/m³)

Reclassified crop pattern percentage (%)	Crop Type	Yield (kg/ha)	Yield (kg)	Unit Gross Revenue of Crop (€/kg)	Total Gross Revenue (€)	Irrigation need percentage*	Actual water demand (m³)	UGR (€/m³)
20.89	Alfalfa	14000	7606750	0.24	1825620	20.798	1544755	1.182
42.57	Corn	10496	11623879	0.23	2673492	42.388	3148315	0.849
5.88	Kiwi fruit	21165	3238612	0.55	1781236	21.552	1600734	1.113
30.66	Sunflower	3190	2544574	0.5	1272287	15.263	1133637	1.122
Total Area (ha):	2601.18					*Calculated according to CROPWAT		

Table A2.63 Koiliaris crop unit gross revenue (€/m³)

Reclassified crop pattern percentage (%)	Crop Type	Yield (kg/ha)	Yield (kg)	Unit Gross Revenue of Crop (€/kg)	Total Gross Revenue (€)	Actual water demand (m³)	UGR (€/m³)
10.17	Annual Crops	7000	989800	2.9	2870420	70700000	0.041
79.48	Olive Trees	3500	3864000	9	34776000	331200000	0.105
7.23	Citrus Trees	5000	502500	2	1005000	50250000	0.020
3.09	Vineyards	10000	430000	3.5	1505000	15050000	0.100
Total Area (ha):	1389					467200000	

Table A2.64 Tarquinia crop unit gross revenue (€/m³)

Crop pattern percentage (%)	Crop Type	Yield (kg/ha)	Yield (kg)	Unit Gross Revenue of Crop (€/kg)	Total Gross Revenue (€)	Irrigation need (m³/ha)	Actual water demand (m³)	UGR (€/m³)
4	Short rotation forage	10000	760000	0.22	167200	2591	196916	0.849
4	Fruit trees	16500	1254000	0.9	1128600	2996	227696	4.957
2	Corn	10000	380000	0.37	140600	6294	239172	0.588
90	Vegetables	80000	136800000	0.14	19152000	5942	10160820	1.885
Total Area (ha):	1900							

Table A2.65 Deir Alla water exploitation index

	Baseline			RCP4.5			RCP8.5		
Demand Node	Supply delivered from Rivers (mio m^3)	Total Recharge (mio m^3)	WEI (%)	Supply delivered from Rivers (mio m^3)	Total Recharge (mio m^3)	WEI (%)	Supply delivered from Rivers (mio m^3)	Total Recharge (mio m^3)	WEI (%)
Wadi Rajib	12.93	13.03	99.30	100.93	101.08	99.85	100.58	100.96	99.62

Table A2.66 Deir Alla groundwater exploitation index

	Baseline			RCP4.5			RCP8.5		
Demand Node	Supplied Delivered from GWs (mio m^3)	Total Recharge (mio m^3)	GEI (%)	Supplied Delivered from GWs (mio m^3)	Total Recharge (mio m^3)	GEI (%)	Supplied Delivered from GWs (mio m^3)	Total Recharge (mio m^3)	GEI (%)
Kurnub	4.55	4.57	99.69	35.45	35.45	100.00	35.40	35.40	100.00
Zarqa	0.90	0.91	98.90	7.05	7.05	100.00	7.05	7.05	100.00

Table A2.67 Gediz water exploitation index

	Baseline			RCP4.5			RCP8.5		
Demand Node	Supply delivered from Rivers (mio m^3)	Total Recharge (mio m^3)	WEI (%)	Supply delivered from Rivers (mio m^3)	Total Recharge (mio m^3)	WEI (%)	Supply delivered from Rivers (mio m^3)	Total Recharge (mio m^3)	WEI (%)
Gediz	10113.00	61476.65	16.45	68628.94	281139.25	24.41	61538.00	260529.07	23.62

PRIMA IN THE MEDITERRANEAN AREA
This project is part of the PRIMA programme supported by the European Union.
GA n° [2041] [LENSES] [Call 2020 Section 1 Nexus IA]

Table A2.68 Doñana water exploitation index

	Baseline			RCP4.5			RCP8.5		
Demand Node	Supply delivered from Rivers (mio m³)	Total Recharge (mio m³)	WEI (%)	Supply delivered from Rivers (mio m³)	Total Recharge (mio m³)	WEI (%)	Supply delivered from Rivers (mio m³)	Total Recharge (mio m³)	WEI (%)
Arrojo Madre de la Marismas	28.72	76.59	37.50	612.13	1393.32	43.93	621.58	1326.74	46.85
Arrojo de la Rocina	16.80	47.01	35.74	327.66	742.36	44.13	328.53	654.69	50.18
Guadiamar	13.65	91.82	14.86	6.90	2384.46	0.28	6.97	2249.98	0.31
Other Contributions	104.34	118.85	87.79	2260.77	2347.28	96.31	2288.19	2347.28	97.48

Table A2.69 Doñana groundwater exploitation index

	Baseline			RCP4.5			RCP8.5		
Demand Node	Supplied Delivered from GWs (mio m³)	Total Recharge (mio m³)	GEI (%)	Supplied Delivered from GWs (mio m³)	Total Recharge (mio m³)	GEI (%)	Supplied Delivered from GWs (mio m³)	Total Recharge (mio m³)	GEI (%)
Almonte GW	42.39	263.32	16.10	2129.13	5347.35	39.81	2129.13	5338.88	39.88
La Rocina GW	107.46	245.20	43.82	2122.44	4985.48	42.57	2122.44	4977.61	42.64
Manto Eolico Litoral de Donana GW	72.08	283.26	25.44	1339.08	5749.80	23.28	1339.08	5740.70	23.32
Marismas GW	119.27	107.85	>100.00	2259.93	2245.91	>100.00	2259.93	2245.91	>100.00

Table A2.70 Pinios – Agia groundwater exploitation index

	Baseline			RCP4.5			RCP8.5		
Demand Node	Supplied Delivered from GWs (mio m^3)	Total Recharge (mio m^3)	GEI (%)	Supplied Delivered from GWs (mio m^3)	Total Recharge (mio m^3)	GEI (%)	Supplied Delivered from GWs (mio m^3)	Total Recharge (mio m^3)	GEI (%)
Agia groundwater	220.94	224.42	98.44	584.79	573.70	>100.00	582.45	591.32	98.49

Table A2.71 Pinios – Delta water exploitation index

	Baseline			RCP4.5			RCP8.5		
Demand Node	Supply delivered from Rivers (mio m^3)	Total Recharge (mio m^3)	WEI (%)	Supply delivered from Rivers (mio m^3)	Total Recharge (mio m^3)	WEI (%)	Supply delivered from Rivers (mio m^3)	Total Recharge (mio m^3)	WEI (%)
Pinios River	79.05	56536.20	0.14	211.89	148867.80	0.14	211.16	148867.80	0.14

Table A2.72 Pinios – Delta groundwater exploitation index

	Baseline			RCP4.5			RCP8.5		
Demand Node	Supplied Delivered from GWs (mio m^3)	Total Recharge (mio m^3)	GEI (%)	Supplied Delivered from GWs (mio m^3)	Total Recharge (mio m^3)	GEI (%)	Supplied Delivered from GWs (mio m^3)	Total Recharge (mio m^3)	GEI (%)
Pinios Delta groundwater	195.44	284.29	68.74	553.30	684.44	80.84	546.11	720.07	75.84

Table A2.73 Koiliaris groundwater exploitation index

	Baseline			RCP4.5			RCP8.5		
Demand Node	Supplied Delivered from GWs (mio m^3)	Total Recharge (mio m^3)	GEI (%)	Supplied Delivered from GWs (mio m^3)	Total Recharge (mio m^3)	GEI (%)	Supplied Delivered from GWs (mio m^3)	Total Recharge (mio m^3)	GEI (%)
DEYAX	27.36	433.55	6.31	113.63	104.68	>100.00	112.20	105.63	>100.00
OAK	63.38	73.94	85.71	491.81	163.63	>100.00	7.05	7.05	>100.00
TOEB	1.86	90.87	2.04	0.38	3.23	11.73	0.33	3.50	9.64

Table A2.74 Tarquinia water exploitation index

	Baseline			RCP4.5			RCP8.5		
Demand Node	Supply delivered from Rivers (mio m^3)	Total Recharge (mio m^3)	WEI (%)	Supply delivered from Rivers (mio m^3)	Total Recharge (mio m^3)	WEI (%)	Supply delivered from Rivers (mio m^3)	Total Recharge (mio m^3)	WEI (%)
River Marta	100.07	348.43	28.72	2496.39	27970.42	8.92	2400.01	25439.76	9.43

This publication reflects only the author's view and the PRIMA Foundation is not responsible for any use that may be made of the information it contains

This project is part of the PRIMA programme supported by the European Union.
GA n° [2041] [LENSES] [Call 2020 Section 1 Nexus IA]